

**Characterization of T cell responses to
EBV-associated gastric carcinoma using
a single TCR cloning platform**

Nadia Khan

Imperial College London

Department of Infectious Diseases
Centre for Immunology and Vaccinology

Thesis Submitted for the Degree of Doctor of Philosophy

March 2020

Declaration of Originality

I, Nadia Khan, declare that all the work presented in this thesis is my own work, and that any information used here from other published, unpublished sources or collaborations is correctly referenced.

Copyright Declaration

The copyright of this thesis rests with the author and is made available under a Creative Commons Attribution Non-Commercial No Derivatives licence. Researchers are free to copy, distribute or transmit the thesis on the condition that they attribute it, that they do not use it for commercial purposes and that they do not alter, transform or build upon it. For any reuse or redistribution, researchers must make clear to others the licence terms of this work.

Acknowledgements

First and foremost, I would like to thank Almighty God for giving me the strength, ability and opportunity to complete this PhD. Without His blessings, none of it would have been possible. All praise is to Him alone.

I would like to thank Professor Xiao-Ning Xu for his enthusiasm and for the opportunity to undertake this research. I also thank Imperial College London for providing me with the scholarship to implement this PhD. I would like to say a big thank you to all of my friends and colleagues in the Centre for Immunology and Vaccinology for all their encouragement over the past 4 years- I have learned so much from everyone. In particular, I would like to thank Dr. Michael Liu for always being helpful, for patiently answering my endless questions, and for meticulously reading my thesis chapters. Also, thank you to Dr. Weiwei Ma, Dr. Scarlett Turner, Dr. Alex Cocker, Dr. Alessia Dalla Pria, Parisa Amjadi, Dominic Smith and Sima Fulford for their support, and for always offering great advice. A big thank you to Dr. Nesrina Imami for all of her invaluable guidance and discussions, this thesis probably would not have been possible without her expert assistance and encouragement. Also, a massive thank you to Dr. Peter Kelleher for reading my thesis and for taking the time to give me such detailed mock vivas.

Thank you to Dr. Hua Wongwiwat for patiently introducing me to the world of PCR primers and Gibson Assembly during my first year. I would also like to acknowledge Professor Hiroshi Hamana from the University of Toyama, Japan, for his advice on the TCR cloning vector.

Last, but not least, I would like to give my sincere and heartfelt thanks to all of my family members, old and new, for their continued support and prayers over the past few years. To my husband who has patiently supported me and reassured me through it all- thank you for having faith in me when I didn't have faith in myself to complete this PhD.

My biggest thanks and deepest gratitude go to my parents, who have always been an inspiration through their hard work and continued sacrifices for the whole family. Thank you for everything. Although I can never repay you for all of your sacrifices, I pray that I have made you proud. I dedicate this PhD to you both.

Abstract

Adoptive T-cell therapy has emerged as a powerful treatment for many cancers. T-cell receptor (TCR)-engineered T-cells are genetically modified to express full-length tumour-specific TCRs and have demonstrated encouraging results in the treatment of numerous solid cancers.

Here, I outline the development and validation of a highly accessible novel single TCR cloning platform. Using optimized TCR-specific PCR and cloning primers, and Gibson Assembly techniques, the streamlined platform allows efficient cloning of any TCR without expansion in culture. The platform clones TCR genes into a novel universal retroviral vector backbone for stable expression in target cells for crucial functional characterization, epitope mapping and MHC-restriction analysis.

The capability of the platform was demonstrated via identification and cloning of dominant TCRs specific to ZEBRA, a highly immunogenic lytic stage EBV antigen. These TCRs comprised up to 21% of sequences in two healthy donors and were successfully expressed in a TCR-deficient T-cell line and in primary T-cells. Transduced T-cells upregulated the early activation marker CD69 and secreted TNF- α and IFN- γ upon stimulation, demonstrating preserved functional ability of the cloned TCRs.

Characterization of a previously undiscovered TCR from one healthy donor revealed its curious ability to recognise antigen presented on two different autologous HLA alleles, HLA-A*02:01 and HLA-B*35:01. Such cross-reactivity to HLA molecules within the same donor has not been described in literature and may hold promise for T-cell therapy for patients carrying either, or both, HLA types. Moreover, functional studies suggested that ZEBRA-specific TCR-transduced primary T-cells could recognise and mediate killing of EBV-associated gastric carcinoma cells after virus latency reversal with HDAC inhibitors.

The data suggests that combination therapy comprising latency reversal agents to reactivate the lytic stage of EBV infection, followed by adoptive T-cell therapy with TCR-engineered T-cells specific to highly immunogenic lytic stage antigens, may be a promising novel approach to the treatment of EBV-associated malignancies.

Table of Contents

Declaration of Originality	2
Copyright Declaration	3
Acknowledgements	4
Abstract	5
List of Figures	10
List of Tables	12
Chapter 1: Introduction	13
1.1 T cells	14
1.1.1 T cell development and generation of T cell receptors	14
1.1.2 Organization, rearrangement and variability of the TCR- $\alpha\beta$ genes	15
1.1.3 T cell co-receptors and MHC molecules	20
1.1.4 T cell activation	21
1.1.5 CD8+ T cells	23
1.2 T cell-based Immunotherapies	26
1.2.1 Adoptive Cell Therapy using TILs	28
1.2.2 TCR Engineering and Gene Therapy	28
1.2.2.1 CAR-T cell therapy	29
1.2.2.2 TCR gene therapy	30
1.2.2.3 Strategies for Improvement of TCR gene therapy	31
1.2.2.4 Adoptive Cell Therapy for Virus-associated Cancers	31
1.3 Technologies for T cell repertoire analysis and TCR cloning	34
1.3.1 Bulk Methods	35
1.3.2 Single-Cell Methods	35
1.3.2.1 High-throughput methods for TCR repertoire analysis	36
1.3.2.2 Conventional single cell TCR sequencing and cloning	37
1.4 Epstein-Barr Virus	40
1.4.1 Pathobiology of EBV	40
1.4.2 The EBV ZEBRA protein and lytic cycle activation	44
1.4.3 The Immune response to EBV	45
1.4.3.1 The T cell response to primary EBV infection	45
1.4.3.2 The T cell response during persistent EBV infection	49
1.4.4 Latent EBV and tumorigenesis	50
1.4.4.1 EBV-associated Gastric Carcinoma	54
1.4.4.2 Molecular and cellular characteristics of EBVaGC	54
1.4.4.3 Approaches for the treatment of EBVaGC	55
1.4.4.3.1 EBV-specific Immunotherapy and Latency Reversal	56
1.5 Objectives, Aims and Hypothesis	59
Chapter 2: Materials and Methods	61
2.1 Materials used in this thesis	62
2.1.1 Antibodies	62
2.1.2 Vectors	62
2.1.3 HDAC Inhibitors	62
2.1.4 Cell Lines	63
2.2 Blood processing for isolation of PBMCs from healthy donors	64
2.2.1 Isolation of PBMC from whole blood by density gradient centrifugation	64
2.2.2 Counting cells using Trypan blue staining and light microscope	64

2.3	Identification and isolation of ZEBRA-specific CD8 ⁺ T cells	65
2.3.1	Screening of healthy donors for IFN- γ responses to EBV ZEBRA peptide pool	65
2.3.2	Peptide stimulation for detection of EBV ZEBRA-specific CD8 ⁺ T cells	66
2.3.3	IFN- γ Capture Assay	66
2.3.4	Staining and single cell sorting of IFN- γ positive CD8 ⁺ T cells	67
2.4	Single TCR Cloning	70
2.4.1	Overview	70
2.4.2	RT-PCR on single T cells	72
2.4.3	Second PCR of paired TCR $\alpha\beta$ sequences	76
2.4.4	Third PCR to introduce cloning sites	78
2.4.5	Agarose Gel Electrophoresis	80
2.4.6	Extraction and purification of TCR- α and - β PCR products	80
2.4.7	Sequencing of TCR genes	80
2.5	Constructing the vector backbone for TCR cloning	81
2.5.1	Vector Linearization	81
2.5.2	Preparation of the TCR constant genes	82
2.5.3	Cloning of the TRAC gene into the vector	84
2.6	Gibson assembly cloning of TCR genes	87
2.6.1	The Gibson assembly reaction	87
2.6.2	Transformation of Stable competent E coli	89
2.6.3	Preparation of Single Colony Starting Cultures	89
2.6.4	Extraction of Bacterial Plasmids and screening for correct inserts	89
2.6.5	Analysis of Sequencing Results and Production of Vector for Transfection	91
2.7	Generation of Retroviral particles	91
2.7.1	Transfection of PlatGP with retroviral vector	91
2.7.2	Transduction of PG13 retroviral packaging cells	92
2.7.3	Transduction of target T cells for expression of antigen-specific TCR	93
2.7.3.1	Transduction of a TCR-negative T cell line	93
2.7.3.2	Transduction of a primary T cells	93
2.8	Knockdown of endogenous TCRs	94
2.9	TCR functional assays	96
2.9.1	Generation of lymphoblastoid cell lines (B cell lines)	96
2.9.2	Peptide stimulation assays	97
2.10	Peptide epitope mapping	98
2.11	HLA-restriction assays	99
2.12	Measurement of secreted cytokines in supernatant	99
2.13	Cell viability assay to assess killing by TCR-transduced primary T cells	100
2.14	Culture of the gastric carcinoma cells AGS and OE19	102
2.15	Treatment of gastric carcinoma cells with HDACi	102
2.16	Assessing recognition and killing of HDACi-treated cells by primary T cell clones	103
2.17	Data analysis	104
Chapter 3: Establishment of a Single T cell Receptor Cloning Platform		105
3.1	Introduction	106
3.1.1	Chapter-specific aims	108
3.2	Optimization of single TCR cloning method	109
3.2.1	The 5'RACE PCR method	109

3.2.2	The Multiplex RT-PCR method for single TCR cloning	114
3.2.3	Design and verification of novel cloning primers	121
3.3	Proof of concept of our single TCR cloning platform	123
3.3.1	Screening PBMCs for IFN- γ responses to EBV ZEBRA antigen	123
3.3.2	Isolation and single-cell sorting of EBV ZEBRA-specific CD8 ⁺ T cells	125
3.4	PCR and sequencing of EBV ZEBRA-specific T cells	127
3.5	Construction of the TRAC_pMX-IRES-GFP retroviral vector	131
3.5.1	Gibson Assembly Cloning and screening of bacterial clones	134
3.6	Retroviral vector transfection and transduction of SKW3 cells	141
3.6.1	Expression of EBV-specific TCRs on SKW3 cells	143
3.6.2	Functional analysis of SKW3 TCR clones	146
3.7	Knockdown of endogenous TCRs	152
3.7.1	siRNA design and cloning	153
3.7.2	Knock-out of TCRs from Jurkat cells and Primary T cells	158
3.8	Discussion	161
3.8.1	Summary	161
3.8.2	Optimization of a single TCR cloning method	163
3.8.3	PCR and sequencing of EBV ZEBRA-specific T cells	165
3.8.4	Cloning and expression of EBV-specific T cells in SKW3 cells	167
3.8.5	Functional analysis of SKW3 TCR clones	168
3.8.6	Knock-down of endogenous TCRs via RNAi	169
3.8.7	Future work	170
Chapter 4: Characterization of EBV ZEBRA-specific T cell receptors		172
4.1	Introduction	173
4.1.1	Chapter-specific aims	174
4.2	Characterization of TCR4 from Donor 1	175
4.2.1	HLA restriction of TCR4	175
4.3	Epitope mapping of TCRs	177
4.4	Characterization of TCRs from Donor 2	185
4.5	Discussion	190
4.5.1	Summary	190
4.5.2	TCR4 recognizes two overlapping peptide epitopes presented on both HLA-A*02:01 and HLA-B*35:01	192
4.5.3	TCRs from donor 2 recognise various epitopes within the same peptide region of ZEBRA, presented on various HLA molecules	195
4.5.4	Clustering of ZEBRA-specific TCR epitopes	196
Chapter 5: Recognition of EBV-associated Gastric Carcinoma Cells by ZEBRA-specific TCRs		199
5.1	Introduction	200
5.1.1	Chapter-specific aims	202
5.2	HDACi treatment of EBV-associated gastric carcinoma cells	203
5.3	EBV-specific TCRs recognise ZEBRA peptide-pulsed gastric cells	211
5.4	EBV-specific TCRs recognise ZEBRA on HDACi-treated EBVaGC cells	213
5.5	Expression of EBV-specific TCRs in primary T cells	215
5.6	Recognition of exogenous ZEBRA antigen by primary T cells transduced with ZEBRA-specific TCRs	217

5.7	TCR-transduced primary T cells recognise HDACi-treated EBVaGC cells	221
5.8	Discussion	230
5.8.1	Summary	230
5.8.2	EBVaGC cells express lytic stage antigen ZEBRA after HDACi-treatment	230
5.8.3	EBV-specific SKW3 T cells recognise ZEBRA on HLA-matched gastric carcinoma cells	231
5.8.4	EBV-specific TCRs can be expressed in primary T cells and can recognise ZEBRA peptide-pulsed autologous B cells	232
5.8.5	TCR-transduced primary T cells recognise HDACi-treated EBVaGC cells and mediate killing	234
5.8.6	Future work	235
Chapter 6: Discussion		237
6.1	Results Summary	238
6.2	General Discussion	240
6.3	Future Directions	247
6.4	Final Conclusions	248
References		250
Appendices		278

List of Figures

Chapter 1

Figure 1. 1 Genomic Organization of the TCR Loci	17
Figure 1. 2 The TCR complex	19
Figure 1. 3 The Requirements of T cell activation	22
Figure 1. 4 Mechanisms of CTL-mediated killing.....	25
Figure 1. 5 Types of adoptive T cell therapy	27
Figure 1. 6 Structure and configuration of the EBV genome during latent and lytic states.....	41
Figure 1. 7 The EBV infection cycle and establishment of persistence.....	43
Figure 1. 8 The T cell response to EBV infection	48
Figure 1. 9 The latency types of EBV-associated cancers and their immunogenicity.....	52

Chapter 2

Figure 2. 1 Gating strategy for single-cell sorting of peptide-specific CD8 ⁺ T cells	69
Figure 2. 2 Overview of the single TCR cloning protocol.....	71
Figure 2. 3 Nucleotide sequences of codon-optimized constant gene fragments for construction of complete TCR vectors.....	83
Figure 2. 4 Overview of TCR vector backbone construction	85
Figure 2. 5 BamHI-Linearized TRAC_pMXs_IRES_GFP	86
Figure 2. 6 Representative calculations and workflow of the Gibson assembly reaction protocol.....	88

Chapter 3

Figure 3. 1 Schematic of 5'RACE PCR Method	110
Figure 3. 2 Agarose gel showing 5'RACE PCR products.....	111
Figure 3. 3 Partial TCR beta sequence obtained from 5'RACE PCR	112
Figure 3. 4 Amplification of TCR α and β genes from PBMCs and Jurkat cells.....	115
Figure 3. 5 Amplification of TCR α and β genes from Jurkat cells and primary T cells.....	117
Figure 3. 6 Jurkat cell TCR- α PCR product sequence alignment	118
Figure 3. 7 Jurkat cell TCR- β PCR product sequence alignment	119
Figure 3. 8 PCR efficiency of new cloning primers	122
Figure 3. 9 Screening of healthy donors via IFN- γ ELISpot for reactivity against EBV ZEBRA.....	124
Figure 3. 10 Gating strategy for single-cell sorting of peptide-specific CD8 ⁺ T cells.....	126
Figure 3. 11. Single EBV ZEBRA-specific TCR PCR products from TCR donors.....	128
Figure 3. 12 The pMX-IRES-GFP retroviral vector and ligation of the TRAC gene	132
Figure 3. 13 Schematic overview of Gibson Assembly method.....	136
Figure 3. 14 Schematic of Gibson Assembly of TCR α and β genes, P2A linker and vector.....	138
Figure 3. 15 Screening of Gibson Assembly product-transformed E. coli	140
Figure 3. 16 Transduction efficiency of PG13 cells	142
Figure 3. 17 Gating strategy to assess TCR expression on transduced SKW3 cells.....	144
Figure 3. 18 TCR expression on transduced SKW3 cells.....	145
Figure 3. 19 Representative gating to analyse CD69 expression on peptide-stimulated SKW3 clones	147
Figure 3. 20 Optimization of peptide stimulation time for SKW3-TCR4	148
Figure 3. 21 Upregulation of CD69 on SKW3 clones after peptide stimulation	150
Figure 3. 22 Secretion of cytokines IL-2, TNF- α and IFN- γ by SKW3 clones	151
Figure 3. 23 Alignment of wild type TCR β constant genes with codon-optimized TCR β constant gene and selection of target sequences	155
Figure 3. 24 Map of the pRFP_C_RS_shRNA vector	156
Figure 3. 25 Fluorescence microscope images confirming RFP vector transduction	157
Figure 3. 26 Knock-down of TCR in Jurkat cells and in primary T cells with siRNA	159
Figure 3. 27 Summary of Single TCR PCR workflow	162

Chapter 4

Figure 4. 1 Peptide pulsing of partially histocompatible BCLs to determine HLA-restriction of TCR4	176
Figure 4. 2 The 18mer epitope mapping of TCR4	179
Figure 4. 3 TCR4 recognizes two overlapping 11mers on both HLA*02:01 and HLA-B*35:01	182
Figure 4. 4 TCR4 does not recognise peptide presented on HLA-C*07:01	183
Figure 4. 5 HLA restriction mapping of TCRs from Donor 2	186
Figure 4. 6 Epitope mapping of donor 2 TCRs.....	188
Figure 4. 7 Clustered distribution of T cell epitopes within EBV ZEBRA antigen	197

Chapter 5

Figure 5. 1 The gating strategy for assessment of ZEBRA induction Vs toxicity post-HDACi treatment.....	205
Figure 5. 2 The effect of increasing doses of HDACi treatment on EBVaGC cells	206
Figure 5. 3 Assessment of ZEBRA induction in EBV-associated gastric carcinoma cells post-HDACi treatment	208
Figure 5. 4 Percentage of ZEBRA positive gastric carcinoma cells post-HDACi treatment.....	209
Figure 5. 5 CD69 upregulation on ZEBRA-specific SKW3 T cells post peptide-pulsing of gastric cells.....	212
Figure 5. 6 SKW3 T cell clones produce cytokines upon recognition of HDACi-induced ZEBRA on gastric carcinoma cells	214
Figure 5. 7 Transduction efficiency of primary T cells with TCR-encoding retrovirus	216
Figure 5. 8 Gating Strategy for B cell killing assay	218
Figure 5. 9 Killing of ZEBRA peptide-pulsed B cells by activated T cell clones	219
Figure 5. 10 Time course staining of HDACi-treated gastric cell death.....	223
Figure 5. 11 Specific interaction of HLA-matched T cells with HDACi-treated gastric cells is associated with cell death.....	224
Figure 5. 12 TCR4-transduced primary T cells kill HDACi-treated EBVaGC cells	225
Figure 5. 13 Donor 2 ZEBRA-specific primary T cell clones kill HDACi-treated OE19_rEBV cells.....	226
Figure 5. 14 ZEBRA-specific primary T cells secrete IL-2, IFN- γ and TNF- α in response to HDACi-treated gastric carcinoma cells.....	228

Chapter 6

Figure 6. 1 Summary of Single TCR Cloning Platform	239
--	-----

List of Tables

Chapter 2

Table 2. 1 Antibodies used in this thesis	62
Table 2. 2 Vectors used in this thesis.....	62
Table 2. 3 HDACi used in this thesis.....	62
Table 2. 4 Cell lines used in this thesis.....	63
Table 2. 5 Flow cytometry staining panel for single cell sorting of IFN- γ positive CD8 ⁺ T cells	67
Table 2. 6 RNase-inhibiting catch buffer reagents	67
Table 2. 7 RT-PCR primer mix	72
Table 2. 8 TCR- α RT-PCR Forward primers	73
Table 2. 9 TCR- β RT-PCR Forward primers	74
Table 2. 10 The RT-PCR reverse primers	75
Table 2. 11 The components of the RT-PCR mastermix	75
Table 2. 12 RT-PCR cycle conditions	75
Table 2. 13 Primers used in the 2nd PCR	76
Table 2. 14 The TCR- α 2nd PCR mastermix components	76
Table 2. 15 The TCR- β 2nd PCR mastermix components	77
Table 2. 16 Second PCR conditions	77
Table 2. 17. Third PCR/cloning primers.....	78
Table 2. 18 The components of the TCR- α 3rd-PCR mastermix.....	79
Table 2. 19 The components of the TCR- β 3rd-PCR mastermix.....	79
Table 2. 20 The 3rd-PCR conditions for both TCR- α and TCR- β genes.....	79
Table 2. 21 Overnight linearization reaction of pMX_IRES_GFP vector.....	81
Table 2. 22 Double restriction enzyme digest reaction of Gibson products	90
Table 2. 23 The primers used to sequence the Gibson assembly products	90
Table 2. 24 The oligonucleotide sequences for the construction of siRNA vectors	94
Table 2. 25 T cell clone activation status staining panel	98
Table 2. 26 HLA typing of TCR donors 1 and 2	99
Table 2. 27 BCL viability assay staining panel	100
Table 2. 28 HLA typing of donors 1 and 2, and of the gastric carcinoma cells.....	102

Chapter 3

Table 3. 1 TCR α and β genes sequenced from single-sorted primary T cells	120
Table 3. 2 The sequences of the original 3 rd PCR primers and our novel 3 rd PCR primers.....	121
Table 3. 3. Single EBV ZEBRA-specific TCRs from TCR Donor 1	129
Table 3. 4. Single EBV ZEBRA-specific TCR genes from TCR Donor 2	130
Table 3. 5 Gibson Assembly fragments and their overlapping sequences for TCR cloning.....	138
Table 3. 6 The siRNA oligonucleotides and their component sequences	156

Chapter 4

Table 4. 1 The HLA alleles of TCR Donor 1	175
Table 4. 2 The 18mer ZEBRA peptides in each pool	178
Table 4. 3 Summary of peptides recognised by TCR4 after presentation on autologous BCL	181
Table 4. 4 The HLA alleles of TCR Donor 2	185
Table 4. 5 Epitope (9mer) mapping of Donor 2 TCRs	189
Table 4. 6 Summarized characteristics of cloned EBV ZEBRA peptide-specific TCRs.....	191

Chapter 5

Table 5. 1 The HLA-A, -B and -C alleles of TCR Donors and the Gastric cell lines.....	203
---	-----

1 Introduction

1.1 T cells

The cells of the adaptive immune system can recognise specific details of pathogens owing to their enormous repertoire of receptors. These cells are the T and B lymphocytes, both of which originate from progenitor cells in the bone marrow. T cells migrate to the thymus in the form of thymocytes to complete their development. They are instrumental in orchestrating cell-mediated immunity, the central element of adaptive immunity, against intracellular pathogens (Abbas and Janeway, 2000, Parkin and Cohen, 2001, Janeway et al., 2005).

The adaptive immune response is not immediate and can take at least 5 days to become activated due to necessary priming and proliferation of naïve antigen-specific lymphocytes. Upon full activation however, its immense power can allow complete eradication of most infections. After elimination of the threat, T cells reduce in numbers, but a fraction remain as memory cells in circulation, allowing a faster and more robust antigen-specific response should the same pathogen be encountered again. Herein lies the concept of vaccination (Janeway, 2001), and the importance of immunotherapy and identification of antigens responsible for the induction of such powerful and long-lasting immune responses.

1.1.1 T cell development and generation of T cell receptors

Upon entering the thymus, thymocytes do not express any cell-surface molecules which distinguish them as T cells; they lack the molecules of the T-cell receptor (TCR) complex and the co-receptors CD4 and CD8, hence they are known as double-negative (DN) thymocytes. These DN thymocytes can commit to the majority $\alpha\beta$ -T cell lineage or the minority $\gamma\delta$ -T cell lineage (Egerton et al., 1990, Janeway, 2001). During development of $\alpha\beta$ -T cells in the thymus, initial activation of the RAG1/RAG2 genes leads to rearrangement of the TCR β -chain genes, resulting in a productive TCR β -chain. This TCR β -chain pairs with an invariant temporary pre-TCR α -chain, and this pre-TCR is expressed alongside CD3 molecules. This allows initial signalling, survival and increased cell proliferation, and the thymocyte begins to express both CD4 and CD8 co-receptors, thus leading to double positive (DP) thymocytes. The rearrangement of the TCR- α chain locus soon follows, and the first round of positive and negative selection of T cells begins; the DP thymocytes interact with epithelial cells in the thymus which express self-major histocompatibility complex (MHC) class I and II molecules (Sebzda et al., 1999). Whether the DP thymocytes survive depends on the levels of signalling

mediated by the recognition of these self-MHC molecules by the TCR. If the signalling mediated by the TCR is too strong or too weak, the T cells undergo negative selection in the form of apoptosis or anergy (Sebzda et al., 1999). Only those thymocytes whose TCRs can recognise self-MHC appropriately are allowed to survive, i.e. are positively selected, ensuring all T cells in the periphery can recognise self-MHC presenting peptides. DP thymocytes that are positively selected progress through the thymus and eventually lose either of their CD4 or CD8 molecules, depending on whether they recognised peptide on MHC class II or MHC class I, respectively. Those T cells that recognised peptide on MHC class I will retain only their CD8 molecule expression and develop into CD8⁺ CTLs. Those that recognised peptide on MHC class II will retain only their CD4 molecule expression and develop into CD4⁺ helper T cells (Teh et al., 1988, Kaye et al., 1989). It has been suggested that stronger TCR signalling leads to development of CD8⁺ T cells, whereas weaker signalling leads to CD4⁺ T cell development (Bommhardt et al., 1999).

The thymocyte is now single positive (SP) and progresses to the medulla, where the second round of positive and negative selection, known as central tolerance, takes place. Here, the TCRs interact with self-peptide-MHC complexes presented on epithelial cells and DC. Only those thymocytes whose TCRs produce an intermediate level of signalling upon recognition of self-peptides will survive and mature, resulting in positive selection and progression into mature T cells (von Boehmer et al., 1989, Zerrahn et al., 1997). Those T cells that recognise self-peptides with an affinity that is too high or too low undergo apoptosis. This induction of central tolerance is critical in limiting the risks of autoimmunity after the T cell leaves the thymus and enters the periphery (Abbas and Janeway, 2000).

T cells can be classed as $\alpha\beta$ -T cells or $\gamma\delta$ -T cells, depending on the types of chains present in the heterodimer of their TCR. In this thesis, the term TCR shall be used to refer to the $\alpha\beta$ -TCR only.

1.1.2 Organization, rearrangement and variability of the TCR- $\alpha\beta$ genes

Both the α and β chains of the TCR consist of a non-variable region known as the constant (C) region and a variable (V) region. The α and β chains are connected via an interchain disulphide bond in the C region, and extend into the lipid bilayer, anchoring the TCR onto the T cell membrane (Allison et al., 1982, Kappler et al., 1983, Lefranc and Lefranc, 2001a). In humans, the TCR- α (TRA) chain locus is situated on chromosome 14, whilst the locus for the TCR- β (TRB) chain is on chromosome 7 (Caccia et al., 1984, Collins et al., 1985).

The organisation of the human TRA and TRB gene loci are illustrated in Figure 1. 1. Each locus is composed of separate C, V, joining (J) gene segments, whilst addition diversity (D) gene segments are also present in the β chain locus. The TCR- α chain locus has approximately 40 functional V gene segments, each of which is associated with a preceding leader (L) sequence. Further along the locus are the TRA-Joining (TRAJ) gene segments, of which there are about 60, and a single TRA-Constant (TRAC) gene. The TRAC gene is composed of 4 separate exons, the first two of which encode the extracellular portions of the TRAC domain, and the remaining two of which encode the transmembrane domains (Janeway et al., 2005, Lefranc and Lefranc, 2001a).

The TCR- β (TRB) chain locus has approximately 45 V (TRBV) segments and their associated L sequences. The TRB locus has two separate clusters of gene segments; each of these TRB gene clusters is composed of a single TRBD segment, with either 6 or 7 TRB-Joining (TRBJ) gene segments, followed by one of two closely homologous TRB-Constant (TRBC) regions, TRBC1 or TRBC2 (Lefranc and Lefranc, 2001b, Janeway et al., 2005, Rowen et al., 1996).

The TCR chains are generated during T cell development in the thymus, via rearrangement of gene segments. In the TCR- α chain this occurs between the V and J gene segments, whereas rearrangement in the TCR- β chain also includes the D gene segments; a single V gene segment is joined to a single J gene segment, and the DNA between the two segments is removed. This recombined V-J gene creates the variable regions of the TCR chains, and after transcription this is then joined onto a single C gene to produce the respective TCR chain mRNA (Grawunder et al., 1998, Lefranc and Lefranc, 2001b, Roth, 2014, Turner et al., 2006).

During T cell development, the signal received through the pre-TCR inhibits further TCR- β gene rearrangement (Uematsu et al., 1988). However, the alleles of the TCR- α genes do not cease their rearrangement in this manner. Thus it is possible to observe T cells with two different types of TCR α chains, even if only one is expressed on the surface (Padovan et al., 1993).

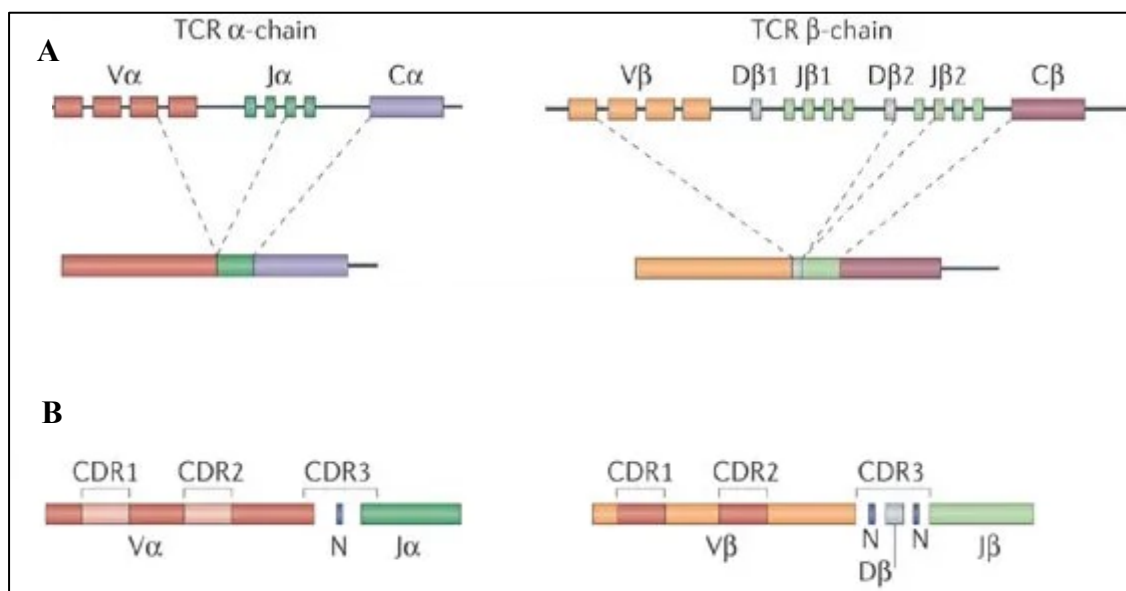


Figure 1. 1 Genomic Organization of the TCR Loci

- A) The human T Cell Receptor α and β chain loci are formed of several V, D and J gene segments which undergo rearrangement during T cell development. The TCR- α locus is formed of approximately 40 V gene segments and approximately 60 J gene segments, along with a single C gene. The TCR- β locus is formed of approximately 45 V gene segments and two separate clusters which each contain a single D gene, several J gene segments, and a C gene each.
- B) Complementarity-determining regions (CDRs) are regions of hypervariability within the TCR V regions; the use of different V α and V β genes create various CDR1 and CDR2 regions in each TCR, contributing to the diversity of the TCR repertoire. The CDR3 is the most variable region of the TCR and is composed of the recombined V(D)J genes, with additional diversity created through point mutations at the VDJ junctions. Image adapted from Turner et al., 2006.

Adjacent to the sites where VDJ gene segment recombination takes place, there are conserved non-coding DNA sequences which guide the process and are recognised by the enzymes involved, including RAG1/RAG2. These enzymes mediate breaks in the DNA sequence and allow exonuclease enzymes to remove nucleotides at the ends of the breaks, with new random nucleotides added via the enzyme terminal deoxynucleotidyl transferase (TdT). Finally, the newly modified ends of the DNA strand breaks are joined together by DNA ligase (Grawunder et al., 1998). Thus, in addition to the combinatorial diversity created through V(D)J gene segment rearrangement and the bringing together of different α and β chains, the modification of nucleotides between the joining regions creates junctional diversity, adding to the huge repertoire of TCR available for antigen recognition (Shinkai et al., 1992, Grawunder et al., 1998, Ramsden et al., 1994).

Variability of the TCR chains is particularly focussed in certain segments of the V regions, with three of these hypervariable (HV) regions being present in each chain, known as HV1, HV2 and HV3. When the α and β chains come together as a folded heterodimer, the HV domains from each chain are brought together and form the antigen binding site on the complete TCR molecule (Sun et al., 1995). The two HV1, HV2 and HV3 regions from the α and β chains form the CDR1, CDR2 and CDR3 regions in the folded TCR molecule, respectively (depicted schematically in Figure 1. 1b). The CDR1 and CDR2 regions make up the outer regions of the antigen-binding site and are made up of regions encoded by the V gene segments, thus they are non-variable and are referred to as “germline derived” (Garcia and Adams, 2005). This contrasts with the CDR3 loop, which is made up of regions encoded by the V, D and J gene segments, is highly variable and thus forms the centre of the antigen-recognition site. CDRs 1 and 2 are less variable and interact mainly with the MHC molecule during antigen presentation, whereas the highly variable CDR3 loop binds the specific peptide antigen as well as interacting with the presenting MHC molecule (Hennecke and Wiley, 2001, Janeway, 2001).

The combination of the gene rearrangement mechanisms described above lead to the formation of a large TCR repertoire diversity, with each TCR having a unique antigen specificity. The human periphery is estimated to contain up to 10^8 different TCRs (Arstila et al., 1999). Compatible TCR α and β chains come together after translation, fold in the correct conformation and fuse. This fusion occurs in the TRAC and TRBC regions via a disulphide bond that forms between cysteine residues on both chains. The TCR- $\alpha\beta$ heterodimer is then glycosylated and expressed on the cell surface membrane alongside CD3 molecules for signalling (Figure 1. 2) (Miles et al., 2011).

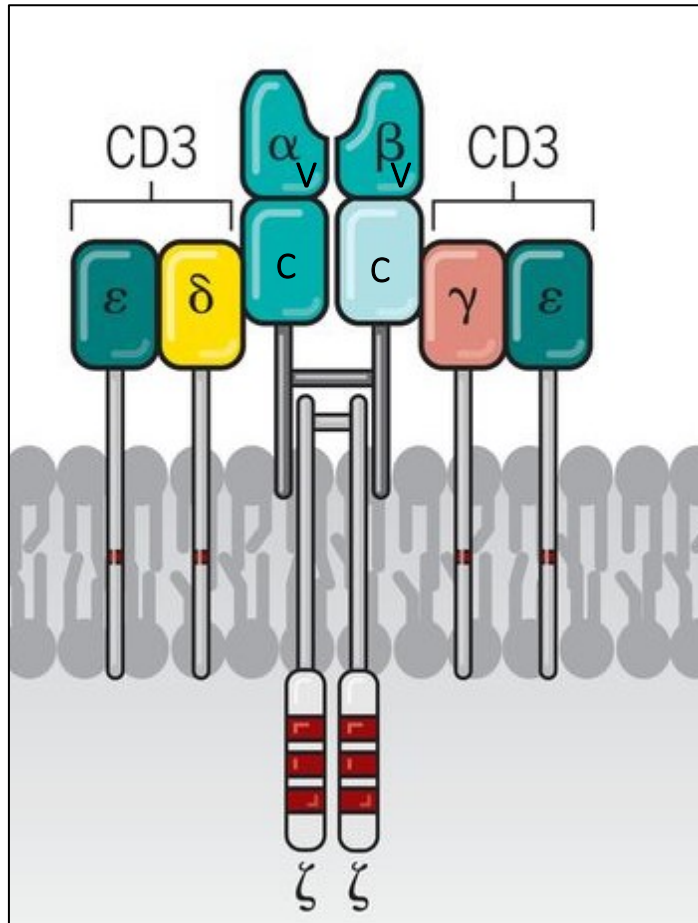


Figure 1. 2 The TCR complex

The TCR α and β chains are expressed in a complex with CD3 group of proteins and the ζ chains, which have Immunoreceptor Tyrosine-based Activation Motifs (ITAMs, in red) in their intracellular regions for intracellular signal conduction and T cell activation.

Figure taken from June et al., 2018, with permission from AAAS.

1.1.3 T cell co-receptors and MHC molecules

Although it can recognise minute details of the MHC and its presented peptide antigen, by itself the TCR heterodimer is inadequate for initiation of intracellular signalling within the T cell. The TCR is thus in a complex with several conserved signalling molecules including the CD3 family of proteins (made of one CD3 δ , one CD3 γ and two CD3 ϵ chains) and the TCR- ζ chain homodimers (Figure 1. 2) (Weiss and Littman, 1994, van der Merwe and Dushek, 2011). These signalling chains contain immunoreceptor tyrosine-based activation motifs (ITAMs) in their cytoplasmic tails. The ITAMs are phosphorylated during TCR binding to the correct pMHC complex, leading to a cascade of intracellular signalling events, discussed further in section 1.1.4 (Smith-Garvin et al., 2009).

There are two major categories of $\alpha\beta$ -T cells depending on the type of co-receptor they express; CD4⁺ or CD8⁺. Both co-receptors are cell-surface glycoproteins that associate closely with the TCR. They are known to enhance T cell recognition of pMHC complexes and augment T cell activation by 100-fold by binding to the conserved portions of their respective MHC molecule (Hennecke and Wiley, 2001, Rudolph et al., 2006).

Foreign antigen peptides presented on MHC molecules can be of two types; if they are derived from endosomal proteolysis of antigens, they are displayed on MHC Class II molecules on the APC surface and induce differentiation of CD4⁺ helper T cell subset. If the antigen has been derived from cytosolic degradation of intracellular pathogens such as viruses, they are processed and displayed on MHC Class I molecules of the infected cell, and induce activation of CD8⁺ cytotoxic T cells (Braciale et al., 1987).

MHC molecules are transmembrane proteins that bind antigen in grooves present in their extracellular domain. Class I MHC proteins have a closed groove that typically binds short peptides between 8-10 amino acids long (Matsumura et al., 1992). MHC Class II proteins possess a groove that is open at the ends and thus can bind longer peptides of between 13-20 amino acids (Wieczorek et al., 2017). The backbone of an MHC molecule is composed of amino acid residues that are relatively conserved, which is where the CD4 and CD8 co-receptors bind. In addition, there are clusters of polymorphic residues in and around the peptide-binding cleft, known as anchor residues, allowing the MHC molecules to accommodate the vast array of peptide antigens that they may be required to present (Hennecke and Wiley, 2001, Rudolph et al., 2006, van Bleek and Nathenson, 1991).

1.1.4 T cell activation

After development and successful positive selection, naïve T cells migrate out of the thymus and into the lymphoid organs. During infection, dendritic cells (DC) which have captured antigen from elsewhere in the body will also migrate to the lymphoid organs in search for the T cell that expresses the TCR specific for that antigen. In the periphery, the T cell is activated, beginning a rapid clonal expansion of identical antigen-specific T cells and creating a massive population of effector cells. After the threat has been cleared, the majority of these effector T cells die, but a small number remain as memory T cells, ready to rapidly expand again should the antigen be encountered again (Janeway, 2001).

There are stringent requirements for the successful activation of T cells, with three main signals needed (Figure 1. 3)(Gutcher and Becher, 2007). The first of these is the recognition of a specific peptide antigen displayed in the peptide-binding cleft of the MHC molecule; termed antigen specificity and MHC-restriction. MHC-restriction involves the recognition of polymorphic residues of the MHC molecules by residues in the CDR1 and CDR2 domains of the TCR- α chain (Rudolph et al., 2006). In parallel, the simultaneous binding of the CD4 or CD8 co-receptor to conserved residues in the MHC molecule must occur.

The second signal is the bringing together of the T cell and the antigen presenting cells (APC) such as DC, so that costimulatory molecules on the APC can interact with the receptors on the T cells (Smith-Garvin et al., 2009). The costimulatory molecule CD80/CD86 on the APC binds to CD28 on the T cell surface and delivers anti-apoptotic signals to the T cells, stimulating their activation and IL-2 production (Smith-Garvin et al., 2009). Other co-stimulatory molecules include 4-1BB (CD137) and CD27, the former is important in activation of CD8⁺ T cells, whereas the latter has been shown to be required in the development of T cell memory (Tan et al., 1999a, Hendriks et al., 2000).

The third signal needed for full T cell activation is the production of cytokines by the APC, which is influenced by the type of pathogen whose presence initiated the response, and in turn determines the subtype into which the naïve T cell will differentiate (Lenschow et al., 1996, Hennecke and Wiley, 2001, Huppa and Davis, 2003). The combination of all three activation signals leads the T cell to produce IL-2, whose autocrine action allows proliferation of the T cell and development into an effector cell.

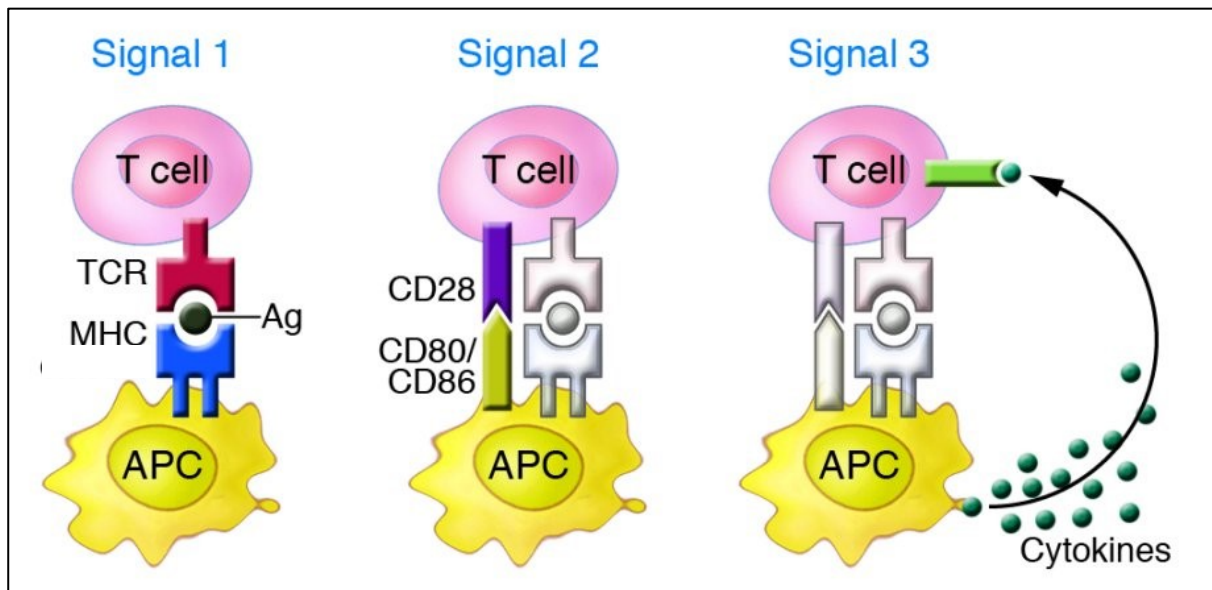


Figure 1. 3 The Requirements of T cell activation

Three signals are necessary for antigen-specific T cell activation; Signal 1 is the presentation of peptide in the context of a specific MHC molecule on the antigen presenting cell (APC), to the antigen-specific TCR.

Signal 2 is the binding of co-stimulatory molecules CD80/CD86 on the APC to CD28 on the T cell.

Signal 3 is the production of particular cytokines by the APC, which bind to cytokine receptors on the T cells and polarize them towards the relevant phenotype, e.g. Th1 cells in the context of viral infections.

Image taken from Gutcher and Becher, 2007.

There are several postulations regarding the manner in which TCR recognition of pMHC molecules on the cell surface can lead to biochemical changes in the intracytoplasmic regions of CD3, a process known as TCR triggering (van der Merwe and Dushek, 2011). Perhaps the most widely accepted model is the co-receptor heterodimerization model, in which the CD4 or CD8 co-receptor and its associated protein kinase, LCK, is brought in closer proximity to the TCR complex due to the co-receptor's interactions with the presenting MHC molecule. A CD45 molecule on the T cell surface is also brought near these molecules and its associated tyrosine phosphatase removes inhibitory phosphate groups. The phosphorylation of the CD3 ζ chains triggers activation of another protein kinase, ZAP-70, which can initiate the important signalling pathways that culminate in activation of transcription factors such as NF κ B and NFAT, leading to specific gene transcription, and finally T cell activation and differentiation (van der Merwe and Dushek, 2011, Janssen and Zhang, 2003).

1.1.5 CD8⁺ T cells

The type of effector cell that the naïve T cell differentiates into after activation depends firstly on the class of T cell; because CD4⁺ T cells recognise antigen from extracellular pathogens on MHC II molecules, they will differentiate into CD4⁺ helper T cells which secrete specific cytokines to assist other cells to achieve their effector functions (Nakayamada et al., 2012). CD8⁺ T cells on the other hand recognise antigen from intracellular pathogens presented on MHC Class I molecules and differentiate into cytotoxic T cells which can eliminate the infected cell (Andersen et al., 2006).

During an intracellular infection, such as a viral infection, the activation of innate immune cells triggers the production of IL-12 and IFN- γ by innate cells. During antigen presentation, this IL-12 acts as the third signal to allow naïve CD4⁺ T cells to differentiate into helper CD4⁺ Th1 cells which then provide cytokine help for the activation of CD8⁺ T cells (Nakayamada et al., 2012, Janeway, 2001).

Although CD8⁺ T cells can produce some cytokines, their main role is the elimination of infected or malignant host cells, thus they are known as cytotoxic T lymphocytes (CTLs) (Andersen et al., 2006). In addition to the recognition of specific antigen on MHC I of the target cell, and co-stimulatory molecule interaction from DC, CD4⁺ T cell-derived cytokines such as IL-2 and IFN- γ are also needed for the optimal activation of CTLs. For a CTL response with lasting immunological memory, CD4⁺ T cell help is indispensable (Janssen et al., 2003).

CTLs kill their target cells through a variety of different mechanisms (Figure 1. 4) (Andersen et al., 2006). At the point of contact between the CTL and the target cell, known as the immunological synapse (Grakoui et al., 1999), the activated CTL will rapidly release preformed granules which contain the effector proteins perforin and granzymes; perforin polymerises on the target cell membrane, forming pores through which granzymes are delivered directly into the target cell (Basu et al., 2016). These pores will either lyse the cell through osmosis, leading to a proinflammatory response to the cell death, or the granzymes will induce apoptosis through the activation of caspases (Lieberman et al., 2002, Andersen et al., 2006). CTLs can also kill through direct cell-to-cell contact; Fas ligand on the CTL can bind to the death receptor Fas on the target cell, activating intracellular pathways that lead to apoptosis in the target cell (Andersen et al., 2006). CTLs also secrete IFN- γ and TNF- α which contribute to the proinflammatory environment and recruitment and activation of phagocytes, in addition to induction of target cell death (Russell and Ley, 2002, Delves and Roitt, 2000).

After elimination of the intracellular pathogen, most of the activated CTLs die through apoptosis, but a minority (up to 10%) survive as CD45RO⁺ memory cells (Williams and Bevan, 2007). The memory T cells can be categorized as central memory (T_{CM}) and effector memory (T_{EM}) subtypes (Hamann et al., 1997, Sallusto et al., 2004). T_{CM} cells constitutively express CCR7 and CD62L, enabling them to home to the lymphoid organs in a similar manner to naïve T cells. These T_{CM} cells respond to antigen quicker than naïve T cells and do not require co-stimulation, allowing quick and effective functional response to secondary infections via production of cytokines (Sallusto et al., 2004). T_{EM} cells on the other hand do not express CCR7, nor do they always express CD62L. They are characterized by rapid effector function mediated by perforin and cytotoxic cytokine production. It is thought that in response to repeat encounter with a pathogen, T_{CM} cells home to lymphoid organs to quickly differentiate into effector cells, whereas T_{EM} cells remain at the original site of infection, ready to rapidly carry out their effector functions (Sallusto et al., 2004). Thus, T cell memory grants a much more rapid and effective response to secondary encounter with antigen, allowing faster elimination of the pathogen.

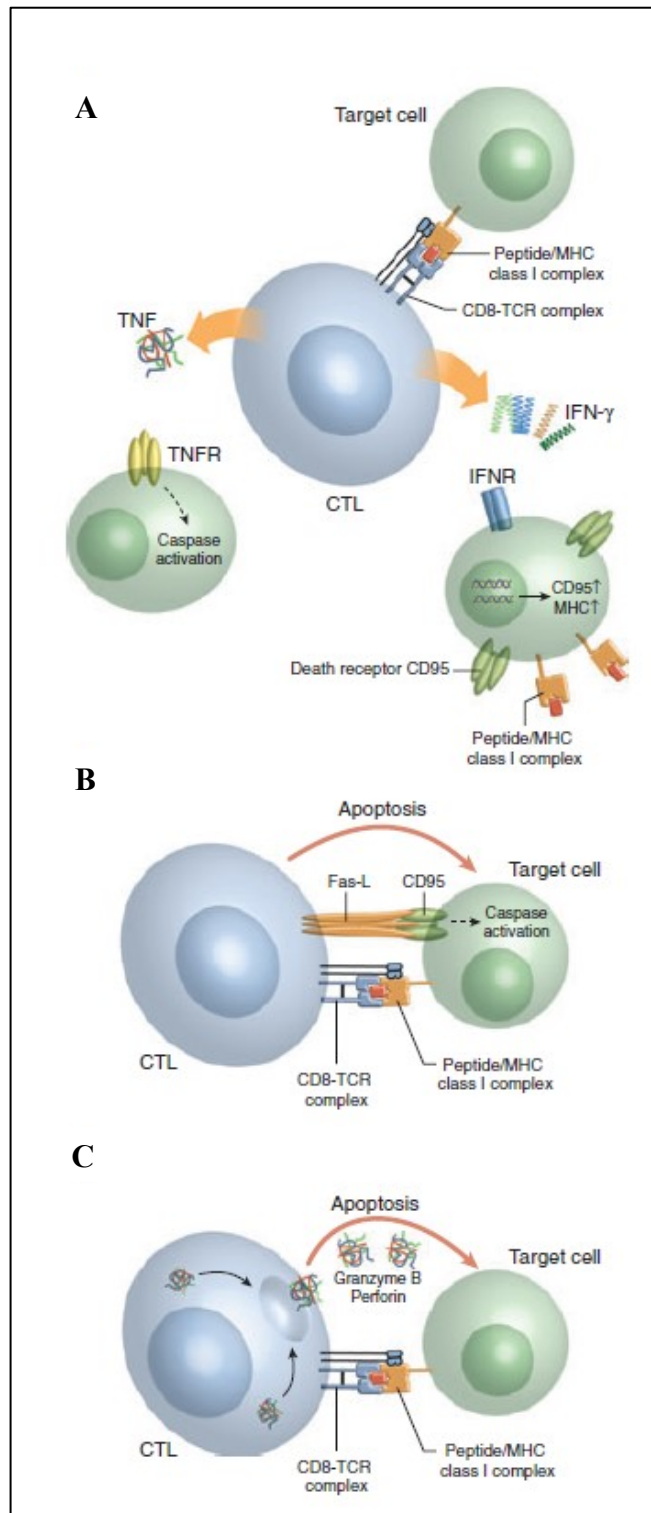


Figure 1. 4 Mechanisms of CTL-mediated killing

The mechanisms of killing by CTLs include (A) the release of the cytotoxic cytokines TNF- α and IFN- γ , (B) the direct induction of apoptosis in the target cell via binding of Fas-ligand to the death receptor Fas in the target cell, (C) the direct killing of the target cell through the release of perforin and granzyme B. Image taken from (Andersen et al., 2006)

1.2 T cell-based Immunotherapies

It is well known that the incidence rates of cancer are greater in immunosuppressed and immunodeficient individuals compared to those who are immunocompetent (Grulich et al., 2007, Duan and Grunebaum, 2018). In addition, the presence of tumour-infiltrating lymphocytes (TILs) correlates with good prognosis, and their therapeutic use has demonstrated great success (Zhao et al., 2019, Rosenberg et al., 1988, Rosenberg et al., 1994, Galon et al., 2006). Thus the role of the immune system in the prevention and elimination of cancer is well established.

The use of the immune system in the treatment of diseases is known as immunotherapy, and can be categorized broadly as adoptive cell therapy (ACT) and immune checkpoint blockade (Ribas and Wolchok, 2018, Morgan et al., 2006). Whilst the former utilizes the infusion of antigen-specific T cells into the patient to target the cancer cells, the latter uses antibodies that block immune checkpoints such as PD-1/PD-L1 and CTLA-4/CD80 interactions, thereby enhancing existing T cell responses against the target cells (Ribas and Wolchok, 2018).

ACT aims to reconstitute and enhance the immune system with effective, antigen-specific T cells. Early studies demonstrated ACT to be successful at treating advanced cancer in numerous patients (Rosenberg et al., 1988, Rosenberg et al., 1994, Dudley et al., 2002, Morgan et al., 2006). Currently there are three main approaches to ACT (Figure 1. 5); these include the transfer of ex-vivo expanded TILs obtained directly from patient tumours, and the infusion of genetically engineered T cells, either modified with specific full-length $\alpha\beta$ -TCRs or with chimeric antigen receptors (CAR) (June et al., 2015).

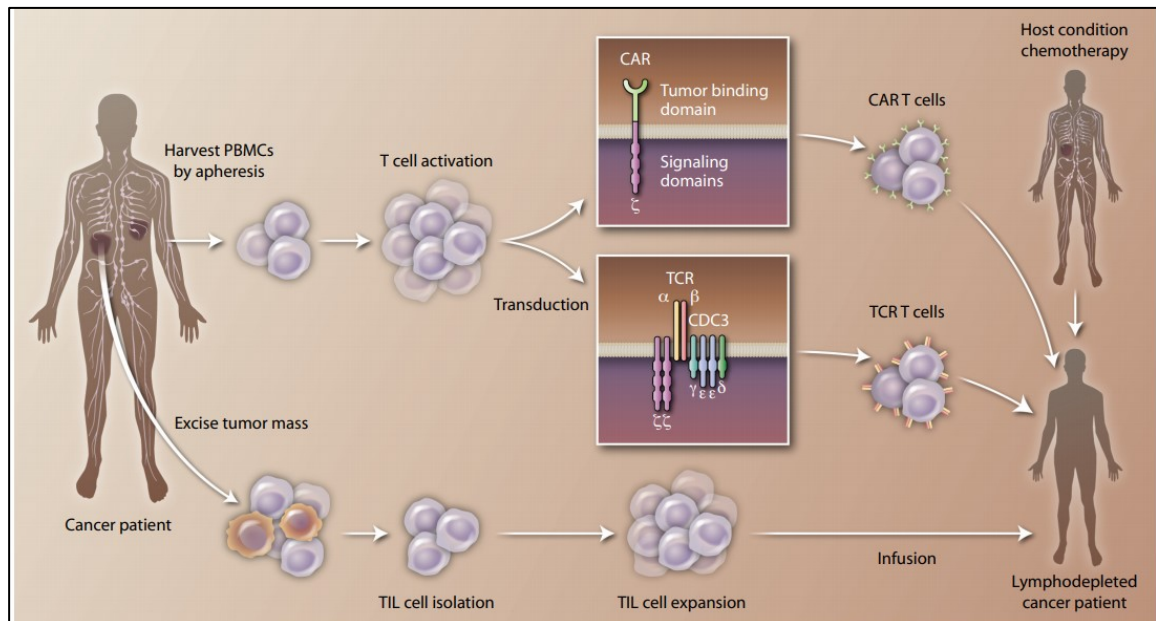


Figure 1. 5 Types of adoptive T cell therapy

Adoptive T cell therapy consists of obtaining T cells from the patient (through apheresis or tumour excision), followed by one of three approaches: the genetic modification of activated T cells via viral transduction of CAR or TCR, to produce CAR-T and TCR-T cells, respectively, or the ex-vivo expansion of TILs. The antigen-specific cells are infused back into the patient after lymphodepletion. CAR: chimeric antigen receptor, TIL: tumour-infiltrating lymphocyte.

Figure taken from (June et al., 2015), with permission from AAAS.

1.2.1 Adoptive Cell Therapy using TILs

In early studies, it was demonstrated that freshly extracted TILs could mediate specific lysis of autologous tumour cells, but that these effects were short lived (Rosenberg et al., 1988). Since this study, critical developments in TIL-ACT have been achieved, such as the prior depletion of existing lymphocytes and administration of exogenous IL-2 before re-infusion of *in vitro*-expanded TILs (Dudley et al., 2002). They have led to numerous reports of successful cancer regression, many without additional toxicities (Dudley et al., 2002, Kawakami et al., 1994, Hunder et al., 2008).

One of the benefits of using ex vivo-expanded TILs include the polyclonal nature of the cells; they may have specificity for different tumour antigens, some of which may be vital for tumour progression, thus mediating long term regression of the tumours (Lu et al., 2014). However, there are many obstacles in the use of TILs for the treatment of several cancers, including difficulties in identifying and isolating tumour-specific T cells from the patient, in obtaining a therapeutically useful number of tumour-specific T cells, and the lengthy ex vivo expansion times which can lead to terminally-differentiated T cells that have limited lifespan in vivo (Ping et al., 2018).

1.2.2 TCR Engineering and Gene Therapy

The obstacles associated with utilizing TILs can be overcome using TCR engineering technologies, which allow re-directing of T cell specificities through genetic modification. This alternative way of generating large numbers of tumour-specific cells consists of cloning antigen-specific $\alpha\beta$ -TCRs or the generation of CARs, which have the potential to be “off the shelf” treatments that can be universally used amongst patients. These technologies have demonstrated notable clinical outcomes in several different cancers, including melanoma, colon cancer, and myeloma (Morgan et al., 2006, Robbins et al., 2011, Rapoport et al., 2015, Parkhurst et al., 2011, June et al., 2015).

TCR engineering technologies often use viral vectors to deliver and express the target gene within the cell. They are a popular choice due to their simple genomes and ability to integrate into the target cell genome, allowing stable, long-term expression of the gene of interest (Barquinero et al., 2004). However there is an associated risk with the use of retroviral vectors due to their preferred sites of integration near promoter sites, which can lead to development of cancer (Sinn et al., 2005, Hacein-Bey-Abina et al., 2003). Another popular

vector type is the lentiviral vector, which has a lower chance of integration near promoter regions and is thus considered a relatively safer option for gene therapy (Trono, 2003). Alternatively, non-viral transposons have been shown to mediate highly efficient transfer of TCR genes to target cells and confer levels of antitumor activity that are comparable to retroviral vector systems (Peng et al., 2009, Chicaybam et al., 2013).

1.2.2.1 CAR-T cell therapy

A CAR incorporates an Ag-binding domain, often a single chain variable fragment from a specific antibody, linked via a hinged region to the transmembrane signalling domains of the CD3- ζ chain, and co-stimulatory domains from CD28 or CD137. Due to the presence of all of these necessary domains, the CAR molecule can redirect and fully activate the T cell after recognition of the specific surface antigen (Guedan et al., 2019, June et al., 2018). The use of the single chain variable fragment to recognise cell-surface antigens bypasses the requirement of antigen processing and presentation on MHC molecules (Gross et al., 1989).

The use of CARs has shown promising results in the treatment of previously hard to-treat B cell malignancies, and more recently in a solid tumour (Porter et al., 2015, Till et al., 2008, Park et al., 2018). In one clinical trial, infusion of autologous T cells transduced with an anti-CD19 CAR encoded by a lentiviral vector led to complete remission in 90% of patients with leukaemia (Maude et al., 2014). Following success of clinical trials, CAR-T cells that target CD19 have been recently approved in the by the US Food and Drug Administration (FDA) and the European Commission (EC) for the treatment of various forms of leukaemia (Guedan et al., 2019, June et al., 2015). In addition CAR-T cell treatment has recently been approved for use by the NHS in the UK, and is being used to treat certain B cell leukaemias.

One of the disadvantages associated with CAR-T cell therapy is the accompanying toxicity, which can often be greater than that seen with ACT using TILs or TCR-transduced cells (Kalos et al., 2011). Such toxic effects include severe cytokine release syndrome and neurological complications (Gust et al., 2017, Kalos et al., 2011, Maude et al., 2014). A major disadvantage is that despite great advances in treatment of haematological cancers, CAR-T cell therapy for solid tumours has not shown the same success. This is owing to several reasons, including the difficulties in finding the ideal target antigen; in contrast to B cell leukaemia which universally express CD19 on their surface, most solid tumours often express tumour associated antigens (TAAs) which may be enriched on the tumour but also present at lower levels on other non-cancerous cells. This significantly increases the risk of on-target off-tumour toxic effects and can be fatal (Morgan et al., 2010, Richman et al., 2018,

Garber, 2018). Although a fundamental advantage of CAR-T cells over conventional $\alpha\beta$ -TCR-bearing cells is that they are not compelled by MHC restriction, this feature is also a double-edged sword because the CARs cannot therefore recognise viral antigens which are processed and presented on the MHC of virus-associated cancer cells (Garrido et al., 1997). They can only recognise complete molecules on the cell surface, thus limiting their target range.

1.2.2.2 TCR gene therapy

TCR-transduced T cells (TCR-T cells) are genetically modified to express full-length $\alpha\beta$ -TCRs specific for any desired antigen. Unlike CAR-T cells, these TCR-engineered T cells have the benefits of recognising peptide antigens presented on MHC molecules, possessing their own native affinities and the ability to signal intracellularly to mediate effector functions. In order to generate these TCR-T cells, the antigen-specific cell is isolated and their TCR genes are cloned into retroviral vectors for transduction into primary T cells, allowing re-direction of the antigen-specificity of the T cell. This method has been used in numerous studies and has shown to be an efficient way to redirect specific antigen-reactivity of T cells (Clay et al., 1999, Hughes et al., 2005, Ahmadi et al., 2011). Such TCR-T cells have shown promising clinical responses in the treatment of solid cancers (Parkhurst et al., 2011, Robbins et al., 2011, Morgan et al., 2006, Rapoport et al., 2015, Dudley et al., 2002). Morgan et al first demonstrated that autologous T cells engineered to express MART-1-specific TCRs could mediate notable clinical responses in melanoma patients (Morgan et al., 2006). After treatment of 31 patients with the TCR-T cells, an objective regression of metastatic melanoma was seen in four patients (13%). In addition, adverse melanocyte toxicity was not observed in any patient, and the engineered cells persisted 1 year after infusion in two patients in whom regression of metastatic lesions were seen (Morgan et al., 2006).

Varying levels of success of using TCR-engineered T cells has also been demonstrated against other cancers, including in esophageal cancer, multiple myeloma and synovial cell sarcoma (Rapoport et al., 2015, Robbins et al., 2015, Robbins et al., 2011, Kageyama et al., 2015). Moreover, an affinity enhanced T-cell therapy targeting NY-ESO-1 showed promising clinical results and was approved by the FDA in early 2016 for use in synovial sarcoma patients (Stadtmauer et al., 2019).

However, alongside the great progress in ACT with TCR-engineered T cells, there have been reports of severe adverse effects in some studies. The use of modified, higher-affinity TCRs

against tumour-associated antigens has led to systemic toxicity and even fatalities due to cross-reactivity between the affinity-enhanced TCRs and healthy cells (Johnson et al., 2009, Parkhurst et al., 2011, Linette et al., 2013, Morgan et al., 2013). These studies demonstrate not only the severe dangers of manipulating antigen-specific TCRs by interfering with the fine-tuning of physiological tolerance mechanisms, but also the potential risks associated with utilizing TCRs that target self-antigens which are expressed on healthy cells as well as target cells.

1.2.2.3 Strategies for Improvement of TCR gene therapy

CAR-T cell therapy has largely overshadowed TCR-engineered T cells due to its success against B cell leukaemia. Other reasons for the rapid advancement of CAR-T therapy over TCR-engineered T cells may be due to problems associated with the introduction of transgenic TCRs into primary T cells. Firstly, the existence of the endogenous TCRs hampers the expression levels of the transgenic heterodimeric TCRs due to competition between them for binding with CD3, which has been shown to limit transgenic TCR expression (Ahmadi et al., 2011). Secondly, and more importantly, there is a risk of mispairing between the chains of the endogenous and transgenic TCRs creating mixed dimers and posing the risk of potentially dangerous TCRs which can lead to fatal autoimmunity (van Loenen et al., 2010, Bendle et al., 2010).

Several strategies have been explored by groups to overcome these problems. These include the addition of non-native cysteine residues within the transduced TCR chains to improve their pairing via additional disulphide bonds, the use of murine constant genes to generate hybrid TCRs, and codon optimization to enhance transduced TCR expression (Cohen et al., 2007, Cohen et al., 2006, Scholten et al., 2006). Another approach is the genomic knockout or knockdown of the endogenous TCR at the RNA level (Bunse et al., 2014, Provasi et al., 2012). This disruption of endogenous TCR expression involves various methods including the use of short-interfering RNA (siRNA,) CRISPR-Cas9 or TALENs, all targeting the constant genes of the TCR α or β genes and reducing their transcription or translation (Bunse et al., 2014, Ochi et al., 2011, Knipping et al., 2017, Legut et al., 2018).

1.2.2.4 Adoptive Cell Therapy for Virus-associated Cancers

In contrast to targeting tumour-associated antigens using ACT, a promising alternative in the treatment of virus-associated cancers is the targeting of viral antigens themselves. Using

virus-specific T cells (VSTs) in ACT against viral infections is attractive because they can distinguish between infected and non-infected cells. ACT using VSTs has shown durable clinical responses against several virus-associated cancers (Riddell et al., 1992, Ma et al., 2015, Stevanovic et al., 2015).

In the context of chronic Epstein-Barr Virus (EBV) infection, many groups have shown the feasibility and safety of using EBV-specific T cells (EBVSTs) as an efficient way to treat EBV-related cancers in transplant patients, with the VSTs shown to persist for up to 6 years (Sun et al., 2002, Barker et al., 2010, Heslop et al., 1996, Rooney et al., 1995). Haque and colleagues demonstrated successful use of EBVSTs to treat post-transplantation lymphoproliferative disease (PTLD), a common complication of solid organ transplants and bone marrow transplants (Haque et al., 2002). Subsequently, in a larger study, the group reported favourable clinical responses in over 50% of patients six months after treatment, with 14 out of 33 PTLN patients achieving complete remission (Haque et al., 2007).

Notably, these studies used EBVSTs from partially HLA-matched healthy donors from a frozen bank of CTLs, and reported no GVHD, demonstrating that using partially HLA-matched allogenic VSTs is safe, effective and potentially more efficient than expanding autologous T cells (Haque et al., 2002).

Furthermore, Bollard and colleagues treated 14 EBV-positive Hodgkin's disease patients with EBVSTs, reporting successful expansion and trafficking of cells to tumour sites, and decrease in viral load. Five patients had sustained remission after 40 months of treatment (Bollard et al., 2004).

In comparison to EBV-positive B cell lymphomas, few studies have reported using EBVSTs in the context of EBV-associated epithelial cancers. In a study by Straathof et al, 4 out of 10 nasopharyngeal carcinoma (NPC) patients had clinical remissions after treatment with EBVSTs (Straathof et al., 2005). Others have explored the possibility of ACT for EBV-associated epithelial cancers in pre-clinical studies (Cho et al., 2018, Lee et al., 2000, Orentas et al., 2001). One of the reasons for this disparity is likely to be the relative types of EBV latency expressed by the different cancers, which dictate their levels of immunogenicity (Moosmann et al., 2010, Khanna et al., 1999, Saiki et al., 1996). Although EBV-associated gastric carcinoma (EBVaGC) is one of the least immunogenic, expressing only the EBNA-1 antigen, the tumours are known to be infiltrated with TILs whose presence is associated with better prognosis compared to EBV-negative gastric carcinoma (Iizasa et al., 2012, Grogg et al., 2003, Kang et al., 2016, Saiki et al., 1996). However, EBVaGC cells are known to express high levels of PD-L1, and the surrounding TILs have been shown to be PD-1

positive, thus suggesting a major mechanism of cancer escape and progression via mediation of exhaustion of infiltrating T cells (Sasaki et al., 2019, Crescenzi et al., 2017). Although ACT has been explored as a potential treatment for gastric cancer and shown positive clinical outcomes, there are no reports of ACT being used to specifically target EBVaGC (Zhang et al., 2015, Han et al., 2018). Therefore, ACT of engineered EBV-specific T cells may be an avenue which should be explored for the immunotherapy of EBVaGC.

1.3 Technologies for T cell repertoire analysis and TCR cloning

As discussed above, TCR-engineering technologies for adoptive therapies offer several advantages compared to *ex vivo* expansion of naturally-occurring autologous or donor T cells. Engineering the T cells allows the precise selection of cells bearing antigen-specific TCRs which are most suitable and effective in their function, and allows rapid production of large numbers of specific T cell clones for infusion (Sadelain et al., 2017).

For the identification and selection of the most potent TCRs, the TCR repertoire needs to be analysed within a given population of T cells. TCR sequences which are polyclonal, i.e. identical CDR3 sequences that are found in more than one T cell, indicate polyclonal expansion in response to the same antigen epitope. Thus the most frequent, or most dominant, TCRs may be effective in the immune response against that antigen (Chen et al., 2012, Abdel-Hakeem et al., 2017, Callan et al., 1996). Identification and isolation of these dominant TCRs can allow them to be cloned and their functions to be analysed, leading to development of potential immunotherapies (Durgeau et al., 2018). To this end, several methods of TCR repertoire analysis and cloning have been described, each having their own advantages and draw-backs.

Traditional methods of TCR cloning involve expansion of the Ag-specific T cells in culture, which is not only time-consuming but can lead to bias through loss of certain T cell clones or selective outgrowth of others, in addition to terminal differentiation of T cells (Heslop et al., 1996, Linnemann et al., 2013). In addition, they often involve the use of tetramers for selection and enrichment of expanded clones, which requires prior knowledge of the TCR, or epitope and MHC restriction (Trautmann et al., 2005). Although this is useful for TCRs which are already well-characterized, it is not a viable option for studies where the TCR of interest is unknown.

Conventional antibody-based methods for the analysis of the TCR repertoire include flow cytometry and more recently, CyTOF (Faint et al., 1999, Lin and Maecker, 2018). Although they are rapid, they are limited by the lack of available antibodies against all TCR variable genes, and by their inability to provide specific information about the CDR3 regions of the TCR.

The most effective methods for the sequencing and cloning of TCRs are molecular techniques that avoid long term expansion of antigen-specific T cells in culture and use PCR to specifically amplify the T cell DNA prior to sequencing. They can be broadly classed as

bulk methods, where several thousand T cells are analysed in parallel, or as single-cell methods (Han et al., 2014, Hamana et al., 2016, Freeman et al., 2009). Although they each have their own advantages and draw-backs, their selection depends on the intended individual objectives of each study.

1.3.1 Bulk Methods

Recent powerful high-throughput next generation (NGS) sequencing methods used to study and compare TCR diversity often employ the use of bulk sequencing of pooled T cell populations. They involve the amplification of sequences, whether from RNA or DNA, from thousands of TCRs simultaneously in a single reaction, followed by their reading in the one sample to create a TCR library. Such RNA and DNA-based bulk T cell sequencing methods are valuable for the purposes of characterizing T cell clonality and identifying antigen-specific TCRs, however they often require the use of advanced, outsourced high-throughput technology (Linnemann et al., 2013, Gong et al., 2017, Howie et al., 2015). Moreover, they cannot rapidly produce ready-to-express TCRs for cloning and functional characterization without additional costs and time. Crucially, many bulk methods cannot easily provide information about the pairing of the TCR α and β chains from a specific T cell, impairing the ability to fully understand the complex characteristics of the whole TCR. Several studies have focused on characterization of only the TCR β repertoire as it has a higher combinatorial potential relative to the TCR α chain due to its additional D gene (Costa et al., 2015, Alves Sousa et al., 2019, Becattini et al., 2015). In addition, a T cell possesses only a single productively rearranged β chain gene whilst this is not the case for the α chain gene; both α alleles continue to rearrange until positive selection, so two potential α chains can be expressed in a large fraction of $\alpha\beta$ -T cells (Padovan et al., 1993). Thus, the TCR β repertoire has often been considered to represent diversity in the T cell repertoire (Li et al., 2015, Freeman et al., 2009). However, both the TCR α and β chains must be identified in order to reconstitute the complete TCR for functional analysis, for use in therapy and for antigen-binding studies. With many bulk sequencing methods, the α and β pair of the TCR of interest must be determined using DNA barcoding or complicated statistical analysis, which is often impractical and inaccessible for in-house methods (Han et al., 2014, Howie et al., 2015).

1.3.2 Single-Cell Methods

Single-cell methods of TCR sequencing enable convenient and direct pairing of both the α and β chains of the TCR. This allows determination of the antigenic specificity of the TCR,

in addition to providing information about clonal relationships when analysing large repertoires of T cells. They can be broadly categorized into high-throughput NGS-based technologies, and lower-throughput conventional sequencing-based methods, each of which have their own advantages and caveats.

1.3.2.1 High-throughput methods for TCR repertoire analysis

Several high-throughput single cell methods have recently been described, some of which have combined the ability to not only describe the paired CDR3 sequences of TCRs, but also link them to phenotypic characteristics, reveal ancestry between clones, and determine antigen-specificities (Stubington et al., 2016, Han et al., 2014, Hu et al., 2018, Munson et al., 2016). Han et al sought to devise a novel method which could integrate a single TCR sequence with information about the T cell function within a heterogeneous population (Han et al., 2014). This is important as different T cells which possess the same TCR can have distinct functions, thus linking this information can enable identification of cells which have undergone clonal expansion, and which cells display plasticity and have changed their functional phenotype. This clever methodology involves the use of many primers against all known human TCR genes, and many more primers specific for CD4+ T cell transcription factors and proinflammatory and inhibitory cytokines. Individual barcodes are incorporated into each PCR product in order to link the α and β TCR chains. The barcode is a short sequence of nucleotides which is added to each unique cDNA, enabling the transcripts to be traced back to their original cell. The resulting sequences demonstrated extremely high success rates; productive TCR β sequences were obtained in up to 92% of wells, one of the most efficient described in literature to date. In addition, the fact that the method uses deep sequencing enabled the detection of multiple TCR α sequences from one T cell, whereas traditional Sanger sequencing cannot easily do this. This innovative technique can cleverly link TCR sequences with the cell's phenotype without the need for lengthy expansion, laborious manual purification and time-consuming functional studies. However although the authors claim that the method retains information about the TCR pair so that it can be expressed for functional studies, this is very difficult as their RT-PCR primers flank only the CDR3 region of the TCR genes, excluding the amplification of the CDR1 and CDR2 regions which are necessary for correct MHC binding and influence the affinity of the binding of the TCR (Chlewicki et al., 2005). Thus, because their primers do not capture the entire length of the TCR sequence, the product cannot be used directly for functional studies without further steps to produce the full length TCR sequence. This drawback was addressed recently in a

method whereby the latter primers were used to design a cloning and expression system for assessment of specificity of antigens (Hu et al., 2018). Hu and colleagues created a library of vectors containing all the known TCR α and β variable genes alongside the constant gene and cloned in the CDR3 regions obtained from antigen specific T cells, before transferring this into a retroviral vector for expression in TCR-deficient Jurkat reporter cells which had been modified to express luciferase activity after TCR activation. The reporter cells could then be used to rapidly assess the antigen specificity of the transduced TCRs through luciferase expression, IL-2 or CD69 upregulation. Although this method combines high-throughput single TCR sequencing and TCR cloning and expression for functional characterization, it is still relatively lengthy compared to other cloning methods due to the extensive subcloning steps. Owing to this, it is impractical and highly laborious, and although the authors claim it is a controlled system whereby the avidity of the TCRs for their peptides can also be determined, this will depend on various factors such as the level of expression of the different TCRs on the reporter cells, and the level of expression of the HLA molecules on the antigen-presenting cells.

A computational method by Stubbington et al, named TraCeR, found several antigen-specific cells which shared the same TCR β sequence but had different TCR α sequences (Stubbington et al., 2016). The finding highlights that paired TCR- $\alpha\beta$ sequencing is especially important when analysing T cell repertoires as the existence of two TCR chain recombinants can mean that the TCR- $\alpha\beta$ pair can change, and that analysing just the TCR β sequence as others have done is not an adequate representation of T cell clonality.

1.3.2.2 Conventional single cell TCR sequencing and cloning

High throughput NGS-based methods of TCR sequencing and repertoire analysis, whether involving bulk or single cells, are highly efficient with respect to the sequencing and analysis of a large number of T cells simultaneously. Although they are able to provide information about the clonality of T cells in a given population, and possibly their basic functional phenotypes and antigen-specificity, they are costly and cannot produce full-length TCR genes which can be easily cloned for functional assays. In contrast, conventional TCR sequencing and cloning technologies involving amplification of the TCR from a single cell cDNA, although low throughput and laborious in comparison, are highly practical and can produce libraries of correctly paired TCR genes which can be conveniently expressed in target cell lines (Hamana et al., 2016, Simon et al., 2014, Guo et al., 2016). In addition, they are popular due to their low overall cost and accessibility. Although they lead to only a tiny fraction of the

overall TCR repertoire being discovered due to the smaller number of cells analysed at once, these convenient methods are necessary for their application in cloning antigen-specific TCRs for expression and full functional characterization. Such methods encompass single cell approaches that allow the simple pairing of TCR α and β chain sequences without the need for complicated computational protocols and extensive artificial gene synthesis for later cloning. These conventional single cell methods can be broadly grouped into two main approaches, both of which present advantages and drawbacks; multiplex PCR methods that use several different primers for all the known TCR variable region genes, and single-primer methods such as Rapid Amplification of cDNA Ends (RACE) PCR which uses only a single primer against the known TCR constant.

The use of a single TCR constant gene-specific primer is a convenient approach in which the TCR RNA is reverse transcribed using a single primer specific to the constant gene of both the TCR α and β chains, and has been adopted by several groups whilst amplifying TCRs (Kobayashi et al., 2013, Sun et al., 2012, Simon et al., 2014, Wälchli et al., 2011).

Kobayashi et al described an elegant method which they referred to as “human TCR efficient cloning within 10 days” or hTEC10 (Kobayashi et al., 2013). Their approach involved the production of TCR cDNA from the RNA of an antigen-specific T cell using a single reverse primer specific to TCR α and β constant region genes. This is a RACE -PCR, whereby an mRNA template is amplified between the known constant region gene and the unknown variable region gene. The method described by Kobayashi and colleagues is elegant and simple. Its simplicity lies in its use of universal primers which can be used to amplify any TCR regardless of the sequence, without the need for several V-region specific primers which would need lengthy optimisation. However, it is not the most efficient method of TCR amplification and cloning for several reasons; firstly, the products obtained through the PCR are not full length TCRs owing to the semi-nested nature of the PCRs, and secondly these PCR products must be sequenced and subjected to further PCRs to incorporate cloning sites (Kobayashi et al., 2013). The additional steps would add more time to the 10 days specified by the authors, in addition to the fact that the cells must be expanded for two days to aid the detection of antigen-specific T cells. A major failing of this method however is that the TCR sequences obtained can be incomplete, missing part or all of the V-region gene. This is due to incomplete reverse transcription in the first stage of the RACE PCR, and the authors later acknowledged that this rendered this RACE- PCR method highly flawed (Hamana et al., 2016). Thus, although the use of RACE-PCR bypasses the need for multiple primers to amplify the variable regions of unknown TCR sequences, this method of TCR cloning is not

always successful or efficient when expanding and cloning TCRs from single cells for functional characterization (Hamana et al., 2016, Kobayashi et al., 2013).

A popular alternative to RACE-PCR is the multiplex PCR method to amplify TCRs (Dash et al., 2011, Hamana et al., 2016, Shitaoka et al., 2018, Sun et al., 2012). This involves the direct amplification of cDNA from T cells using a set of primers which anneal to all the known variable region genes for TCR α and β genes. This can entail up to 50 primers each for α and β but ensures that every possible TCR can be amplified from the variable region through to the constant region. One of the limitations of many existing methods of multiplex PCR for TCR amplification however is that the primers used only amplify the CDR3 region (Kim et al., 2012, Guo et al., 2016). These methods mainly utilize the TCR sequences obtained for repertoire analysis purposes and are therefore unsuitable for cloning full-length TCRs for functional analysis. A fast and efficient method to screen and clone full-length, paired TCR α and β genes from single Ag-specific T cells was described by Hamana et al (Hamana et al., 2016). The group reported that TCR $\alpha\beta$ pairs were amplified from over 80% of cells, demonstrating the high efficiency of the PCR method. They applied this PCR method to amplify EBV-specific TCRs and expressed them in a luciferase reporter cell line to analyse their specificity and function. The authors bypassed the traditional method of cloning the TCR genes into retroviral vectors for stable expression in the target cell line as this is lengthy (Hamana et al., 2016). Instead they transformed the PCR products into transcriptionally active PCR (TAP) fragments which could be directly transfected into the luciferase reporter cell line for screening. This effective method can be used to rapidly clone, express and functionally analyse TCRs from single cells within just a week. The reported rate of amplification of the TCR pairs is excellent (>80%), and although the use of so many primers may be difficult to optimise, the production of full length TCRs is ideal for cloning purposes. Furthermore, the use of the TAP fragments and reporter cells is a clever way to rapidly express the TCRs and screen them using luciferase activity, saving weeks of time compared to producing retrovirus particles for transduction before functional screening (Cooray et al., 2012, Parente-Pereira et al., 2014). However, this is only suitable for rapid screening purposes and not direct killing assays as the TCRs are expressed in HEK293T cells and not a T cell line. Thus, although this may be a rapid and efficient method to clone and screen antigen-specific T cells, it is neither suitable for the purpose of characterizing the full potential of T cells bearing the transduced TCR, nor for direct use in immunotherapy as the TAP products cannot be transduced stably into primary T cells from patients.

Thus, there are several advantages and limitations associated with each TCR cloning method, and the selection of a suitable method will depend on the specific requirements of each study.

1.4 Epstein-Barr Virus

Epstein-Barr Virus (EBV, also known as human herpesvirus 4) was first discovered in tissue from Burkitt's lymphoma in the 1960s and has since been shown to be the cause of several lymphomas and carcinomas (Epstein, 2012, Cohen, 2000). Initial infection often occurs during childhood and does not cause any notable clinical symptoms (Fleisher et al., 1979). However, if primary infection occurs during adolescence or adult life, infectious mononucleosis (IM) occurs, which is characterized by acute fever, pharyngitis and swollen lymph nodes (Sprunt and Evans, 1920). Resolution of infection leads to latent, persistent infection within B cells (Thorley-Lawson et al., 2013). EBV is the most common persistent virus infection in humans, with 95% of the world's adult population being asymptomatic life-long carriers (Tzellos and Farrell, 2012). The persistent nature of EBV is attributable to some of its main characteristics, including attainment of latent infection in B cells and its ability to evade recognition and elimination by the immune system. Latent EBV infection is associated with different types of B cell cancers such as Burkitt's lymphoma, and post-transplantation related lymphomas. EBV is also associated with epithelial cancers such as nasopharyngeal carcinoma and a certain subtype of gastric carcinoma (Neparidze and Lacy, 2014). Annually, there are over 140,000 deaths from EBV-associated malignancies globally (Khan and Hashim, 2014), thus the virus is an important target for cancer prevention, therapy and vaccine design.

1.4.1 Pathobiology of EBV

The structure of EBV consists of a double stranded DNA genome surrounded by a nucleocapsid, which is itself encased by the viral envelope consisting of glycoproteins (Cohen, 2000). The genome of EBV encodes over 80 genes, and exists in a linear form within the replicating virus, but as a circular episome within the nucleus of the latently-infected cell (Baer et al., 1984, Lindahl et al., 1976). The structure and configuration of EBV DNA during its latent circular form, and lytic linear form is shown in Figure 1. 6. The EBV DNA can be digested by the restriction enzyme BamHI, producing several fragments of varying sizes, classified as A to Z. The designation of the translatable genes is based on these fragments; for example, the gene BZLF1 is within in the BamHI "Z" fragment.

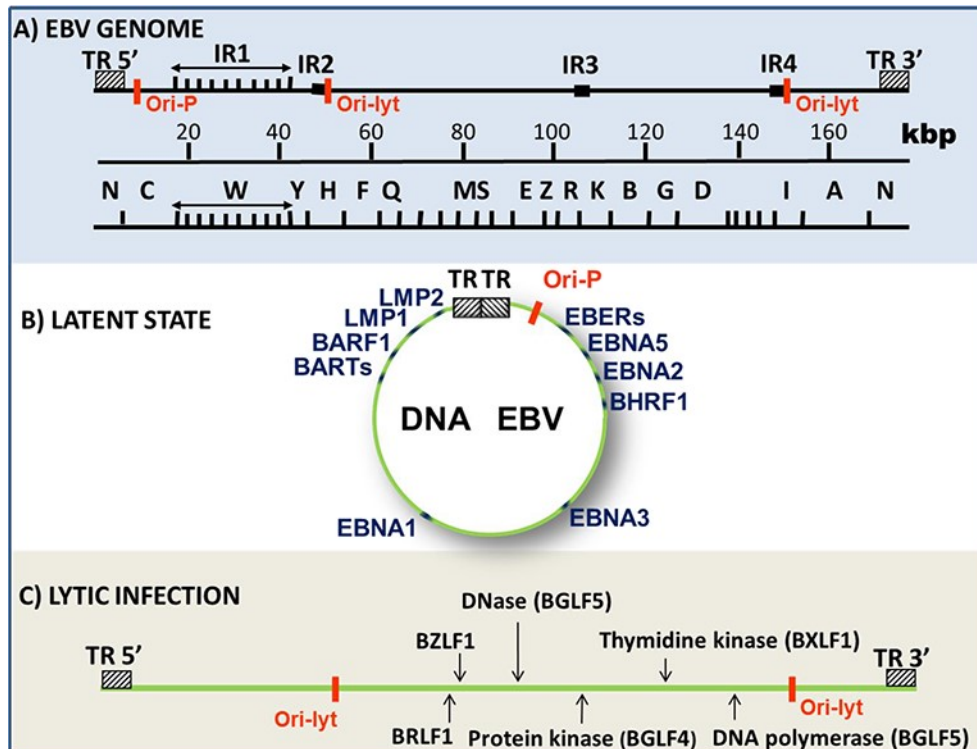


Figure 1. 6 Structure and configuration of the EBV genome during latent and lytic states

A) The EBV genome consists of approximately 172kb which make up over 80 lytic and latent genes. The DNA is made up of short and long sequence domains formed of internal repeats (IR1-4), flanked by short terminal repeats (TR). The origin of replication used in the latent stage of infection is known as Ori-P, and those used in lytic infection are designated as Ori-lyt (shown in red). The EBV genome can be digested by the restriction enzyme BamHI, producing various-sized fragments designated A-Z. The lytic and latent genes fall within these fragments. B) During latent infection, the EBV genome exists as a circular episome, expressing only 10% of its genes. C) The EBV genome exists in linear form during the lytic, infectious phase and expresses viral proteins such as BZLF1 and BRLF1, which are crucial for continuation of lytic infection and virus particle production. Many genes such as BXLF1 encode enzymes involved in DNA metabolism. IR: internal repeat, TR: terminal repeat. Figure taken from (Oker, 2016).

EBV is transmitted through saliva during the infectious lytic phase of the viral life cycle and infects epithelial cells of the throat and of the cervix, and B cells (Sixbey et al., 1984, Sixbey et al., 1986, Pope et al., 1968). The virus envelope glycoprotein gp350 binds to the CD21 molecule on the target cell and induces endocytosis, allowing viral entry into the cell (Nemerow et al., 1987, Tanner et al., 1987, Neparidze and Lacy, 2014). Primary infection in epithelial cells initiates the lytic phase of the viral life cycle, involving replication and high levels of viral shedding from infected cells in the oropharynx. The virus infects locally infiltrating B cells and leads to spread of the infection via growth-transforming infection of B cells in the tonsils. EBV evades the immune response from within these B cells, establishing latently infected memory B cells, and promotes their differentiation into plasma cells. Within these plasma cells, the virus can replicate spontaneously and release virions for infection of new B cells and viral transmission. Thus B cells are a major reservoir for persistence of EBV (Rickinson and Kieff, 2007, Miller, 1990). The infected B cells enter the memory B cell pool and establish lifelong persistence by downregulating all gene expression and becoming truly latent (Figure 1. 7) (Taylor et al., 2015, Münz, 2019).

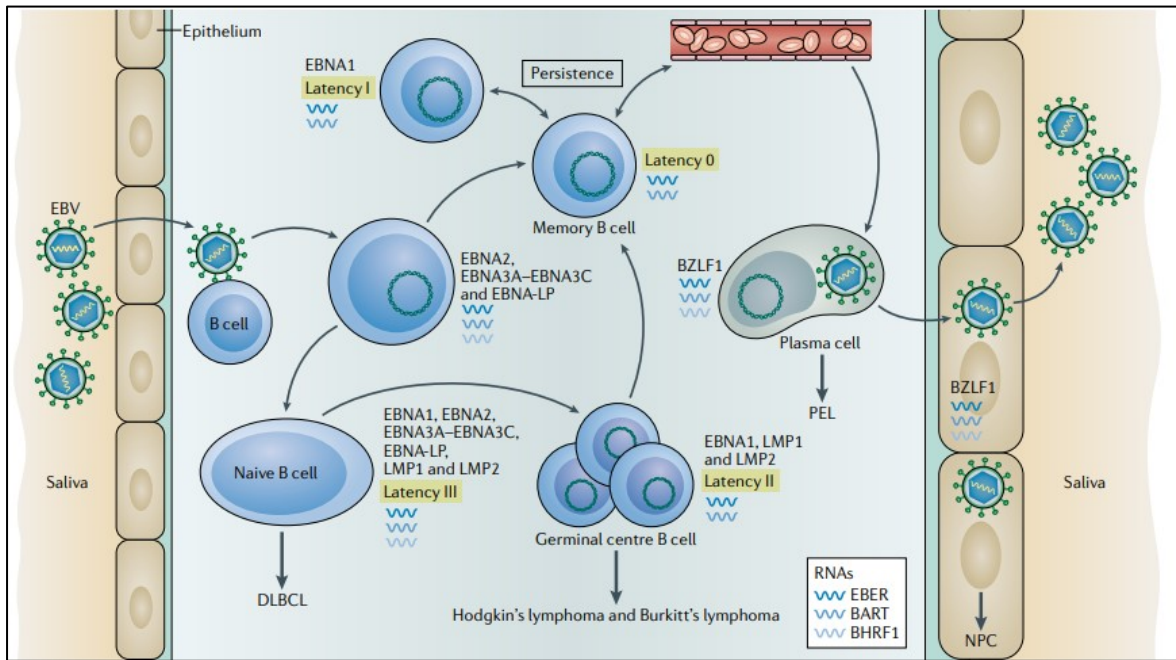


Figure 1. 7 The EBV infection cycle and establishment of persistence

EBV infects the mucosal epithelium from saliva and transfers across to B cells in the tonsils. B cell infection leads to EBNA-2-mediated proliferation and infection of memory B cells or naïve B cells. Infection of memory B cells can lead directly to generation of a viral reservoir through establishment of true latency where no EBV proteins are expressed (latency type 0). During homeostatic proliferation, the memory B cells enter latency type I transiently. Spontaneous reactivation of infected memory B cells (via cognate antigen recognition) and plasma cell differentiation leads to reactivation of latent EBV in the reservoir. Lytic replication in plasma cells is associated with plasmacytoma primary effusion lymphoma (PEL), and also release of new virions back into saliva for viral transmission. Epithelial infection can lead to EBV-associated carcinomas.

Infection of naïve B cells on the other hand can lead to latency type III transformation in the germinal centre where all the latent proteins are expressed. Differentiation of infected B cells via this pathway leads to latency type II, and may lead to diffuse large B cell lymphoma (DLBCL), Hodgkin's lymphoma and Burkitt's lymphoma.

Expression of EBV genes at each stage is depicted, in addition to expression patterns of the viral non-coding RNAs. Figure taken from Münz, 2019.

1.4.2 The EBV ZEBRA protein and lytic cycle activation

During lytic infection, the EBV genes are expressed as a regulated cascade; the immediate early genes, followed by the early genes, and finally the late genes. The immediate early genes, *BZLF1* and *BRLF1*, encode transactivator proteins ZEBRA (BamHI Z Epstein-Barr virus Replication Activator), and Rta respectively (Hardwick et al., 1988, Rooney et al., 1989, Countryman et al., 1987).

Phosphorylation of ZEBRA results in activation of ZEBRA, allowing lytic replication and progression of the virus life cycle (Baumann et al., 1998). ZEBRA is therefore critical for the initiation of the complete EBV lytic cascade, and its role in pathogenesis and infection of new cells is indispensable (Grogan et al., 1987, Takada et al., 1986, Countryman and Miller, 1985). The crucial roles of ZEBRA are owed to its function as a transcriptional activator of the early genes of the EBV lytic cycle. Its primary target is the *BRLF1* gene leading to expression of Rta, and together they activate downstream lytic genes (Liu and Speck, 2003, Sinclair et al., 1991). They synergistically trigger the expression of subsequent early lytic genes, which encode enzymes and proteins involved in viral DNA replication (Feederle et al., 2000). During the late stage of the lytic cycle, after viral DNA amplification, genes for viral structural proteins are expressed and virions are produced for release (Feederle et al., 2000).

Structurally, ZEBRA belongs to a large group of conserved transcription factors which all possess similar structures; ZEBRA contains a transcriptional activation domain (amino acids [aa] 1-166), a regulatory domain (aa 167-177), a basic DNA recognition domain (aa 178 to 194), and a dimerization domain (aa 198-225) (Flemington et al., 1992, Farrell et al., 1989). Phosphorylation of specific residues in the regulatory domain modulates functions such as DNA binding and DNA replication (Kolman et al., 1993).

ZEBRA has also been shown to affect the host immune response by inhibiting the actions of IFN- γ and TNF- α , thus directly contributing to immune evasion (Morrison et al., 2004, Morrison et al., 2001).

ZEBRA is the most immunodominant antigen of EBV compared to other lytic stage proteins, and numerous CD8⁺ T cell epitopes presented by HLA-A, -B and -C have been defined (Rist et al., 2015b). Its recognition leads to a potent immune response consisting of cytokine production and T cell-mediated killing (discussed in further detail in section 1.4.3.1 (Steven

et al., 1997, Bogedain et al., 1995). It is known that healthy carriers sustain high frequencies of ZEBRA-specific memory T cells, and that these potentially help in controlling virus spread during spontaneous reactivation during persistent infection (Elliott et al., 1997, Tan et al., 1999b).

The crucial role of ZEBRA supports its targeting in antiviral and oncolytic treatments. Earlier strategies explored the induction of overexpression of ZEBRA in order to kill EBV-associated tumours as replication of virus can lead to cell death in vitro (Feng et al., 2002, Kawanishi, 1993).

1.4.3 The Immune response to EBV

The immune response to EBV consists of initial antiviral innate responses such as those mediated by NK cells, which can recognise and kill EBV-infected cells (Williams et al., 2005). This is evidenced by patients with X-linked lymphoproliferative disease who are unable to control primary EBV infection due to defects with NK cell signalling (Parolini et al., 2000). There is also a strong serological response to EBV, and antibodies are targeted towards viral structural proteins, lytic stage and latent stage antigens (Vetsika and Callan, 2004). Patients with IM display production of IgM and IgG antibodies specific for viral capsid antigens and EBNA antigens, respectively, and these are still detectable in serum during persistent infection (Garzelli et al., 1984, Vetsika and Callan, 2004).

1.4.3.1 The T cell response to primary EBV infection

The majority of studies describing the T cell response to primary EBV infection are based on IM patients, whose excessive symptoms occur after a 6 week incubation period, and contrast greatly to the asymptomatic primary infection acquired by the majority of people in childhood (Fleisher et al., 1979, Dunmire et al., 2015). It is well established that both CD4⁺ and CD8⁺ T cell activity is crucial for the control of primary and persistent EBV (Strang and Rickinson, 1987). This is highlighted by the increased incidence of EBV-associated pathologies in immunosuppressed patients (Hanto et al., 1981, Ziegler et al., 1982, Palendira and Rickinson, 2015). Symptomatic primary EBV infection, i.e. IM, is characterized by profound clonal and oligoclonal expansion of CD8⁺ T cells bearing identical or similar TCRs, suggesting that they are driven by antigen (Callan et al., 1996). Tetramer-staining has also confirmed that these cells display cytotoxicity when stimulated *ex vivo* with peptide-loaded cells, whether from IM patients or from healthy carriers, highlighting their potent antigen-specific function (Steven et al., 1997, Steven et al., 1996, Hislop et al., 2001).

CD8⁺ T cells specific for lytic EBV proteins show a defined hierarchy in terms of their antigen-specificity; the majority of the cells are specific for immediate early lytic stage antigens BZLF1 and BRLF1, and their recognition leads to cytokine production and CTL-mediated killing of infected cells (Steven et al., 1997, Bogedain et al., 1995). A smaller proportion display specificity for the early lytic antigens, followed by the late lytic antigens (Woodberry et al., 2005, Abbott et al., 2013, Pudney et al., 2005, Steven et al., 1997, Callan et al., 1998). This immunodominance reflects the varying levels of antigen-presentation on infected cells; as the lytic cycle progresses, there is an impairment of the cell's ability to present antigen due to immunoevasion tactics of the virus (Quinn et al., 2014).

Also observed, albeit at a much lower frequency, are CD8⁺ T cells specific for some latent stage proteins such as EBNA3 and LMP2 (Hislop et al., 2002, Catalina et al., 2001).

Tetramer studies have demonstrated that these EBV-specific T cells display activated or memory phenotypes during primary infection, with increased expression levels of activation markers CD38, HLA DR, and CD45RO and low levels of the homing molecule CD62L, indicating their high activity levels (Callan et al., 1998). Moreover, significant responses to EBNA1 epitopes were seen in IM patients (Blake et al., 2000). However, whilst up to 44% of total CD8⁺ T cells in peripheral blood were shown to be specific to a single epitope within the lytic antigen ZEBRA in one individual, only up to 5% have been found to be specific to latent stage epitopes in another study, highlighting the stark dominance of these lytic stage antigens in the T cell response (Callan et al., 1998, Blake et al., 2000).

In contrast to the CD8⁺ T cell response, the CD4⁺ T cell response during primary EBV infection is less skewed towards certain lytic antigens and does not display evidence of immunodominance hierarchies (Long et al., 2011). This has been suggested to be due to the mechanism of antigen presentation to these CD4⁺ T cells, which involves the release of the antigens from the infected cells, and uptake and presentation by dendritic cells and B cells (Long et al., 2011).

Although initial studies reported that oligoclonal expansion was not observed in the CD4⁺ T cell compartment during IM, a recent study demonstrated that primary infection does in fact induce oligoclonal expansion of Th1-like CD4⁺ T cells (Maini et al., 2000, Meckiff et al., 2019). These CD4⁺ T cells were found to produce effector cytokines IFN- γ , TNF- α and IL-2, and to express perforin and granzyme B during IM (Meckiff et al., 2019). Furthermore, another ex vivo study of CD4⁺ T cells using tetramers has shown that the CD4⁺ T cell response is greater than previously thought, and that EBV-specific cells can make up to 1.5%

of the total CD4⁺ T cells in IM patients (Long et al., 2013). The discrepancy in observations of CD4⁺ T cell frequencies between various studies is likely to be due to the recent use of epitope-specific HLA II tetramers as opposed to the more limited cytokine secretion assays in earlier studies (Long et al., 2013, Meckiff et al., 2019).

In contrast to the CD8⁺ response, CD4⁺ T cell responses have been shown to be mainly latent antigen-specific, both during IM and in healthy carriers (Precopio et al., 2003, Meckiff et al., 2019, Amyes et al., 2003, Taylor et al., 2015). A summary of the T cell responses against the lytic and latent antigens of EBV is shown in Figure 1. 8, taken from a detailed review by Taylor et al (Taylor et al., 2015). The figure displays summarized data from studies comparing the CD4⁺ and CD8⁺ T cell responses to numerous EBV lytic and latent proteins. Blood from more than 30 individuals was screened using IFN- γ ELISpot assays on peptide libraries (Taylor et al., 2015).

Both the CD4⁺ and CD8⁺ T cell clones retract in numbers following recovery and persist as memory cells which can be activated *ex vivo* (Hislop et al., 2001, Maini et al., 2000, Hislop et al., 2002).

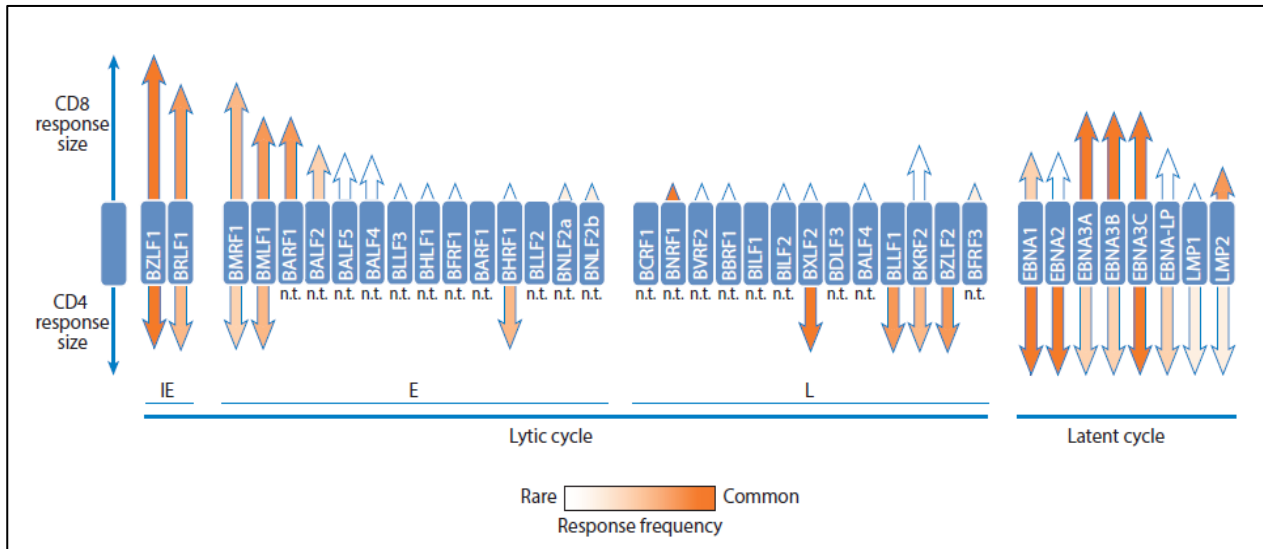


Figure 1. 8 The T cell response to EBV infection

The T cell response to EBV infection involves both CD8+ (upper arrows) and CD4+ (lower arrows) T cells. The CD8+ T cell response mainly targets lytic cycle proteins whereas the majority of CD4+ T cell responses are directed against latent cycle proteins. There is a clear hierarchy of immunodominance between the lytic cycle proteins recognised by CD8+ T cells, with immediate early (IE) proteins being most immunodominant, followed by early (E) and late (L) antigens. The CD8+ T cell response to latent antigens is mainly focussed on the EBNA3 antigens. There is no clear hierarchy of immunodominance amongst CD4+ T cell lytic cycle proteins, and the most common responses are seen towards the EBNA proteins in the latent cycle.

The height of the arrows indicate the mean size of the IFN- γ response within the study cohort towards that protein. The intensity of orange shading depicts more commonly seen responses. The CD8 and CD4 responses are not shown to the same scale; the CD8+ T cells responses are up to 20x greater (Taylor et al., 2015).

Abbreviations- E, early; EBNA, EBV nuclear antigen; EBV, Epstein-Barr virus; IE, immediate early; L, late; LMP, latent membrane protein; n.t., not tested. Figure taken from (Taylor et al., 2015).

During asymptomatic EBV infection, studies have shown that although a virus-specific CD8⁺ T cell response is induced, it is lower in magnitude than in IM despite high levels of EBV DNA being detected. Despite this, T cell response in asymptomatic infection is nonetheless able to control EBV infection (Fleisher et al., 1979, Jayasooriya et al., 2015, Silins et al., 2001). These studies suggest that the fundamental differences in the clinical presentations between asymptomatic EBV infection and IM are due to an exaggeration of the CD8⁺ T cell response during the latter, and that IM is an immunopathological disease (Silins et al., 2001, Taylor et al., 2015). It has been suggested that this exaggerated response during primary infection in adulthood is related to the cross-recognition of EBV epitopes by pre-existing memory T cells specific for other pathogens, such as influenza, which are not usually present during early childhood when asymptomatic primary infection occurs (Clute et al., 2005).

Following the dramatic CD8⁺ T cell response seen in IM, resolution leads to contraction of the EBV-specific T cell population. A virus-specific memory pool is established whose immunodominance hierarchy reflects that seen during primary infection; lytic-specific cells make up 2% of T cells whilst the latent epitope-specific T cells make up 0.5% of the virus-specific memory pool (Taylor et al., 2015).

1.4.3.2 The T cell response during persistent EBV infection

CD8⁺ T cells specific to both lytic and latent antigens are easily detected in peripheral blood of healthy carriers, with the former being more abundant than the latter (Tan et al., 1999b). Indeed, tetramer staining by Tan et al demonstrated that CD8⁺ T cells specific for a specific HLA-B*08-restricted epitope of the ZEBRA antigen made up to 5.5% of CD8⁺ T cells (Tan et al., 1999b). Furthermore, the lytic antigen hierarchy seen during IM is also reflected in memory cells (Abbott et al., 2013). Lytic antigen-specific T cells are believed to control virus replication within the oropharynx and spontaneous reactivation in latently-infected B cells (Tan et al., 1999b).

CD8⁺ T cells targeting the latent antigens include T cells specific to the dominant EBNA3A, 3B, and 3C proteins, whereas responses against EBNA1, EBNA2, and LMP2 are less frequent (Taylor et al., 2015). Hislop et al described a study of EBV-specific memory T cells during latent infection reporting a contrast in the phenotypes of lytic epitope-specific CD8⁺ T cells compared to latent epitope-specific CD8⁺ T cells (Hislop et al., 2001). Whilst the

former cell types were heterogeneous in their expression of CD45RO/RA and CD28, the latter were consistently CD45RO⁺ and CD28⁺. Despite this phenotypic difference, all types of cells displayed cytotoxicity and cytokine production upon epitope recognition *ex vivo*. The group also found that CCR7⁺ cells failed to produce cytokines in response to their specific antigen, whereas cells lacking CCR7 produced IFN- γ and TNF- α . This was interesting because they also noted that the latent epitope-specific CD8⁺ T cell population expressed higher levels of CCR7 compared to lytic epitope-specific CD8⁺ T cells (Hislop et al., 2001). These observations suggest that the lack of cytokine production by latent antigen-specific T cells during latent infection could be a factor allowing persistence of the virus.

The CD4⁺ T cell response in healthy carriers is smaller than that of the CD8⁺ T cells but retains the wide range of epitopes targeted during primary infection (Long et al., 2013). In addition, CD4⁺ memory T cells have been shown to be uniform in their phenotype; regardless of whether they recognise lytic or latent antigens, they lack activation markers and can be either central memory (CCR7⁺) or effector memory (CCR7⁻) (Long et al., 2013). A study by Ning et al demonstrated that CD4⁺ and CD8⁺ T cells in healthy long-term carriers produced multiple cytokines and possessed cytotoxic capacity, although polyfunctional CD4⁺ T cells were found to lack CD107 expression (Ning et al., 2011). In contrast to the immunodominance hierarchy of latent proteins recognised by memory CD8⁺ T cells, EBNA1 is a more frequent target of CD4⁺ T cells compared to EBNA3 and LMP2 (Ning et al., 2011).

The delicate balance between the memory T cells and EBV enables the virus to persist asymptotically in its human host. When this balance is disrupted, EBV is able to cause various types of cancer through a range of techniques.

1.4.4 Latent EBV and tumorigenesis

An arsenal of host cell manipulation and immune evasion techniques grant EBV the ability to cause persistent infection and cancer. These include downregulation of viral proteins throughout various stages of latency, thus reducing immunogenicity, and direct interference with host immunity.

Although infection of memory B cells can allow the establishment of “true latency” during persistent disease where no viral proteins are produced, there are other types of latency which involve the expression of various combinations of EBV antigens (Figure 1. 7, Figure 1. 9). Thus, transformation of infected cells leads to various types of EBV-associated cancers,

which are classified into one of three types of latency depending on the distinct patterns of latent protein expression. Complete latency within memory B cells is latency type 0, whereas latency type I is limited to only expressing EBNA1, and includes Burkitt lymphoma (BL) and EBV-associated gastric cancer (EBVaGC). Latency type II expresses EBNA1 and all the LMP proteins, and includes Hodgkin Lymphoma and nasopharyngeal carcinoma. Latency III is characterized by the expression of all the latency proteins and is only seen in lymphomas associated with immunosuppression, such as PTLD and HIV-associated lymphomas (Neparidze and Lacy, 2014, Gottschalk and Rooney, 2015). The immunogenicity of the EBV-associated cancers correlates with the number of latent antigens expressed, thus PTLD (type III latency) is the most immunogenic type of EBV-associated cancer, whereas BL and EBVaGC (type I latency) are the least immunogenic (Figure 1. 9).

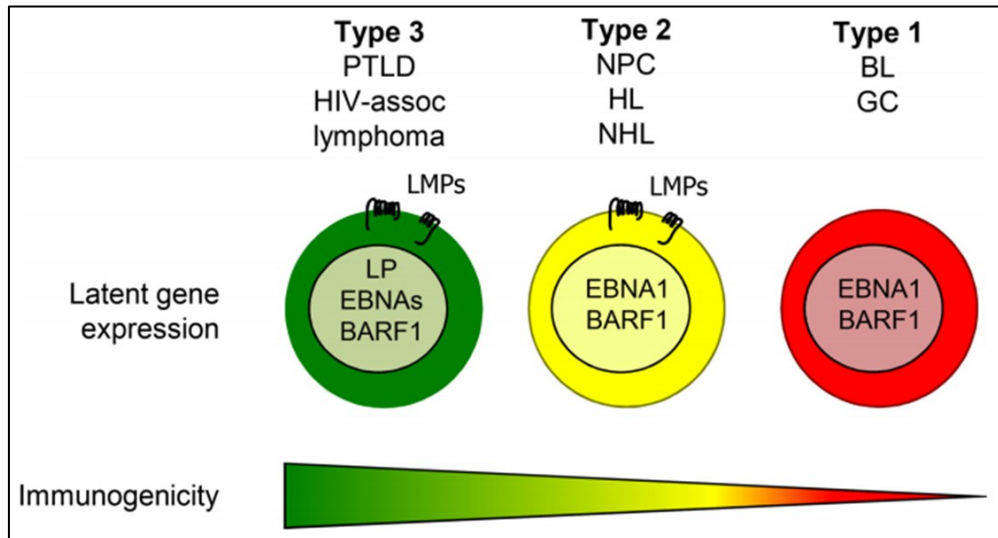


Figure 1. 9 The latency types of EBV-associated cancers and their immunogenicity

The various types of EBV-associated cancers are classed as various latency types according to the number of latent EBV antigens and oncogenes they express. Latency type III cancers express all the EBV latency proteins, whilst their expression is reduced in latency type II and I cancers. The immunogenicity of the EBV-associated cancers correlates with the number of latent antigens expressed.

PTLD: post-transplantation lymphoproliferative disease; HIV-associated lymphoma; NPC: Nasopharyngeal carcinoma; HL: Hodgkin lymphoma; NHL: Non-Hodgkin Lymphoma; BL: Burkitt-lymphoma; GC: gastric carcinoma; BARF1: BamH1-A-Reading Frame-1.

Image taken from (Gottschalk and Rooney, 2015).

The detailed mechanisms by which EBV leads to oncogenesis is not fully clear, but it is known that the viral proteins interfere with host cell growth, inhibit the immune response, and prevent apoptosis via several cellular signalling pathways. Although latent EBV has been widely believed to be solely responsible for development of virus-associated cancers, it has recently been proposed that the lytic cycle may also play a major role in tumorigenesis (Münz, 2019). This is through “conditioning” of the tumour-microenvironment through mechanisms such as production of immunosuppressing IL-10, suppression of tumour peptide presentation, and inhibition of immune cell chemoattraction (Münz, 2019).

The EBV latent genes encode several proteins which are essential for persistence and host cell transformation; six nuclear proteins (EBNA1, 2, 3A-C and LP), three cytoplasmic latent membrane proteins (LMP1, 2A/B), and the BARTs which act as precursors for microRNAs, in addition to the non-translated EBV-encoded RNAs (EBERs) (Neparidze and Lacy, 2014). The EBNA proteins affect gene regulation and most are required for B cell transformation. LMP1 is a transforming protein and acts as a major oncogene by mimicking CD40 signalling, leading to activation of several cell signalling pathways, and upregulation of the anti-apoptosis protein bcl-2 (Kang and Kieff, 2015, Neparidze and Lacy, 2014). Additionally, the BCRF1 lytic gene encodes a viral homologue to the immune suppressive cytokine IL-10, which can inhibit inflammatory cytokine production by T cells and NK cells, providing the virus with a survival advantage (Moore et al., 1990). EBNA1, which is the only EBNA protein expressed in latency type I cancers, is known to avoid presentation on HLA-I molecules owing to an inhibitory signal generated by its internal glycine-alanine repeats, thus avoiding recognition by CTLs during latent infection (Levitskaya et al., 1995).

Thus, there is a great deal of evidence that EBV allows the propagation of cancers by directly interfering with immune surveillance and causing T cell exhaustion. In parallel, EBV expresses several viral miRNAs which can repress host cellular proteins such as those involved in apoptosis, thus contributing to cellular transformation (Iizasa et al., 2012). Epigenetic changes such as DNA methylation are involved in the escape of EBV from the immune system as well as in tumorigenesis. During latent infection, the viral genome is methylated, thus silenced, allowing viral escape. Fernandez et al reported that in contrast to free particle virus, which displays no methylation, in latent EBV present in tumours such as NPC, extensive methylation of the EBV genome was present (Fernandez et al., 2009).

1.4.4.1 EBV-associated Gastric Carcinoma

Gastric cancers are one of the leading causes of cancer-related mortality globally, and EBV is associated with approximately 9% of these (Ferlay et al., 2010, Singh and Jha, 2017). The prevalence of EBVaGC varies globally although there are regional patterns of increased incidences seen. For example, there are more cases in the USA and South American nations compared to China, where the frequencies are approximately 16% and less than 5% respectively. These differences have been suggested to be due to certain genetic polymorphisms which predispose to infection with different EBV strains (Iizasa et al., 2012, Carrasco-Avino et al., 2017, Shibata and Weiss, 1992). In addition, EBVaGC has been found to be significantly associated with predominance in males under 60 years of age (Naseem et al., 2018).

EBVaGC are often adenocarcinomas found in the upper parts of the stomach (Shinozaki-Ushiku et al., 2015). The detailed mechanisms of EBV infection of gastric tissue remain unclear compared to those of B cell infection via CD21. One theory concerns the chronic gastritis which precedes gastric carcinoma. It is speculated that this attracts lymphocytes carrying EBV, and the inflamed epithelium secretes products that induce EBV production from infected B cells (Lin et al., 2016, Farrell, 2019). It has been demonstrated that EBV coated with IgA can bind to the polymeric IgA receptor in saliva, which can then bind to transmembrane proteins within the epithelial cell surfaces, allowing endocytic internalization of the virus (Gan et al., 1997). Another theory is that EBV is swallowed from the oral epithelium and survives the stomach acids to infect inflamed gastric cells (Farrell, 2019).

1.4.4.2 Molecular and cellular characteristics of EBVaGC

EBVaGC is characterized by a distinct molecular phenotype. EBV-encoded RNAs (EBERs) are present in all the carcinoma cells and express a single genotype, indicating that they had expanded from a single EBV-infected clone. This suggests direct involvement of the virus in tumorigenesis (Imai et al., 1994, Kuzushima et al., 1999). Compared with EBV-negative gastric cancers, there is a lack of p53 mutations, but extensive DNA hypermethylation (Zhang, 2014). Matsusaka et al reported that infection of EBV-negative gastric cells with recombinant EBV caused increased DNA methylation, which led to gene repression (Matsusaka et al., 2011). Additionally, Hino et al showed that in EBVaGC, the latent protein LMP2A leads to CpG island methylation and loss of the tumour suppressor gene PTEN (Hino et al., 2009). Hypermethylation of numerous other genes have also been specifically observed

in EBVaGC (Iizasa et al., 2012).

The immunophenotype of EBVaGC has been shown to include dense infiltration of perforin-expressing CD8⁺ T cells, with greatly increased numbers of TILs and higher expression of MHC II and other inflammation-induced adhesion molecules, compared to EBV-negative GC (Saiki et al., 1996, Kuzushima et al., 1999). Furthermore, there was direct contact between the CD8⁺ T cells and the carcinoma cells (Saiki et al., 1996). These observations are in line with the overall predicted better prognoses associated with EBVaGC relative to EBV-negative GC (Kang et al., 2016).

Kuzushima and colleagues showed that TILs isolated from EBVaGC contained high levels of HLA class I-restricted CTLs which could specifically recognise and kill EBV-infected autologous cells in vitro (Kuzushima et al., 1999). However, their experiments showed that these CTLs were not specific to the other known EBV latent antigens, such as EBNA3 or LMP1, which are not expressed in EBVaGC. They reasoned that as EBVaGC do not express the antigens commonly recognised by EBV-specific CTLs, that the CTLs in the TILs could be targeting cellular proteins present within the tumour or its pro-inflammatory environment (Kuzushima et al., 1999). Thus, despite the dense infiltration of TILs seen in EBVaGC, there are many mechanisms through which the virus can persist and cause cancer. One of these may be linked to PD-L1 expression, which is increased greatly in EBVaGC (Naseem et al., 2018, Sasaki et al., 2019). PD-L1 interaction with the PD-1 receptor on T cells leads to inhibition of T cell activation and proliferation. This induces their apoptosis and exhaustion, possibly explaining why despite extensive infiltration by TILs, the immune system is unable to eliminate EBVaGC.

1.4.4.3 Approaches for the treatment of EBVaGC

Currently, surgery with adjuvant chemotherapy or radiation is the only successful treatment for most gastric carcinomas and there is no specific treatment for EBVaGC (Camargo et al., 2014, Orditura et al., 2014). However, at advanced stages, relapse occurs after surgical resection in over half of patients, and 5-year survival is less than 10% (Orditura et al., 2014). EBVaGC has been observed to be resistant to certain chemotherapy options compared to EBV-negative gastric carcinoma cells (Shin et al., 2011). Alternative treatment options for advanced stage EBVaGC may encompass improving the immune response to the cancer cells, such as immune-checkpoint blockade (Kang et al., 2017). Although the effects of checkpoint inhibitor treatment on gastric cancers are currently being investigated, they do not

necessarily consider EBV status (Fuchs et al., 2017). The PD-1/PD-1L interaction has been the target of some studies of immunotherapy against gastric carcinoma to date (Kang et al., 2017, Muro et al., 2016, Kim et al., 2018). Although Muro et al did not confirm the EBV status of the gastric carcinoma cells, Kim et al did so, and demonstrated the highest response rates in EBV-positive gastric cancer (Kim et al., 2018). This study highlights the immune suppressing nature of EBVaGC and provides a possible explanation for its persistence despite infiltration of TILs. Ideally, in view of the observation that PD-L1 is increased in EBVaGC, it will be important to confirm the efficacy of checkpoint inhibitor treatments on PD-L1+ EBVaGC patients (Kang et al., 2017).

1.4.4.3.1 EBV-specific Immunotherapy and Latency Reversal

An alternative immunotherapy against EBVaGC is adoptive T cell therapy with EBV-specific CTLs. This has shown highly effective results in trials with other EBV-associated malignancies (Haque et al., 2001, Straathof et al., 2005, Wildeman et al., 2012, Cho et al., 2018b). The rationale is that re-introduction of large numbers of EBV-specific T cells can be advantageous to the immune system as they can potentially overcome viral escape mechanisms and clear infection (Sadelain et al., 2017).

However, the EBV-associated cancers targeted in the aforementioned studies exhibit different EBV latency types involving expression of more immunogenic antigens, compared with the limited immunogenicity of EBVaGC (Young and Dawson, 2014, Iizasa et al., 2012, El-Sharkawy et al., 2018). Viral latency reversal has been proposed as a way to overcome this inadequate immunogenicity; the rationale being that reactivating latent virus to the highly immunogenic and replicating lytic state renders the virus susceptible to antiviral agents or recognition by the immune system (Archin et al., 2012, Deeks, 2012). Numerous studies have demonstrated the efficacy of this “shock and kill” approach, whereby latent viruses are “shocked” out of latency and subsequently “killed” in their replicative, vulnerable state (Lee et al., 2015, Hui et al., 2016, Hui and Chiang, 2010, Wildeman et al., 2012, Clutton and Jones, 2018). Indeed, many groups have explored the potential of treating HIV with latency reversal agents in order to target the latent viral reservoir in search for a full “sterilizing cure” (Archin et al., 2012, Deeks, 2012, Sung et al., 2015, Sung et al., 2018, Walker-Sperling et al., 2016). Using this approach, Sung et al combined HIV latency reversal with ex vivo-expanded HIV epitope-specific autologous CTLs and observed reduction in HIV+ CD4+ T cells. Their data demonstrated that transferred HIV-specific T cells could recognise and mediate clearance of latently-infected CD4+T cells in vitro after latency reversal (Sung et al., 2015).

One of the leading groups of potent latency reversal agents are the histone deacetylase inhibitors (HDACi), which have been shown to successfully induce lytic reactivation of latent EBV (Wildeman et al., 2012, Hui et al., 2016). DNA chromatin are wrapped around histone proteins, which are modified in a reversible manner in order to control gene expression. When the histones are acetylated by enzyme histone acetyltransferases (HATs), they become negatively charged and can no longer bind to the DNA tightly, thus creating a more open chromatin structure, allowing binding of transcription factors and gene expression (Bose et al., 2014, Richon, 2006). Conversely, histone deacetylases (HDACs) remove acetyls from the histones, allowing histones to bind to DNA more tightly, creating a more compact, condensed DNA structure which is inaccessible to transcription factors (Bose et al., 2014). HDAC expression is known to be abnormal in cancers, with increased expressions associated with advanced disease and poor prognosis (Li and Seto, 2016).

HDACi block the removal of acetyl groups by the HDACs, thus remodelling the DNA chromatin, modifying gene expression to allow recruitment of transcription factors and also inhibiting recruitment of DNA silencing complexes (Bose et al., 2014, Clutton and Jones, 2018). In addition, HDACi have been shown to create cytotoxic effects in cancer cells such as induction of DNA damage and promotion of apoptosis (Bose et al., 2014, Hui et al., 2012). An important issue of consideration is the effect of HDACi on T cells, as they have been suggested to impair T cell proliferation, recognition of antigen, and T cell function, though these effects are yet to be confirmed in clinical studies (Clutton and Jones, 2018).

HDACi are grouped into 5 specific classes according to the HDACs that they act on; some are isoform-selective inhibitors which only target specific types of HDACs, whereas other are pan-inhibitors which do not display any selectivity (Eckschlager et al., 2017). Vorinostat, also known as SAHA, belongs to class I, the hydroxamic acids, and was the first HDACi approved by the FDA in the US and is used against T cell lymphoma (Eckschlager et al., 2017, Bubna, 2015). A newer HDACi, Chidamide, belongs to the benzamide class (class III) and has also shown promising results against T cell lymphoma via the stimulation of cell-mediated immunity mediated by increased gene expression (Ning et al., 2012). Furthermore, a novel HDACi which also belongs to class I is CXD101 (Celleron Therapeutics). It has been shown to have a dual function mechanism which minimises toxicity whilst still mediating anti-tumour activity (Eyre et al., 2016).

The DNA remodelling property of HDACi has been shown to upregulate transcription of highly immunogenic lytic stage antigens in EBV-infected cells such as ZEBRA. Hui et al reported that the HDACi romidepsin could potentially induce lytic cycle reactivation in NPC

and EBVaGC cells in vitro and in vivo (Hui et al., 2016). Furthermore, they demonstrated that these reactivated cells could then be susceptible to treatment with the antiviral agent ganciclovir, which inhibits virus replication and kills reactivated virus-infected cells. Their data showed significant tumour mass reduction and cell death when the HDACi was used in combination with ganciclovir (Hui et al., 2016). A previous report from the group had shown that SAHA also induced strong reactivation of the EBV lytic cycle in NPC cells but not in lymphoma cells, suggesting that the agents have preferential reactivation action in epithelial malignancies compared to lymphoid cancers (Hui and Chiang, 2010).

In another study, Wildeman et al used a different HDACi, valproic acid, alongside ganciclovir as a combination treatment. They demonstrated that this duo induced lytic cycle reactivation and cell death in NPC cell lines, mediated tumour apoptosis and improved patient quality of life when tested in 3 patients (Wildeman et al., 2012). Thus, reactivation of the viral lytic stage is a potentially effective way to overcome the lack of immunogenicity associated with latency type I and II EBV-associated cancers, rendering the virus susceptible to treatment with antiviral treatments.

1.5 Objectives, Aims and Hypothesis

Objectives

As discussed above, several groups have demonstrated the efficacy of using adoptively-transferred CTLs against EBV-related cancers which are of type III latency and are thus more immunogenic. On the other hand, other groups have used lytic reactivation as a tool to render the virus susceptible to killing in the context of latency type I and II cancers (Hui et al., 2016, Hui and Chiang, 2010, Wildeman et al., 2012, Zheng et al., 2015). No studies however have explored the outcome of combining lytic stage EBV reactivation with lytic antigen-specific CTL therapy using TCR-engineered T cells. Combining the two would harness the potent immune response that is observed during primary lytic EBV infection, which may allow the elimination of EBV-associated cancers.

Moreover, studies which used the transfer of EBV-specific T cells to treat EBV-associated malignancies used adoptive transfer of clonally expanded donor cells. Although effective, it is very time consuming and slow in practice due to the large number of cells needed for infusion and potential bias between clonal outgrowth (Moosmann et al., 2010, Haque et al., 2002). Instead, the reconstitution of large numbers of EBV-specific T cell repertoires through TCR-engineered T cells will aid in the fast-tracking of such adoptive treatments.

Optimization of a fast and efficient single TCR cloning platform will allow rapid production of virus-specific T cells for treatment and prevention of EBV-related diseases (Karpanen and Olweus, 2015).

Aims

The overall aim of this thesis is to establish a simple and practical single T cell cloning method to identify EBV ZEBRA-specific TCRs which mediate killing of reactivated EBV-infected cells, and would therefore be the best candidates for TCR-gene therapy against EBV-associated cancers.

There are three key sub-aims:

1. To establish a practical and efficient method of single TCR cloning to sequence and clone antigen-specific T cells
2. To utilize this platform to clone and characterize protective TCR species in an *in vitro* model of EBV infection
3. To test the ability of these lytic stage antigen-specific TCR-engineered T cells to recognise EBV after virus reactivation with latency reversal agents

Hypothesis

After reactivation of latent EBV infection, lytic stage antigen-specific TCR-engineered T cells will recognise and kill EBV-infected cells.

2 Materials and Methods

2.1 Materials used in this thesis

2.1.1 Antibodies

Table 2. 1 Antibodies used in this thesis

Antibody	Fluorochrome	Clone	Volume per 1 x10 ⁶ cells (µl)
CD3	APC-H7	SK7	1.25
CD4	PE-Cy7	SK3	0.63
CD8	BV421	RPA-T8	0.63
TCRαβ	APC	T10B9	1.25
CD69	PE	FN50	2.5
EBV ZEBRA	PE	BZ1	50µl of 1:200 diluted antibody
CD19	BV421	HIB19	1.25
Live/Dead	AmCyan	-	2100µl of 1µl in 1600µl dH2O dilution
Dead cell eFluor 780	APC-H7	-	1

2.1.2 Vectors

Table 2. 2 Vectors used in this thesis

Retroviral Vector	Source	Resistance genes	Experiment
pMXs_IRES_GFP (RTV-013)	Cell Biolabs	Ampicillin (E. coli)	TCR expression
pRFP_C_RS_shRNA (TR30014)	Origene	Chloramphenicol (E. coli) Puromycin (Mammalian)	siRNA Knockdown

2.1.3 HDAC Inhibitors

Table 2. 3 HDACi used in this thesis

HDACi	Source
SAHA	SelleckChem
Chidamide	Chipscreen Biosciences Ltd, Shenzhen, China
CXD101	Kind gift from Prof Xin Lu, Oxford University

2.1.4 Cell Lines

Table 2. 4 Cell lines used in this thesis

Cell Line	Cell Type	Source
Jurkat (Clone E6-1)	T cell line	ATCC
SKW3	TCR-deficient cell line	ATCC
Plat-GP	Transient retroviral packaging cell line	Cell Biolabs
PG13	Stable retroviral packaging cell line	ATCC
AGS_rEBV_GFP	rEBV_GFP-infected gastric carcinoma	Oxford*
OE19_rEBV_GFP	rEBV_GFP-infected gastric carcinoma	Oxford *
AGS_WT	Gastric adenocarcinoma cell line	Oxford *
OE_19 WT	Esophageal adenocarcinoma cell line	Oxford*
.221_A2	.221 B cell line modified to express HLA-A*02:01	CIV ¹
B Cell Lines	Various EBV-lymphoblastoid cell lines from donors	CIV ²

*These cells were kindly gifted by Professor Xin Lu, Ludwig Institute for Cancer Research, Oxford University

¹ The .221 cell line was modified previously in our lab

² These LCLs (B cell lines, BCLs) were generated from patient or donor blood in our lab and are stored in our liquid nitrogen inventory

2.2 Blood processing for isolation of PBMCs from healthy donors

2.2.1 Isolation of PBMC from whole blood by density gradient centrifugation

Whole blood from healthy donors was collected in lithium heparin collection tubes before transferring into a 50ml Falcon tube, and the collection tubes were washed with PBS before transferring the contents to the same 50 ml tube. The blood was topped up with more PBS to give a final volume of 40-50 ml. In a clean 50 ml Falcon tube, 10 ml of room temperature Histopaque (Sigma) was transferred before the PBS-diluted blood was very slowly layered on top of the Histopaque layer, using the slowest setting on the pipette aid. The tubes were centrifuged at 2000 rpm (800g) for 20 min, at room temperature with the brakes set to the off/zero position. The PBMC layer was collected using a sterile Pasteur pipette, transferred to a 15 ml Falcon tube and washed in 15 ml PBS by centrifugation at 1500 rpm for 5 min with brakes on. The supernatant was decanted, and the cell pellet resuspended in 10 ml of R10 media before being counted.

2.2.2 Counting cells using Trypan blue staining and light microscope

Isolated PBMCs were counted using a standard light microscope and Trypan blue stain (Sigma), allowing the determination of total number of viable cells only. Trypan blue was mixed at a 1:1 dilution with cells and 10 μ l of this mixture is loaded onto the counting chamber of a haemocytometer. Viable cells in three of the 9 squares were counted and an average number of cells determined, multiplied by the dilution factor of 2, and multiplied by 10,000 to determine the concentration of cells per ml.

The counted cells were used immediately for ZEBRA peptide pool stimulation, or divided amongst wells of a 6-well tissue culture plate and rested overnight at 37°C.

2.3 Identification and isolation of ZEBRA-specific CD8+ T cells

2.3.1 Screening of healthy donors for IFN- γ responses to EBV ZEBRA peptide pool

Healthy donors from our lab were screened for CD8+ T cell responses to EBV Lytic stage antigen ZEBRA using IFN- γ ELISpot. All steps were performed under sterile conditions in a safety hood besides the final development and washing stages.

On day 0, the wells of the ELISpot plate were pre-wet with 50 μ l of 70% ethanol in H₂O and left at room temperature for 1-3 minutes. The ethanol was then discarded, and the plate blotted and washed 4 times with 180 μ l per well of sterile PBS. The plates were then coated with 100 μ l per well of 10mg/ml anti-human IFN- γ monoclonal antibody 1-D1K in sterile PBS and incubated at 4°C overnight. The next day, the plates were washed once with 180 μ l per well of sterile PBS before adding 180 μ l of sterile R10 media to each plate. The plates were incubated at 37°C 5 % CO₂ for at least 2 hours or overnight at 4°C.

The EBV ZEBRA peptide pool was made up of 47 18mer peptides overlapping by 10 amino acids (Appendix Table 11). The pool was prepared at a 10x working stock of 20 μ g/ml and then diluted in R10 to give a final assay concentration of 2 μ g/mL per peptide. In addition to the peptide pool a 10X (4.5% DMSO) working stock mock pool, and 10X stock of PHA as a positive control, were used.

The blocked plates were removed from the incubator and the blocking solution decanted before addition of 50 μ l of peptide pool, mock or PHA diluted in R10 to the appropriate wells. Counted PBMCs were resuspended in R10 at 4 x 10⁶ cells/ml, and 50 μ l transferred to each well before incubating at 37°C for 20-24 hours.

On the final day, a biotinylated mouse-anti human IFN- γ antibody (7-B6-1) was prepared by diluting to 1 μ g/mL in antibody diluent (0.5% BSA/PBS). After mixing, the antibody solution was passed through a 0.22 mm filter using a syringe into to a clean tube to remove antibody aggregates.

The wells of the plates were washed with 180 μ l of PBS/ Tween 0.05% six times, blotting the plate on paper tissue between each wash, avoiding drying out of the plates. Immediately after blotting the residue from the last wash, 100 μ l of biotinylated antibody was added to each plate and incubated at room temperature for 4 hours.

The ABC peroxidase complex was prepared for the development of the ELISpot by adding 1 drop of solution A and 1 drop of solution B to every 5 mL PBS/Tween 0.05% and mixing well before storing at room temperature in the dark for 30 minutes.

After incubation with the 2nd antibody, the plates were washed 6 times as before with PBS/Tween. The ABC solution was diluted 1 in 2 immediately before use and 100ul/well added to the wells of each plate before incubating for 1-1.5 hours at room temperature in the dark. After incubation, the plates were washed 3 times as before with PBS/ Tween 0.05% and then 3 times with PBS. Finally, 100ul of AEC substrate was added to each well and incubated for 4 minutes at room temperature. After 4 minutes, the reaction was stopped by washing the plate under running tap water immediately and blotting dry. The plates were left to dry in the dark overnight before counting the spots in each well using an ELISpot reader.

2.3.2 Peptide stimulation for detection of EBV ZEBRA-specific CD8+ T cells

PBMCs from the 2 donors who responded to the EBV ZEBRA peptide pool in the IFN- γ ELISpot assays were used to identify and isolate ZEBRA-specific CD8+ T cells. Fresh PBMCs, either rested overnight or freshly isolated were washed and counted. Of the total cells, approximately 1×10^6 PBMCs were used for an unstimulated negative control, and 25-30 $\times 10^6$ cells were used for peptide stimulation at a concentration of 2×10^6 cells/ml. The final volume was adjusted to accommodate for the ZEBRA peptide pool which was at a 10x concentration of 20 $\mu\text{g/ml}$. After addition of the peptide pool, the final volume of cells was divided into wells of a 12-well tissue culture plate, approximately 3mls per well. Peptide stimulation was performed for 6 hours at 37°C before wrapping in foil and storing in 4°C overnight prior to IFN- γ capture assay.

2.3.3 IFN- γ Capture Assay

An IFN- γ secretion assay (Human IFN- γ Secretion Detection Kit (PE), Miltenyi Biotech) was performed as per manufacturer's instructions to capture IFN- γ on the surface of antigen-specific T cells after peptide-stimulation and isolate them through staining. Briefly, the peptide-stimulated cells and unstimulated cells were washed in cold MACS buffer at 300 \times g for 10 minutes before incubating in IFN- γ catch reagent and incubating for 45 minutes at 37 °C under slow continuous rotation. Following the secretion period, the cells were washed and stained with the IFN- γ -PE detection antibody (provided in the kit) for 10 minutes on ice before washing. The supernatant was aspirated completely before proceeding to T cell staining for FACS analysis and sorting. The magnetic beads and column provided were omitted from the protocol.

2.3.4 Staining and single cell sorting of IFN- γ positive CD8+ T cells

The IFN- γ -PE detection antibody-stained cells were incubated with 100 μ l Live/Dead stain, which was first diluted 1 in 1600 in dH₂O to make the working stock, for 20 minutes in the dark at room temperature. The cells were then washed in 3mls PBS containing 2.5% FBS at 1500rpm for 5 minutes and counted, before adding antibodies according to the quantities in Table 2. 5.

Table 2. 5 Flow cytometry staining panel for single cell sorting of IFN- γ positive CD8+ T cells

Antibody	Fluorochrome	Clone	Volume per 1 x10 ⁶ cells (μ l)
CD3	APC-H7	SK7	1.25
CD4	PE-Cy7	SK3	0.63
CD8	BV421	RPA-T8	0.63
Live/Dead	AmCyan	-	100 μ l of 1 μ l in 1600 μ l dH ₂ O dilution

Table 2. 6 RNase-inhibiting catch buffer reagents

Reagent	Volume per well (μ l)	Volume per 96 well plate (μ l)
RNase-free H ₂ O	1.92	192
1M Tris (pH 8)	0.018	1.8
RNase Out (Invitrogen)	0.048	4.8

Cells were incubated for 20 minutes at room temperature in the dark, alongside single-stained compensation beads, before washing and counting. The counted cells were adjusted to approximately 2 x10⁶ cells /ml and filtered through FACS tubes with filter caps (BD) for cell sorting using the FACS Aria III cell sorter (BD).

The peptide-specific T cells from the IFN- γ secretion assay were single-sorted into wells of 96-well PCR plates preloaded with 2 μ l RNase-inhibiting lysis buffer (Table 2. 6). The RNase-inhibiting catch buffer was made fresh on the day of sorting and kept on ice until use. As it is a hypotonic solution, it lyses the cell, and immediate freezing of the cells after sorting

protects RNA integrity.

The catch buffer was made and dispensed into each well immediately before use, and the plates kept on ice until sorting. The cells were sorted according to the gating strategy in Figure 2. 1. Immediately after sorting, the plates were centrifuged briefly for 30 seconds in a pre-chilled centrifuge to pellet the cells, sealed and frozen at -80°C until PCR was performed.

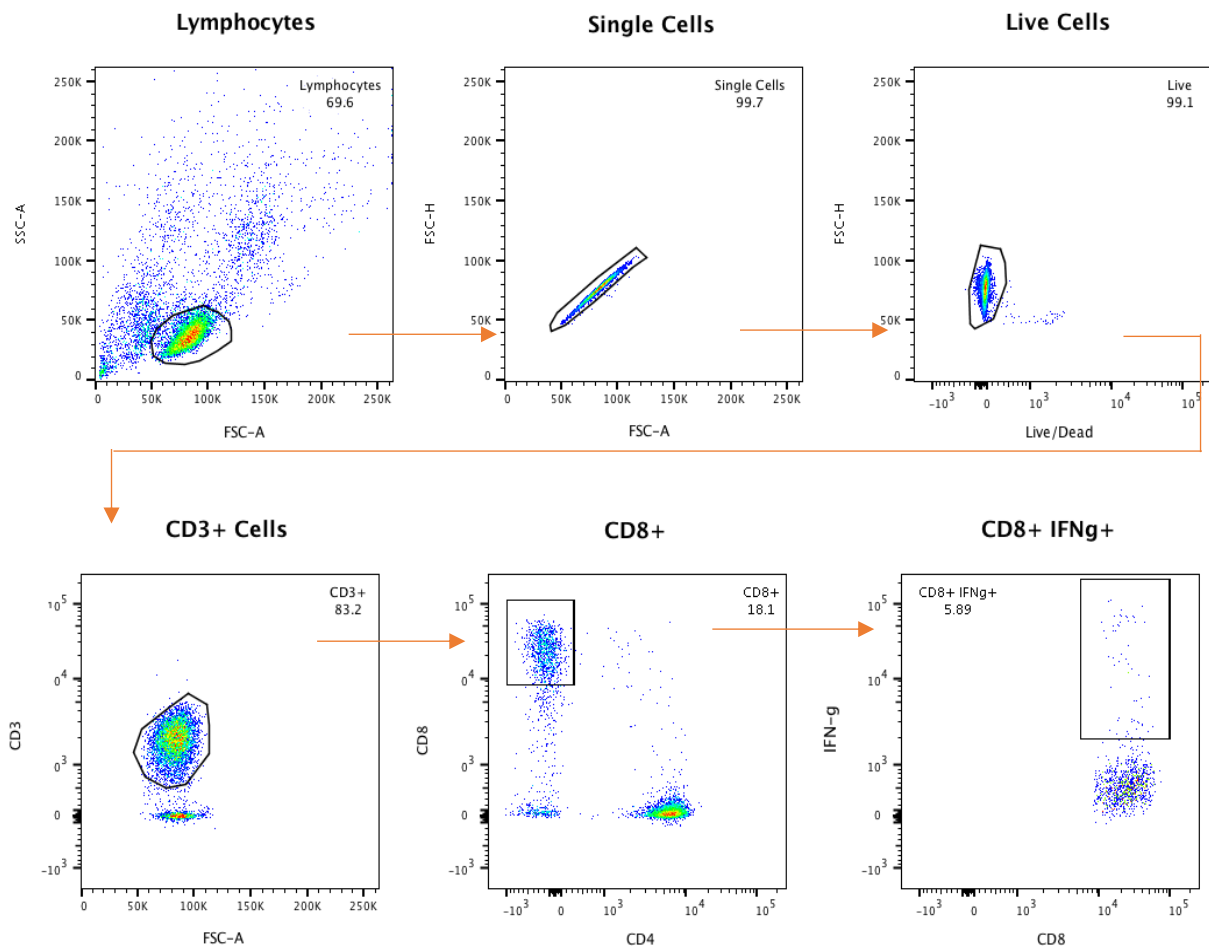


Figure 2. 1 Gating strategy for single-cell sorting of peptide-specific CD8⁺ T cells

After stimulation with ZEBRA peptide pool, IFN- γ capture assay and staining, PBMCs were first gated on lymphocytes and singlets, before gating on live cells, CD3⁺ cells, CD3⁺ CD8⁺ CD4⁻ cells, and finally CD8⁺ IFN- γ ⁺ cells for single cell sorting into 96-well PCR plates. Percentage population of each gate is shown.

2.4 Single TCR Cloning

2.4.1 Overview

In order to specifically amplify the paired TCR α and β genes from single T cells, a series of polymerase chain reactions (PCRs) were performed on the single-sorted antigen-specific T cells; the PCR method published by Hamana et al. (Hamana et al., 2016) was used as a basis for the PCRs. The PCR conditions and the primer sequences for the RT-PCR and 2nd PCR are the same as in the paper, but the primers used in the 3rd PCR are new. They have been modified to include sequences to accommodate the cloning of the TCR genes into my chosen retroviral vector, for subsequent expression of the TCRs in target cells for functional analysis and characterization. An overall workflow of the PCR method is shown in Figure 2. 2.

All PCR steps were performed on the Veriti Thermocycler (Applied Biosciences).

All primers arrived lyophilized and were resuspended with nuclease-free water to a stock concentration of 100 μ M before preparing a 10 μ M working solution.

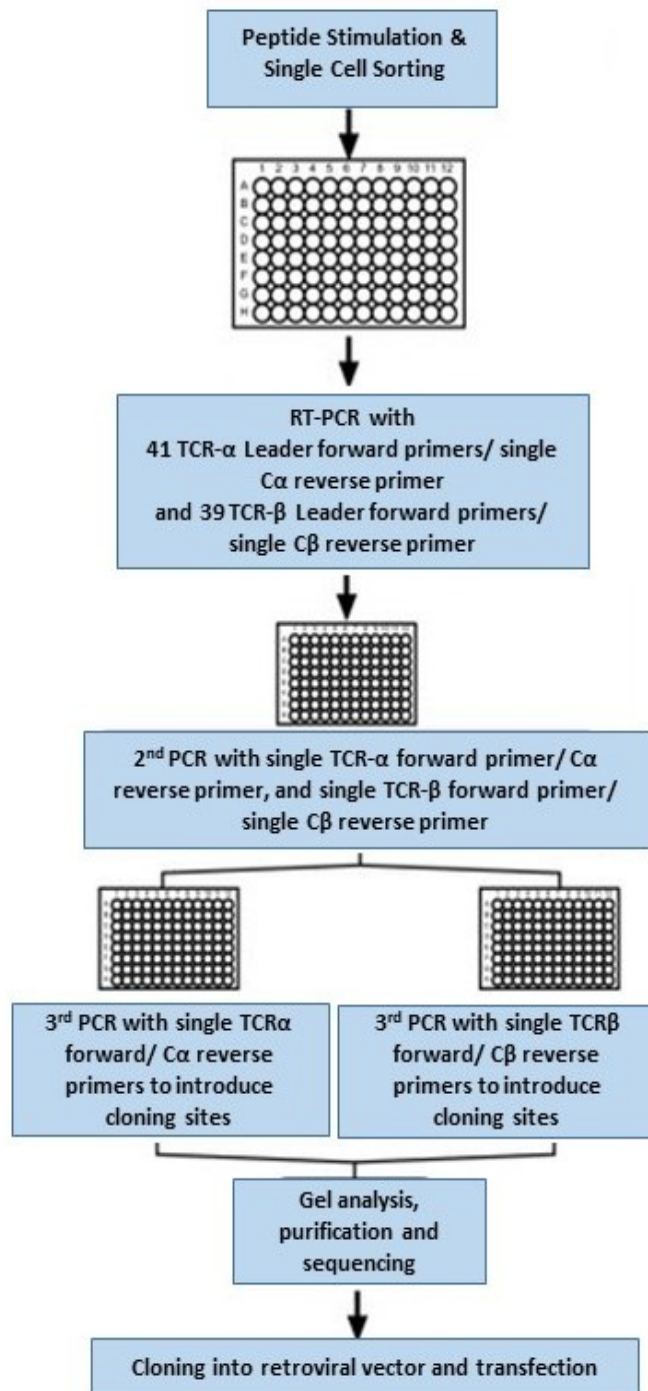


Figure 2. 2 Overview of the single TCR cloning protocol

PBMCs from donors were stimulated with peptide pool for 6hrs, and IFN γ ⁺CD8⁺T cells were single-cell sorted into wells of a 96-well PCR plate. Several rounds of PCR were performed to amplify paired TCR $\alpha\beta$ genes, before cloning the genes into a retroviral vector for expression in target cells for analysis.

2.4.2 RT-PCR on single T cells

To amplify both the TCR- α and - β genes and produce cDNA for further amplification, an RT-PCR was performed. First, an RT-PCR primer mix was prepared according to Table 2. 7. The RT-primer mix contained 41 different TCR- α forward primers (Table 2.8) and 39 different TCR- β forward primers (Table 2. 9), in addition to one TCR- α and - β reverse primer each (Table 2. 10). The forward primers target the individual leader (L) sequences of every known TCR- α and TCR- β variable (V) region gene as listed on the Immunogenetics Database (IMGT.org). The two reverse primers target exon 3 of the TCR- α and TCR- β constant (C) genes. This combination of primers allows the amplification of the full reading frames of both the TCR genes; full leader-variable-joining-constant (LVJC) region genes for TCR- α and full leader-variable-diversity-joining-constant (LVDJC) region genes for TCR- β . The 5' of each forward primer in the RT-mix had a universal α or β adapter region which facilitated binding of the primers in the 2nd PCR. The RT-PCR primer mix was used to prepare a mastermix for the reaction according to Table 2. 11 and the reaction performed according to the conditions listed in Table 2. 12. Following this, 5 μ l was added directly into the wells of the single-sorted T cells on ice.

Table 2. 7 RT-PCR primer mix

Primer	Concentration (uM)
Each AL forward primer	0.44
Each BL forward primer	0.44
Ca_RV1	2.22
Cb_RV1	2.22

Table 2. 8 TCR- α RT-PCR Forward primers

Primer Name	Primer Sequence (5'-3')
AL-1-1	TGGAGGAGAACCCTGGACCTatgtggggagctttcctct
AL-2	TGGAGGAGAACCCTGGACCTatggctttgcagagcactct
AL-3	TGGAGGAGAACCCTGGACCTatggcctctgcacccatctc
AL-4	TGGAGGAGAACCCTGGACCTatgaggcaagtggcgagagt
AL-5	TGGAGGAGAACCCTGGACCTatgaagacatttctggatt
AL-6	TGGAGGAGAACCCTGGACCTatggagtcattctgggagg
AL-7	TGGAGGAGAACCCTGGACCTatggagaagatcgggagacc
AL-8-1	TGGAGGAGAACCCTGGACCTatgctcctgttctcatacc
AL-8-2	TGGAGGAGAACCCTGGACCTatgctcctgctgctcgtccc
AL-8-3	TGGAGGAGAACCCTGGACCTatgctcctggagcttatccc
AL-9-1	TGGAGGAGAACCCTGGACCTatgaattcttctccaggacc
AL-9-2	TGGAGGAGAACCCTGGACCTatgaactattctccaggctt
AL-10	TGGAGGAGAACCCTGGACCTatgaaaaagcatctgacgac
AL-12-1	TGGAGGAGAACCCTGGACCTatgatataccttgagagtttt
AL-12-3	TGGAGGAGAACCCTGGACCTatgatgaaatccttgagagt
AL-13-1	TGGAGGAGAACCCTGGACCTatgacatccattcgagctgt
AL-13-2	TGGAGGAGAACCCTGGACCTatggcaggcattcgagcttt
AL-14	TGGAGGAGAACCCTGGACCTatgtcactttctagcctgct
AL-16	TGGAGGAGAACCCTGGACCTatgaagcccacccctcatctc
AL-17	TGGAGGAGAACCCTGGACCTatggaaactctcctgggagt
AL-18	TGGAGGAGAACCCTGGACCTatgctgtctgcttctctgctc
AL-19	TGGAGGAGAACCCTGGACCTatgctgactgccagcctgtt
AL-20	TGGAGGAGAACCCTGGACCTatggagaaaatgttgagagt
AL-21	TGGAGGAGAACCCTGGACCTatggagaccctctgggacct
AL-22	TGGAGGAGAACCCTGGACCTatgaagaggatattgggagc
AL-23	TGGAGGAGAACCCTGGACCTatggacaagatcttaggagc
AL-24	TGGAGGAGAACCCTGGACCTatggagaagaatcctttggc
AL-25	TGGAGGAGAACCCTGGACCTatgctactcatcacatcaat
AL-26-1	TGGAGGAGAACCCTGGACCTatgaggctggtggcaagagt
AL-26-2	TGGAGGAGAACCCTGGACCTatgaagttggtgacaagcat
AL-27	TGGAGGAGAACCCTGGACCTatggtcctgaaattctccgt
AL-29	TGGAGGAGAACCCTGGACCTatggccatgctcctgggggc
AL-30	TGGAGGAGAACCCTGGACCTatggagactctctgaaagt
AL-34	TGGAGGAGAACCCTGGACCTatggagactgttctgcaagt
AL-35	TGGAGGAGAACCCTGGACCTatgctccttgaacatttatt
AL-36	TGGAGGAGAACCCTGGACCTatgatgaagtgtccacaggc
AL-38-1	TGGAGGAGAACCCTGGACCTatgacacaggttagcttgc
AL-39	TGGAGGAGAACCCTGGACCTatgaagaagctactagaat
AL-40	TGGAGGAGAACCCTGGACCTatgaactcctctctggactt
AL-41	TGGAGGAGAACCCTGGACCTatggtgaagatccggcaatt

Table 2. 9 TCR-β RT-PCR Forward primers

Primer Name	Primer Sequence (5'→ 3')
BL-2	AAGGATCCGAATTCCTGCAGGatggataacctggctctatg
BL-3-1	AAGGATCCGAATTCCTGCAGGatgggctgcaggctcctctg
BL-4-1	AAGGATCCGAATTCCTGCAGGatgggctgcaggctcctctg
BL-5-1	AAGGATCCGAATTCCTGCAGGatgggctccaggctcctctg
BL-5-4	AAGGATCCGAATTCCTGCAGGatgggccctgggctcctctg
BL-5-6	AAGGATCCGAATTCCTGCAGGatgggccccgggctcctctg
BL-5-8	AAGGATCCGAATTCCTGCAGGatgggaccaggctcctctt
BL-6-1	AAGGATCCGAATTCCTGCAGGatgagcatcgggctcctctg
BL-6-2	AAGGATCCGAATTCCTGCAGGatgagcctcgggctcctctg
BL-6-4	AAGGATCCGAATTCCTGCAGGatgagaatcaggctcctctg
BL-6-5	AAGGATCCGAATTCCTGCAGGatgagcatcggcctcctctg
BL-6-6	AAGGATCCGAATTCCTGCAGGatgagcatcagcctcctctg
BL-7-2	AAGGATCCGAATTCCTGCAGGatgggcaccaggctcctctt
BL-7-3	AAGGATCCGAATTCCTGCAGGatgggcaccaggctcctctg
BL-7-6	AAGGATCCGAATTCCTGCAGGatgggcaccagtctctatg
BL-7-7	AAGGATCCGAATTCCTGCAGGatgggtaccagtctctatg
BL-7-9	AAGGATCCGAATTCCTGCAGGatgggcaccagcctcctctg
BL-9	AAGGATCCGAATTCCTGCAGGatgggcttcaggctcctctg
BL-10-1	AAGGATCCGAATTCCTGCAGGatgggcacaggctcttctt
BL-10-2	AAGGATCCGAATTCCTGCAGGatgggcaccaggctcttctt
BL-10-3	AAGGATCCGAATTCCTGCAGGatgggcacaaggttgttctt
BL-11-1	AAGGATCCGAATTCCTGCAGGatgagcaccaggcttctctg
BL-11-3	AAGGATCCGAATTCCTGCAGGatgggtaccaggctcctctg
BL-12-3	AAGGATCCGAATTCCTGCAGGatggactcctggacctctg
BL-12-4	AAGGATCCGAATTCCTGCAGGatgggctcctggacctctg
BL-12-5	AAGGATCCGAATTCCTGCAGGatggccaccaggctcctctg
BL-13	AAGGATCCGAATTCCTGCAGGatgcttagtctgacctgcc
BL-14	AAGGATCCGAATTCCTGCAGGatggtttccaggcttctcag
BL-15	AAGGATCCGAATTCCTGCAGGatgggtcctgggcttctcca
BL-16	AAGGATCCGAATTCCTGCAGGatgagccaatattcacctg
BL-18	AAGGATCCGAATTCCTGCAGGatggacaccagagtactctg
BL-19	AAGGATCCGAATTCCTGCAGGatgagcaaccagggtgctctg
BL-20-1	AAGGATCCGAATTCCTGCAGGatgctgctgcttctgctgct
BL-24-1	AAGGATCCGAATTCCTGCAGGatggcctccctgctcttctt
BL-25-1	AAGGATCCGAATTCCTGCAGGatgactatcaggctcctctg
BL-27	AAGGATCCGAATTCCTGCAGGatgggccccagctccttgg
BL-28	AAGGATCCGAATTCCTGCAGGatgggaatcaggctcctctg
BL-29-1	AAGGATCCGAATTCCTGCAGGatgctgagtcttctgctct
BL-30	AAGGATCCGAATTCCTGCAGGatgctgctctctctcttgc

Table 2. 10 The RT-PCR reverse primers

Primer	Primer Sequence (5'- 3')
Ca_RV1	AGGTTCGTATCTGTTTCAAAGCTT
Cb_RV1	GGTAAAGCCACAGTCTGCTCTA

Table 2. 11 The components of the RT-PCR mastermix

Reagent	μL per reaction
2×PrimeStar GC buffer	2.5
Nuclease-free water	1.425
RT-PCR Primer Mix	0.45
2.5 mM dNTP	0.4
RNase Inhibitor (40u/μl)	0.1
PrimeScript II RTase (200u/μl)	0.1
PrimeStar HS Polymerase (2.5u/μl)	0.025

Table 2. 12 RT-PCR cycle conditions

Temperature	
Heated Lid 105°C	
40 min at 45 °C	
98 °C for 1 min	
98 °C for 10 sec	30 cycles
52 °C for 5 sec	
72 °C for 1 min	
4 °C store	

2.4.3 Second PCR of paired TCR $\alpha\beta$ sequences

The product of the RT-PCR reaction was diluted 1 in 10 in nuclease-free water, and 2 μ l of the diluted PCR product was used as a template for a semi-nested 2nd PCR step. The TCR- α and - β genes are amplified separately for this step but with the same PCR conditions. This step entails use of a single TCR- α forward and a single TCR- β forward primer, whose sequences are identical to the universal adapter regions in the forward primers from the RT-PCR step. The reverse primers target exon 2 of the TCR- α and - β constant region genes. The primers are listed in Table 2. 13.

The components of the two separate master mixes are listed in Table 2. 14 and Table 2. 15. The TCR- α and TCR- β 2nd PCR reactions are performed simultaneously according to the conditions in Table 2. 16.

Table 2. 13 Primers used in the 2nd PCR

Primer	Primer Name	Primer Sequence (5'-3')
TCR- α Forward	A2F	TGGAGGAGAACCCTGGACCT
TCR- β Forward	B2F	AAGGATCCGAATTCCTGCAGG
TCR- α Reverse	Ca_RV2	TGTGACACATTTGTTTGAGAA
TCR- β Reverse	Cb_RV2	CTGTGCACCTCCTTCCCA

Table 2. 14 The TCR- α 2nd PCR mastermix components

Mastermix	μL per reaction
2 \times PrimeSTAR GC Buffer	10
Nuclease-free water	5.5
2.5 mM dNTP	1.6
10 μ M A2F F primer	0.4
10 μ M Ca_RV2_R primer	0.4
PrimeSTAR HS DNA polymerase	0.1

Table 2. 15 The TCR-β 2nd PCR mastermix components

Mastermix	μL per Reaction
2×PrimeSTAR GC Buffer	10
Nuclease-free water	5.5
2.5 mM dNTP	1.6
10 μM B2F F primer	0.4
10 μM Cb_RV2_R primer	0.4
PrimeSTAR HS DNA polymerase	0.1

Table 2. 16 Second PCR conditions

Temperature	
98 °C for 1 min	
98 °C for 10 sec	35 cycles
52 °C for 5 sec	
72 °C for 30 sec	
4 °C store	

2.4.4 Third PCR to introduce cloning sites

During the third PCR step, the TCR genes are amplified further, and cloning sites are incorporated using the primers listed in Table 2. 17.

The TCR- α 3rd forward primer contains part of the P2A linker sequence in its 5' end. This is used to connect the TCR- α and - β genes in the same vector during the cloning step. The TCR- α 3rd reverse primer has the reverse complement sequence to a portion of the TCR- α constant (TRAC) gene which is present in the modified vector backbone. The TCR- β forward primer has a 5' sequence that overlaps with the sequence of the linearized vector, and the reverse primer has part of the TCR- β constant (TRBC) gene in its 3' end that is also present in the linker sequence. These overlaps between the modified vector, the TCR- α and - β PCR fragments and the P2A linker allow the cloning of both the TCR- α and - β pair genes into the same vector via the Gibson Assembly cloning method.

The TCR- α and - β products of the 2nd PCR were diluted 1 in 10 in nuclease-free water, and 2 μ l was added to 18 μ l aliquots of mastermix which was prepared with the components listed in Table 2. 18 and Table 2. 19. The reaction is then performed according to the conditions described in Table 2. 20.

Table 2. 17. Third PCR/cloning primers

Primer	Primer Sequence (5'- 3')
P2A_A3_F	GTTGAAGCAGGCTGGAGACGTGGAGGAGAACCCTGGACCT
pMX_B3_F	GACCATCCTCTAGACTGCCGGATCTAGCTAGTTAATTAAGTGGCG CCGGAATTAGATCTCTCGAGAAGGATCCGAATTCCTGCAGG
TRAC_RV3	GGTGAATAGGCAGACAGACTT
TRBC_RV3	GTGGCCAGGCACACCAGTG

Table 2. 18 The components of the TCR- α 3rd-PCR mastermix

Mastermix	μL per Reaction
2 \times PrimeSTAR GC Buffer	10
Nuclease-free water	5.5
2.5 mM dNTP	1.6
10 μ M P2A_A3 F primer	0.4
10 μ M TRAC_RV3_R primer	0.4
PrimeSTAR HS DNA polymerase	0.1

Table 2. 19 The components of the TCR- β 3rd-PCR mastermix

Mastermix	μL per Reaction
2 \times PrimeSTAR GC Buffer	10
Nuclease-free water	5.5
2.5 mM dNTP	1.6
10 μ M pMX_B3 F primer	0.4
10 μ M TRBC_RV3_R primer	0.4
PrimeSTAR HS DNA polymerase	0.1

Table 2. 20 The 3rd-PCR conditions for both TCR- α and TCR- β genes

Temperature	
Heated Lid 105°C	
98 °C for 1 min	
98 °C for 10 sec	35 cycles
52 °C for 5 sec	
72 °C for 30 sec	
4 °C store	

2.4.5 Agarose Gel Electrophoresis

In order to visualise the amplification of the TCR genes, the products of the 3rd PCR were analysed on a 1% agarose gel. To make the gel, agarose was added to 1x TBE buffer (Invitrogen) to a final concentration of 1% and heated in the microwave until fully dissolved. The solution was cooled down and stained with SYBR-Safe DNA gel stain (Invitrogen) before pouring into a large gel case with the appropriate combs. The entire 3rd PCR products were mixed with 6x gel loading dye (NEB) and the whole reaction loaded into the gel alongside a 100bp DNA ladder (NEB). The gel was run at 130V for one hour in 1x TBE to fully separate the bands for extraction and sequencing.

2.4.6 Extraction and purification of TCR- α and - β PCR products

The agarose gels were visualised via a blue light transilluminator (Thermofisher) and the DNA bands at ~550 bp were excised. The bands were purified using Qiaquick gel extraction kit (Qiagen) and prepared for sequencing. The remainder of the 3rd PCR products were stored at -20°C ready for cloning into the retroviral vector.

2.4.7 Sequencing of TCR genes

The gel-purified TCR genes were sent for Sanger sequencing using the 3rd PCR primers and the sequences of each TCR- α and - β 3rd PCR product was analysed using the V-Quest analysis tool on the IMGT database. The variable and joining genes of each TCR chain were determined alongside the CDR3 regions, and the sequences were also checked for the presence of the cloning sites needed for subsequent Gibson Assembly.

Every TCR $\alpha\beta$ pair was tallied according to how many single T cells carried the same TCR $\alpha\beta$ sequence. The paired TCR sequences were then ranked according to how frequent they were within the entire analysed TCR repertoire of that particular donor. The TCRs which made up the highest percentages of all the TCRs obtained from a single donor were deemed to be the most dominant, and these were chosen to be cloned into the vector for expression and analysis.

2.5 Constructing the vector backbone for TCR cloning

To produce the EBV-specific TCR clones, the TCR- α and - β genes from the most dominant TCRs were cloned into the retrovirus vector pMXs_IRES_GFP.

Before cloning, modification of the vector was needed so it would contain the TCR α constant region (TRAC) for full length TCR to be expressed in the target mammalian cells.

2.5.1 Vector Linearization

The pMXs_IRES_GFP vector was first prepared for receiving the TRAC gene. The vector was linearized via digestion with the restriction endonucleases BamHI-HF and NotI-HF (both NEB) using the overnight linearization reaction outlined in Table 2. 21.

The reaction was incubated at 37°C overnight and then treated with 5 μ l of calf intestinal phosphatase (CIP, NEB) for 1 hour at 37°C to remove the phosphorylated ends of the DNA, thus preventing vector re-ligation. The CIP-treated reaction was loaded into a 0.8% agarose gel and run at 140V for 90 minutes alongside an uncut control. The DNA band containing fully linearized vector was excised from the gel before purification using the Qiaquick Gel Purification kit (Qiagen), quantified via Nanodrop (Thermofisher), and stored at -20°C until further use.

Table 2. 21 Overnight linearization reaction of pMX_IRES_GFP vector

Reagent	Volume (μl)
CutSmart Buffer (NEB)	10
BamHI-HF	2
NotI-HF	2
Vector (1 μ g/ μ l)	10
Nuclease-free water	76
Total reaction volume	100

2.5.2 Preparation of the TCR constant genes

The TCR $\alpha\beta$ constant genes (TRAC and TRBC genes, respectively) were codon-optimized and modified with additional non-native cysteine residues according to the modified constant genes used by Hamana et al (Hamana et al., 2016). These gene sequences were obtained through email communications with the lead author. These modifications would permit optimal expression of the genes in human cells and also promote correct pairing of the exogenous TCR α and β chains owing to the additional cysteine residues forming additional disulphide bonds. The modified constant region genes (Figure 2. 3) were synthesised as gene fragments (GeneArt Strings, Thermofisher). The lyophilized gene fragments were resuspended according to the manufacturer's instructions and stored at -20°C until use. The TRAC gene was digested with BamHI and NotI in a 1 hour reaction at 37°C to produce cohesive overhangs for efficient cloning into the linearized vector. The digestion reaction was purified using the MiniElute Reaction Clean up kit (Qiagen) before ligating into the vector.

Codon-optimized and cysteine- modified TRAC gene fragment

GTCTggatccGTGTACCAGCTGAGAGACTCTAAATCCAGTGACAAGTCTGTCTGCCTATTCACCGACTTCGACAGCCAGACCAACGTGAGCCAGAGCAAGGACAGCGACGTGTACATCACCGACAAGTGCCTGGACATGAGAAGCATGGACTTCAAGAGCAACAGCGCCGTGGCCTGGAGCAACAAGAGCGACTTCGCCTGCGCCAA CGCCTTCAACAACAGCATCATCCCCGAGGACACCTTCTTCCCCAGCCCCGAGAGCAGCTGCGACGTGAAG CTGGTGGAGAAGAGCTTCGAGACCGACACCAACCTGAACTTCCAGAACCTGCTGGTGATCGTGCTGAGAA TCCTGCTGCTGAAGGTGGCCGGCTTCAACCTGCTGATGACCCTGAGACTGTGGAGCAGCTGAgcggccgcA CTT

Codon-optimized and cysteine-modified TRBC_P2A Linker Fragment

CACACCCAAAAGGCCACACTGGTGTGCCTGGCCACAGGCTTCTTCCCCGACCACGTGGAGCTGAGCTGGT GGGTGAACGGCAAGGAGGTGCACAGCGGCGTGTGCACCGACCCCCAGCCCCTGAAGGAGCAGCCCCGC CTGAACGACAGCAGATACTGCCTGAGCAGCAGACTGAGAGTGAGCGCCACCTTCTGGCAGAACCCCAGA AACCACTTCAGATGCCAGGTGCAGTTCTACGGCCTGAGCGAGAACGACGAGTGGACCCAGGACAGAGCC AAGCCCGTGACCCAGATCGTGAGCGCCGAGGCCTGGGGCAGAGCCGACTGCGGCTTACCAGCGTGAGC TACCAGCAGGGCGTGCTGAGCGCCACCATCCTGTACGAGATCCTGCTGGGCAAGGCCACCCTGTACGCCG TGCTGGTGAAGGAGAAAGGACTTCGGAAGCGGAGCTACTAACT

Figure 2. 3 Nucleotide sequences of codon-optimized constant gene fragments for construction of complete TCR vectors

The codon-optimized and cysteine-modified TRAC gene fragment was used to modify the pMXs_IRES_GFP vector. The codon-optimized and cysteine-modified TRBC gene fragment was used in the Gibson assembly reaction to complete the TCR β gene. Additional non-native cysteine residues are in red. In the TRAC fragment, end sequences in lowercase are restriction endonuclease sites. In TRBC fragment, the P2A sequence is present at the 3' and is shown in bold.

2.5.3 Cloning of the TRAC gene into the vector

The TRAC gene was ligated into the linearized pMXs_IRES_GFP vector upstream of the IRES gene using T4 DNA (NEB) ligase according to manufacturer's instructions at room temperature, for 4 hours before diluting the reaction 1 in 10 with nuclease-free water. The diluted reaction was then used to transform *E. coli* DH5alpha competent cells (ThermoFisher); a 50µl aliquot of the competent cells were thawed on ice and gently mixed before transferring to 12ml polypropylene tubes (Sigma) and addition of 1µl of the diluted ligation reaction. The mixture was incubated on ice for 20 minutes before heat-shocking at 42°C for exactly 45 seconds, followed by further incubation of the tubes on ice for 5 minutes. This was followed by the addition of 950µl of pre-warmed LB media and incubation at 37°C for 1 hour with shaking at 225rpm. The culture was then plated on LB agar plates containing 100µg/ml of ampicillin for selection of transformed bacteria and incubated overnight at 37°C. The following day, single colonies were picked, grown in 5mls LB media with 100µg/ml ampicillin. After 16hrs of growth at 37°C, the plasmid was extracted from each culture using Qiaprep Miniprep kit (Qiagen).

A double restriction enzyme digest was performed on the miniprep using BamHI-HF and NotI-HF, as per manufacturer's instructions, to screen for clones positive for the 424bp TRAC insert. DNA from positive clones was selected for sequencing with the TRAC-specific primer 5'-GAGACTCTAAATCCAGTGAC-3'.

After confirming correct sequence and insertion of the TRAC gene into the vector, 750 µl of the initial starting culture from the corresponding clone was used to inoculate 50ml of LB Amp media in 250ml conical flasks. The culture was grown overnight at 37°C shaking at 250rpm to allow propagation of large amounts of bacteria containing the correct vector. The following day, a Qiaprep Midiprep kit (Qiagen) was used to extract and purify the vector from the culture before quantification.

The TRAC_pMXs_IRES_GFP vector was linearized in an overnight reaction using BamHI-HF before agarose gel-purification as described above. Cutting the vector with BamHI opens up the vector at the 5' end of the inserted TRAC (Figure 2. 4 and Figure 2. 5) for efficient cloning of the TCR genes via Gibson Assembly cloning.

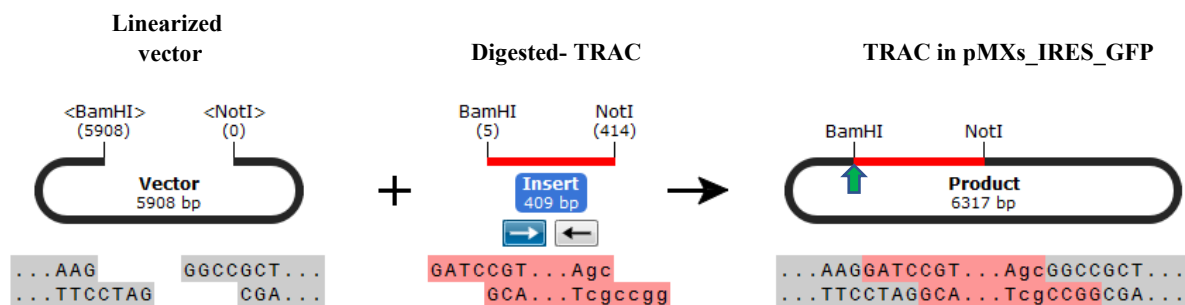


Figure 2. 4 Overview of TCR vector backbone construction

The pMXs_IRES_GFP vector was first linearised via restriction enzyme digest with BamHI and NotI to prepare it for accepting the TRAC gene. The TRAC gene was also cut with the same enzymes and ligated into the vector. The complete vector was cut again with BamHI upstream of the inserted TRAC gene (green arrow), to produce a linearized complete vector for TCR cloning.

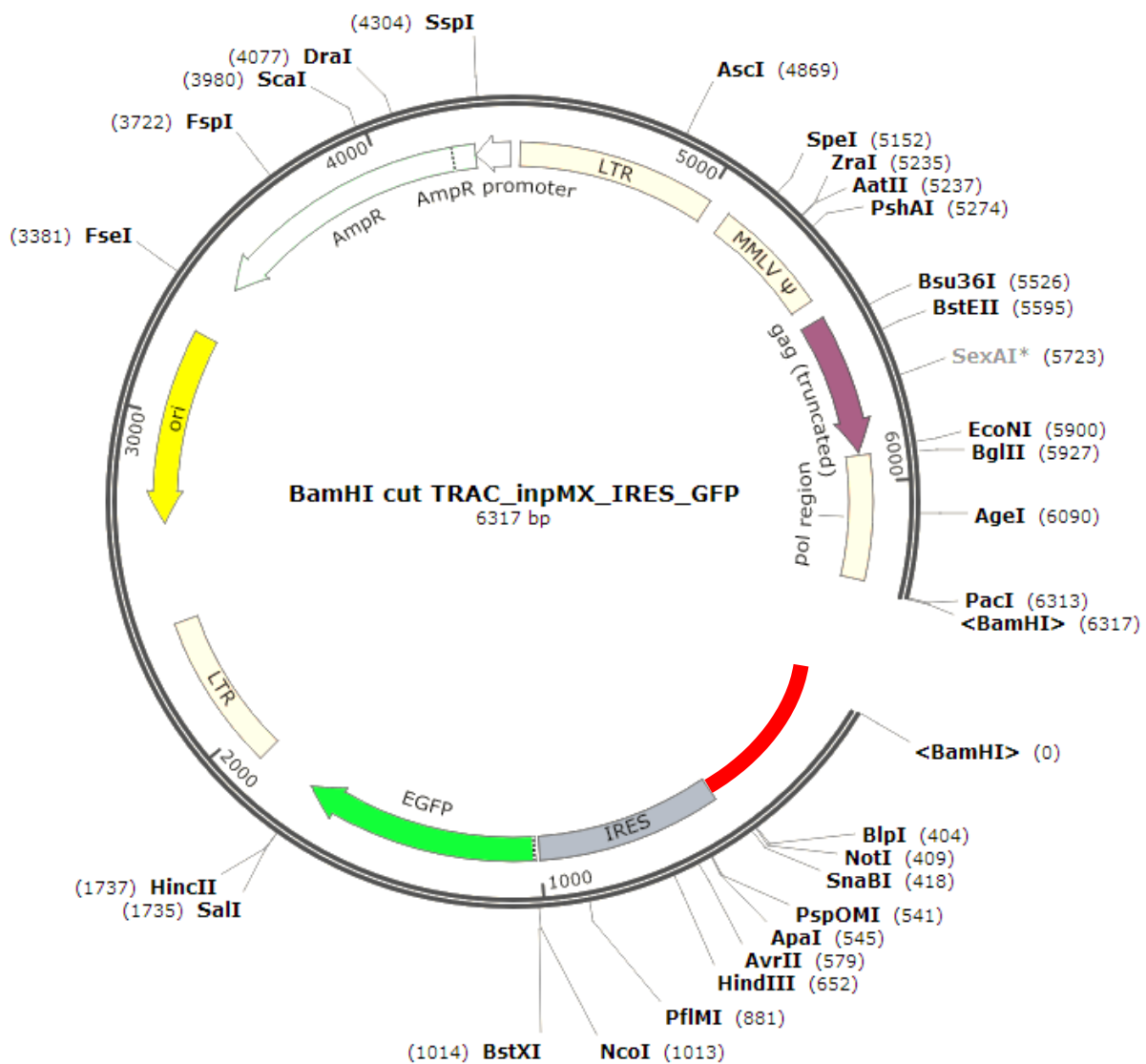


Figure 2. 5 BamHI-Linearized TRAC_pMXs_IRES_GFP

The TRAC gene (red gene block) was inserted into the pMXs_IRES_GFP vector and the complete vector cut at the BamHI site to linearize and open up the vector in preparation for Gibson Assembly.

2.6 Gibson assembly cloning of TCR genes

The paired TCR α and β genes from a single TCR were cloned into the linearized TRAC_pMXs_IRES_GFP vector so that both TCR- α and - β genes are expressed from the same vector. The TCR α and β genes will be linked within the vector using a P2A gene fragment, which allows equimolar levels of expression of both the TCR- α and - β genes from the same vector. All the fragments had overlapping sequences to enable their seamless assembly without prior digestion with restriction enzymes to produce sticky ends.

2.6.1 The Gibson assembly reaction

The Gibson assembly cloning reaction consists of joining 0.04 μ mol of the vector with 0.2 μ mol each of the TCR PCR product, linked by a TRBC_P2A linker fragment. Each of these is a different fragment which will then be assembled together to make a complete TCR expression vector. Figure 2. 6 illustrates how the required volume of each fragment is calculated, and the reaction conditions for a single TCR $\alpha\beta$ pair cloning reaction. The reaction is performed in a single 0.2ml PCR tube in one step using the NEB HiFi Assembly mastermix (New England Biosciences).

Gene: TCR4	TCR α (μ l)	TCR β (μ l)	Linker (μ l)	Vector (μ l)
Fragment	F1	F2	F3	F4
Concentration (ng/ μ l)	30	19	20	49
Length (bp)	550	550	531	6317

Equations for volume of fragments required:

$$\text{pmols} = (\text{weight in ng}) \times 1,000 / (\text{base pairs} \times 650 \text{ daltons})$$

Fragments F1-3:

$$\mu\text{l} = (0.5 \times 650 \times \text{Length of fragment (bp)}) / (\text{DNA concentration (ng}/\mu\text{l)}) \times 1000$$

Vector:

$$\mu\text{l} = (0.04 \times 650 \times \text{Length of fragment (bp)}) / (\text{DNA concentration (ng}/\mu\text{l)}) \times 1000$$

Fragment	F1	F2	F3	F4			
	TCR α	TCR β	Linker	Vector	Mastermix	H2O	Total (μ l)
	(μ l)	(μ l)	(μ l)	(μ l)	(μ l)	(μ l)	
TCR4	2.38	3.76	3.45	2.08	15	3.32	30

Incubate at 4 hours at 50°C

Store at -20°C

Figure 2. 6 Representative calculations and workflow of the Gibson assembly reaction protocol

TCR4 is used as an example of how the volumes needed of each fragment in a TCR cloning reaction are calculated, and how they make up the individual component fragments of a single Gibson reaction. The respective TCR α , TCR β , P2A linker and linearized vector volumes are added to a tube with the NEB HiFi Assembly mastermix and incubated for up to 4 hours at 50°C before storage.

2.6.2 Transformation of Stable competent E coli

The products of the Gibson Assembly cloning reaction were transformed into competent NEB Stable *E. coli*. After thawing a tube (50 μ l) of the cells on ice, 2 μ l of the cooled Gibson Assembly cloning reaction was added, followed by flicking of the tube to mix. The tube was placed on ice for 30 minutes before heat shocking at 42°C for exactly 30 seconds. The tube was incubated on ice for a further 5 minutes before addition of 950 μ l of room temperature NEB 10-beta/Stable Outgrowth medium which was supplied with the cells. The tubes were incubated horizontally at 30°C for 1 hour with shaking at 250rpm. After a 1-hour recovery period, 25-50 μ l of the cell mixture was spread on LB ampicillin plates and incubated at 30°C for 24 hours.

2.6.3 Preparation of Single Colony Starting Cultures

After 24 hours of incubation at 30°C, the plates were examined by eye for bacterial colonies. Single, separated colonies were picked and used to inoculate 5mls of LB media with 100 μ g/ml ampicillin. At least 8-10 colonies were picked from each TCR cloning reaction to ensure selection of a correctly-assembled insert. These starting cultures were grown for 12-16 hours, shaking at 250rpm at 30°C, before plasmid extraction.

2.6.4 Extraction of Bacterial Plasmids and screening for correct inserts

After growing the single colony starter cultures overnight, the plasmid was extracted using the Qiaprep Spin Miniprep kit (Qiagen). The DNA was quantified using the NanoDrop 8000 Spectrophotometer (Thermo Fisher Scientific). A 50 μ l double restriction enzyme digest was set up for each colony to screen for the presence of a correctly-assembled 1800 base pair insert of the full TCR α and TCR β genes with the P2A linker gene. The reaction conditions are outlined in Table 2. 22.

The miniprep plasmid digests which produced only two correct bands (indicating the 1800bp fragment and 7kb vector), were prepared for sequencing; 800ng of each plasmid was sent for sequencing using the specific sequencing primers in Table 2. 23.

Table 2. 22 Double restriction enzyme digest reaction of Gibson products

Reagent	μL
Plasmid DNA	1μg
CutSmart Buffer 10x	5
NotI HF	1
BamHI HF	1
Nuclease-free water	to 50μL final volume
	Incubate at 1hr 37°C

Table 2. 23 The primers used to sequence the Gibson assembly products

Sequencing Primer	Primer Sequence 5'-3'
pMXs_IRES_GFP_F	GACGGCATCGCAGCTTGGATACAC
TRBCmid_F	CGCCACCATCCTGTACGAGAT

2.6.5 Analysis of Sequencing Results and Production of Vector for Transfection

The sequencing results were analysed using the SnapGene Viewer program and assessed for presence of the correct TCR $\alpha\beta$ sequences, including the constant genes, and V and J regions, in addition to the presence of the full P2A sequence. To produce a purer plasmid of higher yield that is suitable for mammalian cell transfection, the bacterial starter cultures from the successful clones were propagated in larger volumes for extraction of plasmid using a Midiprep kit (Qiagen). For this, 750ul of the starter culture was used to inoculate 100mls of LB media with 100 μ g/mL ampicillin. The cultures were incubated shaking at 250 rpm at 30°C for 12-16 hours, and the Midiprep Kit was used to extract up to 4 μ g of purified plasmid DNA. This was then sent for sequencing again using the same primers as above to confirm that no point mutations had occurred in the plasmid during culture.

2.7 Generation of Retroviral particles

An efficient method of gene transfer into cells is using retroviral vector infection. This allows stable expression of the gene of interest in target cells. The production of TCR-encoding retroviral particles was achieved through several steps, including the use of two retroviral packaging cell lines, PlatGP and PG13, which produce high titres of retroviral particles. Both packaging cell lines were passaged and maintained in T75 flasks in D10 media, composed of DMEM media with high L-Glutamine, with added 10% FCS and 1% PenStrep. Trypsin-EDTA (Gibco) was used every 3 days once the cells reached 90% confluence, to passage the cells 1:5.

2.7.1 Transfection of PlatGP with retroviral vector

The PlatGP cell line (Cell Biolabs) is based on the 293T cell line but produces higher titres of retroviral particles with transient transfection. They contain the gag and pol genes which are needed for packaging of the retroviral particle, but require co-transfection of an expression vector such as the pCMV_VSV-G envelope vector which encodes the Env protein that allows the produced retroviral particles to be infective. PlatGP cells were used to produce high titres of virus for storage, and for efficient subsequent transfection of a stable transfection packaging cell line.

The PlatGP cells were recovered from liquid nitrogen and cultured for 5 days before transfection. On the day before transfection, 1.6- 1.8 million PlatGP cells were plated in several wells of a 6-well plate with 2ml D10. The next day, wells which had cells that were

70-90% confluent were selected for transfection. To prepare the transfection solution, the warmed serum-free medium, Opti-MEM (Gibco), was aliquoted into FACS tubes in a volume of 200 μ l per transfection reaction. The vectors were then added; 0.5 μ g VSV-G vector and 2 μ g TCR_pMXs_IRES_GFP vector. After 5 minutes of incubation at room temperature, 7 μ l of X-tremeGENE HP Transfection Reagent (Sigma) was then added, and the solution was incubated at room temperature for 15 minutes, before transfecting the cells, distributing the solution among the target well in a dropwise manner. The cells were then returned to the incubator and the medium was replaced with 2ml fresh D10 after 18 hours. The supernatant contained retrovirus particles which could be harvested after 48hrs and 72hrs post-transfection. When harvesting the viral supernatant, the media was collected in tubes and centrifuged at 300g for 5min to pellet floating cells, before aliquoting the virus-containing supernatant and storing at -80°C.

2.7.2 Transduction of PG13 retroviral packaging cells

As PlatGP cells cannot survive for more than 3-4 days after transfection, they cannot be used as a stable source of retroviral vector production. A second, stable transfection retroviral packaging cell line, PG13, was therefore used for this purpose.

On the day before transduction, 0.3 million PG13 cells were plated in wells of a 6-well plate in order to achieve 30% confluence for transduction.

The next day, the centrifuge was warmed to 32°C and viral supernatant from PlatGP cells were thawed on ice. Once thawed, polybrene (Sigma) was added at a concentration of 6 μ g/ml to the virus and mixed. The positive charge of Polybrene neutralizes the charge on the surface of the virus and the target cell surface, so they do not repel each other, thus enhancing their contact and increasing the efficiency of transduction.

The virus-Polybrene solution was used to replace the medium of the PG13 cells in the 6-well plate. The plate was wrapped with cling-film and centrifuged at 100g at 32°C for 2hrs. The cells were returned to the incubator and after 24 hours, the media was replaced with fresh D10. The transduced cells were trypsinized from the wells 48 hours after transduction and transferred to a T75 flask. On this day, the PG13 cells can be assessed for GFP expression, indicating successful transduction with the virus. After 2 more days, the PG13 cells were passaged and a portion of the cells frozen for storage in freezing media made of 90% FBS+10% DMSO. Five days after transduction, the PG13 supernatant was harvested in the same way as the PlatGP supernatant and frozen at -80°C.

2.7.3 Transduction of target T cells for expression of antigen-specific TCR

The retroviral particles produced by the PG13 packaging cells were used to transduce TCR-deficient SKW-3 T cell line and later, primary T cells from an EBV-negative healthy donor.

2.7.3.1 Transduction of a TCR-negative T cell line

The SKW-3 T cell line (DSMZ) was used to assess the infection efficiency of the retroviral particles, and also to assess the functional ability of the expressed TCRs. These cells are deficient for TCR $\alpha\beta$, but CD4⁺ and CD8⁺ and are cell-surface negative for CD3. They possess CD3 in their cytoplasm, but these are only expressed on the surface alongside a fully formed TCR. These SKW-3 cells were therefore used as a target cell line to assess expression of transduced TCRs.

On the day before transduction, wells of a non-Tissue Culture treated 24-well-plate were coated with 1 ml of 15 μ g/ml RetroNectin solution (Clontech) and stored at 4°C overnight. On the day of transduction, the solution was removed and the wells were washed with 2ml PBS before adding 1.5ml PG13 viral supernatant to each well.

One million SKW-3 cells were transferred to each well and the plate wrapped in cling-film before centrifuging at 100g for 2hrs at 32°C. The cells were returned to the incubator. The media was replaced after 24 hours with fresh R10 media (RPMI media supplemented with 10% FCS, 1% L-glutamine and 1% PenStrep).

Two days after transduction, the SKW3 cells were analysed via flow cytometry for expression of TCR using 1.25 μ l of anti-CD3-APC-H7 and 1.5 μ l of anti-TCR $\alpha\beta$ -APC antibodies per million cells. The cells were gated on lymphocytes, singlets and then GFP, before gating for CD3 against TCR and compared to non-transduced SKW3 cells.

The cells were cultured for approximately 10 days before the GFP⁺ CD3⁺ TCR⁺ cells were sorted using the FACS Aria II, expanded, frozen, and used for assays.

2.7.3.2 Transduction of a primary T cells

In order to fully characterize the functions and killing capabilities of the transduced TCR clones, primary T cells were transduced with the EBV-specific TCRs. PBMCs from a healthy donor who had previously tested negative for responses against ZEBRA were isolated and plated at a density of 3 million cells/ml in a six-well-plate (4ml per well). The T cells were activated using CD3/CD28 Dynabeads (Thermofisher) at a 1:1 ratio for 3 days in the

presence of IL-2 (100U/ml). Transduction of the activated primary T cells was performed in the same way as the SKW-3 cell transduction, except for the addition of IL-2 (50U/ml) to each well prior to centrifugation with virus supernatant. The next day after transduction, the R10 media was replaced and supplemented with fresh IL-2 (50U/ml). The efficiency of transduction in the primary T cells were assessed 2-3 days after infection by analysing the GFP expression. The cells were then expanded for a further 10 days, with addition of 50U/ml IL-2 every two-three days, before the CD3⁺ CD8⁺ GFP⁺ T cells were sorted. The sorted cells were either used immediately for functional studies or cultured for up to 7 days. Cell numbers permitting, a portion of the cells were also cryopreserved in liquid nitrogen.

2.8 Knockdown of endogenous TCRs

siRNA was used to knock down endogenous TCR β chains in primary T cells. The siRNA was designed so it targeted only the endogenous TCR β and not the transgenic TCR. This was achieved through designing siRNA against sequences in the TCR β gene which were mismatched between the wild type TCR constant gene and the codon-optimized TCR constant genes. Three suitable siRNA sequences were used in the design of oligonucleotides (Table 2. 24) whose sequences consisted of the sense target DNA sequence joined to the antisense by a hairpin loop sequence and a poly-T transcription termination signal. These sequences were flanked by the restriction enzyme sites BamHI and HindIII.

Table 2. 24 The oligonucleotide sequences for the construction of siRNA vectors

Oligo	BamHI+ 4nt	TRBC DNA sense	loop	TRBC DNA antisense	Termination	HindIII +4nt
TRBC2F	GTCTGGATCC	GTGACTCCAGATACTGCCTG	TTCAAGAGA	CAGGCAGTATCTGGAGTCAC	TTTTTT	AAGCTTACTT
TRBC3F	GTCTGGATCC	GCCACTTCCGCTGTCAAGTC	TTCAAGAGA	GACTTGACAGCGGAAGTGGC	TTTTTT	AAGCTTACTT
TRBC4F	GTCTGGATCC	GTCCAGTTCTACGGGCTCT	TTCAAGAGA	AGAGCCCGTAGAACTGGAC	TTTTTT	AAGCTTACTT

The pRFP_C_RS_shRNA retroviral vector (Origene) was chosen for the expression of the siRNA. This is a short hairpin RNA (shRNA) vector which contains an U6 promoter to drive transcription of the siRNA gene by RNA polymerase III. The vector was prepared for cloning of the siRNA oligonucleotides by restriction enzyme digest using the BamHI and HindIII and treatment with CIP as with the pMX_IRES_GFP vector mentioned previously. The oligonucleotides arrived lyophilized (Sigma). After resuspension, they were also cut with the BamHI and HindIII enzymes to produce cohesive ends, and the fragments were ligated using T4 DNA ligase (NEB) as before. After transforming into *E. coli* DH5alpha competent cells (Thermofisher), the bacteria were plated onto LB chloramphenicol (34ug/ml) plates for selection, incubated overnight and colonies screened the following days via miniprep and sequencing. The correct vectors were transfected into the retroviral packaging cell lines PlatGP and PG13 as performed for the TCR vectors. An empty vector control was also used in parallel for each siRNA vector. Because the pRFP_C_RS_shRNA possesses a red fluorescent protein (RFP) gene, it was possible to visualise the transduction efficiency in the packaging cell lines. The viral supernatant from the packaging cells was collected and used to transduce Jurkat cells and also activated primary T cells from a healthy donor.

In order to determine the correct concentration of puromycin for selection of transduced cells, a kill curve was performed; approximately 2×10^5 non-transduced Jurkat cells in 100ul were cultured in 96 well plates in the presence of varying doses of puromycin ranging from 5-100ug/ml, and trypan blue staining was used to count the dead cells every day and compared to an untreated control. By day 2, over 85% of the Jurkat cells had died in wells with 10ug or more of puromycin, so this was used as the concentration for selection of transduced cells.

Transduced Jurkat and primary T cells were cultured for two weeks in the presence of 10ug/ml Puromycin, with the media being replaced every 2 days. Two replicates of each test were performed, and cells transduced with virus containing the empty vector were used as a mock treated control. Each day, an aliquot of cells was stained with antibodies against CD3 and TCR to assess the effect on TCR expression post-transduction. Cells were gated on lymphocytes, single cells and then on CD3 vs TCR. The MFI levels of the TCR in each siRNA test was measured and calculated as a percentage of the MFI TCR in the empty vector control on the same day.

2.9 TCR functional assays

In order to test the ability of the transduced TCR to recognise its cognate peptide and function correctly, peptide stimulation assays were performed using the ZEBRA peptide pool, and the upregulation of CD69 was analysed on the BD LSR II flow cytometer.

Autologous lymphoblastoid cell lines were produced for the antigen-presentation of peptides to the TCR clones.

2.9.1 Generation of lymphoblastoid cell lines (B cell lines)

B cell lines (BCL) were made using PBMCs from the TCR donors using an EBV-immortalization method already established in the lab.

The EBV used to infect the donor TCRs was obtained from supernatant from the B95-8 cell line. This is a lymphoblastoid cell line which was made by infecting marmoset B cells with human EBV. Supernatant containing EBV from the cell line was collected previously and cryopreserved in liquid nitrogen for future use.

Donor PBMCs were prepared to a concentration of 2×10^6 cells/ml in R10. An aliquot of 1ml of cells was kept aside to be used as a negative control for EBV transformation; in these cells no EBV was included but CpG and Cyclosporin A (Sigma) were added. To all the samples, CpG was added at a concentration of 1.5mg/ml to enhance immortalization in the presence of EBV, and Cyclosporin A was added at a final concentration of 1 μ g/ml to inhibit T cell-mediated killing of infected B cells. For the infection of donor cells, 1ml of EBV supernatant was added to every 10mls of PBMCs, before 250 μ l of the cell suspension was distributed into individual wells of a 48 well plate. The cells were incubated at 37°C for 1 week, when the R10 media had turned very yellow and the cells showed clumps when observed under the microscope at 10x magnification. A further 250 μ l of fresh R10 with 1 μ g/ml cyclosporin A was added slowly to each well, avoiding breaking up the clumps. After another week of incubation, the cells were transferred to 24 well plates in 500 μ l of fresh R10 + 1 μ g/ml Cyclosporin A. This step was repeated a week later when the cells were transferred to 12 well plates, and then to T25 flasks after another week. Transferring was performed using a disposable Pastette to avoid breaking up the clumps. A week or 10 days after culturing in T25 flasks, the cells were counted, with some being prepared for storage in liquid nitrogen, and others continued to be cultured for assays.

2.9.2 Peptide stimulation assays

The autologous BCLs were used to present the ZEBRA peptide pool to the T cell clones in order to examine the functional ability of the transduced TCRs. Initially, recognition of the cognate peptide by the TCR was assessed through upregulation of CD69 on the cell surface post co-culture with peptide-pulsed BCLs. The stimulations were performed at an Effector:Target ratio (E:T) of 2:1, with 2 million T cell clones being used per 1 million pulsed BCLs. Four replicate wells were used for each condition, with each replicate being used to analyse cells at different time points post-stimulation. The pulsing of the BCLs was performed for 1 hour at 37°C in volumes of 300ul per stimulation reaction. The cells were pulsed with 10ug/ml ZEBRA peptide pool. After 1 hour of incubation, the pulsed cells were washed 3 times in R10 and counted before 1 million pulsed BCLs were dispensed into the relevant wells of a round-bottomed 96-well plate. The T cell clones were counted and 2 million T cells dispensed into the relevant wells to a final volume of 300ul per reaction. As negative controls, BCLs on their own without peptide, in addition to BCLs pulsed with 10ug/ml irrelevant peptide, were used. PHA was used at a concentration of 5ug/ml for the positive control. PBMCs stimulated with PHA were also used as a positive control for T cell activation. Wells pre-coated with 1 µg/ml anti-CD3 OKT3 antibody and 1µg/ml anti-CD28 antibody (eBioscience) were also used as additional positive controls.

For the initial peptide stimulation assay, cells were stimulated for either 6 hours or 18 hours. At each time point, the cells from the relevant wells were transferred into FACS tubes and the wells were rinsed to capture any remaining cells before washing in 2mls of PBS and counting. The cells were stained according to the staining panel in Table 2. 25 and flow cytometry was performed to assess upregulation of CD69 on the surface of the T cells. In all subsequent peptide stimulation experiments, cells were stimulated for 18 hours before washing and staining. The cells were gated on lymphocytes, singlets, GFP+, CD8+ CD4- (as the SKW-3 line is known to be positive for both CD4 and CD8), CD3+ TCR+, then for CD69+ status. The MFI CD69 in experimental wells was compared to the background levels in the negative controls.

Table 2. 25 T cell clone activation status staining panel

Antibody	Fluorochrome	Clone	Volume per 1 x10⁶ cells (µl)
CD3	APC-H7	SK7	1.25
TCR $\alpha\beta$	APC	T10B9	1.25
CD4	PE-Cy7	SK3	0.63
CD8	BV421	RPA-T8	0.63
CD69	PE	FN50	2.5

2.10 Peptide epitope mapping

The epitope specificities of the transduced TCRs were determined using a series of peptide stimulation assays involving various peptide pools and their individual component 18mer peptides, before characterisation of specific 9mer epitopes for each ZEBRA-specific TCR.

The initial ZEBRA peptide pool consisted of 47 x 18mer peptides overlapping by 10 amino acids. In order to identify the specific peptide recognized by each TCR, 7 mini pools consisting of 6 peptides each, and a final mini pool comprised of 5 peptides were prepared with the concentration of each peptide in the pool at 30ug/ml. These 8 mini pools were used to pulse autologous BCLs for each TCR clone and the peptide stimulation and flow cytometry staining performed as above. The mini pools which induced a positive response from the T cell clones, in the form of CD69 upregulation, were split into their individual component 18mer peptides and used for another round of peptide stimulation. The individual 18mer which induced CD69 upregulation in the TCR clone was chosen for the design of 8mer, 9mer, 11mer and 13mer truncated peptides for TCR epitope mapping.

2.11 HLA-restriction assays

In order to further characterize the EBV ZEBRA-specific TCRs, the HLA restriction of each was determined. To do this, the CIV liquid nitrogen inventory was searched for BCLs from donors who had only one matching allele to TCR donors 1 and 2, outlined in Table 2. 26. For example, a BCL that was positive only for HLA- A*02:01 but negative for HLAs - A*11:01, -B*35:01, -B*49:01, -Cw*04:01 and -Cw*07:01 was used to assess whether the TCRs from donor 1 were restricted to HLA-A*02:01.

The partially histocompatible BCLs were recovered and cultured for at least 10 days before performing the peptide stimulation assays by pulsing each BCL with the ZEBRA peptide pool and assessing CD69 upregulation on the TCR clone after 18 hours co-culture.

Table 2. 26 HLA typing of TCR donors 1 and 2

Donor	TCRs	HLA-A		HLA-B		HLA-C	
1	4	A*02:01	A*11:01	B*35:01	B*49:01	Cw*04:01	Cw*07:01
2	9, 16, 34, 131, 132	A*23:01	A*31:01	B*18:01	B*40:01	Cw*03:04	Cw*07:01

2.12 Measurement of secreted cytokines in supernatant

The supernatant from all peptide-stimulation and cytotoxic killing assays were collected in 96-well plates and stored at -20°C for future analysis of secreted cytokines. These analytes were measured using U-Plex plates on the Mesoscale Discovery system (MSD, United States). This is a multiplex sandwich immunoassay system that uses specific linkers which bridge analytes in the supernatant to detection antibodies conjugated to electrochemiluminescent labels. Presence of the analytes being assayed in the sample causes spots of light to form in specific electrodes in the well, which is scanned by the MSD machine and quantified by the built-in software using to a known standard. We chose to use this MSD system to measure secreted cytokines as opposed to using a standard ELISA because this system allows the quantification of multiple analytes from one sample in a single well of a 96-well plate; we measured TNF- α , IFN- γ and IL-2 from all the samples. In addition, the MSD system has a much higher sensitivity than standard ELISAs.

2.13 Cell viability assay to assess killing by TCR-transduced primary T cells

The killing ability of primary T cells transduced with EBV ZEBRA-specific TCRs was assessed using a target cell viability assay instead of a radioactive chromium-release assay. Primary T cells from a healthy donor who had previously screened negative for responses to ZEBRA peptide pool were used for transduction. The GFP⁺ CD8⁺ sorted T cells were co-cultured for 18hours with BCLs pulsed with 10µg/ml ZEBRA peptide pool, at an E:T ratio of 2:1 in round-bottom 96-well plates. The BCLs used were autologous to the donor from which that TCR was derived. An irrelevant peptide-pulsed control was used for each TCR clone, as well as a BCL only control. After 18hrs, the cells were removed and washed in a FACS tube with PBS, before counting and staining according to the panel shown in Table 2. 27. Immediately before acquiring on the flow cytometer, 5000 counting beads were added immediately.

Table 2. 27 BCL viability assay staining panel

Antibody	Fluorochrome	Clone	Volume per 1 x10⁶ cells (µl)
CD3	APC-H7	SK7	1.25
CD19	BV421	HIB19	1.25
Live/Dead	AmCyan	-	100µl of 1µl in 1600µl dH2O dilution

After the cells were stained, washed and resuspended, 5000 CountBright Absolute Counting Beads (Invitrogen) were added to each sample and vortexed, before acquiring 5000 events gated on the beads on medium flow rate. The addition of the beads acts as an internal counting standard so that the absolute cell counts can reliably be calculated and normalized between each sample and its control. Acquiring 5000 events from each sample ensured that the same number of cells were taken up for each condition. During analysis, the cells were gated on lymphocytes and singlets, live cells, and CD19 vs CD3. The number of live BCLs present in each condition was counted and percentage cell death calculated. This was compared between cognate peptide-pulsed BCLs and irrelevant-peptide-pulsed BCLs in relation to the BCL only control. The following equation was used to calculate the % target cell death:

$$\frac{\text{BCL only} - \text{Peptide-pulsed BCL}}{\text{BCL only}} \times 100$$

2.14 Culture of the gastric carcinoma cells AGS and OE19

Gastric carcinoma cells were used as target cells in order to test the cytotoxic killing ability of the EBV-specific T cell clones. The gastric adenocarcinoma cell lines AGS and OE19 were used, in addition to their artificially infected counterparts. The latter had been infected with recombinant EBV which expressed GFP, generating AGS_rEBV_GFP and OE19_rEBV_GFP cell lines. The cell lines were gifted by Professor Xin Lu, University of Oxford. The HLA types of both the cells compared to those of the TCR donors are shown in Table 2. 28. The matched HLA-A and –B alleles are highlighted in red, indicating that these gastric cells are suitable for use as targets to TCRs restricted to the matching HLA alleles

Table 2. 28 HLA typing of donors 1 and 2, and of the gastric carcinoma cells

Donor	TCRs	HLA-A		HLA-B		HLA-C	
1	4	A*02:01	A*11:01	B*35:01	B*49:01	Cw*04:01	Cw*07:01
2	9, 16, 34, 131, 132	A*23:01	A*31:01	B*18:01	B*40:01	Cw*03:04	Cw*07:01
EBV ⁺ Gastric cell line							
	AGS	A*02:01	A*02:01	B*52:01	B*52:01	Cw*03:03	Cw*03:03
	OE19	A*01:01	A*02:01	B*18:01	B*45:01	Cw*05:01	Cw*07:01

After recovering, the gastric cells were cultured in R10 media, and passaged 1 in 5 every 2 days via trypsinization. The rEBV_GFP⁺ cell lines were similarly cultured in R10 but were supplemented with 400µg/ml of G418 (Geneticin, Gibco) to select for the rEBV_GFP-infected cells.

2.15 Treatment of gastric carcinoma cells with HDACi

In order to test the killing ability of the ZEBRA-specific T cell clones, latent infection in the rEBV-infected gastric cells was reversed using HDAC-inhibitors (HDACi). The cells were treated with either 2.5µM of CXD101 (gifted by Prof Xin Lu, Oxford University), 5µM of Chidamide, or 5µM of SAHA. DMSO was used as a negative control.

Approximately 10 x 10⁵ AGS_rEBV_GFP and OE19_rEBV_GFP cells were plated in 6mm culture dishes the day before treatment to allow the cells to adhere and grow to 50%

confluence. The next day, the media was removed, and the cells treated for 48 hours with the HDACi or DMSO. After 48 hours, the cells were dissociated with trypsin-EDTA and counted. The dissociated cells were either stained for FACS analysis immediately, or they were plated at an E:T ratio of 10:1 with T cells for functional assays. In the latter case, the gastric cells were plated in the wells of a flat-bottomed 96-well plate and left to adhere for 4-6 hours before the addition of T cell clones.

2.16 Assessing recognition and killing of HDACi-treated cells by primary T cell clones

The IncuCyte S3 Live-Cell analysis system was used to analyse the interactions between the T cell clones and the HDACi-treated gastric cells over a period of 24 hours. The cells were cultured at an E:T ratio of 10:1 and IncuCyte® Cytotox Red Reagent for counting dead cells was added to each well at the start of incubation. The treated AGS_rEBV_GFP cells were co-cultured with the HLA-A*02:01-restricted TCR4 primary T cell clones, and the HLA-mismatched control clone, TCR9. The OE19_rEBV_GFP cells were co-cultured with the TCR4 clones, in addition to the HLA-B*18:01-restricted TCR clones TCR9, TCR131 and TCR132. The IncuCyte analysis system was set up to record images of the 96 well plates at 0, 8, 12, 18 and 24 hours during the incubation, and all images were recorded at 10x magnification. After 24 hours incubation, the supernatant was removed from the wells for quantification of cytokines.

The ability of the clones to kill the target cells was assessed using the automated IncuCyte analysis software; initially the background levels of fluorescence were set according to the control wells in the plate. A GFP threshold level was set to distinguish between the GFP-low T cells and the GFP-high gastric cells; in addition to being considerably larger in cell size, the GFP levels in the gastric cells were considerably brighter than the T cells, making it easy to distinguish between the two cell types. The Cytotox Red apoptosis marker that was added to the wells at the start of co-culture was taken up by dead cells, and the overlap area of this red fluorescence with larger, very bright GFP cells was measured in μM^2 per replicate well at each set time point.

2.17 Data analysis

SnapGene software was used for analysis of DNA sequences and to verify cloning methods. Flow cytometry data was analysed on FlowJo version 10 software, and graphs were created using GraphPad Prism.

The MSD analysis system was used to assess the cytokine data from the culture supernatants. The IncuCyte analysis system was used to analyse the killing assay data involving primary T cell clones and HDACi-treated gastric carcinoma cells.

GraphPad Prism was used to perform the Wilcoxon's matched pairs signed rank test to analyse statistical significance between cell death in HDACi-treated cells and DMSO-treated cells at the same time points.

Establishment of a Single T cell Receptor Cloning Platform

3.1 Introduction

T cells are critical in the control of viral infections and malignancies. Their antigen-specific activation induces effector functions such as cytokine production and target cell killing. In some chronic viral infections and cancers however, specific effector T cells can become exhausted, resulting in their dysfunction and persistence of disease (Wherry et al., 2007). In addition, large numbers of highly reactive effector T cells might be required for control and elimination in many cases but is not possible due to tolerance mechanisms. Immunotherapies such as TCR gene therapy and adoptive T cell therapy are promising solutions for these obstacles (June et al., 2015, Ping et al., 2018, Sadelain et al., 2017). This involves transfer of the α and β genes encoding the antigen-specific $\alpha\beta$ TCR into autologous T cells, or in vitro expansion of T cells, and reinfusion into the patient. This has been shown to induce a potent protective T cell response in the case of numerous malignancies (Clay et al., 1999, Johnson et al., 2009b, Parkhurst et al., 2011, Rosenberg et al., 1994, Rapoport et al., 2015b). Efficient screening and selection of the most potent T cells is critical for the success of treatment.

A key challenge to the effective application of this approach however is the efficient isolation and cloning of full-length Ag-specific TCRs. Several variations of TCR cloning techniques currently exist in literature; traditional culture-based methods involve expansion of the Ag-specific T cells *in vitro*, which is significantly time consuming, expensive, and can lead to bias through loss of certain T cell clones or selective outgrowth of others (Heslop et al., 1996, Linnemann et al., 2013). Molecular methods on the other hand can be used to avoid long term expansion of cells and can be broadly grouped into two main approaches; analysis of bulk T cell populations, and single T cell analysis. Bulk methods can characterise TCR repertoires in large populations of cells, but the TCR α and β pairs of the TCR of interest must be determined using additional steps such as DNA barcoding during analysis, or statistical analysis, both of which can become complicated and expensive (Linnemann et al., 2013, Han et al., 2014, Howie et al., 2015, Stubbington et al., 2016). In addition, they are often unsuitable for TCR cloning purposes as their primers are usually not designed to capture the entire length of the TCR sequences, and the TCR α and β pairs cannot readily be cloned for expression.

The more conventional, single cell approach to TCR cloning on the other hand allows the convenient pairing of defined antigen-specific TCR α and β chain sequences without the need for complicated and lengthy algorithmic protocols. There are several such PCR methods, including 5' Rapid Amplification of cDNA Ends PCR (RACE- PCR) and multiplex PCR

methods (Kobayashi et al., 2013, Sun et al., 2012, Simon et al., 2014). Many limitations exist in current single cell methods, one of which is that the cells often need to be expanded in culture before isolation of antigen-specific TCRs. In addition, in many protocols the primers used are often only designed to amplify specific parts of the TCR genes, for example the CDR3 region, for repertoire analysis purposes, and are therefore unsuitable for cloning full-length TCRs (Han et al., 2014, Hu et al., 2018, Kim et al., 2012, Guo et al., 2016). Furthermore, several of these single cell approaches require RNA purification which is an additional step that can compromise the stability of the template, or they use tetramers to isolate cells specific to known antigen epitopes, which is not applicable when the aim is to identify new antigens or when the TCR and MHC restriction are unknown (Kobayashi et al., 2013, Linnemann et al., 2013). Finally, many of the TCR cloning protocols described require extensive manipulation of the TCR gene products after PCR amplification to allow cloning of full-length TCRs into vectors (Guo et al., 2016, Hu et al., 2018, Hamana et al., 2016, Kobayashi et al., 2013).

A simple and accessible platform to screen and clone paired TCR α and β genes in a streamlined way would therefore address many of the issues associated with existing protocols. Such a simplified platform will grant convenience and efficiency of TCR cloning in any basic laboratory setting, fast tracking clinical applicability by aiding the design of new TCR gene-therapies.

Significant limitations to efficacy and safety aspects concerning TCR gene therapy remain despite its great clinical promise. One of these is the potential mispairing that can occur between the α and β chains of the transgenic TCR and the endogenous TCR in the target cell. In addition to the reduced expression levels of the transgenic TCR due to competition with the endogenous TCR, this can create a scenario where new TCR pairs are generated which do not recognise the cancer target, rendering the treatment useless. Even worse, mispairing can lead to generation of TCRs which are autoreactive, creating potentially lethal consequences (van Loenen et al., 2010, Bendle et al., 2010).

There have been several reported efforts to avoid mispairing of TCRs, including engineering the transgenic TCR to pair correctly via introduction of additional disulphide bonds, and reduction of endogenous TCR expression using genomic knockout or knockdown at the RNA level (Bunse et al., 2014, Provasi et al., 2012). Several studies have shown that reducing the expression of endogenous TCR enhances the efficacy and expression levels of the transduced TCRs, avoiding mispairing and the lethal effects of potential autoreactivity (Bunse et al.,

2014, Legut et al., 2018, Ochi et al., 2011, Sun et al., 2019).

Thus, a simplified and easily applicable method of endogenous TCR knockdown would be helpful to assess the full function of cloned and transduced TCRs. Such a system would enable examination of the TCR specificity and function in primary T cells without interference from endogenous TCRs. Moreover, in clinical applications the ideal TCR gene therapy vector would incorporate a direct TCR replacement strategy, knocking down the endogenous TCRs in the target cell and replacing them with the tumour-specific TCRs for optimum therapeutic outcomes.

3.1.1 Chapter-specific aims

There were 3 key aims for this chapter of the thesis;

1. To establish a practical and efficient single TCR cloning platform
2. To utilize this platform to clone EBV ZEBRA-specific TCRs and assess their function
3. To design a method to knockdown endogenous TCR in primary T cells

3.2 Optimization of single TCR cloning method

A single cell PCR method was established in order to clone the TCR $\alpha\beta$ pairs of Ag-specific cells. To this end, various approaches were considered; these included a 5'RACE PCR method using single primers at each PCR step, and a multiplex Reverse Transcription-PCR (RT-PCR) method using several different primers in the RT-PCR step.

3.2.1 The 5'RACE PCR method

In order to establish our single TCR cloning method, we evaluated a recently published 5'Rapid amplification of cDNA ends (RACE) PCR approach for its suitability for our platform (Kobayashi et al., 2013). The authors claimed that this method could successfully clone and express single antigen-specific TCRs within 10 days, which was desirable as we wished to set up a fast and reliable TCR cloning method in our lab. The 5'RACE PCR method, outlined in Figure 3. 1, involves several steps to amplify the variable, diversity, joining and constant (VDJC) gene regions of the TCR genes. The resulting nested PCR products were analysed on a 1% agarose gel (Figure 3. 2) and products of approximately 500 base pairs (bp) were purified and sent for sequencing. The primers and conditions used for the PCR are outlined in Appendix 1.

We largely followed the method outlined by Kobayashi et al (Kobayashi et al., 2013), with the aim to initially establish the protocol on a larger number of T cells to maximise the sensitivity before translating it to the single T cell level. Initially, RNA extracted from 1 million PBMCs was used to produce cDNA using a stand-alone reverse transcription reaction. In parallel, RT primers specific for the cellular enzyme Glyceraldehyde 3-phosphate dehydrogenase (GAPDH) were used as a positive control for the reverse transcriptase reaction. A poly-G tailing reaction was performed on the newly synthesised cDNA, and various volumes of this were used as a template for the 1st PCR step. Following a final nested PCR step, the resulting product was analysed for the presence of a ~650-700bp product. As evident from the gel shown in Figure 3. 2 two TCR- α products and one TCR- β product can be seen (500-700bp). These products were sequenced and analysed using the V-Quest Alignment tool on the International ImmunoGenetics (IMGT.org) database. The sequencing results for these bands however showed incomplete sequences; the alignment of a representative incomplete TCR β sequence is shown in Figure 3. 3.

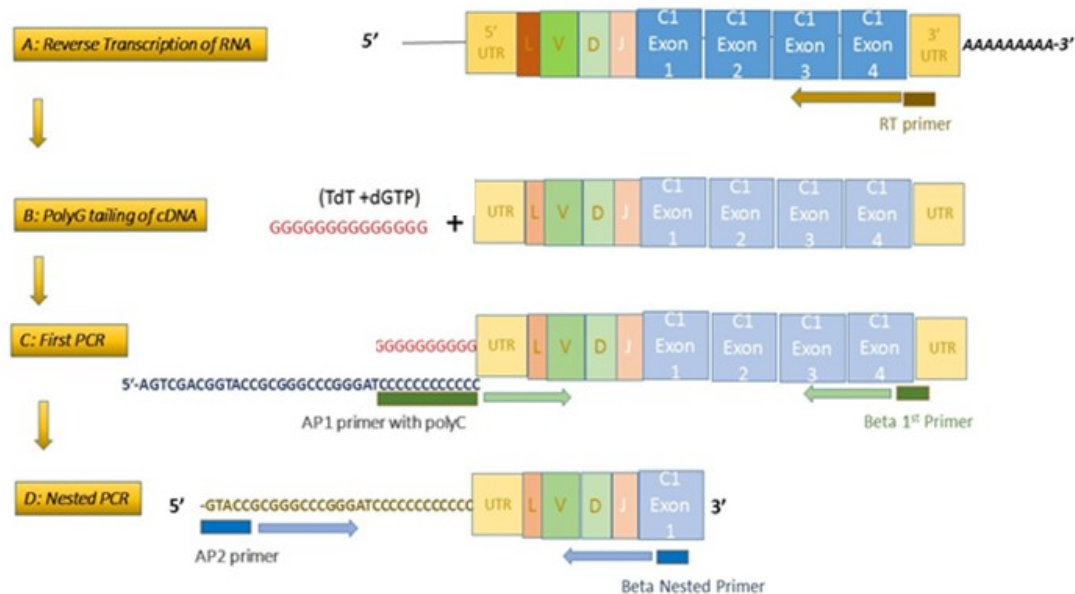


Figure 3. 1 Schematic of 5'RACE PCR Method

The series of steps comprising the 5'RACE PCR method for TCR amplification based on (Kobayashi et al., 2013) are shown. On the left, in the yellow boxes, are the different reactions at each step. The gene regions of the TCR beta chain mRNA/cDNA are shown; composed of the leader, variable, diversity and joining (LVDJ) genes, and a known constant gene with 4 exons. The primer binding locations for the RT and PCR steps are shown, indicating a single RT primer for the transcription of TCR cDNA from single cell mRNA (Step A), followed by addition of the poly-G tail (Step B), and the first PCR using a universal AP1 primer and 1st reverse primer (Step C), and the final nested PCR (Step D) whose reverse primers bind at exon 1 of the constant gene.

All primer sequences and PCR conditions are based on those published by (Kobayashi et al., 2013), and are listed in Appendix 1.

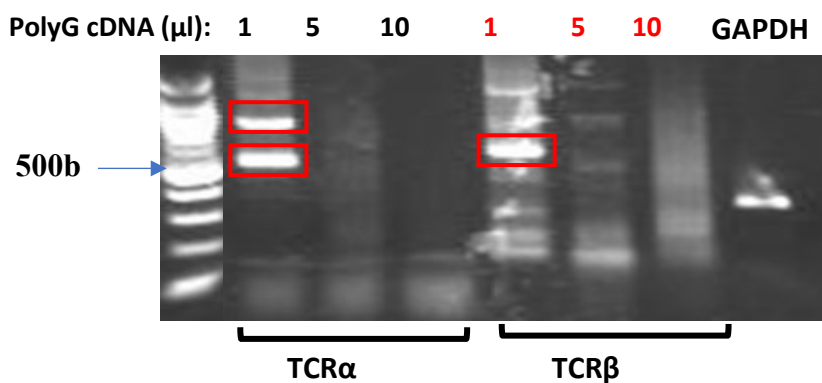


Figure 3. 2 Agarose gel showing 5'RACE PCR products

Total RNA was extracted from 1×10^6 TCR donor PBMCs, cDNA produced, and PCRs performed. GAPDH was used as a positive control, product at approximately 400 bp. The TCR α and β chain products at approximately 500bp and 700bp are outlined in red. Various starting quantities of polyG-tailed cDNA (1, 5 or 10 μ l) were used as template for the reverse transcription reactions. Figure representative of 3 different experiments.

Reference_TRB	-----atgggcaccagcctcctctgctggatggccctgtgtctcctggggg	46
TCRb_PCR_Product	----- -----	60
Reference_TRB	cagatcacgcagatactggagctctccagaaccccagacacaagatcacaagaggggac	106
TCRb_PCR_Product	GGCCCGGATCCCCCCCCCCCCCTCCTCAATCCTAGACACAAGATCACAAAGAGGGGAC * **** ** ** *****	120
Reference_TRB	agaatgtaacttttcaggtgtgatccaatttctgaacacaaccgcctttatttggtagccgac	166
TCRb_PCR_Product	AGAATGTAACTTTTCAGGTGTGATCCAATTTCTGAACACAACCGCCTTTATTGGTACCGAC *****	180
Reference_TRB	agaccctggggcagggcccagagtttctgacttacttccagaatgaagctcaactagaaa	226
TCRb_PCR_Product	AGACCTGGGGCAGGGCCAGAGTTTCTGACTTACTTCCAGAATGAAGCTCAACTAGAAA *****	240
Reference_TRB	aatcaaggctgctcagtgatcggttctctgcagagaggcctaagggatctttctccacct	286
TCRb_PCR_Product	AATCAAGGCTGCTCAGTGATCGGTTCTCTGCAGAGAGGCCTAAGGGATCTTTCTCCACCT *****	300
Reference_TRB	tggagatccagcgcacagagcagggggactcggccatgtatctctgtgccagcagcttag	346
TCRb_PCR_Product	TGGAGATCCAGCGCACAGAGCAGGGGGACTCGGCCATGTATCTCTGTGCCAGCAGCCCC- *****	359
Reference_TRB	cgggacagggggctgaacactgaagctttctttggacaaggcaccagactcacagttgta	406
TCRb_PCR_Product	-----CAGCCGACTGAAGCTTCTTTGGACAAGGCACCAGACTCACAGTTGTA * * *****	407
Reference_TRB	gaggacctgaacaaggtgttcccacccagggctcgtgtgtttgagccatcagaagcagag	466
TCRb_PCR_Product	GAGGACCTGAACAAGGTGTCCCACCCGAGGTCGCTGTGTTGAGCCATCAGAAGCAGAG *****	467
Reference_TRB	atctcccacacccaaaaggccacactggtgtgcctggccaca	508
TCRb_PCR_Product	ATCTCCACACCCAAAAGGCCACACTGGTGTGCCTGGCCACA	509

Figure 3. 3 Partial TCR beta sequence obtained from 5'RACE PCR

A representative partial TCR-β VDJC gene sequence obtained from the 5'RACE PCR is aligned against a reference TCR-β gene sequence from the IMGT.org database. The alignment shows an incomplete V-region sequence. The yellow highlighted dashes and missing asterisks indicate the absent leader sequence in the V-region in the TCR-β PCR product compared to the reference sequence. The asterisks indicate matching nucleotide base pairs between the PCR product sequence and the reference sequence. CDR3 region is highlighted in blue.

As shown by the sequence in Figure 3. 3, the variable region of the TCR β chain is incomplete because the leader sequence is missing, as indicated by the yellow highlighted dashes at the start of the TCR β PCR product sequence. This suggests that the full mRNA sequence of the TCR chains were not transcribed all the way to the 5' end during cDNA synthesis, resulting in incomplete TCR gene sequences. We therefore sought to establish an alternative single TCR cloning protocol which could amplify full-length TCRs suitable for a universal single T cell cloning platform.

3.2.2 The Multiplex RT-PCR method for single TCR cloning

Full-length paired TCR genes from single cells were successfully amplified using a multiplex RT-PCR method. In contrast to the single primer steps of the 5'RACE PCR protocol, the multiplex RT-PCR uses 41 TCR α and 39 TCR β forward primers which target all the known leader (L) sequences of the variable region gene families listed on the IMGT.org database. In addition to these, single gene-specific reverse primers were used to target the TCR α and - β constant genes. This method is based on that published by Hamana et al. (Hamana et al., 2016), but with modified, novel 3rd PCR primers to suit our chosen cloning system. The published method entails an RT-PCR step using a primer mix containing all the TCR α and β leader-specific forward primers, and single reverse primers against the constant regions of the TCR α and β genes. The TCR leader-specific forward primers have universal adapter sequences in their 5' ends which enable binding of a single TCR α or β forward primer in the next step, irrespective of the TCR sequence itself.

The second PCR step specifically amplifies the TCRs using single TCR α and β forward primers. Once again, single reverse primers specific for the constant regions of the TCR α or β genes are used, enabling amplification of the entire LVDJC region of the TCRs. A third PCR step is performed using the second PCR product as a template. In our method, new primers were designed for this step, such that cloning sites were incorporated for downstream cloning into a retroviral vector. The product of the third PCR was purified for sequencing and cloning. All the primers, reagents and PCR conditions and protocols are detailed in the Materials and Methods chapter.

To test the sensitivity and efficiency of this PCR method in our hands, we first established it using RNA obtained from 1 million Jurkat cells and 1 million PBMCs. For both cell types, the TCR α and β genes were successfully amplified, shown as bands of approximately 550bp in Figure 3. 4, which represents the products of the 3rd PCR step.

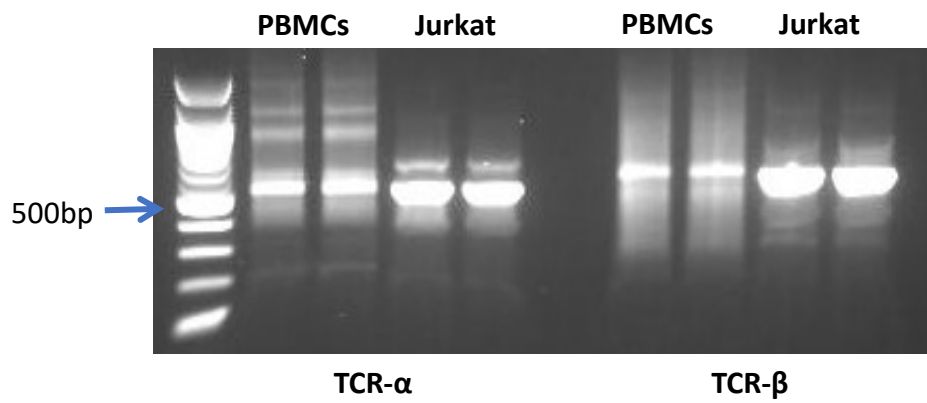


Figure 3. 4 Amplification of TCR α and β genes from PBMCs and Jurkat cells

A 1% TBE agarose gel showing the products of the PCR on DNA from 1 million PBMCs and 1 million Jurkat cells. TCR α and β products are present at ~550bp.

As the PCRs had successfully amplified DNA from 1 million Jurkat cells and PBMCs, we assessed its sensitivity on sorted cells, ranging from 100 sorted cells per well to single-sorted cells per well. Prior to sorting, the cells were rested overnight at 37°C and stained with Live/Dead stain, anti-CD3 and anti-TCR antibodies. In each well, 100, 20, 4, or single cells were sorted into 2µl RNase inhibitor-containing lysis buffer, and control wells were kept empty with no cells added. After sorting, PCR was performed, and the products were run on a 1% agarose TBE gel. The PCR method successfully amplified both TCR α and β genes from Jurkat cells and primary T cells (Figure 3. 5). The gels indicate that for both cell types, strong and defined products are produced from most of the wells, regardless of the number of cells they contained. Overall, the Jurkat cell products are cleaner than the primary T cells product. This may be explained by the monoclonal nature of the cell line which only express TCRs composed of the TRAV8-4, TRAJ3, TRBV12-3 and TRBJ1-2 TCR genes (Redmond et al., 2016). This contrasts with the polyclonal nature of the primary T cells, which could have resulted in more non-specific products. The efficiency of amplification of TCRs from single cells is approximately 75% in both cell types.

To test the specificity and accuracy of the PCR method, the DNA sequences from the single Jurkat cell PCR products were compared to reference Jurkat cell TCR α and β sequences published on the NCBI GeneBank database. Both sequences were aligned on the online sequence alignment software, Clustal Omega (ebi.ac.uk/Tools/msa/clustalo/), and analysed on IMGT.org for TCR α and β gene family usage and statistics. As indicated by the asterisks in the alignments in Figure 3. 6 and Figure 3. 7, the sequences of the Jurkat cell TCR α or β genes amplified by the PCR method matched exactly to that of the known Jurkat TCR DNA sequences and amino acids. This indicates excellent fidelity of the PCR method and supports its reliability when amplifying unknown antigen-specific TCR genes.

Reference_Jurkat	atgctcctgctgctcgtcccagtgctcgaggtgatttttacctgggaggaaccagagcc	60
Jurkat_PCR	atgctcctgctgctcgtcccagtgctcgaggtgatttttacctgggaggaaccagagcc *****	60
Reference_Jurkat	cagtcggtgaccagcttggcagccacgtctctgtctctgaaggagccctggtctgctg	120
Jurkat_PCR	cagtcggtgaccagcttggcagccacgtctctgtctctgaaggagccctggtctgctg *****	120
Reference_Jurkat	aggTGcaactactcatcgtctgttccaccatatctcttctggatgtgcaataccccaac	180
Jurkat_PCR	aggTGcaactactcatcgtctgttccaccatatctcttctggatgtgcaataccccaac *****	180
Reference_Jurkat	caaggactccagcttctcctgaagtacacatcagcggccaccctggtaaaggcatcaac	240
Jurkat_PCR	caaggactccagcttctcctgaagtacacatcagcggccaccctggtaaaggcatcaac *****	240
Reference_Jurkat	ggttttgaggtgaatttaagaagagtgaacctccttccacctgacaaaacctcagcc	300
Jurkat_PCR	ggttttgaggtgaatttaagaagagtgaacctccttccacctgacaaaacctcagcc *****	300
Reference_Jurkat	catatgagcgcgcggctgagtacttctgtgctgtgagtgatctcgaaccgaacagcagt	360
Jurkat_PCR	catatgagcgcgcggctgagtacttctgtgctgtgagtgatctcgaaccgaacagcagt *****	360
Reference_Jurkat	gcttccaagataatctttggatcagggaccagactcagcatccggccaaatatccagAAC	420
Jurkat_PCR	gcttccaagataatctttggatcagggaccagactcagcatccggccaaatatccagAAC *****	420
Reference_Jurkat	cctgacctgccggtgtaccagctgagagactcTaaatccagtgacaagtctgtctgccta	480
Jurkat_PCR	cctgacctgccggtgtaccagctgagagactcTaaatccagtgacaagtctgtctgccta *****	480
Reference_Jurkat	ttcaccgattttgattctcaacaaatgtgtcacaagtaaggattctgatgtgtataTc	540
Jurkat_PCR	ttcaccgattttgattctcaacaaatgtgtcacaagtaaggattctgatgtgtataTc *****	540
Reference_Jurkat	acagacaaaactgtgctagacatgaggtctatggacttcaagagcaacagtgctgtggcc	600
Jurkat_PCR	acagacaaaactgtgctagacatgaggtctatggacttcaagagcaacagtgctgtggcc *****	600
Reference_Jurkat	tggagcaacaaatctgactttgcatgtgcaaacgccttcaacaacagcattattccagaa	660
Jurkat_PCR	tggagcaacaaatctgactttgcatgtgcaaacgccttcaacaacagcattattccagaa *****	660
Reference_Jurkat	gacaccttcttcccagcccagaaagttcctgtgatgtcaagctggtcgagaaaagcttt	720
Jurkat_PCR	gacaccttcttcccagcccagaaagttcctgtgatgtcaagctggtcgagaaaagcttt *****	720
Reference_Jurkat	gaaacagatacgaacctaaactttcaaaaacctgtcagtgattgggttccgaatcctcTc	780
Jurkat_PCR	gaaacagatacgaacctaaactttcaaaaacctgtcagtgattgggttccgaatcctcTc *****	780
Reference_Jurkat	ctgaaagtggccgggttaaatctgctcatgacgctgCGGctgtggtccagc-	831
Jurkat_PCR	ctgaaagtggccgggttaaatctgctcatgacgctgCGGctgtggtccagc *****	832

Figure 3. 6 Jurkat cell TCR- α PCR product sequence alignment

Sequence alignments from published Jurkat TCR- α sequence (upper reference Jurkat sequence) compared to Jurkat PCR product (lower sequence). The asterisks under each pair of bases indicate a match between both PCR and reference sequence nucleotide bases.

Reference_Jurkat	atggactcctggaccttctgctgtgtgtccctttgcatcctgtagcgaagcatacacagat	60
Jurkat	atggactcctggaccttctgctgtgtgtccctttgcatcctgtagcgaagcatacacagat	60

Reference_Jurkat	gctggagttatccagtcaccccgccatgaggtgacagagatgggacaagaagtgactctg	120
Jurkat	gctggagttatccagtcaccccgccatgaggtgacagagatgggacaagaagtgactctg	120

Reference_Jurkat	agatgtaaaccaatttcaggccacaactccctttctggtacagacagaccatgatgctg	180
Jurkat	agatgtaaaccaatttcaggccacaactccctttctggtacagacagaccatgatgctg	180

Reference_Jurkat	ggactggagttgctcatttactttaacaacaacgttccgatagatgattcagggatgcc	240
Jurkat	ggactggagttgctcatttactttaacaacaacgttccgatagatgattcagggatgcc	240

Reference_Jurkat	gaggatcgatttctcagctaagatgcctaataatgcatcatttctccactctgaagatccagccc	300
Jurkat	gaggatcgatttctcagctaagatgcctaataatgcatcatttctccactctgaagatccagccc	300

Reference_Jurkat	tcagaaccaggactcagctgtgtacttctgtgccagcagtttctcgacctgttccggct	360
Jurkat	tcagaaccaggactcagctgtgtacttctgtgccagcagtttctcgacctgttccggct	360

Reference_Jurkat	aactatggctacaccttcggttcggggaccaggttaaccgtttagaggacctgaacaag	420
Jurkat	aactatggctacaccttcggttcggggaccaggttaaccgtttagaggacctgaacaag	420

Reference_Jurkat	gtgttcccaccagggtcgctgtgtttgagccatcagaagcagagatctcccacaccaa	480
Jurkat	gtgttcccaccagggtcgctgtgtttgagccatcagaagcagagatctcccacaccaa	480

Reference_Jurkat	aaggccacactggtgtgcctggccacaggcttcttccccaccagctggagctgagctgg	540
Jurkat	aaggccacactggtgtgcctggccacaggcttcttccccaccagctggagctgagctgg	540

Reference_Jurkat	tgggtgaatgggaaggaggtgcacagtggtgagcagacagaccgcagccctcaaggag	600
Jurkat	tgggtgaatgggaaggaggtgcacagtggtgagcagacagaccgcagccctcaaggag	600

Reference_Jurkat	cagccccctcaatgactccagatactgctgagcagccgctgagggctctcggccacc	660
Jurkat	cagccccctcaatgactccagatactgctgagcagccgctgagggctctcggccacc	660

Reference_Jurkat	ttctggcagaacccccgaaccacttccgctgtcaagtccagttctacgggctctcggag	720
Jurkat	ttctggcagaacccccgaaccacttccgctgtcaagtccagttctacgggctctcggag	720

Reference_Jurkat	aatgacgagtgaccaggatagggccaaaccgctcaccagatcgtcagcgccgaggcc	780
Jurkat	aatgacgagtgaccaggatagggccaaaccgctcaccagatcgtcagcgccgaggcc	780

Reference_Jurkat	tgggtagagcagactgtggctttacctcgggtgcctaccagcaaggggtcctgtctgcc	840
Jurkat	tgggtagagcagactgtggctttacctcgggtgcctaccagcaaggggtcctgtctgcc	840

Reference_Jurkat	accatcctctatgagatcctgctaggaaggccaccctgtatgctgtgctggcagcgcc	900
Jurkat	accatcctctatgagatcctgctaggaaggccaccctgtatgctgtgctggcagcgcc	900

Reference_Jurkat	cttgtgtgatggccatggtcaagagaaaggatttc	936
Jurkat	cttgtgtgatggccatggtcaagagaaaggatttc	936

Figure 3. 7 Jurkat cell TCR-β PCR product sequence alignment

Sequence alignments from published Jurkat TCR-β sequence (upper reference Jurkat sequence) compared to Jurkat PCR product (lower sequence). The asterisks under each pair of bases in indicate a match between both PCR and reference sequence nucleotide bases.

Paired TCR α and β gene products obtained from single-sorted primary T cells were assessed to determine whether the PCR method could amplify a wide range of TCR gene families. The sequences in Table 3. 1 indicate that this method can amplify a wide variety of TCR gene families and that the sequences are complete, including the entire V, J and CDR3 regions.

Table 3. 1 TCR α and β genes sequenced from single-sorted primary T cells

T cell	TCR- α V region	TCR- α J region	TCR- α CDR3	TCR- β V region	TCR- β V region	TCR- β CDR3
1	TRAV8*4*01	TRAJ33*01	CAVSDQGNVQLIW	TRBV10-3*03	TRBJ1-1*01	CAISGSRNTEAFF
2	TRAV6*01	TRAJ2*01	CAVSRHTFDGVDIF	TRBV8*01	TRBJ1-1*01	CVAGTAPKGYWF
3	TRAV4*01	TRAJ22*01	CLVGPTLSARQLTF	TRBV20-1*02	TRBJ1-2*01	CSARGTPEKGYTF
4	TRAV13*01	TRAJ30*01	CAASMNRRDDKIIF	TRBV18*01	TRBJ1-2*01	CASSQESYGYTF
5	TRAV21*02	TRAJ48*01	CAVSAGNEKLTFF	TRBV7-9*03	TRBJ1-1*01	CASSRALEAFF
6	TRAV8-6*02	TRAJ23*01	CAVSRSNQGGKLIF	TRBV28*01	TRBJ2-1*01	CASRVPLXDEYFF
7	TRAV8-6*02	TRAJ40*01	CAVSDQGTQYKIF	TRBV3-1*01	TRBJ1-2*01	CASGTGVGYTF
8	TRAV4*01	TRAJ8*01	CLQNAFQKLVF	TRBV12-3*01	TRBJ1-2*01	CASSFSTNYGYTF
9	TRAV8-6*02	TRAJ23*01	CAVSRSNQGGKLIF	TRBV3-1*01	TRBJ1-2*01	CASSQSTGVGYTF
10	TRAV21*02	TRAJ4*01	CAVRPLIYGYNKLIFF	TRBV28*01	TRBJ2-3*01	CASSLPGYTTQYF
11	TRAV24*01	TRAJ24*02	CALPWGWGKLFQ	TRBV6-4*01	TRBJ1-1*01	CASSDTGNTTEAFF

Therefore, this single TCR PCR protocol can amplify full-length Jurkat cell TCR α and β genes correctly without mutations and is also proficient at amplifying numerous TCR genes from primary T cells in a polyclonal population.

We next applied this multiplex PCR method to amplify TCRs specific to the EBV lytic stage antigen, ZEBRA. Future experiments were designed with the aim of utilizing the single TCR cloning method to isolate and express antigen-specific TCRs in target T cells.

3.2.3 Design and verification of novel cloning primers

In order to clone the paired TCR genes into our chosen vector for expression in target cells, novel cloning primers were designed to be used in the third PCR in place of the original published primers. New primers were designed for TCR α forward, TCR β forward and TCR β reverse. These new primers add the relevant sequences to enable direct and seamless cloning into our chosen vector. The TCR α reverse primer was not changed as it was still compatible with our new protocol.

The third PCR primers were designed to enable any purified PCR product to be directly assembled into the retroviral vector pMX_IRES_GFP for expression studies. Table 3. 2 shows the sequences of the original, published primers, compared to the new primers used in our protocol. The PCR efficiency of the new cloning primers was confirmed and compared to the published primers (Figure 3. 8).

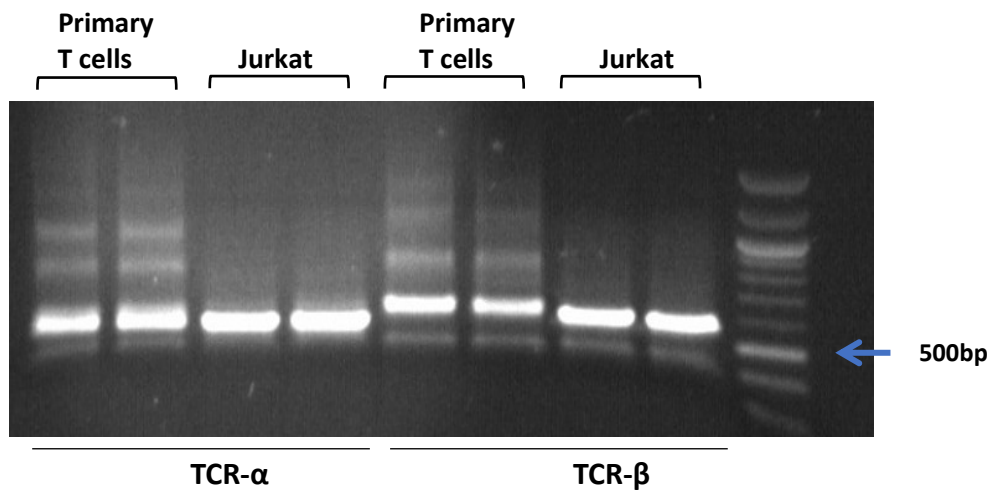
Table 3. 2 The sequences of the original 3rd PCR primers and our novel 3rd PCR primers

Primer	Original 3 rd PCR primers	New 3 rd PCR Cloning primers
TCR α F	TGGAGGAGAACCCTGGACCT	GTTGAAGCAGGCTGGAGACGTGGAGGAGAACCCTGGACCT
TCR α R ¹	GGTGAATAGGCAGACAGACTT	GGTGAATAGGCAGACAGACTT
TCR β F	GTGGCCAGGCACACCAGTGT	GACCATCCTCTAGACTGCCGGATCTAGCTAGTTAATTAAGTG- GCGCCGGAATTAGATCTCTCGAGAAGGATCCGAATTCCTGC- GG
TCR β R	AAGGATCCGAATTCCTGCAGG	GTGGCCAGGCACACCAGTG

¹ TCR α Reverse primer has not been changed from the original published primer sequence

The novel cloning primers produced PCR products which were stronger and more defined on the agarose gel compared to the published primers (Figure 3. 8). In particular, the amplification efficiency of the TCR- α gene from primary T cells had increased dramatically, as demonstrated by the brighter bands. This confirmed that the novel cloning primers could be used successfully to prepare the TCR genes for direct cloning into the vector.

A. New primers



B. Original Primers

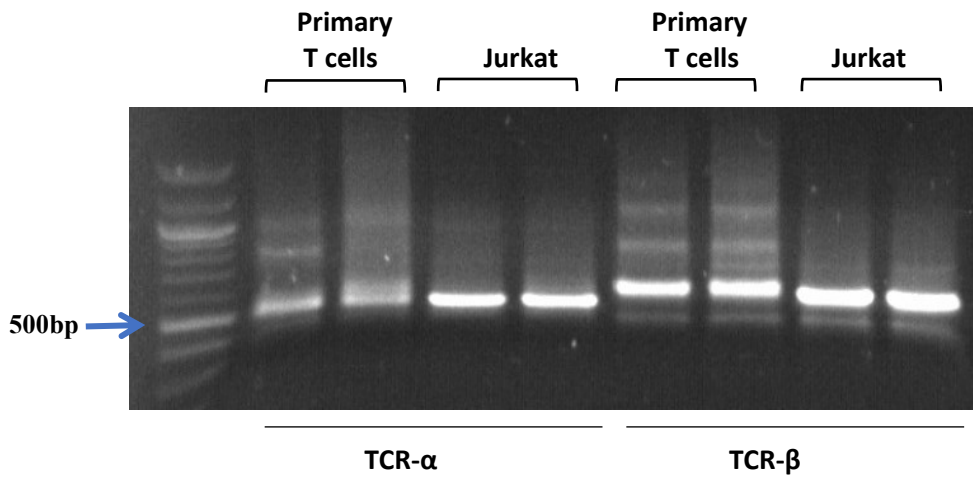


Figure 3. 8 PCR efficiency of new cloning primers

The novel PCR primers (A) were tested alongside the original PCR primers (B) to confirm the efficiency of PCR on single-sorted cells.

3.3 Proof of concept of our single TCR cloning platform

In order to test our single TCR cloning system in its ability to clone antigen-specific TCR pairs, and retain their functional ability in target cells, EBV-specific T cells were used as a proof of concept. We aimed to isolate and express TCRs specific to the EBV lytic stage antigen ZEBRA and test their functions. In addition to enabling assessment of the efficiency of our platform to accurately clone single TCRs, this would also permit evaluation of the suitability of the EBV-specific TCRs as a potential immunotherapy for EBV-associated cancers.

3.3.1 Screening PBMCs for IFN- γ responses to EBV ZEBRA antigen

In order to obtain EBV-specific TCRs for cloning, whole blood was obtained from healthy donors in the lab and their PBMCs were tested for IFN- γ responses towards the EBV lytic stage antigen, ZEBRA. A pool of overlapping ZEBRA peptides, 18mers overlapping by 10 amino acids (Appendix 2), was used to stimulate the PBMCs for 24 hours in an IFN- γ ELISpot. This screening experiment was performed by Dr. Michael Liu in the CIV lab. Out of 11 healthy donors in the lab, two donors, HC3 and HC11 showed IFN- γ responses towards the ZEBRA peptide (Figure 3. 9). Fresh PBMCs from these two donors were later obtained for further stimulation and single cell sorting.

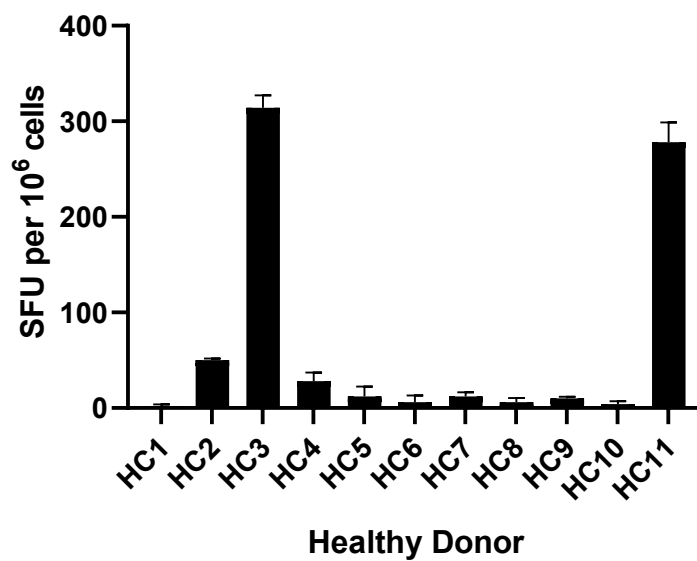


Figure 3. 9 Screening of healthy donors via IFN- γ ELISpot for reactivity against EBV ZEBRA

PBMCs from 11 healthy donors were screened for responses to the EBV immediate early lytic antigen ZEBRA. IFN- γ ELISpots were performed on the stimulated cells and the number of spot forming units (SFU) per 1 million cells was determined. Data shows the mean of 3 replicate wells with error bars representing SEM. HC= Healthy control/donor

3.3.2 Isolation and single-cell sorting of EBV ZEBRA-specific CD8⁺ T cells

PBMCs from the two healthy donors HC3 and HC11 (hereafter referred to as TCR donors 1 and 2, respectively) who showed positive IFN- γ responses towards the EBV ZEBRA pool were selected for the isolation of ZEBRA-specific T cells. The IFN- γ capture assay from Miltenyi Biotech was used to specifically label IFN- γ producing T cells after peptide stimulation. This enabled identification of live IFN- γ -producing cells without the need for intracellular cytokine staining, which requires permeabilization and fixation of the cells, thus resulting in cell death. For the single TCR cloning PCRs, cells must be alive and intact, with no degradation of their RNA.

For the isolation of ZEBRA-specific T cells, fresh PBMCs were obtained from the donors and stimulated for 6 hours with 2 $\mu\text{g/ml}$ of ZEBRA peptide pool. The stimulated cells were stained with live/dead stain, followed by anti-IFN- γ , anti-CD3, anti-CD4 and anti-CD8 antibodies as per the protocol provided in the kit. The manufacturer's protocol was largely followed except for the use of the magnetic column sorting, which was omitted as we found it to be unsuitable for our purpose due to low starting numbers of IFN- γ producing cells. The cells were single-cell sorted according to the gating strategy in Figure 3. 10, into wells of 96-well PCR plates preloaded with 2 μl fresh RNase-inhibiting lysis buffer. Up to two 96-well plates of single-sorted CD4⁻ CD8⁺ IFN- γ ⁺ T cells were obtained for each TCR donor, and the sorted plates were immediately frozen at -80°C.

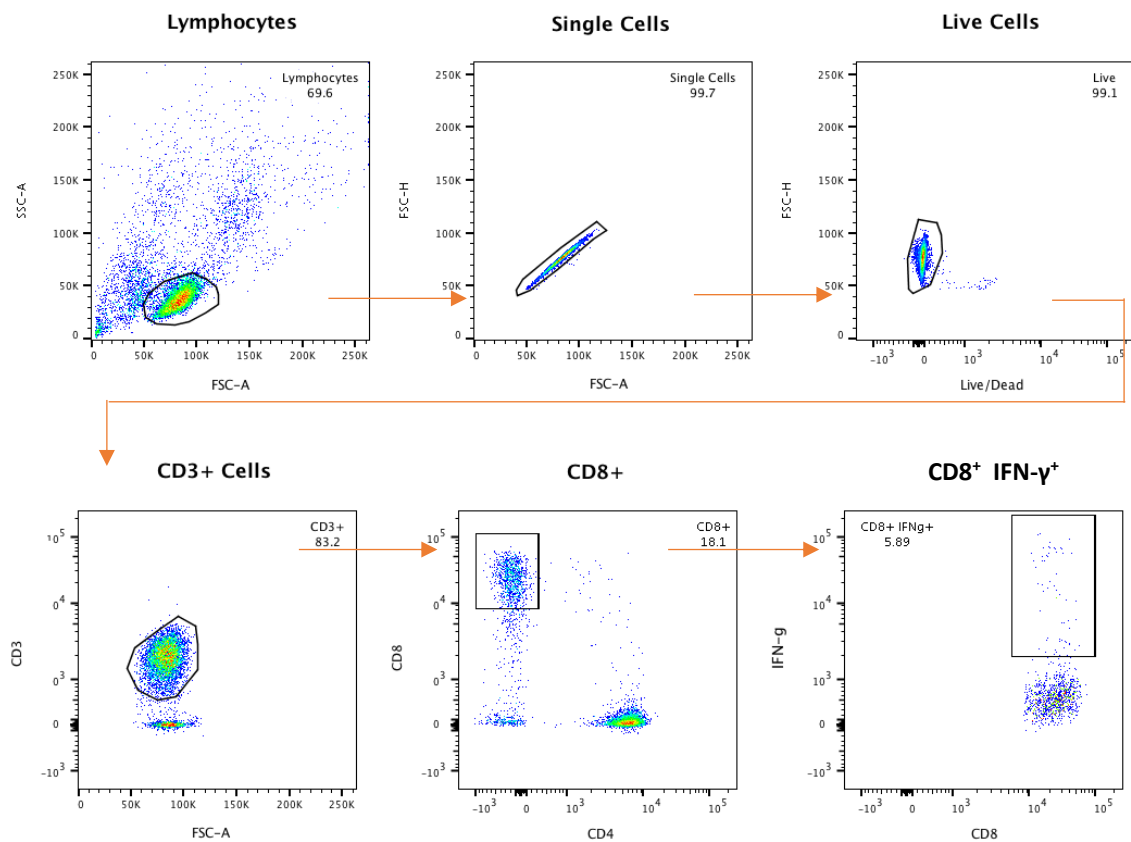


Figure 3. 10 Gating strategy for single-cell sorting of peptide-specific CD8⁺ T cells

After stimulation with ZEBRA peptide pool, IFN- γ capture assay and staining, PBMCs were first gated on lymphocytes and singlets, before live cells were gated on CD3⁺ cells, followed by CD8⁺ CD4⁻ cells, and finally CD8⁺ IFN- γ ⁺ cells for single cell sorting into 96-well PCR plates. Percentage population of each gate is shown.

3.4 PCR and sequencing of EBV ZEBRA-specific T cells

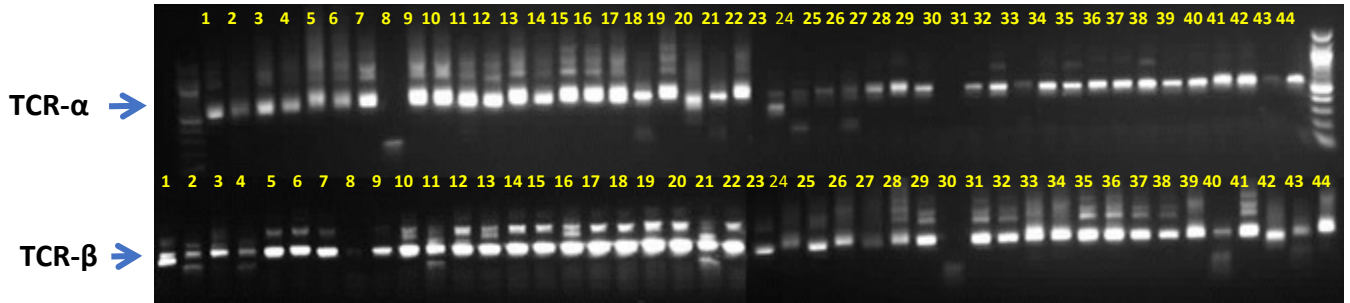
The multiplex PCR method was performed on the single-sorted cells, and the products were run on agarose gels for visualization (Figure 3. 11). The method was able to achieve between 75% to 95% paired TCR α and β amplification products from a single T cell, which is one of the highest reported efficiencies compared to other methods in the literature, which range from 50% to 90% (Han et al., 2014, Simon et al., 2014, Hamana et al., 2016, Kobayashi et al., 2013). The TCR products were purified and sequenced to verify the presence of cloning sites and of productive TCR gene sequences.

The sequencing results were evaluated using the sequence analysis program on IMGT.org for information on TCR α and β gene family usage. This program aligns the input TCR sequence against all the known TCR genes in its database and determines which TCR V and J family the TCR gene product belongs to. In addition, the CDR3 region at the junction of these regions is also determined, alongside statistics on any mutations compared to the database sequences.

Approximately 100 single TCR products were sent for sequencing from each donor, and of these, the majority had sequences which showed productive paired TCR α and β sequences. A few sequences however showed unproductive sequences in one or both TCR genes. This may have been due to degradation of the RNA template or poor quality of the purified PCR products. These non-productive genes were excluded from the repertoire analysis as they did not represent successful paired TCR gene products.

The paired TCR α and β genes from each donor were ranked according to frequency and thus clonal dominance (Table 3.3. and Table 3.4). TCR sequences which were only found in one T cell were not included in these tables. The full details of the repertoire of sequenced TCRs from both donors are listed in Appendices 3 and 4.

A



B

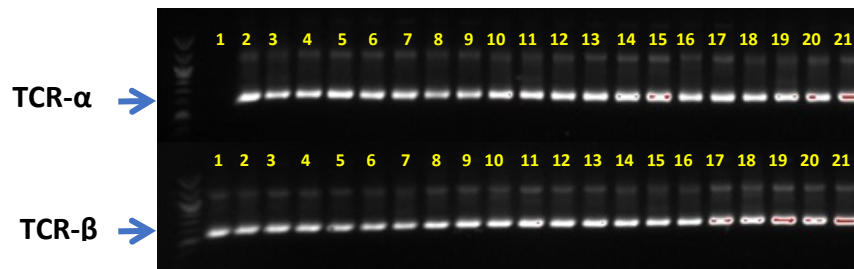


Figure 3. 11. Single EBV ZEBRA-specific TCR PCR products from TCR donors

Representative gels of the 3rd PCR step products showing a selection of paired TCR gene products from TCR donors 1 and 2 (A and B, respectively). The 500bp mark is shown by arrows, all well-defined PCR products at ~550bp were purified and sequenced.

Table 3. 3. Single EBV ZEBRA-specific TCRs from TCR Donor 1

TCR	TRAV	TRAJ	CDR3 α	TRBV	TRBJ	CDR3 β	% ¹
1	TRAV1-2*01	TRAJ6*01	CAVLSSGGSYIPTF	TRBV12-3*01	TRBJ1-2*01	CASSFSTCSANYGYTF	21
10	TRAV3*01	TRAJ13*02	CAVRDYNSGGYQKVTF	TRBV10-3*02	TRBJ1-5*01	CASSTGDSNQPQHF	13
4	TRAV20*02	TRAJ24*02	CAFFSWGKQLQF	TRBV3-1*01	TRBJ1-2*01	CASSQSPGTGVGYTF	13
7	TRAV8-6*02	TRAJ40*01	CAVSDQGTYKYIF	TRBV10-3*02	TRBJ1-5*01	CASSTGDSNQPQHF	6
2	TRAV4*01	TRAJ8*01	CLQNAFQKLVF	TRBV10-3*02	TRBJ1-5*01	CASSTGDSNLPQHF	6
16	TRAV3*01	TRAJ13*02	CAVRDYNGNGYQKVTF	TRBV28*01	TRBJ2-1*01	CASRVPGNLDEQFF	5
19	TRAV3*01	TRAJ13*02	CAVRDYNSGGYQKVTF	TRBV12-3*01	TRBJ1-2*01	CASSFSTCSANYGYTF	5
3	TRAV8-6*02	TRAJ40*01	CAVSDQGTYKYIF	TRBV12-3*01	TRBJ1-2*01	CASSFSTCSANYGYTF	4
17	TRAV8-4*01	TRAJ3*01	CAVSDLEPNSSASKIIF	TRAV35*02	TRBJ1-2*01	CAGHFSTCSANYGYTF	4
18	TRAV3*01	TRAJ13*02	CAVRDYNSGGYQKVTF	TRBV28*01	TRBJ2-1*01	CASRVPLDEQFF	4
20	TRAV1-2*01	TRAJ6*01	CAVLSSGGSYIPTF	TRBV28*01	TRBJ2-1*01	CASRVPLDEQFF	3
61	TRAV20*02	TRAJ24*02	CAFFSWGKQLQF	TRBV7-9*01	TRBJ1-1*01	CASSQPTEAFF	3
14	TRAV20*02	TRAJ24*02	CAFFSWGKQLQF	TRBV28*01	TRBJ2-1*01	CASRVPLDEQFF	3

TRAV= TCR α Variable gene, TRAJ= TCR α joining gene, TRBV= TCR β Variable gene, TRBJ= TCR β joining gene. CDR3 α and CDR3 β columns show the amino acid sequence of the TCR α and β CDR3 regions, respectively.

¹The percentage shown represents the total percentage of paired TCRs with identical TCR α and β gene V, J and CDR3 regions in the selection of TCRs analysed from this donor (n:77). TCRs which only appeared once are not included in the table.

Table 3. 4. Single EBV ZEBRA-specific TCR genes from TCR Donor 2

TCR	TRAV	TRAJ	CDR3 α	TRBV	TRBJ	CDR3 β	% ¹
8	TRAV12-3*01	TRAJ26*01	CAMRNYGQNFVF	TRBV25-1*01	TRBJ1-3*01	CASSDTGgentiYF	15
131	TRAV26-2*01	TRAJ47*01	CILRDGVGYGNKLVF	TRBV9*02	TRBJ2-3*01	CASEDRGGTDTQYF	14
16	TRAV13-2*01	TRAJ12*01	CAEKGWSSYKLI	TRBV30*02	TRBJ1-2*01	CAWVDGVLDGYTF	14
9	TRAV13-1*02	TRAJ42*01	CAASKEGGGSQGNLIF	TRBV20-1*02	TRBJ2-1*01	CSARDRGEHPPNDQFF	10
132	TRAV14*01	TRAJ52*01	CAMREGSGVGTSYGKLT	TRBV29-1*01	TRBJ2-5*01	CSAAGTSGSGETQYF	8
34	TRAV29*01	TRAJ16*01	CAASEGGQKLLF	TRBV7-9*03	TRBJ2-4*01	CASSAPNSDSAKNIQYF	8
25	TRAV13-1*02	TRAJ42*01	CAASKEGGGSQGNLIF	TRBV12-3*01	TRBJ1-2*01	CASSFSTCSANYGYTF	3
51	TRAV14*01	TRAJ54*01	CAMREVQGAQKLVF	TRBV4-2*01	TRBJ1-3*01	CASSLSETGTGNTIYF	3
23	TRAV1-2*01	TRAJ6*01	CAVLSSGGSYIPTF	TRBV12-3*01	TRBJ1-3*01	CASSFSTCSANYTIYF	3
29	TRAV13-1*02	TRAJ42*01	CAASKEGGGSQGNLIF	TRBV20-1*02	TRBJ2-1*01	CSARDRGEHPPDEQFF	3
45	TRAV8-6*02	TRAJ40*01	CAVSDQGTYKYIF	TRBV10-3*02	TRBJ1-5*01	CASSTGDSNQPQHF	3
46	TRAV8-6*02	TRAJ40*01	CAVSDQGTYKYIF	TRBV12-3*01	TRBJ1-2*01	CXSSFSTCSANYGYTF	3
14	TRAV26-2*01	TRAJ47*01	CILRDGVNYGNKLVF	TRBV9*02	TRBJ2-3*01	CASEDRNSGDTQYF	2
15	TRAV29*01	TRAJ16*01	CAASEGGQKLLF	TRBV9*01	TRBJ2-1*01	CASSVPSGGAGEQFF	2

TRAV= TCR α Variable gene, TRAJ= TCR α joining gene, TRBV= TCR β Variable gene, TRBJ= TCR β joining gene. CDR3 α and CDR3 β columns show the amino acid sequence of the TCR α and β CDR3 regions, respectively.

¹The percentage shown represents the total percentage of paired TCRs with identical TCR α and β gene V, J and CDR3 regions in the selection of TCRs analysed from this donor (n:138). TCRs which only appeared once are not included in the table.

3.5 Construction of the TRAC_pMX-IRES-GFP retroviral vector

In order to express the EBV-specific TCRs in target cells, six of the most dominant paired TCR α and β chains from each donor were cloned into a retroviral vector. The retroviral vector expression system was chosen for this purpose as it leads to integration of the viral genes into the dividing host cell genome, thus allowing stable expression of the TCR genes in the target cells (Robbins et al., 1998). The retrovirus vector pMX-IRES-GFP (Figure 3. 12 A) was used for TCR cloning; it contains the Moloney murine leukaemia virus (MMLV) long terminal repeats (LTRs) for initiation of transcription of the transgene, a packaging signal and a multiple cloning site for the insertion of the TCR genes (Kitamura et al., 2003). In addition, it contains a green fluorescent protein (GFP) gene which is expressed alongside the TCR transgene in the target cells. This is owing to the internal ribosome entry site (IRES) sequence present upstream of the GFP gene. The IRES sequence enables recruitment of the ribosome for translation of the mRNA of a subsequent gene without the need for a second initiation signal after the first transgene (Pelletier and Sonenberg, 1988, Renaud-Gabardos et al., 2015). Therefore, in this case, any cells expressing the cloned TCRs will also express GFP, facilitating identification of successfully transduced cells. An ampicillin resistance gene is also present in the pMX-IRES-GFP vector for selective bacterial culture of vector-containing *E. coli*.

Before the vector could be used for TCR cloning, it was modified to include the TCR- α constant gene (TRAC) for successful expression of the full length TCR α chain (Figure 3. 12 B).

A



B

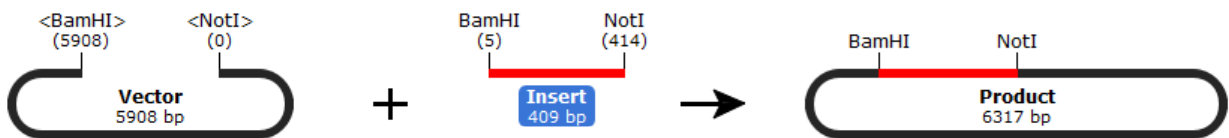


Figure 3. 12 The pMX-IRES-GFP retroviral vector and ligation of the TRAC gene

A) The map shows the full pMX-IRES-GFP vector; the 5963 bp vector contains the MMLV LTRs and packaging signal (light orange-coloured boxes), and a truncated gag gene (purple). The BamHI and NotI sites used for insertion of the TRAC gene are indicated. These sites are followed by an IRES gene (grey) and an enhanced GFP gene (bright green). The bacterial origin of replication (Ori) is also present (yellow), alongside the ampicillin resistance gene and promoter (light green).

B) The workflow for ligating the TCR- α constant (TRAC) gene into the cut vector to produce TRAC_pMX-IRES_GFP is shown. The red 409bp insert represents the TRAC gene. The compatible BamHI and NotI sites are indicated on the vector and the insert. The vector map and cloning schematic were created using the SnapGene software.

The pMX-IRES-GFP vector was cut by restriction digest with BamHI-HF and NotI-HF enzymes and the TRAC gene was inserted (Figure 3. 12 B). This produced the novel TRAC_pMX-IRES-GFP vector which served as the universal vector backbone for all the TCR clones. The complete TRAC-pMX-IRES_GFP vector was cut with BamHI immediately upstream of the TRAC gene in order to linearize it for cloning of the TCR α and β genes, and this open vector was used in every subsequent TCR cloning reaction.

The inclusion of the TRAC gene in the vector backbone modifies the pMX_IRES_GFP vector to create a novel cloning vector that is universally suitable for the insertion of TCRs obtained using our PCR primers. This new vector serves two purposes; firstly, it addresses the fact that the TCR α PCR product does not contain the full TCR α constant region because the reverse primer binds within exon 1 of the constant gene, excluding exons 2-4 from the final product. Secondly, addition of the TRAC gene sequence to the vector provides essential sequence overlap with any given TCR α PCR product, enabling seamless cloning.

The TCR β constant (TRBC) gene was included as a separate gene fragment to be included in every TCR cloning reaction. Both the TRAC and TRBC genes were synthesized as gene fragments by ThermoFisher Scientific. The sequences used in their synthesis are codon-optimized and include additional cysteine residues, as per the sequences published by Hamana and colleagues (Hamana et al., 2016). These modifications of the TCR α and β constant genes not only allow their optimal expression in target human cells, but also avoid potential mispairing of endogenous and exogenous TCR chains. This is due to the additional disulphide bond created between the second cysteine residues on both the TCR α and β chains, which ensure that the transduced TCR chains have greater affinity for each other than the endogenous TCR chains (Cohen et al., 2007). The codon-optimized sequences are outlined in Figure 2.3, in the Materials and Methods chapter.

3.5.1 Gibson Assembly Cloning and screening of bacterial clones

The six most dominant TCRs from Donors 1 and 2 were selected for cloning into the linearized TRAC_pMX-IRES-GFP vector. The expression vector was designed to be bicistronic, incorporating the paired TCR α and β genes in a single retroviral vector, linked by the P2A sequence GGAAGCGGAGCTACTAACTTCAGCCTGTTGAAGCAGGCTG GAGACGTGGAGGAGAACCCTGGACCT. This is a sequence which is found in the porcine teschovirus and codes for a self-cleaving peptide, P2A. It is a member of the 2A group of peptides which were first discovered in the picornavirus family, located between two proteins (Ryan et al., 1991). They allow translation of two sequential proteins in a “stop-go” manner, thereby allowing translation of two proteins from a single start codon. The P2A peptide is self-cleaving; it has a cleavage site (indicated by *) between the final glycine and proline residues of its C-terminal (-LLNFDLLKLAGDVESNPG*P-) (Wang et al., 2015). A P2A sequence between two genes of interest causes ribosomal “skipping” during translation, resulting in the absence of a peptide bond between the two proteins, thus allowing production of two separate protein products (Wang et al., 2015). By using the P2A sequence as a linker between the paired TCR α and β genes in our TCR vector, we are able to achieve expression of both TCR α and β genes from the same vector, from a single promoter sequence, and at equimolar levels. A disadvantage of using the P2A sequence includes retention of a few amino acids from the sequence on both genes after cleavage, which may affect function of the proteins. However, this rarely seems to be a problem as the 2A sequences are a popular way of ensuring co-expression of several different genes in various systems in the published literature (Donnelly et al., 2001, Szymczak et al., 2004). For the purpose of our cloning protocol via Gibson assembly, the codon-optimized TCR β constant (TRBC) gene is included upstream to the sequence of the P2A linker within the fragment. This provides the homologous sequence overlap that is required between the TCR β PCR product and the P2A fragment for annealing during Gibson assembly, but also allows expression of the full codon-optimized TRBC gene (Gibson et al., 2009).

The Gibson Assembly method was used to clone the TCR α and β genes, and the P2A sequence into the single modified retroviral vector, TRAC_pMX-IRES-GFP. With most traditional cloning methods, the genes and vectors are first digested with restriction enzymes, producing cohesive ends which are compatible with standard ligation protocols. However, when large numbers of unknown TCR genes are being amplified, this labour-intensive method of cloning is not suitable. This is firstly because without initial sequencing of each

TCR gene, it would not be possible to guarantee that the TCR gene does not also contain the restriction enzyme site within its sequence before digestion. If the site were found to be present in the TCR sequence, mutagenesis reactions would need to be used to modify the sequence to change it from the restriction site, which is not only time-consuming, but may also have unknown effects on the TCR chain itself, affecting downstream protein expression and function.

Thus, we sought to design a cloning platform which avoids the use of restriction enzyme digest of every TCR fragment, creating an easy, direct and seamless method of insertion of any amplified TCR product into the pre-prepared vector backbone. In contrast to conventional cloning methods, the Gibson assembly method relies on the joining of DNA fragments which have homologous ends, and allows the seamless assembly of several different fragments of DNA sequences into one complete vector without the need for restriction enzyme digests (Figure 3. 13) (Gibson et al., 2009). The method uses three different enzymes in the same mastermix; a 5' endonuclease to chew back the 5' ends of the DNA fragments, DNA polymerase to repair the ends of the DNA after the homologous overlapping ends of the adjacent fragments have annealed, and DNA ligase to seal the nicks in the DNA. Because the extension is based on the pairing of the overlapping homologous DNA ends, there are no mutations inserted and the joints between the fragments of the vector are seamless, creating a continuous stretch of DNA (Gibson et al., 2009).

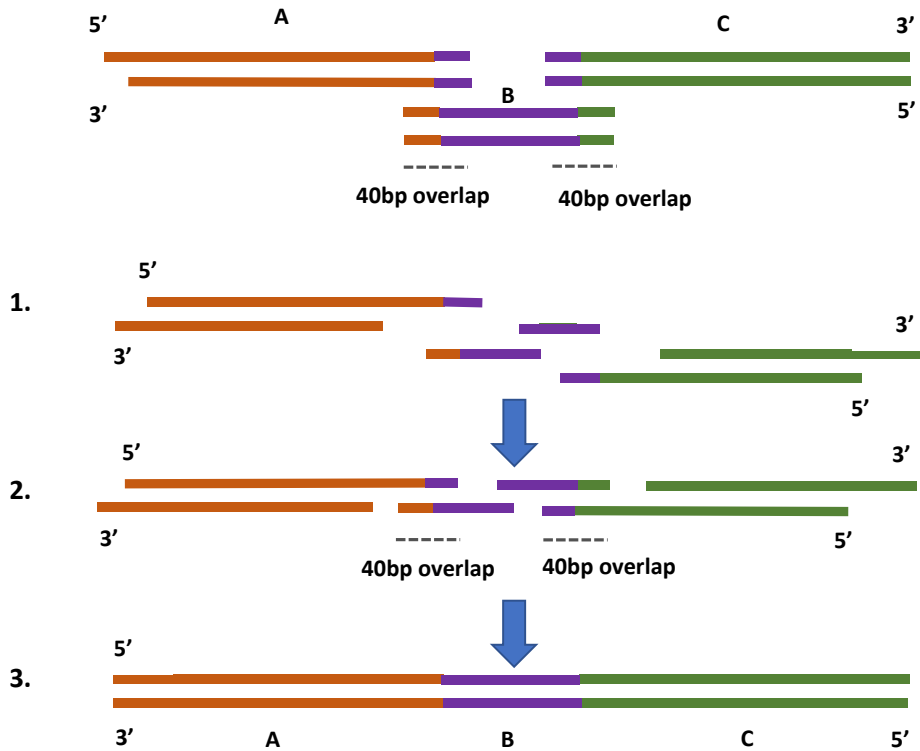


Figure 3. 13 Schematic overview of Gibson Assembly method

The Gibson Assembly method (Gibson et al., 2009) consists of the joining of separate DNA fragments (A, B and C in top panel) which contain homologous overlaps in the ends of their sequences (indicated by matching colours). The assembly takes place in 3 main steps; (1) the T5 exonuclease chews back the 5' ends of the DNA fragments, revealing 3' overhangs. (2) The DNA fragments anneal and the overhangs are brought in close proximity to each other, allowing (3) the repair of the chewed back ends by DNA polymerase and ligase enzymes using the overlapping sequences as templates, forming a seamless stretch of DNA sequence.

In our method the overlapping sites are incorporated into the ends of the TCR genes using the novel third PCR primers, and a single modified universal retroviral vector stock is prepared beforehand through restriction enzyme digest. In addition, the TRBC_P2A linker fragment is synthesised as a gene fragment (ThermoFisher Scientific) and stored as aliquots, ready to be used in the Gibson Assembly reaction. The overlapping fragments ensure that the PCR products, the linker and the digested vector are compatible for cloning without restriction digest of each PCR product, thus allowing any TCR amplified by our PCR to be inserted directly and efficiently into the pre-cut vector in a single cloning reaction straight after PCR. For the Gibson Assembly protocol, each TCR gene, the universal P2A linker and the linearized vector were treated as separate fragments (Figure 3.14 and Table 3.5). We chose to use the gene orientation of TCR β -P2A-TCR α in the expression vector as this orientation has been previously shown to be optimal for maximum TCR expression and function (Banu et al., 2014). Thus, in our method, TCR β is fragment 1, the universal TRBC_P2A linker is fragment 2, TCR α is fragment 3, and the linearized TRAC_pMX-IRES-GFP vector is fragment 4 (Figure 3. 14). Each fragment has an overhang sequence at its 5' and 3' end which is homologous to the 3' and 5' end, respectively, in its adjacent fragment. This homology is indicated by the matching colours in Table 3.5. When designing the assembled product and the fragment sequences, the compatibility of the overhangs was verified using the SnapGene software; the overlapping sequences in each fragment needs to be a minimum length of 35-40 base pairs, and the melting temperature between each joint ideally above 60°C in order to create secure seams during the assembly reaction, which takes place at 50°C. The more fragments involved in the assembly, the longer the overlap sequences required (Gibson et al., 2009).

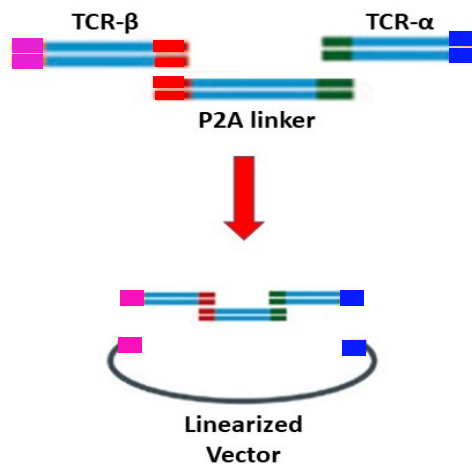


Figure 3. 14 Schematic of Gibson Assembly of TCR α and β genes, P2A linker and vector

Schematic shows the 4 fragments of Gibson Assembly (TCR β , P2A linker, TCR α and the linearized vector) with their overlapping fragments aligned.

Table 3. 5 The Gibson Assembly fragments and their overlapping sequences for TCR cloning

Fragment	Overlap Sequence	Overlaps with
BamHI-linearized TRAC_pMX_IRES_GFP 3' endGTGGGGGTG GACCATCCTCTAGACTGCCG GATCCTAGCTAG	TCR- β gene F primer (pMX-B3-F)
TCR- β F primer (pMX-B3-F)	GACCATCCTCTAGACTGCCGGATCTAGCTAG TTA ATTAAGTGGCGCCGGAATTAGATCTCTCGAGAA GGATCCGAATTCTGCAGG	3' end BamHI-linearized TRAC_pMX_IRES_GFP
TCR- β R primer (TRBC_RV3)	GTGGCCAGGCACACCAGTG	5' of TRBC_P2A linker fragment
TRBC_P2A_linker fragment 5' end	CACTGGTGTGCCTGGCCAC AGGCTTCTTCCCCGA CCACGT.....	TCR- β R primer (TRBC_RV3)
TRBC_P2A_linker fragment 3' endAAGGACTTCGGAAGCGGAGCTACTAACTTCA GCCT GTTGAAGCAGGCTGGAGACGTGGAGGAGA ACCCTGGACCT	TCR- α F primer (P2A_A3_F)
TCR- α F primer (P2A_A3_F)	GTTGAAGCAGGCTGGAGACGTGGAGGAGAACCC TGGACCT	TRBC_P2A_linker fragment 3' end
TCR- α R primer (TRAC_RV3)	GGTGAATAGGCAGACAGACTT	5' of BamHI-linearized TRAC_pMX-IRES-GFP

¹Homologous overhangs are shown in matching colours, in the same colours as in the schematic in Figure 3. 14.

The Gibson Assembly cloning was performed using a commercially available enzyme mastermix (HiFi Assembly Mastermix, NEB). The fragments were assembled together to make a complete TCR expression vector during the 50°C incubation period, when all of the fragments are aligned and seamlessly joined by the enzymes in the mix.

The products of the Gibson Assembly cloning reactions were transformed into competent Stable *E. coli* (NEB), and resulting single colonies were grown as starter cultures overnight. Plasmid DNA from these cultures was used to screen for correctly assembled gene fragments using a double restriction enzyme digest. The plasmids were screened for the presence of an 1800 bp insert representing the correctly-assembled TCR β -P2A-TCR α gene fragments (Figure 3. 15). The efficiency of correct Gibson Assembly cloning ranged from approximately 50-70%. The majority of failed clones were due to apparent mutations of the assembled products themselves; for example, in colonies 4, 7 and 8 there was an assembled product present, however the insert is visibly smaller than the expected 1800 bp size. Upon sequencing it became evident that deletions had occurred, which may have been due to the unstable nature of the retroviral vectors themselves whilst in bacterial culture. One of the drawbacks of retroviral vectors is that repetitive sequences in their LTRs render the vector unstable and prone to homologous recombination and mutations. Despite minimising this by using the Stable *E. coli* strain which lack the endonuclease I gene, thus minimizing degradation of the vector DNA, recombination between DNA regions may still occur, especially in the relatively long recommended culture time of 24 hours. Thus, at least 8-10 different colonies from each TCR cloning reaction plate were selected to maximise the chances of acquiring a correctly-assembled construct consisting of an 1800 bp fragment and ~7 kb vector. The plasmids sequences were analysed for presence of the correct TCR $\alpha\beta$ sequences, including the full constant genes, V and J regions, and for the presence of the full P2A sequence.

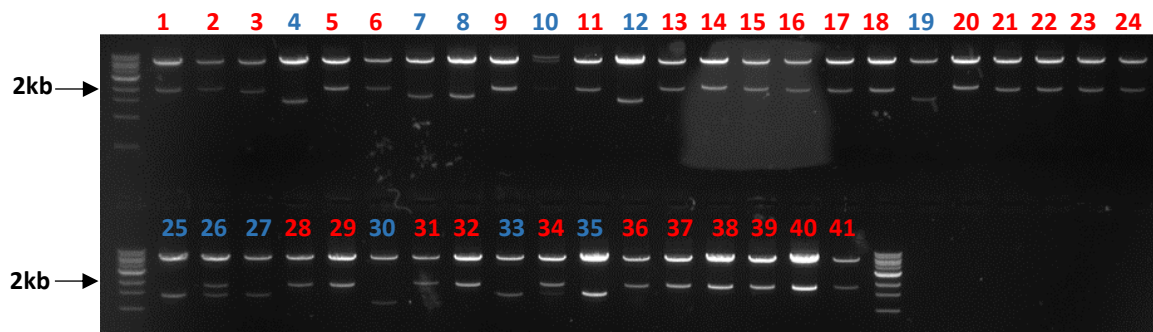


Figure 3. 15 Screening of Gibson Assembly product-transformed *E. coli*

Representative agarose gel showing products of the restriction digest on 41 bacterial colonies after transformation with Gibson Assembly products. The red-labelled wells indicate colonies with the correct inserts of 1800 bp representing the fully-assembled TCR β -P2A-TCR α gene fragments and the ~7 kb vector. The blue labelled wells indicate plasmids with incorrect fragment sizes.

3.6 Retroviral vector transfection and transduction of SKW3 cells

Infection of target T cells with retroviral particles encoding desired TCR $\alpha\beta$ genes requires production of infective retrovirus particles. This was achieved by sequentially using two retroviral packaging cell lines, Plat-GP and PG13, to produce high titres of retroviral particles. The method is loosely based on that by Parente-Pereira et al. (Parente-Pereira et al., 2014). A key advantage of this method is that transduction of the PG13 cells with retroviral particles from PlatGP cells permits higher rates of transduction compared to direct transfection of the PG13 cells with the retroviral vector alone. This ensures that the PG13 cells are highly positive for the vector of interest and no enrichment is needed for further studies (Parente-Pereira et al., 2014).

Although Plat-GP cells were transfected with the most dominant TCRs from each donor; TCRs 1, 10, 4, 7 and 2 from Donor 1 (Table 3. 3) and TCRs 8, 131, 16, 9, 132 and 34 from Donor 2 (Table 3. 4), not all these TCRs were able to be expressed in SKW3 T cells, either due to failure of transfection in Plat-GP, or failed transduction in PG13 or SKW3 T cells, even after repeated attempts. I was able to successfully express and complete assays on TCR4 from donor 1, and five dominant TCRs from donor 2 (TCRs 9, 16, 34, 131 and 132).

Plat-GP cells are a transient source of retroviral particles and cannot survive for more than 3-4 days after transfection. A second retroviral packaging cell line, PG13, was therefore transduced with retroviral particles produced by the Plat-GP cells. As the PG13 cells are transduced by the retroviral particles themselves, the viral genetic information is integrated into the genome of the PG13 cells, thus allowing the formation of a stable, continuous source of TCR-encoding virus. In addition, the PG13 cells stably produce viral particles which are gibbon ape leukaemia virus (GALV) pseudo typed, and are more efficient in their transduction of human T cells compared to the VSV-G pseudo typed viral particles produced by the Plat-GP cells (Parente-Pereira et al., 2014). The transduced PG13 cells were analysed on the flow cytometer for GFP expression 2 days after transduction (Figure 3. 16). The transduction efficiency reached very high levels, ranging from 42% to up to 98% GFP expression. The supernatant from all the PG13 cells was collected from day 5 post-transduction.

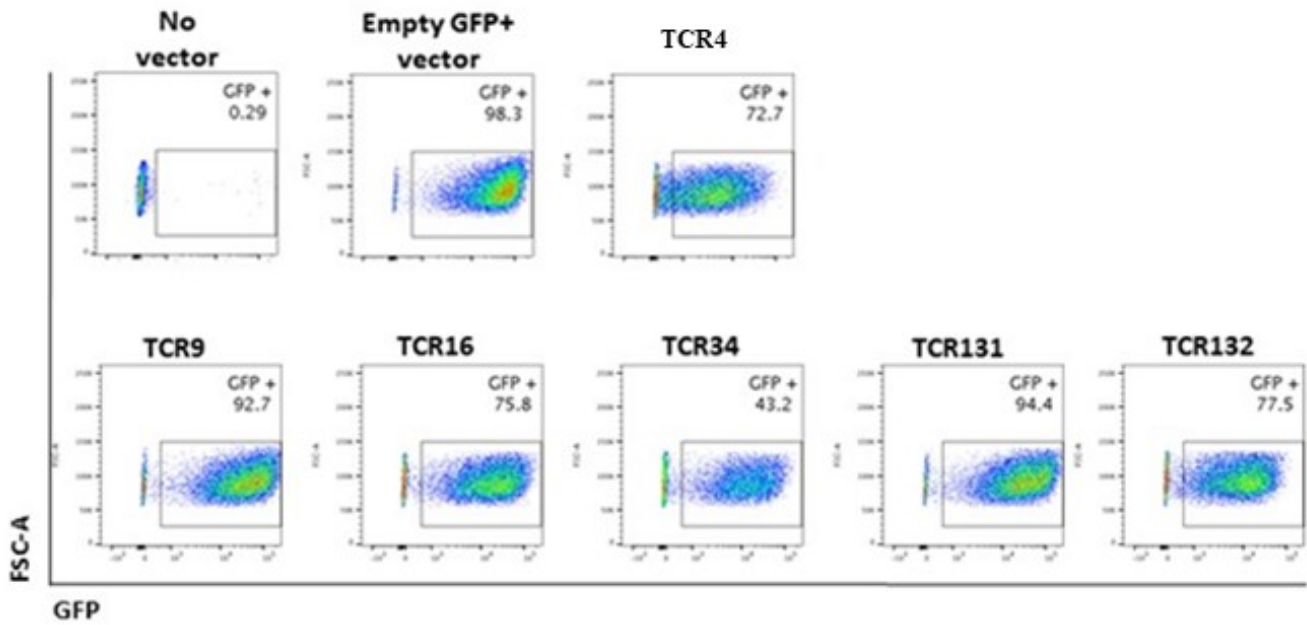


Figure 3. 16 Transduction efficiency of PG13 cells

PG13 cells transduced with viral particles from PlatGP cells and were analysed for GFP expression 48 hours post-transduction. The cells were compared to PG13 cells that had been treated without the vector (no vector negative control), and with an empty vector positive control. PG13 cells transduced with dominant TCRs from Donor 1 (TCR4) and Donor 2 (TCR9, TCR16, TCR34, TCR131 and TCR132) are shown. The values indicate the percentage of GFP⁺ single cells.

3.6.1 Expression of EBV-specific TCRs on SKW3 cells

We chose the T cell line SKW-3 (SKW3) for the expression of the selected antigen-specific TCRs, and to assess the function of the expressed TCRs. These cells are derived from a patient with chronic lymphocytic leukaemia (Hirano et al., 1979) and are known to be TCR $\alpha\beta$ -negative, and lacking in cell surface CD3 expression. CD3 is present in these cells in the cytoplasm, along with other signalling components, but cannot be expressed on the surface in the absence of TCR as these proteins are only expressed stably as a complex (Weiss and Stobo, 1984). The introduction and successful expression of exogenous TCR can therefore be assessed through staining for CD3 as well as TCR $\alpha\beta$.

SKW3 cells were transduced with TCR-encoding retroviral particles produced by PG13 cells, and analysed via flow cytometry for expression of TCR two days later. The cells were gated according to the strategy outlined in Figure 3. 17, and compared to non-transduced SKW3 cells.

Most TCRs selected from Donors 1 and 2 were successfully expressed (Figure 3. 18). From the selected dominant Donor 1 sequences, TCR4 was successfully expressed on SKW3 cells, however TCRs 1, 7 and 10 were not, even with repeated attempts from transfection and viral packaging stages. This failure to express may be due to incompatibility of these TCR chains with the expression vector, or perhaps mutations occurring in the vectors themselves. From the Donor 2 sequences, TCRs 9, 16, 34, 131 and 132 were all successfully expressed on SKW3. Primary T cells were used as a positive control for TCR staining.

The clones were cultured for approximately 10 days before enrichment of the GFP⁺ CD8⁺ CD3⁺ TCR⁺ cells using the FACS Aria II cell sorter.

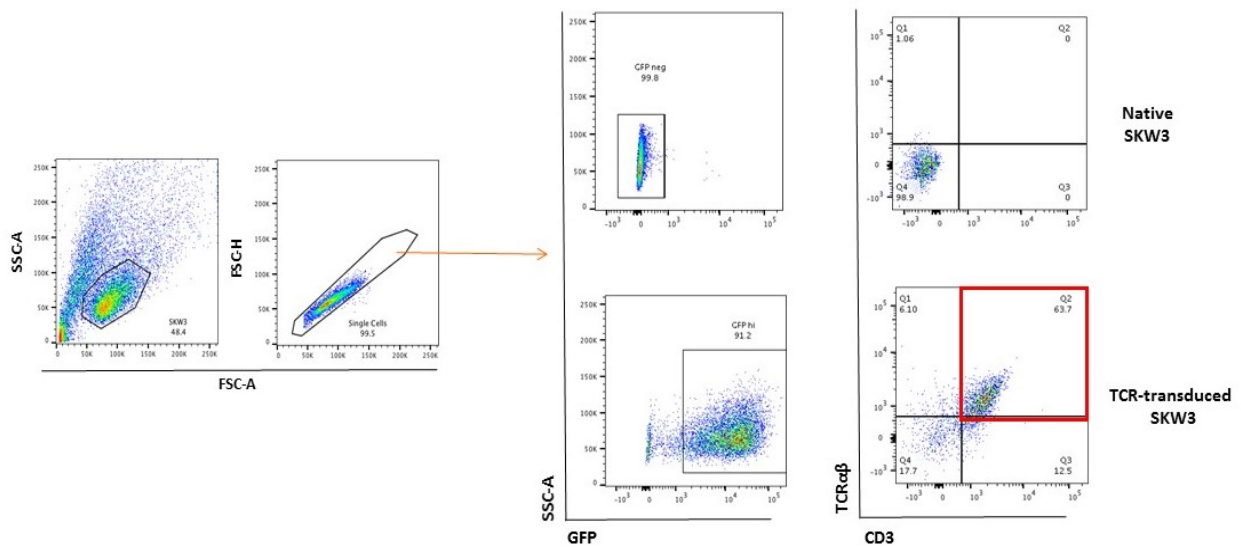


Figure 3. 17 Gating strategy to assess TCR expression on transduced SKW3 cells

TCR_pMX-IRES-GFP-transduced SKW3 T cells were assessed for their TCR expression. The gating strategy is outlined; SKW3 T cells were first gated on lymphocytes, then singlets, before gating on GFP⁺ CD3⁺ TCRαβ⁺ (lower panels, gate highlighted in red box). This was compared to the native SKW3 cells which are deficient in CD3 and TCRαβ (upper panels).

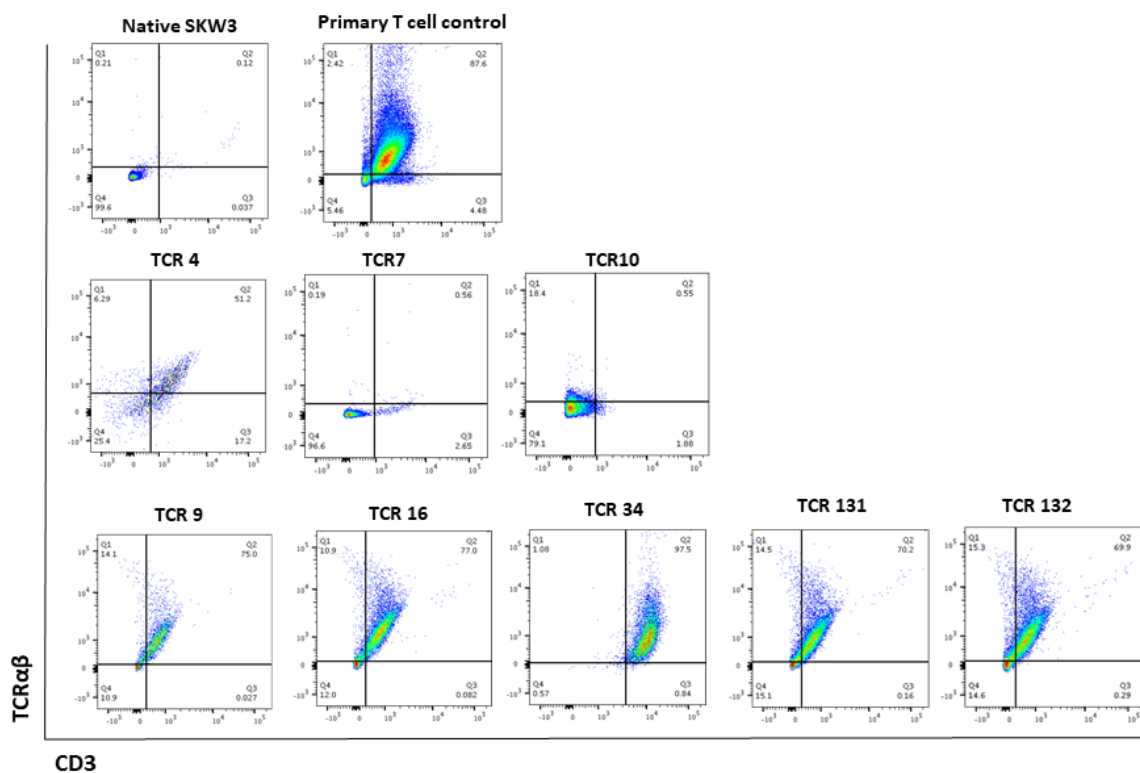


Figure 3. 18 TCR expression on transduced SKW3 cells

Figure showing the flow cytometry plots of CD3 and TCR $\alpha\beta$ staining on SKW3 clones transduced with ZEBRA-specific TCRs. The upper panels show the native SKW3 cells (negative control) and primary T cell control (positive staining control). The middle panels show TCR clones selected from Donor 1 dominant sequences; TCR4 is CD3+ TCR+, but TCR7 and TCR10 did not express CD3 or TCR after transduction. The lower panel shows the clones from Donor 2 dominant TCRs; TCR9, TCR 16, TCR 34, TCR131 and TCR132. Plots shown are representative of 3 experiments performed on the various clones.

3.6.2 Functional analysis of SKW3 TCR clones

The SKW3 T cell clones were assessed for the ability of their transduced TCRs to recognise their cognate EBV ZEBRA antigen. Upregulation of the early activation marker, CD69 on the cell surface, and the production of cytokines TNF- α and IFN- γ were assessed after stimulation with the ZEBRA peptide pool. The mean fluorescence intensity (MFI) was used as a measurement of CD69 expression post-stimulation in order to provide a more meaningful assessment of variations in the relative amounts of proteins expressed per cell (Nguyen et al., 2014).

Peptide pulsing assays were performed using autologous B cell lymphoblastoid lines (BCLs) from the TCR donors generated via EBV-immortalization. These BCLs were pulsed with ZEBRA peptide pool and used to present the cognate peptide to the SKW3 T cell clones for activation at an Effector:Target ratio (E:T) of 2:1. To determine the optimum conditions for stimulation of these SKW3 TCR clones, TCR4-transduced SKW3 were stimulated for either 6 hours or 18 hours, with peptide-pulsed BCLs. The pulsing of the BCLs was performed using either 5 μ M or 10 μ M of the ZEBRA peptide pool. As controls, BCLs with no peptide (BCL only negative control) were used in parallel. Wells coated with 1 μ g/ml anti-CD3 OKT3 antibody were used as a positive stimulation control. Flow cytometry was performed on the cells to assess CD69 upregulation (Figure 3. 19).

The data in Figure 3.20 demonstrates that the SKW3 TCR4 cells were able to be activated by both 5 μ M and 10 μ M of peptide pool-pulsed cells within 6 hours, as shown by increased CD69 levels compared to the BCL only controls. However longer stimulations of 18hrs resulted in much higher levels of CD69 compared to the BCL only control. In addition, there were much higher levels of CD69 expression after stimulation with 10 μ M of peptide pool compared with 5 μ M.

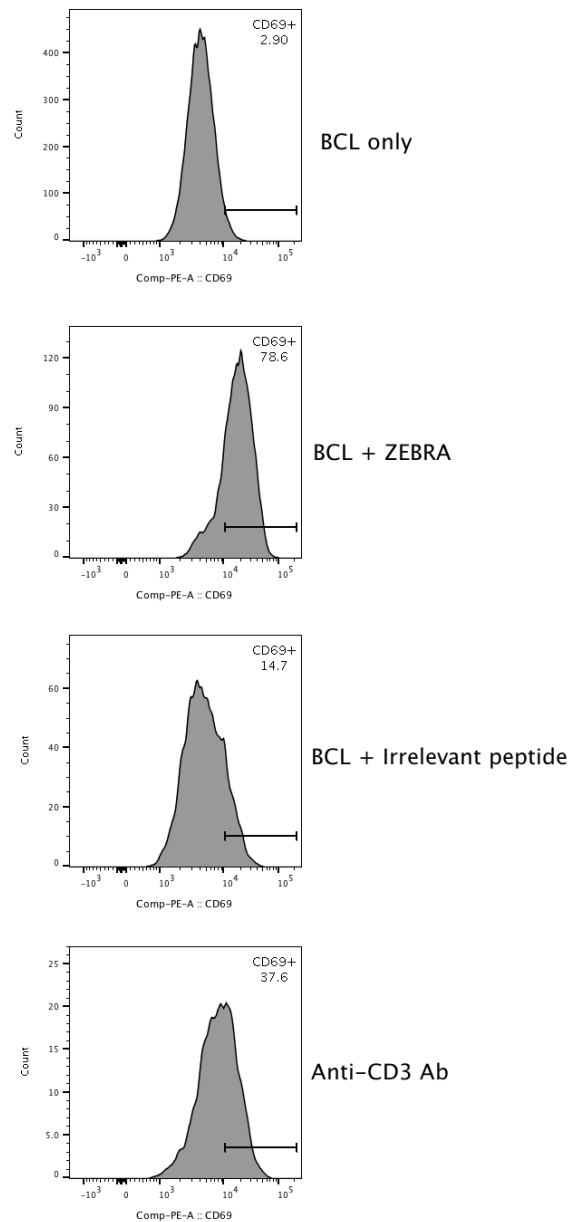


Figure 3. 19 Representative gating to analyse CD69 expression on peptide-stimulated SKW3 clones

SKW3 T cell clones were stimulated with autologous BCLs pulsed with 10 μ M ZEBRA peptide pool and compared to BCL only negative control, an irrelevant peptide (FLRGRAYGL) negative control, and anti-CD3 antibody positive control. The clones were first gated according the strategy in Figure 3.17, before being assessed for CD69 expression. Representative histograms from 3 experiments are shown for each condition. The values shown indicate the % CD69 positive cells compared to the BCL-only control.

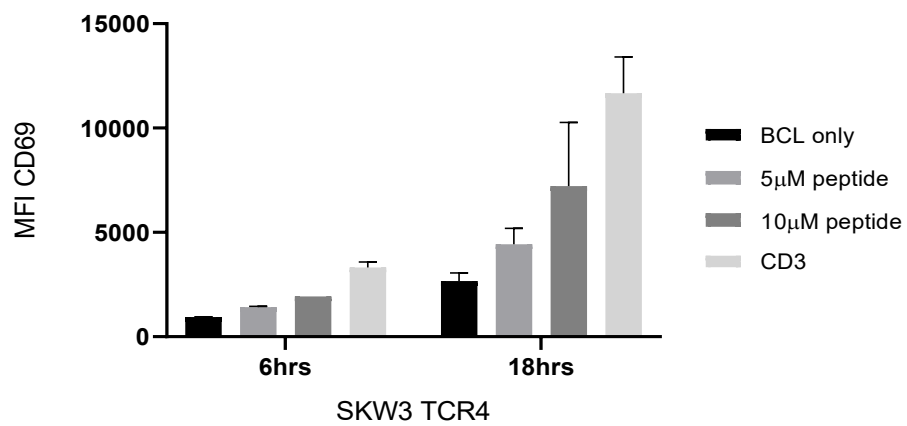


Figure 3. 20 Optimization of peptide stimulation time for SKW3-TCR4

The SKW3-TCR4 cells were used to assess the optimal conditions required for peptide stimulation to achieve T cell clone activation. The cells were stimulated with autologous BCL without peptide as a negative control, or with BCLs pulsed with 5µM or 10µM ZEBRA peptide pool. Cells were incubated in anti-CD3 antibody-coated wells as a positive control. Data shown is the SEM of two replicates obtained from a single experiment.

Considering these results, 10 μ M of ZEBRA peptide pool was used to pulse BCLs and the cells were used to stimulate the TCR clones for 18 hours for all subsequent peptide assays. BCLs pulsed with an irrelevant peptide, FLRGRAYGL, a late stage EBV antigen EBNA-3 epitope, were used as an alternative negative control in later stimulation assays. Peptide stimulation assays were performed on all the SKW3 clones from Donor 1 and Donor 2 TCRs and mean fluorescence intensities (MFI) of CD69 were compared (Figure 3. 21). All the clones showed increased levels of CD69 expression after stimulation with cognate peptide compared to BCL only controls and irrelevant peptide stimulated controls. This indicates that all the transduced TCRs have retained their function throughout the cloning process and can still specifically recognise their cognate peptide in the ZEBRA peptide pool.

The ability of the EBV-specific TCRs to induce production of cytokines after recognition of the ZEBRA peptide antigen was also assessed. The concentrations of TNF- α and IFN- γ were measured in supernatant from the stimulation assays using the Meso Scale Discovery (MSD) U-plex platform, which is similar to an ELISA but allows simultaneous analysis of several analytes from the same well, using limited amounts of supernatant.

The data in Figure 3. 22 indicates that the culture supernatant from the SKW3 TCR clones stimulated with ZEBRA peptide pool contained higher concentrations of IFN- γ and TNF- α compared to irrelevant peptide controls. The ZEBRA peptide-dependent increase in production of these cytokines again indicate that all the transduced TCRs have retained their specificity and function since being isolated on their IFN- γ producing phenotype, cloned and expressed on the surface of the SKW3 T cell line.

These data confirm that the platform for single TCR cloning is efficient, reliable and preserves the integrity of the TCR sequence during cloning, allowing expression of correctly functioning TCRs which retain their ability to recognize their cognate antigen and activate the T cell.

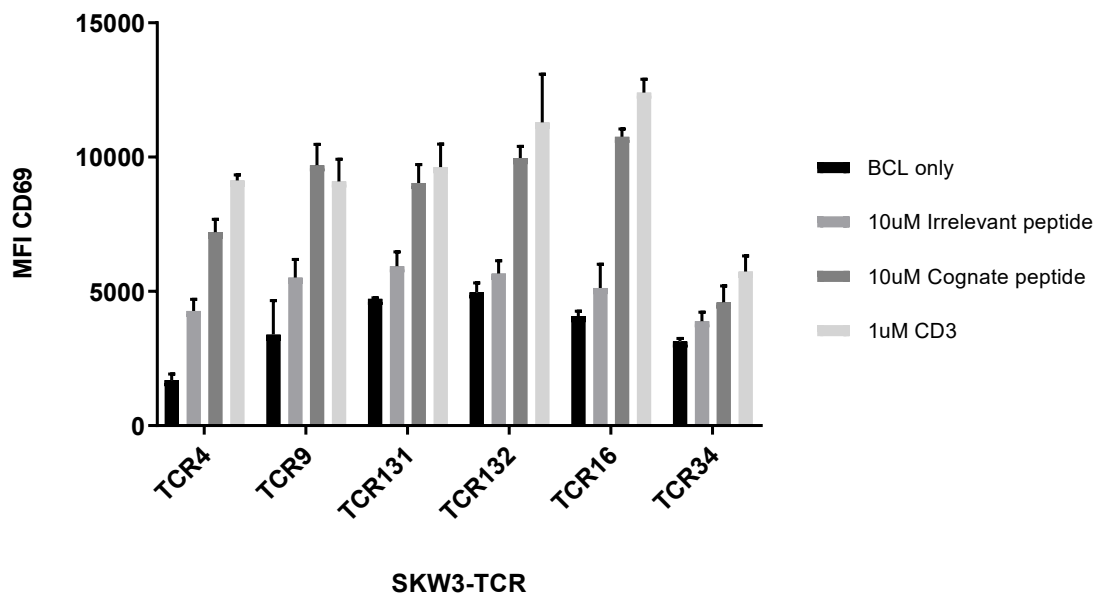


Figure 3. 21 Upregulation of CD69 on SKW3 clones after peptide stimulation

The SKW3 clones were assessed for their ability to recognise ZEBRA peptide presented on autologous BCLs through the upregulation of CD69 on their cell surface. The clones were stimulated with autologous BCLs pulsed with either 10µM cognate peptide, or 10µM irrelevant peptide as a negative control. BCL without peptide was used as a separate negative control and cells were incubated in anti-CD3 antibody-coated wells as a positive control. Data shown is the SEM of two replicates obtained from 2 different experiments.

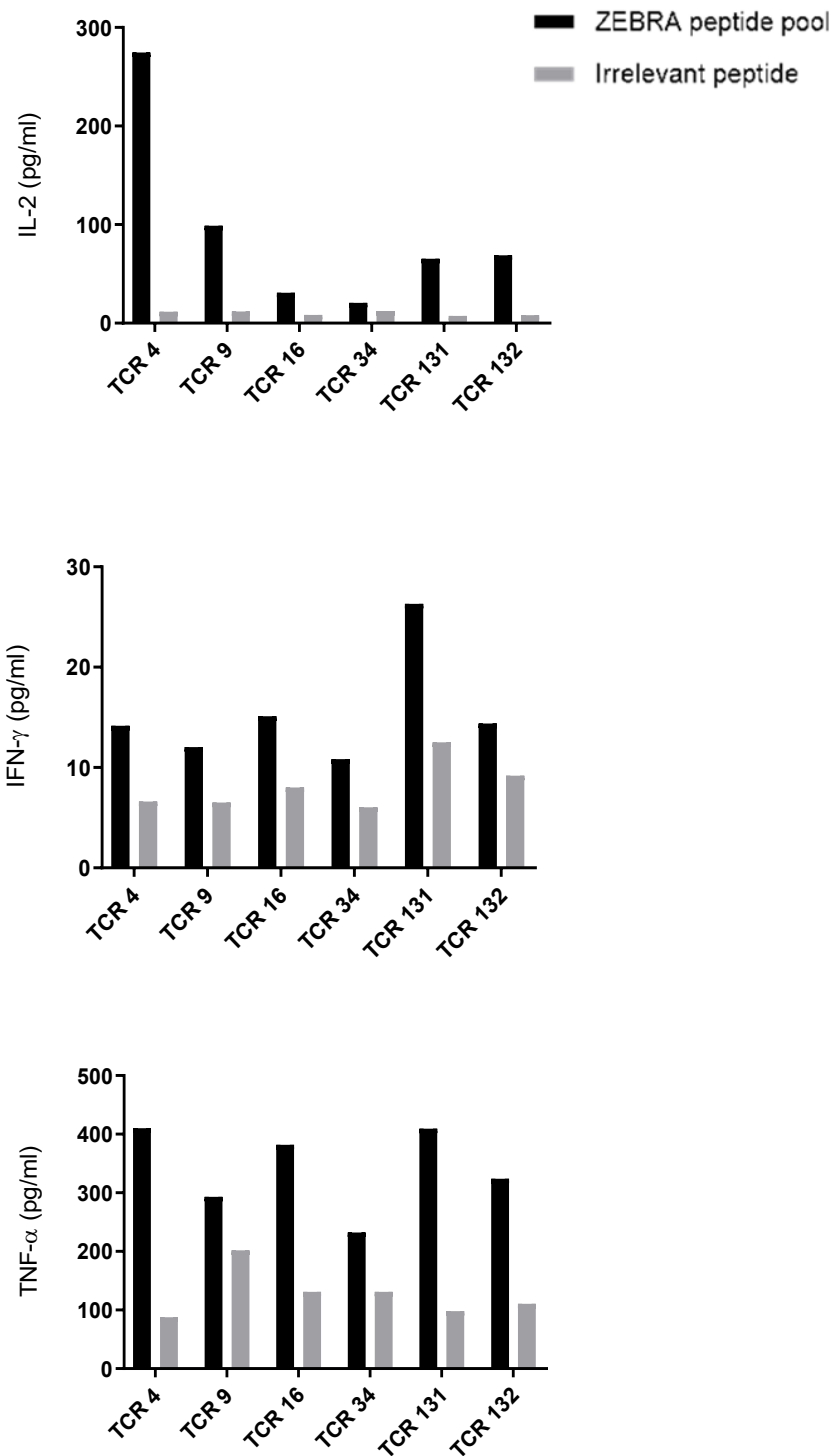


Figure 3. 22 Secretion of cytokines IL-2, TNF- α and IFN- γ by SKW3 clones

Culture supernatant was collected at 18 hours from the peptide stimulation assays from ZEBRA peptide-stimulated and irrelevant peptide-stimulated wells. The concentrations of IL-2, TNF- α and IFN- γ were measured in the supernatant using the MSD multi-array system.

3.7 Knockdown of endogenous TCRs

As proof of concept of our single TCR cloning method and expression had been successfully demonstrated in TCR-deficient SKW3 T cells, the next step was to express these EBV-specific TCRs in primary T cells to examine the functional capability of transduced cells. However, the presence of endogenous TCR in primary T cells can hinder the expression of transgenic TCR, and affect safety (Bunse et al., 2014, Ochi et al., 2011). To this end, we wished to knockdown endogenous TCRs from the target primary T cells to test whether we could enhance the expression of, and consequently the function of, our cloned TCRs. Thus, we used RNA interference (RNAi) to disrupt the expression of endogenous TCR expression in primary T cells. RNAi can be mediated through either small interfering RNA (siRNA) which are chemically synthesised double-stranded RNA, or short hairpin RNA (shRNA), which are produced within the cell nucleus from a vector and cut into siRNA sequences within the cell (Rao et al., 2009). siRNA are a member of the group of small (20-30nts long) noncoding RNAs which are involved in eukaryotic gene expression and processing (Elbashir et al., 2001). The siRNA mediate degradation of mRNA transcripts and silencing of the target gene (Wilson and Doudna, 2013). The use of RNAi was chosen for TCR knock down in our work due to its simplicity in terms of identifying suitable DNA targets; it would not have been possible to use CRISPR or TALENs-based methods with our current system as these require much longer target sequences of at least 20-30 bp, compared to the approximately 18bp target sequence needed by siRNA (Boettcher and McManus, 2015, Bogdanove and Voytas, 2011, Ran et al., 2013, Wilson and Doudna, 2013). The differences between the sequences of our codon-optimized constant genes and the native constant genes (which will be targeted for knockdown, explained in further detail below,) are not long enough to provide the required 20-30bp target for CRISPR or TALENs-based methods, thus they are unsuitable for our current system. Although siRNA would not induce permanent knock-out of the endogenous TCRs at the genetic level, the stable nature of the shRNA retroviral vector would still be sufficient for the generation of a TCR-knockdown primary T cell model. This could be used to test the function of our transgenic TCRs, and this siRNA method has shown recent success in an in vivo model (Brummelkamp et al., 2002, Sun et al., 2019). The aim of this part of the thesis was to initially show that the siRNA could successfully knock-down the endogenous TCR in primary T cells. This would be followed by transduction

of the ZEBRA-specific TCRs into these modified T cells as a direct TCR replacement strategy. These TCR-replaced cells would then be tested for antigen reactivity to the ZEBRA peptide pool with the expectation that they would function better than TCR-transduced primary T cells whose endogenous TCRs have not been knocked down.

3.7.1 siRNA design and cloning

When designing the shRNA vector, it was critical that the produced siRNA would only target the endogenous TCR and not the transgenic TCR. This was achieved via designing siRNA sequences against the TCR genes where there was a mismatch between the wild type constant gene sequence (present in the endogenous TCR), and the codon-optimized TCR constant genes (present in the transgenic TCR). To determine suitable and optimal sequences, specific rules for siRNA design were followed; the selected target mRNA sequence must be between 19-21 nucleotides long, begin with an AA dinucleotide, and have a GC content of 30-50% (Fellmann and Lowe, 2013, Boettcher and McManus, 2015). In order to prevent premature termination, stretches of more than 4 T's and A's were avoided in the target sequence. The potential target mRNA site was then compared to the genome database and checked; those with more than 16-17 continuous base pair homology to other human genes were omitted. Using this method, 3 potential siRNA sequences targeting TCR- β were designed (Figure 3. 23). We decided to focus on initially knocking down TCR- β because a recent study showed that targeting the TCR- β alone is sufficient for significant TCR knockout (Legut et al., 2018). Once this method was established, the aim was to do a simultaneous knockout of TCR α in parallel to ensure full endogenous TCR knock down for maximal disruption (Provasi et al., 2012).

As seen in the alignment in Figure 3. 23 there are several mismatches between the wild type TCR β constant genes 1 and 2, and the codon-optimized TCR β constant gene sequences (as indicated by the pink highlighted nucleotides). However not all mismatched sequences were suitable because they do not comply with the above-mentioned rules of siRNA design. We were thus limited to three suitable sequences; TRBC2, TRBC3, and TRBC4, highlighted by the red, blue and green sequences in the alignment respectively. The selected sequences were used in the design of oligonucleotides for cloning (Table 3. 6). These oligonucleotides were designed to be compatible for cloning into the pRFP_C_RS_shRNA retroviral vector (Figure 3. 24). This vector is specialized for siRNA knock down experiments as it allows transcription of functional short hairpin RNA (shRNA) molecules from the oligo sequence,

expected to target the endogenous TCR β mRNA in the cell (Song and Yang, 2010). The vectors were transfected into the retroviral packaging cell lines PlatGP and PG13 as performed for the TCR vectors, and an empty vector control was also used for each siRNA vector. Because the pRFP_C_RS_shRNA possesses a red fluorescent protein (RFP) gene, it was possible to visualise the transfected cells in the packaging cell lines under the fluorescent microscope (Figure 3. 25).

TRBC2	TCTCCACACCCAAAAGGCCACACTGGTGTGCCTGGCCACAGGCTTCTACCCCGACCACG	120
TRBC1	TCTCCACACCCAAAAGGCCACACTGGTGTGCCTGGCCACAGGCTTCTTCCCTGACCACG	120
CodonOp	----CCACACCCAAAAGGCCACACTGGTGTGCCTGGCCACAGGCTTCTTCCCGACCACG *****	73
TRBC2	TGGAGCTGAGCTGGTGGGTGAATGGGAAGGAGGTGCACAGTGGGGTCAGCACAGACCCGC	180
TRBC1	TGGAGCTGAGCTGGTGGGTGAATGGGAAGGAGGTGCACAGTGGGGTCAGCACAGACCCGC	180
CodonOp	TGGAGCTGAGCTGGTGGGTGAACGGCAAGGAGGTGCACAGGGCGTGTGCACGACCCGC *****	133
TRBC2	AGCCCTCAAGGAGCAGCCCGCCCTCAAATGACTCCAGATACTGCCTGAGCAGCCGCCTGA	240
TRBC1	AGCCCTCAAGGAGCAGCCCGCCCTCAAATGACTCCAGATACTGCCTGAGCAGCCGCCTGA	240
CodonOp	AGCCCTCAAGGAGCAGCCCGCCCTGAACGACAGCAGATACTGCCTGAGCAGCAGACTGA *****	193
TRBC2	GGGTCTCGGCCACCTTCTGGCAGAACCCCGCAAACCACTTCCGCTGTCAAGTCCAGTTCT	300
TRBC1	GGGTCTCGGCCACCTTCTGGCAGAACCCCGCAAACCACTTCCGCTGTCAAGTCCAGTTCT	300
CodonOp	GAGTCTGAGCGCCACCTTCTGGCAGAACCCCGAAACCACTTCAAGATGCAGGTTCAGTTCT * * * * *	253
TRBC2	ACGGGCTCTCGGAGAATGACGAGTGGACCCAGGATAGGGCCAAACCTGTCAACCAGATCG	360
TRBC1	ACGGGCTCTCGGAGAATGACGAGTGGACCCAGGATAGGGCCAAACCCGTCAACCAGATCG	360
CodonOp	ACGGCTCTGAGCGAGAAGCAGCAGTGGACCCAGGACAGAGCCAAACCCGTCAACCAGATCG * * * * *	313
TRBC2	TCAGCGCCGAGGCTGGGGTAGAGCAGACTGTGGCTTACCTCCGAGTCTTACCAGCAAG	420
TRBC1	TCAGCGCCGAGGCTGGGGTAGAGCAGACTGTGGCTTACCTCCGAGTCTTACCAGCAAG	420
CodonOp	TCAGCGCCGAGGCTGGGGTAGAGCGACTGTGGCTTACCTCCGAGTCTTACCAGCAGG * * * * *	373

siRNA	Target sequence
TRBC2	TGACTCCAGATACTGCCTG
TRBC3	CCACTTCCGCTGTCAAGTC
TRBC4	GTCCAGTTCTACGGGCTCT

Figure 3. 23 Alignment of wild type TCR β constant genes with codon-optimized TCR β constant gene and selection of target sequences

The mismatched nucleotides between the native and the codon-optimized sequences are highlighted in pink. The sequences which have these mismatches in them, follow an AA dinucleotide and do not have significant homology to other human genes were selected as siRNA targets (highlighted in bold); TRBC2, TRBC3 and TRBC4, highlighted in red, blue and green respectively are shown.

Table 3. 6 The siRNA oligonucleotides and their component sequences

Oligo	BamHI+ 4nt	TRBC DNA sense	loop	TRBC DNA antisense	Termination	HindIII +4nt
TRBC2F	GTCTGGATCC	GTGACTCCAGATACTGCCTG	TTCAAGAGA	CAGGCAGTATCTGGAGTCAC	TTTTTT	AAGCTTACTT
TRBC3F	GTCTGGATCC	GCCACTTCCGCTGTCAAGTC	TTCAAGAGA	GACTTGACAGCGGAAGTGGC	TTTTTT	AAGCTTACTT
TRBC4F	GTCTGGATCC	GTCCAGTTCTACGGGCTCT	TTCAAGAGA	AGAGCCCGTAGAACTGGAC	TTTTTT	AAGCTTACTT

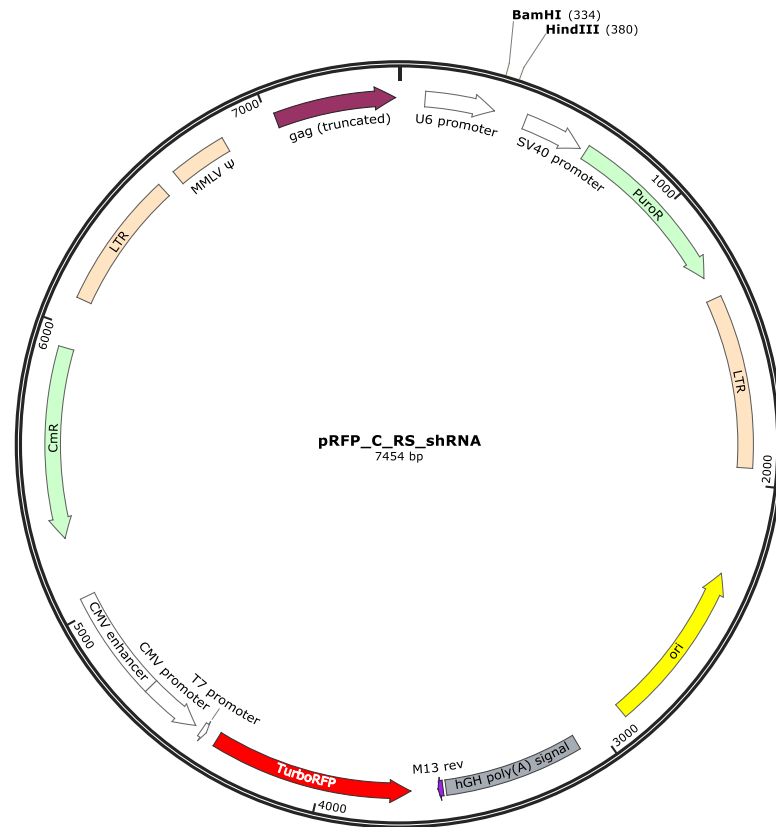


Figure 3. 24 Map of the pRFP_C_RS_shRNA vector

The shRNA oligonucleotides were cloned into the pRFP_C_RS_shRNA vector between the indicated BamHI and HindIII sites for stable production of siRNA.

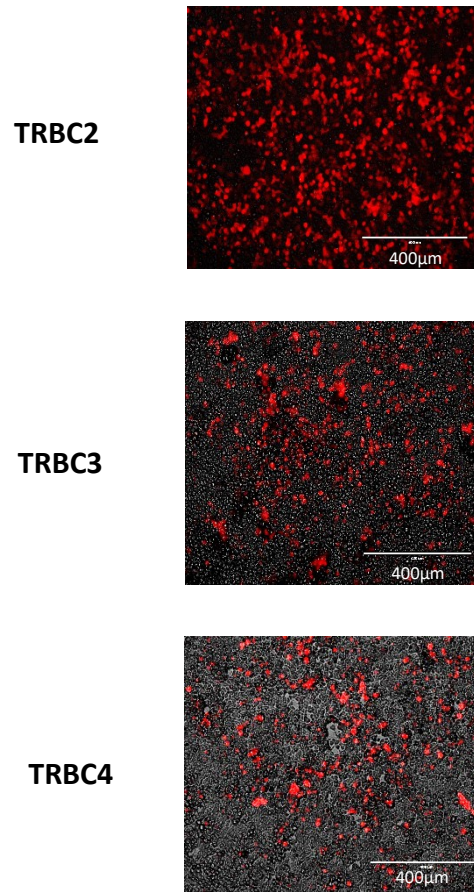


Figure 3. 25 Fluorescence microscope images confirming RFP vector transduction

PG13 packaging cells were transduced and the transduction efficiency of the pRFP_C_RS_shRNA vector was assessed using fluorescence microscopy 5 days later. The images are at 10x magnification and show the RFP-expressing cells. The scale line indicates 400µm.

3.7.2 Knock-out of TCRs from Jurkat cells and Primary T cells

The supernatant from the PG13 packaging cells was collected and used to transduce Jurkat cells and activated primary T cells from a healthy donor. The cells were cultured for two weeks in the presence of puromycin and analysed daily for changes in TCR expression post-transduction. The MFI levels of the TCR in each siRNA test was measured and calculated as a percentage of the MFI TCR expression in the empty vector control (Figure 3. 26).

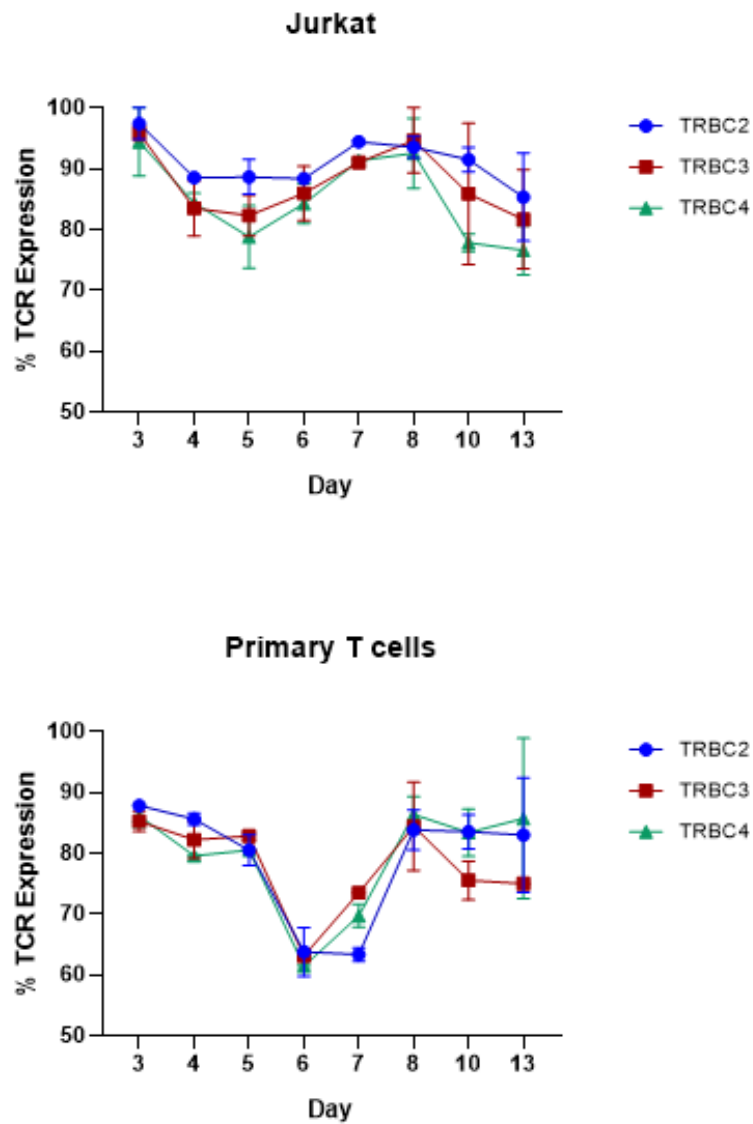


Figure 3. 26 Knock-down of TCR in Jurkat cells and in primary T cells with siRNA

Cells were treated with three siRNA vectors targeting different regions of the TCR β constant gene. Cultured cells were stained and TCR expression levels were compared to a mock-treated control. The data points indicate the MFI TCR as a percentage of the MFI TCR of the mock-treated control. Data shown is the SEM of two replicates from the same experiment.

The data shows that all three siRNA vectors against the TCR β constant region are able to knock-down TCR expression in Jurkat cells and in primary T cells to varying degrees. Despite targeting different regions of the TCR β mRNA, all three siRNAs induce a similar pattern of TCR expression alteration in the respective cells, and this pattern is transient. In Jurkat cells, the TCR expression seems to fluctuate throughout the 13 days of culture; post siRNA treatment, between days 3 and 5 the MFI decreases to as low as 80%, before reverting back between days 6 and 8. At days 10 and 13 however, the TCR expression decreases again to below 80%. A similar pattern of TCR expression fluctuation is seen in primary T cells; although there is a small decrease between days 3 and 5, at day 6 the TCR expression decreases dramatically to approximately 60% and remains low for two days before increasing again to approximately 90%.

The data indicates that the siRNA vectors targeting TCR β may have some impact on the levels of TCR expression in both Jurkat and primary T cells, but the current levels of knock down are not efficient enough for this method to be applied to our TCR cloning platform.

3.8 Discussion

3.8.1 Summary

I have successfully established an efficient single TCR cloning platform in our lab using a multiplex RT-PCR method which can amplify paired TCR $\alpha\beta$ chains from single sorted antigen-specific T cells. The platform is streamlined, accessible and universal, enabling any PCR-amplified TCR $\alpha\beta$ chains to be easily cloned into a single pre-prepared retroviral vector for stable expression in target T cells. Moreover, our platform overcomes several problems associated with conventional primary T cell cloning methods, including lengthy *in vitro* cell culture, and the possibility of certain clones being resistant to out-growth in culture.

A summary of the workflow is shown in Figure 3. 27.

The platform was utilized to clone TCRs from healthy donor CD8⁺ IFN- γ ⁺ T cells specific to the EBV immediate early lytic stage antigen ZEBRA. Cloned TCRs were successfully expressed in the TCR-deficient T cell line SKW3, and their functions were assessed. All the expressed TCRs recognised their cognate antigen in the ZEBRA peptide pool and became activated; they displayed higher levels of the early activation marker CD69 and produced greater amounts of TNF- α and IFN- γ compared to irrelevant peptide-stimulated controls.

A method of shRNA-mediated RNAi was designed to knock down endogenous TCRs from Jurkat cells and primary T cells. Three suitable siRNA sequences were identified and used to construct shRNA retroviral vectors for TCR knock down. Transduction of Jurkat cells and primary T cells resulted in fluctuating levels of TCR expression during a 2-week culture period compared to mock-transduced controls. Although the RNAi may have some impact on the levels of TCR expression in both Jurkat and primary T cells, the current method seems to be transient and may not be efficient for TCR replacement in this cloning platform.

Overall, this chapter demonstrates the validation of an optimized TCR cloning platform which can efficiently and accurately clone full-length TCRs from single live T cells without prior *in vitro* culture, overcoming several barriers associated with current methods of primary T cell cloning.

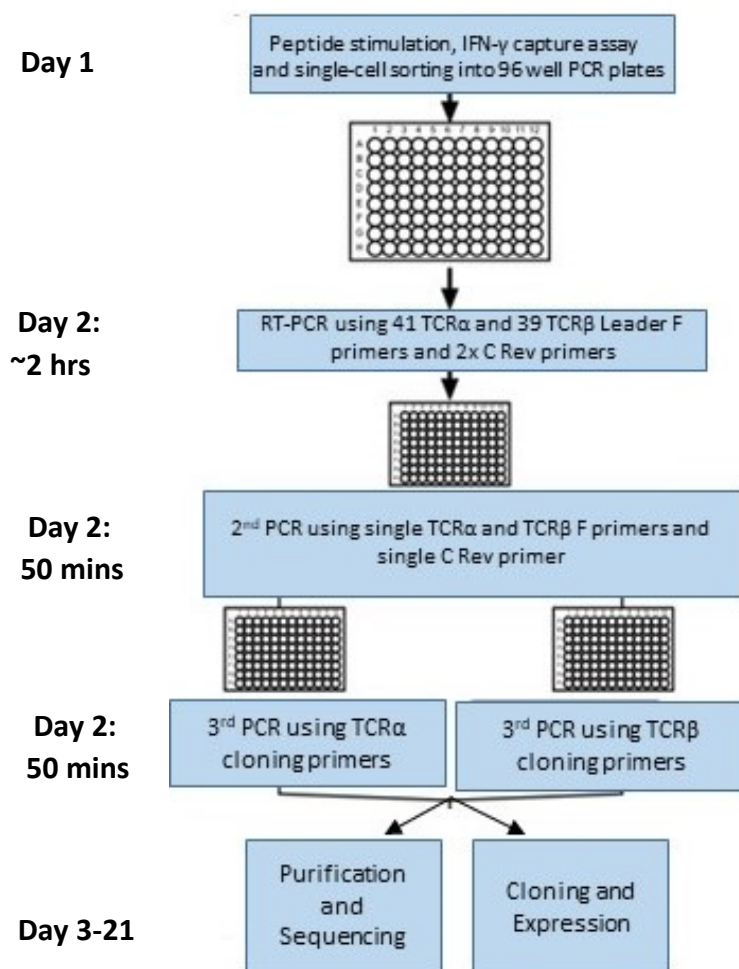


Figure 3. 27 Summary of Single TCR PCR workflow

Schematic showing workflow of single TCR cloning method with expected time frames.

The method begins with peptide stimulation for 6hrs, and single T cell FACS sorting, followed by 3 sets of PCRs. These are followed by purification and sequencing. The sequenced products are selected for cloning and expression in target cells.

3.8.2 Optimization of a single TCR cloning method

In order to optimize a single TCR cloning platform, various approaches to amplifying TCRs were tested. Many published protocols of TCR amplification do not amplify the full-length TCR but focus mainly on the CDR3 regions for repertoire analysis purposes (Han et al., 2014, Hu et al., 2018, Kim et al., 2012, Guo et al., 2016, Dash et al., 2011). Because we were interested in amplifying and cloning the full-length TCR α and β pairs, we selected two alternative protocols to optimise and establish our single TCR cloning platform. The first method tested was the 5'RACE PCR method by Kobayashi et al. (Kobayashi et al., 2013). The attraction of this method was its elegance, simplicity and apparently rapid nature. However as demonstrated by the data in Figure 3. 3, there are some major limitations associated with such a 5'RACE method, one of these being incomplete cDNA synthesis leading to missing crucial V-region sequences. If it is only the CDR3 variable regions that are desired for repertoire analysis purposes then this may be suitable, but even so, the authors expanded the antigen-specific cells in culture prior to PCR amplification, which is time-consuming. Another limitation of this method is that the PCR fragments are not ready to clone directly into a cloning vector. They must be reamplified after sequencing with gene-specific primers to incorporate cloning sites, rendering this method very time-consuming and labour-intensive. This does not support the 10-day clone made by the authors, who did not take into account these additional modifications. Thus, although the use of poly-G tail addition in this manner bypasses the use of multiple V-region specific primer sets, it is not suitable for efficient TCR cloning and characterization purposes.

The problem with incomplete cDNA synthesis was also encountered by the authors themselves, who later acknowledged and addressed the issue in a subsequent paper by designing a multiplex RT-PCR method to amplify full-length TCR chains (Hamana et al., 2016). This RT-PCR method was tried next in our attempt to set up and optimize a single TCR cloning platform. The RT-PCR method uses 41 TCR α and 39 TCR β forward primers which are specific to the Leader sequences of all known TCR $\alpha\beta$ genes. This enables amplification of the full VDJ genes of target TCRs, including the CDR3 region for antigen recognition. As shown in Figure 3. 27, the RT-PCR, 2nd and 3rd PCRs can be performed conveniently in a single day, with the products prepared for sequencing on the same day. As demonstrated by the gels in Figure 3. 4 and Figure 3. 5, the PCR method can successfully amplify full-length TCRs from Jurkat cells and primary T cells. In addition, it was

demonstrated that a variety of TCR α and β genes can be amplified from a polyclonal primary T cell population (Table 3. 1), indicating the capability of this PCR method.

Using the novel cloning primers which replaced the published 3rd PCR primers in my protocol, the platform is able to amplify between 75-95% of TCR $\alpha\beta$ pairs from antigen-specific cells, one of the highest efficiencies reported in the literature, which range from 50% to 90% (Han et al., 2014, Simon et al., 2014, Hamana et al., 2016, Kobayashi et al., 2013). Although there are some nonspecific products present on the gel, this does not affect the outcome as the TCR-specific bands at ~550bp are excised and purified for sequencing and cloning. We verified the accuracy and fidelity of this PCR method by sequencing amplified TCR genes from Jurkat cells, and comparing the obtained sequences with reference Jurkat gene sequences (Figure 3. 6 and Figure 3. 7). There was 100% fidelity between the amplified and reference TCR α and β genes, indicating that the method can accurately amplify TCRs without creating mutations.

The novelty in my cloning primers stems from alterations made to the original final PCR primers that were published by Hamana et al. The original primers were changed to incorporate novel cloning sites to enable Gibson Assembly of paired TCR genes into a retroviral vector, and upon comparison these novel cloning primers yielded a clearer, more defined PCR product than the published primers (Figure 3. 8). Using my novel primers, the TCR cloning platform was designed to enable seamless insertion of any amplified TCR α and β genes into the same retroviral vector via Gibson assembly cloning. The vector backbone had been modified to include a codon optimized TCR α constant region, and once it was generated, it was used for all subsequent TCR cloning experiments. The codon-optimized constant genes of both TCR α and β (kindly provided by Professor Hiroshi Hamana, University of Toyama, Japan, during email communication), contained additional cysteine residues to enable pairing of the transgenic TCR chains, decreasing the chance of the transduced chains mispairing with endogenous TCR α and β chains.

One of the limitations of multiplex PCR-based methods is the potential of better amplification of certain alleles compared to others, thus giving a false interpretation of the relative abundances of TCR sequences. However, this should not be an issue when single-sorted cells are being analysed, as only one TCR α and β chain will be amplified per cell. If the PCR efficiency is low then one may need to question why there is no TCR α or β product from that cell and whether this is due to lack of amplification of those particular TCR alleles or due to low quality or quantity of the starting RNA.

Most PCR-based methods have several limitations, including reaction inefficiencies and mutations inserted from polymerase errors (Kebschull and Zador, 2015, Potapov and Ong, 2017). In the case of repertoire analysis, the latter is problematic because it will not be possible to determine whether base-pair differences in CDR3 regions are legitimate biological polymorphisms, or whether they are a result of polymerase proof-reading errors (Egorov et al., 2015, Oakes et al., 2017).

Compared to other TCR cloning methods in literature, our method is efficient in its ability to amplify paired, full-length TCRs. Crucially, our method bypasses lengthy *in vitro* expansion of T cell clones, which can result in problems with biased outgrowth of some clones over others. Our method captures live, viable antigen-specific T cells after a short period of peptide-stimulation, enabling direct isolation of single IFN- γ ⁺ T cells. Other PCR-based methods which claim to be fast are not as efficient, as incomplete TCR sequences are obtained, either due to shortcomings with the PCR method itself (Kobayashi et al., 2013) or due to design of primers which exclude the crucial sequences of the TCRs outside the CDR3 region (Kim et al., 2012, Guo et al., 2016). In addition, compared to most other TCR cloning methods which report high efficiencies, including higher-throughput methods which can link TCRs to their functional phenotype, our method has many advantages. One of these is its accessibility; it requires no expensive high-throughput sequencing, complicated techniques or separate facilities; it can be performed in any laboratory with basic molecular biology equipment. Establishing this method in-house, although not high-throughput, is less costly than outsourcing to external companies and is easily applicable to TCR projects in the context of any disease.

3.8.3 PCR and sequencing of EBV ZEBRA-specific T cells

We applied our single TCR cloning platform as a proof of concept study to sequence and clone TCRs from EBV ZEBRA antigen-specific T cells. Fresh PBMCs from two healthy donors (whose T cells had previously been seen to produce IFN- γ in response to a ZEBRA peptide pool) were stimulated for 6 hours with the ZEBRA peptide pool before isolating CD8⁺ IFN- γ ⁺ T cells. An IFN- γ capture assay kit from Miltenyi Biotec was used for this as opposed to intracellular cytokine staining of cells because the latter method requires cell permeabilization, thus resulting in cell death and degradation of the RNA template needed for RT-PCR. The capture assay-based method of isolating the peptide pool-stimulated cells yielded approximately 5% of total live cells which were single sorted into 96 well plates. This

percentage of total live ZEBRA-specific CD8⁺ T cells obtained from each donor is in keeping with percentage EBV-specific cells obtained from healthy PBMCs in previous reports (Tan et al., 1999b). Using this method, we obtained approximately 2-3 plates of single sorted cells per donor. PCRs were performed and between 100-150 TCR products were sent for sequencing from each donor. Although the majority of sequences showed productive paired TCR α and β sequences, many sequences showed unproductive sequences in one or both TCR genes. This may have been due to the quality of the purified PCR products or due to low concentrations obtained, for example from the faint products in wells 23-26 in the donor 1 TCR α gel (Figure 3. 11). From the productive sequences obtained, a total of 77 and 138 TCR pairs were sequenced from healthy TCR donors 1 and 2 respectively. The TCRs were analysed and ranked according to frequency, an indication of polyclonal expansion and thus immunodominance (Joglekar et al., 2018, Han et al., 2014). In each of the two healthy donors, the most dominant TCRs contributed to between 10-21% of all the sequenced TCRs (Tables 3.3 and 3.4). Using a similar RT-PCR method, Hamana et al. reported that the most dominant TCRs specific to BRLF1, another EBV lytic stage antigen, made up 42-51% of the sequenced TCRs (Hamana et al., 2016). However, their sorted cells were obtained through tetramer-staining, which offers more specificity compared to peptide-pool stimulation (Tan et al., 1999b). On the other hand, our clonotype dominance data is more comparable to the variable ranges reported by Simon et al. (Simon et al., 2014). Their dominant TCR frequencies ranged between 6% to 54% of CMV antigen-specific TCRs in 4 different donors, and the T cells were also stimulated using a peptide pool before single-cell sorting. The observation that our dominant clonotypes comprised up to a fifth of the sequenced TCRs is significant as it supports their clinical relevance against lytic EBV infection, particularly given the possible diversity of more than 10^7 different TCR combinations in an individual (Arstila et al., 1999).

The labour-intensive method of manual PCR, extraction and sequencing of each TCR α and β product is a major drawback of our method, hindering the efficiency in terms of throughput. As all conventional single cell methods are similar in this regard however, this unfortunately cannot be avoided unless one opts for high-throughput bulk sorting, which would be unsuitable for antigen-specific TCR pair cloning purposes. Thus, the method was able to successfully isolate and amplify EBV ZEBRA-specific single TCR pairs from two healthy donors, providing an insight into the ZEBRA-specific TCR repertoire present in each donor.

3.8.4 Cloning and expression of EBV-specific T cells in SKW3 cells

The Gibson Assembly method (Gibson et al., 2009) employed in our platform enables seamless cloning of any TCR product into the prepared vector, without the need for restriction digest of the TCR fragments. Restriction digest is not only lengthy and labour-intensive, but can also pose a risk of accidental digestion of the TCR product itself should the restriction site be present in the TCR sequence. Although the cloning method itself is highly efficient, yielding approximately 70% of cloning products with correct inserts (Figure 3. 15), the unstable nature of the retroviral vector itself means that mutations can occur in the vector during bacterial growth phase. Due to this, it was necessary to screen several colonies from each Gibson Assembly transformation product in order to increase the chance of locating a successfully assembled, mutation-free clone. This contributed to the labour-intensive drawbacks of this method but ensured greater chances of obtaining a successful construct.

The correctly-assembled retroviral vectors were used to transduce the retroviral packaging cell lines PlatGP and PG13. Although the use of two different types of packaging cell lines adds an extra 3 days to the TCR cloning platform, it is more efficient overall. It is preferable to use retroviral particles produced by PlatGP cells to transduce PG13 cells, than to transfect PG13 cells directly with the vector because transducing the PG13 cells with retroviral particles not only results in stable infection, it also results in higher efficiencies of vector-positive PG13 cells, thus bypassing the need for enrichment of positive cells (Parente-Pereira et al., 2014). Consequently, the transduction efficiency in our PG13 cell lines was very high (Figure 3. 16); empty vector controls were up to 98% positive for GFP compared to the no vector negative control. Similarly, high levels of GFP expression were observed in TCR9 and TCR131 PG13 cells. The GFP levels were approximately between 73-78% in TCR16 and TCR132 PG13 cells, but were as low as 42% in TCR4 and TCR34. These varying levels of transduction efficiency may have been due to the starting concentrations of viral particles in the supernatant collected from PlatGP cells. Perhaps if the supernatant had been ultracentrifuged to concentrate the virus, the efficiencies would have been higher (Bowles et al., 1996).

Some of the dominant TCRs cloned from each donor were not able to be expressed in SKW3 cells. For example, TCR8 from donor 2 was the most dominant, making up 15% of all TCRs obtained from this donor, but no GFP expression was seen in PlatGP cells after transducing with this TCR vector. Similarly, TCRs 7 and 10 from donor 1 failed to be expressed in SKW3 cells (Figure 3. 18). The lack of expression of these TCRs may be explained by

possible mutations in the vector leading to unproductive TCR products, or perhaps by toxicity of the TCR combination to the target cell. This would require further investigation, as perhaps using different target cells may give more success.

Overall, the efficiency of TCR transduction in SKW3 cells is very high, with between 76-98% of GFP⁺ cells expressing CD3 and TCR, indicating efficient cloning of TCR chains into the retroviral vector for stable expression.

3.8.5 Functional analysis of SKW3 TCR clones

Peptide stimulation assays were performed on TCR-transduced SKW3 cells using autologous B cells pulsed with 10 μ M of the ZEBRA peptide pool. All TCR clones showed upregulation of CD69, and increased production of IFN- γ and TNF- α in response to stimulation with ZEBRA peptide pool, compared to the negative controls (Figure 3. 21 and Figure 3. 22). The levels of CD69 upregulation in the clones stimulated with cognate peptide were similar to that achieved by CD3 antibody stimulation for each TCR clone, whereas the irrelevant peptide induced similar levels of CD69 as the BCL only control. This demonstrates the specific and reliable nature of the transgenic TCRs, indicating that they have been accurately cloned from the primary T cells.

The MSD U-plex platform was used to measure the cytokines in the supernatants collected from the stimulation assays. This is a more efficient and very sensitive way of measuring multiple cytokines as a variety of analytes can be measured in a single well, at very low concentrations. Although costly compared to standard ELISAs, it was ideal for measuring the IFN- γ and TNF- α from SKW3 cells as we were uncertain of the levels of cytokines to expect from our clones. The SKW3 TCR clones stimulated with ZEBRA peptide pool produced higher levels of IFN- γ and TNF- α compared to when stimulated with irrelevant peptide (Figure 3. 22). This ZEBRA peptide-dependent increase supports the fact that all the transduced TCRs have retained their specificity and function since being isolated on their IFN- γ producing phenotype, cloned and expressed on the surface of the SKW3 T cell line. In future experiments, the MSD could be used as a standard way to measure the activation and functional ability of the TCR-transduced clones in a highly sensitive way. Costs permitting, this could bypass the use of flow cytometry to analyse CD69 upregulation, thus potentially reducing on experimental time as the cytokines may be measured earlier due to the high sensitivity of the MSD.

Thus, overall the data from the functional assays performed on the EBV-specific TCR clones indicate that our single TCR cloning platform is efficient and reliable. The positive responses

from the transduced SKW3 clones towards the ZEBRA peptide pool, which was used in the initial stages to isolate the cells, indicates that the integrity of the TCR sequence has been preserved during cloning, with seemingly no mutations occurring. The recognition of the antigens confirms expression of correctly functioning TCRs which retain their ability to recognize their cognate antigen and activate the T cell, validating our TCR cloning method.

3.8.6 Knock-down of endogenous TCRs via RNAi

We constructed shRNA retroviral vectors which encoded siRNA to knock down endogenous TCR expression from Jurkat cells and primary T cells. The siRNA sequences were chosen to target sequences in the known constant region of the TCR β constant gene which were mismatched from that of our codon-optimized gene, thus rendering our transgenes resistant to the siRNA. We opted to target only one of the TCR chains for simplicity and because it had been shown previously to be sufficient for endogenous TCR knock down (Legut et al., 2018). To determine suitable sequences, specific rules for siRNA design were followed; the selected target mRNA sequence must be between 19-21 nucleotides long, begin with an AA dinucleotide, and have a GC content of 30-50% (Boettcher and McManus, 2015). In addition, to prevent premature termination, stretches of more than 4 T's and A's were avoided in the target sequence. The potential target mRNA site was then compared to the human genome database and checked; those with more than 16-17 continuous base pair homology to other human genes were disregarded. These design rules limited the potential siRNA targets we could use (Figure 3. 23). We obtained 3 suitable siRNA target sequences and constructed vectors for use in the knock down experiments. The goal was that eventually, the siRNA sequence would be cloned into the TCR vector to be expressed alongside the transgenic TCR, thus acting as a direct TCR replacement vector, knocking down the endogenous TCR in the transduced cell and enabling safe, unhindered expression of the transgenic TCR.

The preliminary data indicated that all three vectors were able to knock-down TCR expression in both Jurkat cells and in primary T cells to some extent, but also displayed great fluctuation in TCR expression across the two-week culture period. For example, in primary T cells at day 6 post-transduction, the TCR expression decreases dramatically to approximately 60% and remains low for two days before increasing again to approximately 90%. The fluctuating levels of TCR expression in the treated cells are concerning and may be attributed to manual or technical errors, such as discrepancies in staining or the functioning of the flow

cytometer on these days. If the levels of TCR expression are true however, perhaps if the cells were sorted for TCR-negative cells (on day 5 for Jurkat cells and day 6 for primary T cells), the stability of the TCR knock down could have been assessed by seeing if the TCRs resurfaced. A more efficient and permanent approach such as the CRISPR method could be used in the future to produce a TCR replacement vector that could be incorporated with our existing platform (Legut et al., 2018). For our current platform however, the sites of mismatch between the codon-optimized and endogenous constant regions sequences are so limited that it would not have been possible to design a CRISPR or TALENs-based TCR knock out system as these require much longer target sequences to be effective (Jinek et al., 2012, Ran et al., 2013, Bogdanove and Voytas, 2011). In addition, the CRISPR-Cas9 system has its own disadvantages which must be considered in future treatment designs (Charlesworth et al., 2018, Crudele and Chamberlain, 2018).

Additionally, only the TCR- β constant region was targeted in our method as it has previously been shown that targeting the TCR- β alone is sufficient for significant TCR knockout and replacement (Legut et al., 2018). Perhaps by targeting the TCR α constant gene simultaneously would have yielded better knock down of the endogenous TCRs due to degradation of both chain genes simultaneously (Provasi et al., 2012). Finally, perhaps co-transfection of all the shRNA vectors to target multiple sites in the endogenous TCR simultaneously would have been more successful as it may have increased the chances and efficiency of RNAi (Ji et al., 2003).

Overall, the apparent transient nature of TCR knock down seen using the current siRNA protocol suggests that it would not be efficient to incorporate it into our existing TCR vectors and further work needs to be done to optimize such a method for future use.

3.8.7 Future work

For future experiments, it may be useful to modify the PCR method to include primers against functional phenotypes in the reverse transcription reaction. For example, the addition of primers against T cell transcription factors and proinflammatory cytokines such as those described by Han and colleagues (Han et al., 2014), would allow the direct selection of T cell subtypes of interest according to their phenotype, without having to express and perform functional assays to identify functionally relevant TCRs.

The cloning system could be improved in its screening of relevant TCRs. In our platform, the

cloned vectors are transfected into packaging cell lines to produce retroviral particles, before transduction of target T cells. Although critical for producing TCR-engineered T cells, this is time consuming during the initial screening process when testing TCR function and specificity. One way to improve this aspect of the system would be to use a reporter cell line system expressing luciferase or GFP. Such a cell line could be transfected with the TCR vector directly and used to stimulate with peptide in order to test for function and specificity using fluorescence as a readout. Other groups have used such systems as a way to overcome the cumbersome nature of retroviral particle production and transduction, demonstrating that reporter cell lines can be used to easily screen for relevant TCRs (Hamana et al., 2016, Guo et al., 2016). Although these cells cannot be used directly for functional and killing assays, they could fast-track the screening stage to select TCRs of interest.

As mentioned previously, the TCR knock down experiments could be improved by trying a different method, such as TALENs or CRISPR-Cas9, to target the endogenous TCR (Berdien et al., 2014, Legut et al., 2018). Further work could involve the improvement of the protocol to include a mechanism for endogenous TCR knock down within the same T cells that the transgenic TCR is to be expressed. This may involve the inclusion of endogenous TCR-specific siRNA, CRISPR or TALENs in the same vector as the TCR, allowing simultaneous knockout of endogenous TCRs and expression of transgenic TCRs (Legut et al., 2018, Ochi et al., 2011, Sun et al., 2019). Such combined gene silencing and TCR transgene expression method has recently been demonstrated successfully in an in vivo model (Sun et al., 2019). Including such a mechanism in our platform would allow the vector to be used as a direct TCR replacement method as opposed to requiring the production of TCR knockout cells beforehand or trying to find HLA-matching donor cells in a TCR knockout line. However major changes in our TCR vector would be required to accommodate the use of such gene-editing methods.

4

Characterization of EBV ZEBRA-specific T cell receptors

4.1 Introduction

Epstein Barr Virus (EBV) is a widespread γ -herpesvirus which establishes lifelong persistent infection in humans (Kieff, 2007). During primary infection in adolescents, EBV replicates in the mucosal epithelia in the oropharynx and is met with a strong CD8⁺ T cell response against lytic stage antigens (Steven et al., 1997, Callan et al., 1998, Hislop et al., 2002, Kieff, 2007). Although most of the virus-infected cells are eliminated by specific T cells, a fraction of infected cells are able to survive within memory B cells, entering the latent stage of infection (Kieff, 2007). In the latent state, EBV expresses a very limited set of genes which permit maintenance of persistent infection in the absence of viral replication (Rowe et al., 1986, Hochberg et al., 2004).

The lytic stage of EBV infection consists of 3 phases; immediate early (IE), early (E) and late (L), with over 80 different lytic EBV proteins expressed along with infectious virus particles (Kieff, 2007). In contrast, only 6-8 viral proteins are expressed during the three latent infection phases. The lytic phase antigens are predominantly recognised by CD8⁺ CTLs, whilst the latent phase antigens are predominantly CD4⁺ specific and less frequent than their CD8⁺ counterparts (Hislop et al., 2007). Both lytic and latent antigen-specific T cells are of interest therapeutically owing to their roles in the different phases of infection; the former are known to exert the greatest effect during primary infection in virus killing and control, whereas the latter are thought to control viral spread during the chronic stages. (Long et al., 2005, Pudney et al., 2005, Hislop et al., 2007).

A hierarchy of immunodominance has been shown of lytic epitope-specific T cells; IE Ag-specific CD8⁺ T cells are most immunodominant, followed by E and then L stage antigens, suggesting impairment of antigen-processing with progression of the lytic cycle (Pudney et al., 2005, Catalina et al., 2001, Abbott et al., 2013). The IE lytic stage antigens BZLF1 (aka ZEBRA, Zta) and BRLF1 (aka Rta), are transcriptional activators which are involved in the propagation of the lytic cycle of infection. They are well known targets of CD8⁺ T cells, leading to the release of antiviral cytokines and target cell death (Steven et al., 1997, Bogedain et al., 1995). ZEBRA is a crucial protein in the EBV lifecycle because it plays an indispensable role in propagating the lytic cycle from the latent viral state. The ZEBRA protein consists of various structural domains; it contains a transactivation domain (amino acids [aa] 1-166), a basic DNA recognition domain (aa 178 to 194), and a coiled-coil dimerization domain (aa 198-225) (Flemington et al., 1992, Farrell et al., 1989). A number of

CD8⁺ T cell epitopes presented by HLA-A, -B and -C have been defined, indicating that polymorphism in the HLA loci ensures diversity in the T cell responses to viruses, minimizing the effects of virus escape mutation (Rist et al., 2015b). Rist et al. demonstrated that many overlapping ZEBRA epitopes exist in clusters whilst other regions are not recognised by CD8⁺ T cells. As the overlapping epitopes are presented by several different HLA alleles which predominate in different parts of the world, the existence of these immunological hotspots could be exploited therapeutically for the design of treatments (Rist et al., 2015b).

Precise mapping of T cell epitopes enables the critical analysis of the immune response via HLA-peptide multimers, and characterization of the HLA-restriction of EBV-specific TCRs can aid directly in vaccine development and adoptive immunotherapy. Thus, in this chapter, the EBV ZEBRA-specific TCRs that were cloned from healthy donors 1 and 2 were characterized in terms of their HLA-restriction and mapped to their specific peptide epitopes. The intriguing characteristics of TCR4, obtained from donor 1, will be discussed first, followed by those of the five TCRs from donor 2.

4.1.1 Chapter-specific aims

There were 2 key aims for this chapter of the thesis;

1. To determine the HLA-restriction of the EBV ZEBRA-specific TCRs cloned from donors 1 and 2
2. To map the precise EBV ZEBRA epitopes which are recognised by each TCR

4.2 Characterization of TCR4 from Donor 1

4.2.1 HLA restriction of TCR4

The HLA restriction of TCR4 from donor 1 was first determined. In order to do this, standard peptide stimulation assays were carried out using a panel of EBV-LCLs (henceforth referred to as BCLs) already established in the lab. The BCLs selected for this panel had known partial histocompatibility for the HLA alleles expressed by donor 1, i.e. each BCL had only one HLA allele which matched the HLA- A, -B, or -C alleles expressed by donor 1. The principle of the assay is that only the BCL that shares a single HLA allele will induce a positive CD69+ response in the T cells, thus indicating the HLA-restriction of the TCR. The HLA-A, -B and -C alleles expressed by TCR donor 1 are shown in Table 4. 1.

The HLA types of the BCL panel used to present peptides to TCR4-expressing SKW3 cells are shown in Appendix 5. The histograms in Figure 4.1 display the data from the peptide pulsing experiment using BCLs which are partially histocompatible to TCR donor 1.

Table 4. 1 The HLA alleles of TCR Donor 1

HLA-A1	HLA-A2	HLA-B1	HLA-B2	HLA-C1	HLA-C2
A*02:01	A*11:01	B*35:01	B*49:01	C*04:01	C*07:01

The data in Figure 4.1 indicate that TCR4 did not respond to ZEBRA peptide-pulsed BCLs expressing HLA-A*11:01 or HLA-B*49:01. Unexpectedly however, there was CD69 upregulation seen on TCR4 cells in response to ZEBRA peptide-pulsed BCLs expressing HLA-A*02:01, as well as BCLs expressing HLA-B*35:01. Although this was surprising, we speculated that perhaps the TCR recognised two separate EBV ZEBRA epitopes presented on the respective HLA molecules. To investigate this, peptide epitope mapping studies were performed on the TCR4 cells.

4.3 Epitope mapping of TCRs

The peptide specificity of all of the EBV-specific TCRs was determined using a series of peptide stimulation assays involving various ZEBRA peptide pools, followed by their individual component 18mer peptides. The 18mer which was recognised was then truncated into 15-, 13-, 11- and 9mers (Appendix 6 and 7) for the specific epitope to be determined. In each assay, the TCR-transduced SKW3 cells were assessed for the upregulation of CD69 on their cell surface in response to the peptides loaded on autologous or selected allogenic BCLs.

The complete ZEBRA peptide pool contained forty-seven 18mer peptides overlapping by 10 amino acids. In order to determine the specific 18mer peptide recognised by the TCRs, the 47 peptides in the complete ZEBRA pool were grouped into 8 smaller pools of 18mers (pools 1-8). These were 7 groups of six overlapping 18mer peptides each, and a final group comprised of the five remaining overlapping 18mers (Table 4. 2) These pools were used to pulse autologous BCLs before peptide stimulation assays were performed as described previously. The pool which induced a positive CD69 response was then divided into its component 18mer peptides (18mers a-f in Table 4. 2) and these were used in a new round of stimulation to map the T cell epitope to its specific 18mer peptide.

Table 4. 2 The 18mer ZEBRA peptides in each pool

Pool	18mer	Sequence
1	1a	MMDPNSTSEDKFTDPY
	1b	STSEDKFTDPYQVPFV
	1c	VKFTDPYQVPFVQAFDQ
	1d	DPYQVPFVQAFDQATRVY
	1e	PFVQAFDQATRVYQDLGG
	1f	FDQATRVYQDLGGPSQAP
2	2a	RVYQDLGGPSQAPLPCVL
	2b	LGGPSQAPLPCVLWVFLP
	2c	QAPLPCVLWVFLPEPLPQ
	2d	CVLWVFLPEPLPQGLTA
	2e	VLPEPLPQGLTAYHVSA
	2f	LPQGGLTAYHVSAAPTGS
3	3a	LTAYHVSAAPTGSWFAP
	3b	VSAAPTGSWFAPQFAPE
	3c	TGSWFAPQFAPENAYQA
	3d	PAPQFAPENAYQAYAAPQ
	3e	APENAYQAYAAPQLFPVS
	3f	YQAYAAPQLFPVSDITQN
4	4a	APQLFPVSDITQNQLTNQ
	4b	PVSDITQNQLTNQAGGEA
	4c	TQNQLTNQAGGEAPQPGD
	4d	TNQAGGEAPQPGDNSTVQ
	4e	GEAPQPGDNSTVQPAAAV
	4f	PGDNSTVQPAAAVLACP
5	5a	TVQPAAAVLACPGANQE
	5b	AAVVLACPGANQEQLAD
	5c	ACPGANQEQLADIGAPQ
	5d	NQEQLADIGAPQPAPAA
	5e	LADIGAPQPAPAAAPARR
	5f	APQPAPAAAPARRTRKPL
6	6a	PAAAPARRTRKPLQPESL
	6b	ARRTRKPLQPESLEECDS
	6c	KPLQPESLEECDSELEIK
	6d	ESLEECDSELEIKRYKNR
	6e	CDSELEIKRYKNRVASRK
	6f	EIKRYKNRVASRKCRAKF
7	7a	KNRVASRKCRAKFKHLLQ
	7b	SRKCRAKFKHLLQHCREV
	7c	AKFKHLLQHCREVASAKS
	7d	LLQHCREVASAKSENDR
	7e	REVASAKSENDRRLRLL
	7f	AKSENDRRLRLLKQMCP
8	8a	NDRRLRLLKQMCPSLDVD
	8b	LLLKQMCPSLDVDSIIPR
	8c	MCPSLDVDSIIPRTPDVL
	8d	DVDSIIPRTPDVLHEDLL
	8e	DSIIPRTPDVLHEDLLNF

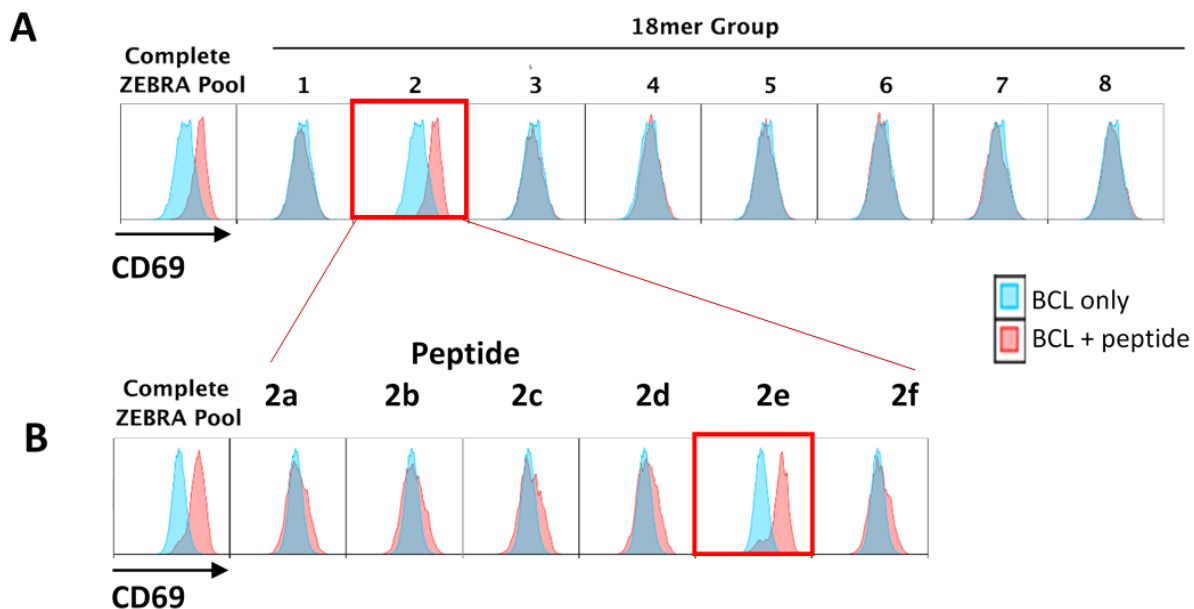


Figure 4.2 The 18mer epitope mapping of TCR4

TCR4 SKW3 cells were stimulated with 18mer pools 1-8 (Panel A) to identify the specific peptide pool to which the T cells responded (highlighted in red box, top). The T cells were then stimulated with the 6 constituent 18mer peptides of pool 2 (2a-2f, Panel B).

In all assays, ZEBRA peptide-stimulated cells were compared to cells incubated with BCLs without peptide. The plots showing a population positive for CD69 upregulation are highlighted in red. The complete ZEBRA peptide pool was used as a positive control.

As shown in Figure 4. 2, after stimulation TCR4 increased CD69 upregulation towards peptide pool 2, compared to BCL only controls. The 18mers that made up pool 2 (peptides 2a-2f) were then used individually to test the TCRs in a second round of peptide stimulations. The stimulation assays show that TCR4 maps to the 18mer VLPEPLPQGQLTAYHVSA (Figure 4. 2, Table 4. 2).

In order to further map TCR4, the VLP 18mer was truncated into all possible 15-, 13-, 11- and 9mers (Mimotopes, Australia). We initially speculated that within this 18mer were 2 different epitopes presented differentially by HLA-A*02:01 and HLA-B*35:01. The TCR4 SKW3 cells were stimulated with autologous BCLs pulsed with these truncated peptides in the same manner as above. Table 4. 3 shows a summary of the results of these peptide stimulation assays. There were no positive CD69 responses seen to any of the 9mer sequences within the VLP 18mer. The related histograms are shown in Appendix 8.

As shown in Table 4. 3, the TCR4 cells recognised all but one 13mer within the VLP 18mer when presented on autologous BCL. They also recognised 4 different overlapping 11mers. In order to determine if the different overlapping 11mer epitopes were recognised differentially on HLA-A*02:01 and HLA-B*35:01, a new panel of BCLs were chosen to present the 11mers to the TCR4 cells. The HLA alleles in each BCL used in this new experiment are shown in Appendix 5. In addition to donor BCLs which were positive for either HLA-B*35:01 or HLA-A*02:01 (IAVI 3572 and IAVI 3374, respectively), a modified version of the .221 human B-lymphoblastoid cell line, the .221_A2 line was used. The original .221 line is known to be negative for all HLA-A and -B alleles, although it has been recently shown to express low levels of HLA-C*01:02 (Partridge et al., 2018). The .221_A2 cells had been previously transfected in our lab to stably express only HLA-A*02:01, thus they were used to confirm whether TCR4 recognises peptide presented on HLA-A*02:01.

Figure 4. 3 shows representative data from the peptide stimulation assays performed to investigate whether different 11mer epitopes are presented independently on HLA-B*35:01 and HLA-A*02:01. Subsequent experiments were performed to confirm and replicate these results (Appendix 9) and two additional BCLs were later used to rule out the potential involvement of HLA-C alleles (HC6 and HK2) (Figure 4. 4).

Table 4. 3 Summary of peptides recognised by TCR4 after presentation on autologous BCL

Peptide Length	Amino Acid Sequence	CD69 status¹
18	VLPEPLPQGQLTAYHVSA	+
13	VLPEPLPQGQLTA	+
13	LPEPLPQGQLTAY	+
13	PEPLPQGQLTAYH	+
13	EPLPQGQLTAYHV	+
13	PLPQGQLTAYHVS	-
13	LPQGQLTAYHVSA	+
11	VLPEPLPQGQL	-
11	LPEPLPQGQLT	+
11	PEPLPQGQLTA	+
11	EPLPQGQLTAY	+
11	PLPQGQLTAYH	-
11	LPQGQLTAYHV	+
11	PQGQLTAYHVS	-
11	QGQLTAYHVSA	-

¹ + and – indicate positive and negative CD69 upregulation, respectively, in response to peptide stimulation, compared to BCL only controls.

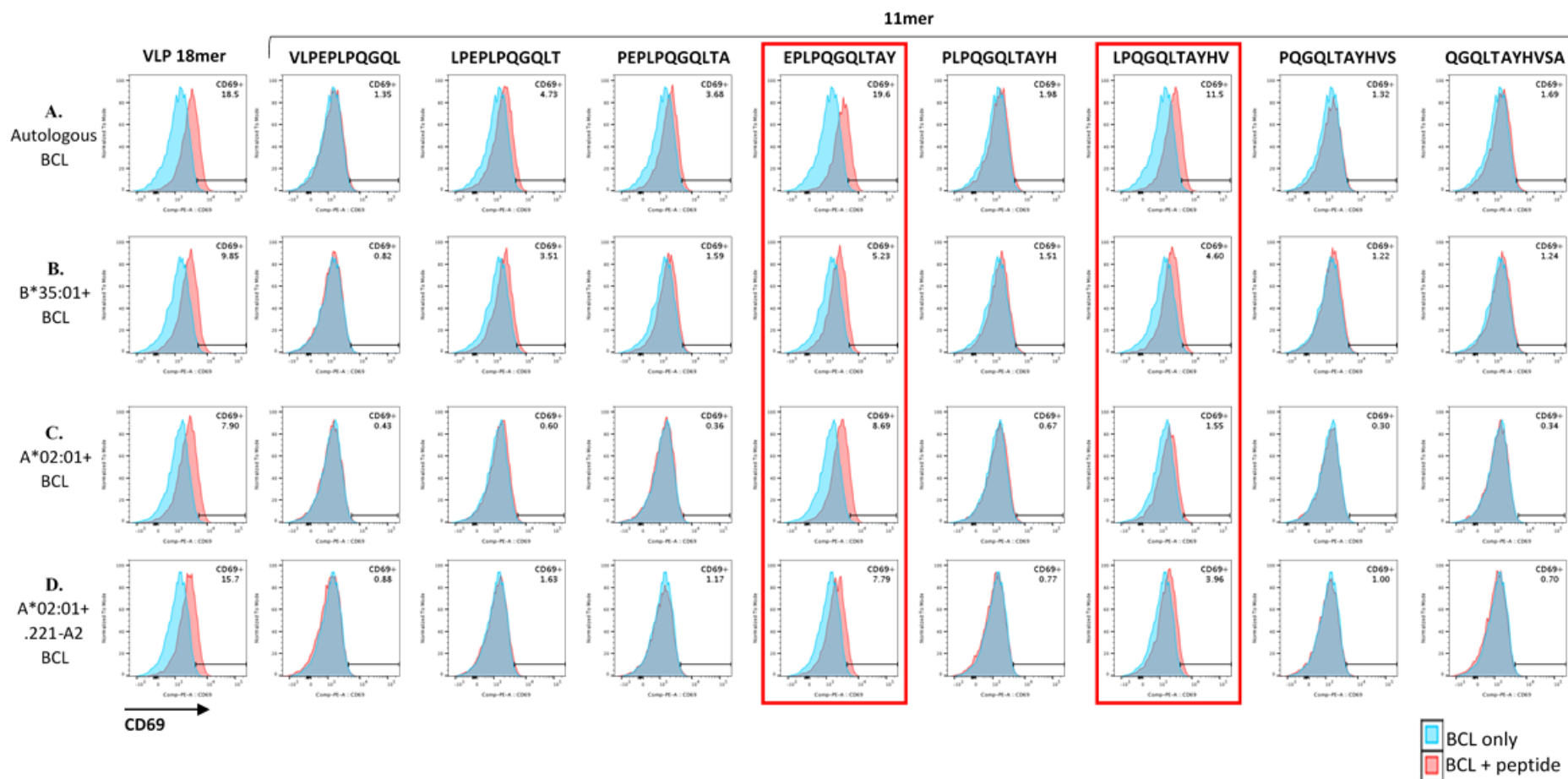


Figure 4.3 TCR4 recognizes two overlapping 11mers on both HLA*02:01 and HLA-B*35:01

Partially histocompatible BCLs (Table 4.5) were used to present the VLP 18mer and its constituent overlapping 11mers to TCR4 SKW3 cells. The histograms in row A show the levels of CD69 upregulation in response to peptide-loaded autologous BCLs, which express both HLA-A*02:01 and HLA-B*35:01. The row B shows the IAVI 3572 BCL which is HLA-B*35:01+ HLA-A*02:01-. Row C shows the IAVI 3374 BCL which is HLA-B*35:01- but HLA-A*02:01+. Row D shows the .221_A2 BCL, which only express HLA-A*02:01 and no other HLA I proteins. ZEBRA peptide-stimulated cells were compared to cells incubated with BCL in the absence of peptide. The 11mers which are recognised by both HLA-A*02:01 and HLA-B*35:01 alleles are highlighted in the red boxes. The data is representative of data from 3 similar experiments.

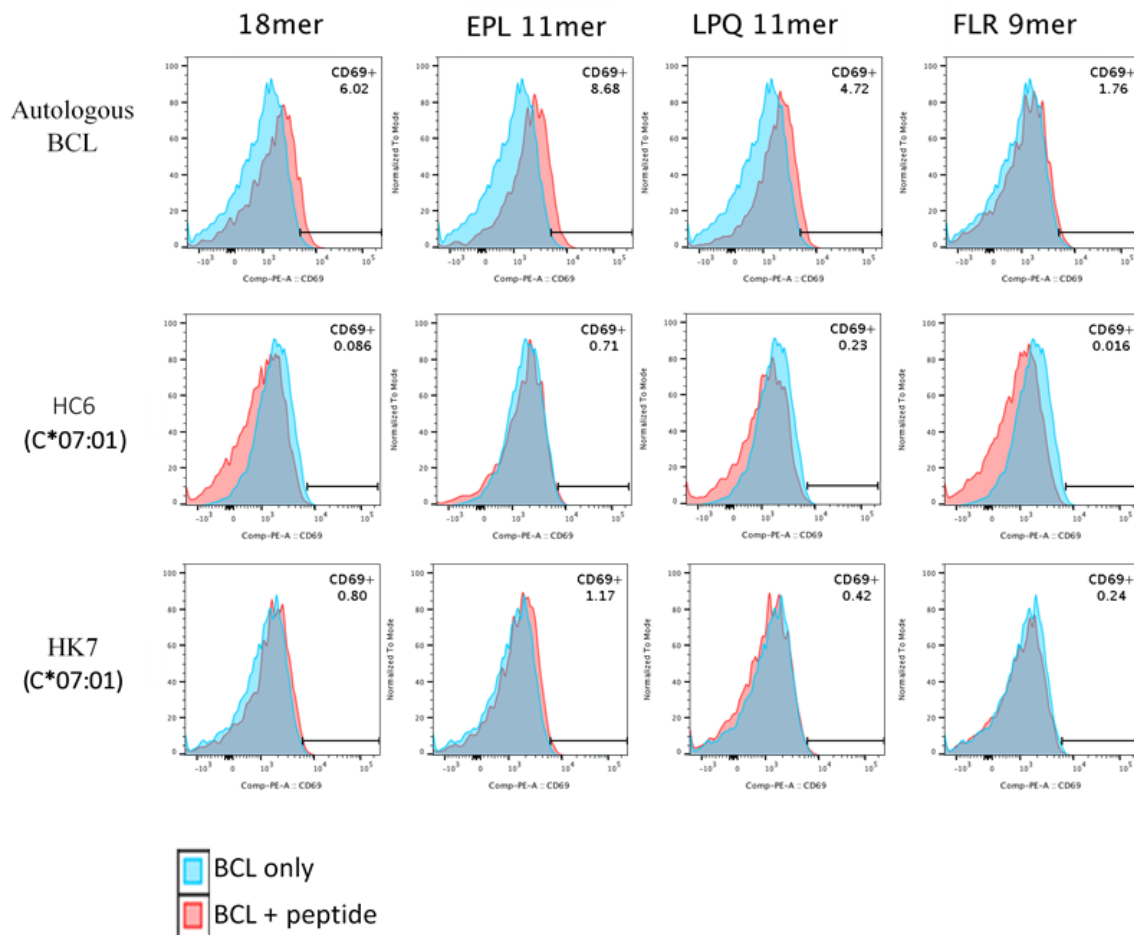


Figure 4. 4 TCR4 does not recognise peptide presented on HLA-C*07:01

Partially histocompatible BCLs (HC6 and HK7) which possessed only HLA-C*07:01 matching to the autologous BCL were used to present the VLP 18mer, EPL 11mer, LPQ 11mer peptides and an irrelevant 9mer peptide FLRGRAYGL to TCR4 SKW3 cells.

CD69 upregulation was measured after 18hrs stimulation and compared to TCR4 cells co-cultured with BCL without peptide.

The data in Figure 4. 3 demonstrates that TCR4 can recognise 2 different, overlapping 11mers EPLPQGQLTAY and LPQGQLTAYHV, and that this occurs when the peptides are presented on HLA-A*02:01 or HLA-B*35:01. The histograms also show that the 11mers LPEPLPQGQLT and PEPLPQGQLTA are also recognized by HLA-B*35:01 but not by HLA-A*02:01.

Figure 4. 4 demonstrates that there is no involvement of HLA-C*07:01 and that it is not presenting the peptides of this region of ZEBRA to TCR4. An irrelevant EBV 9mer (FLRGRAYGL) was used as a control to assess whether the TCR recognises peptide non-specifically. There was no CD69 upregulation on the T cells in response to this irrelevant peptide, indicating that the TCR4 SKW3 T cells specifically recognise the two 11mers EPL and LPQ when presented on HLA-A*02:01 and HLA-B*35:01.

In order to assess whether it is the 9mer LPQGQLTAY that TCR4 is recognizing, as this sequence is present in the overlapping region between the EPL and LPQ 11mers, a separate peptide stimulation assay was performed using 9mers within the VLP 18mer. None of the 9mers provoked activation of the TCR4 SKW3 cells when presented on autologous BCL however (Appendix 8).

4.4 Characterization of TCRs from Donor 2

The five EBV-specific TCRs which were cloned from Donor 2 (TCR9, TCR16, TCR34, TCR131 and TCR132) were also characterized in terms of their HLA-restriction and were epitope mapped. The HLA A, B and C alleles for TCR Donor 2 are shown in Table 4. 4. The HLA types of the partially histocompatible BCL panel used to map the HLA restriction of the TCRs are shown in Appendix 5.

The BCLs were loaded with the complete ZEBRA peptide pool and co-cultured with SKW3 cells expressing TCR9, TCR16, TCR34, TCR131 and TCR132. As previously, CD69 upregulation was assessed after 18 hours and compared to BCL only controls (Figure 4. 5).

Table 4. 4 The HLA alleles of TCR Donor 2

TCRs	HLA-A		HLA-B		HLA-C	
9, 16, 34, 131, 132	A*23:01	A*31:01	B*18:01	B*40:01	C*03:04	C*07:01

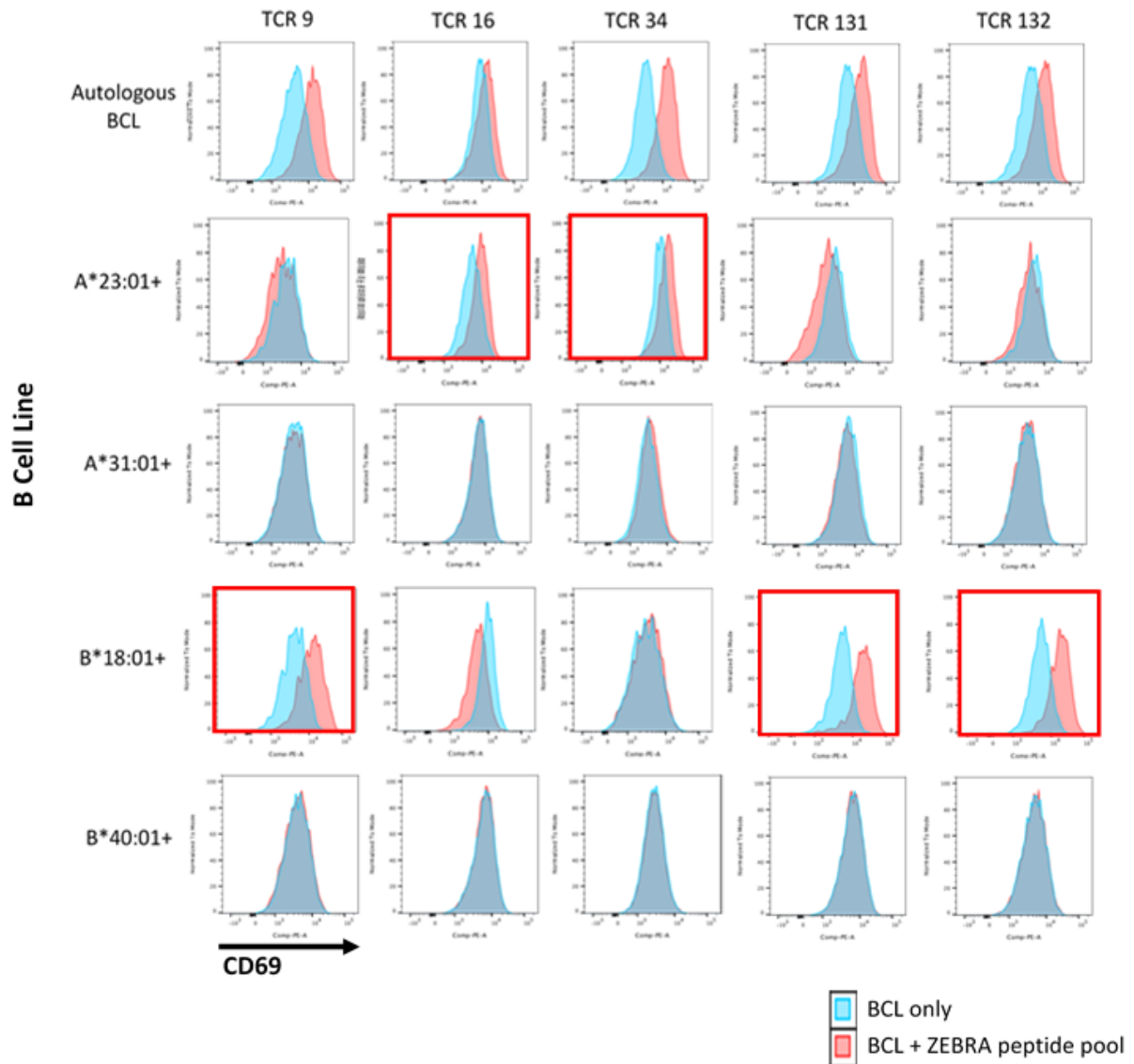


Figure 4. 5 HLA restriction mapping of TCRs from Donor 2

The HLA restrictions of TCRs 9, 16, 34, 131 and 132 were determined through peptide stimulation assays using partially histocompatible BCLs which were loaded with the complete ZEBRA pool. The autologous BCL was used as a positive control. CD69 upregulation was measured after 18hrs stimulation and compared to cells co-cultured with BCLs in the absence of peptide. The plots showing a population positive for CD69 upregulation after presentation by partially histocompatible BCLs are highlighted in red.

Figure 4. 5 demonstrates that the various TCRs derived from Donor 2 are restricted to different HLA alleles; TCRs 9, 131 and 132 show an upregulation of CD69 after stimulation with peptide presented on HLA B*18:01, whilst TCRs 16 and 34 respond to peptide presented on HLA A*23:01. In order to characterize the TCRs further, they were mapped to their peptide epitopes. This was performed in the same manner as for TCR4, initially using the smaller pools derived from the complete ZEBRA peptide pool (Table 4. 2) before stimulating with the constituent 18mers of the activating pool (Figure 4. 6).

All of the Donor 2 TCRs showed a positive response towards pool 6 (Figure 4. 6A), and all mapped to the same 18mer 6e, which is CDSELEIKRYKNRVASRK (Figure 4. 6B and Table 4. 2). The 9mers within the CDS 18mer were loaded onto autologous BCL and CD69 upregulation on the T cells was assessed after 18 hours of stimulation and compared to a BCL only control. The results are presented in Table 4. 5. The histograms depicting the CD69 staining results are shown (Appendix 10).

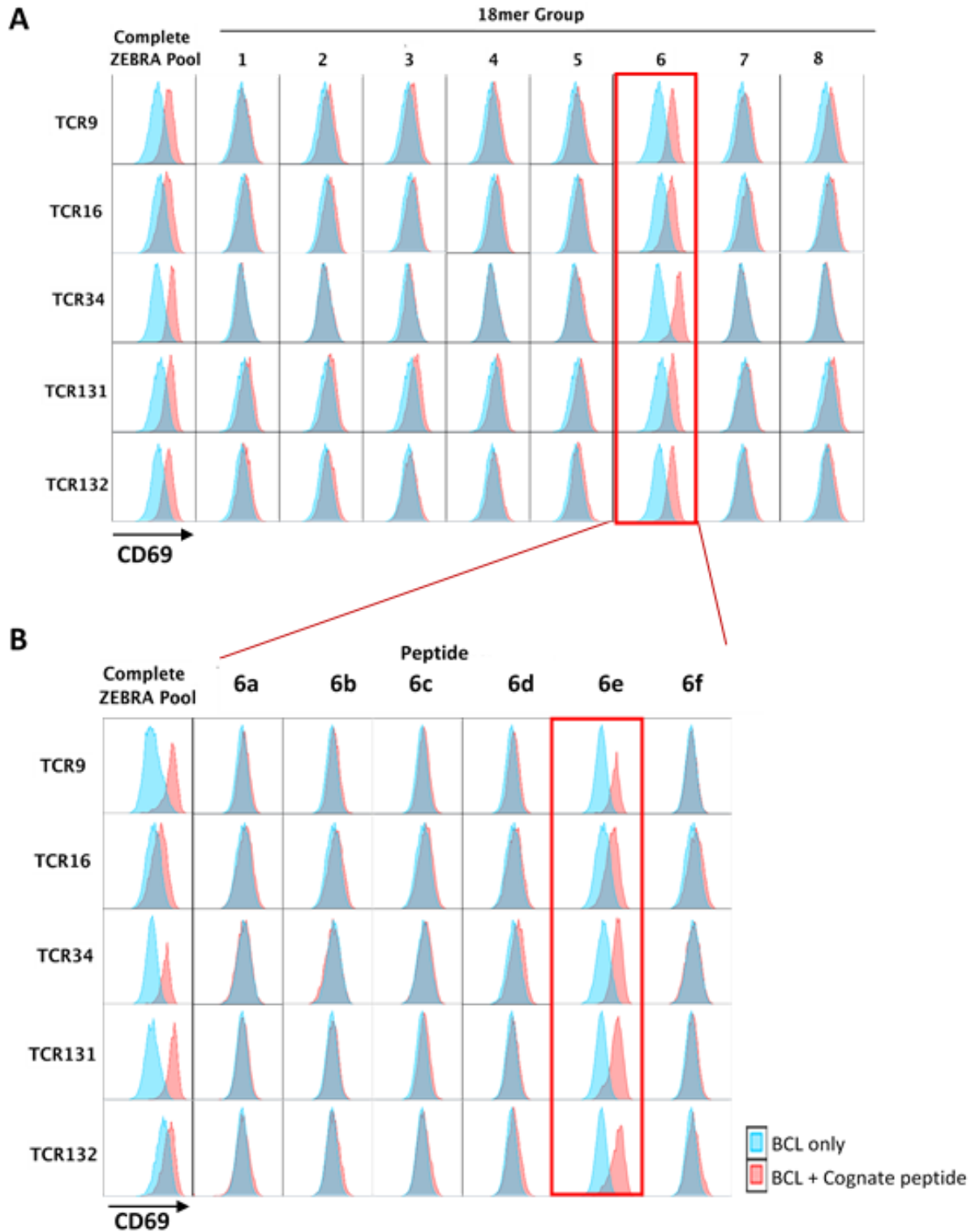


Figure 4. 6 Epitope mapping of donor 2 TCRs

Donor 2 TCRs (TCR9, 16, 34, 131 and 132) were stimulated with 18mer pools 1-8 (Panel A).

The TCR clones were then stimulated with the 6 constituent 18mer peptides of pool 6 (6a-6f, Panel B). In all assays, ZEBRA peptide-stimulated cells were compared to cells incubated with irrelevant peptide-pulsed BCLs. The plots showing a population positive for CD69 upregulation are highlighted in red. The complete ZEBRA peptide pool was used as a positive control.

Table 4. 5 Epitope (9mer) mapping of Donor 2 TCRs

9mer	TCR9	TCR16	TCR34	TCR131	TCR132
CDSELEIKR					+
DSELEIKRY	+			+	
SELEIKRYK					
ELEIKRYKN					
LEIKRYKNR					
EIKRYKNRV		+			
IKRYKNRVA		+			
KRYKNRVAS				+	
RYKNRVASR				+	
YKNRVASRK					

+ represents positive staining for CD69 activation marker after stimulation

The data shows that TCRs 9, 16, 34, 131 and 132 map to different epitopes of the CDS 18mer (Table 4. 5). The HLA-B*18:01-restricted TCRs 9 and 131 are specific for the DSELEIKRY 9mer, whereas TCR 132 maps to the CDSELEIKR 9mer. The HLA-A*23:01-restricted TCR16 maps to two overlapping 9mers with similar levels of CD69 upregulation (Appendix 10). These 9mers, EIKRYKNRV and IKRYKNRVA, both share the 8 amino acid sequence IKRYKNRV, the putative epitope for this TCR. Similarly, HLA-A*23:01-restricted TCR34 shows CD69 upregulation to the overlapping 9mers KRYKNRVAS and RYKNRVASR, which also share an overlapping 8 amino acid sequence, RYKNRVAS.

4.5 Discussion

4.5.1 Summary

In this chapter, the EBV ZEBRA-specific TCRs that were cloned from the two healthy donors have been characterized in terms of their HLA-restriction and their peptide-specificities. Table 4. 6 shows a summary of these characteristics.

As the overlapping epitopes are presented by several different HLA alleles, they could be exploited therapeutically for the design of treatments (Rist et al., 2015b).

The data from this chapter demonstrates an efficient and convenient approach to mapping TCR epitopes and MHC restrictions. Characterization of the HLA-restriction and epitope-specificity of EBV-specific TCRs in this way can aid directly in vaccine development and adoptive immunotherapy.

Table 4. 6 Summarized characteristics of cloned EBV ZEBRA peptide-specific TCRs

Donor	TCR	TCR V/J genes and CDR3		Mapped Peptide	HLA-restriction	
1	4	TRAV20*02 TRBV3-1*01	TRAJ24*02 TRBJ1-2*01	CAFFSWGKIQF CASSQSPGTGVGYTF	EPLPQGQLTAY & LPQGQLTAYHV	A*02:01 & B*35:01
2	9	TRAV13-1*02 TRBV20-1*02	TRAJ42*01 TRBJ2-1*01	CAASKEGGGSQGNLIF CSARDRGEHPPNDQFF	DSELEIKRY	B*18:01
2	16	TRAV13-2*01 TRBV30*02	TRAJ12*01 TRBJ1-2*01	CAEKGWDSYKLIIF CAWVDGVLDGYTF	IKRYKNRV	A*23:01
2	34	TRAV29*01 TRBV7-9*03	TRAJ16*01 TRBJ2-4*01	CAASEGGQKLLF CASSAPNSDSAKNIQYF	RYKNRVAS	A*23:01
2	131	TRAV26-2*01 TRBV9*02	TRAJ47*01 TRBJ2-3*01	CILRDGVGYGNKLVF CASEDRGGTDTQYF	DSELEIKRY	B*18:01
2	132	TRAV14*01 TRBV29-1*01	TRAJ52*01 TRBJ2-5*01	CAMREGSGVGTSYGK CSAAGTSGSGETQYF	CDSELEIKR	B*18:01

4.5.2 TCR4 recognizes two overlapping peptide epitopes presented on both HLA-A*02:01 and HLA-B*35:01

TCR4 is one of the dominant EBV ZEBRA-specific TCRs sequenced from healthy donor 1, making up 13% of all the TCRs sequenced from this donor (Appendix 3). Initial HLA-restriction assays using the complete ZEBRA peptide pool to stimulate the TCR4-transduced SKW3 T cells suggested that TCR4 can recognise ZEBRA peptide presented on both HLA-A*02:01 and HLA-B*35:01, but not on HLA-A*11:01 or HLA-B*49:01 (Figure 4.1). We speculated that perhaps the TCR recognised two separate EBV ZEBRA epitopes presented on the respective HLA molecules. Peptide epitope mapping studies were performed on the TCR4 cells to further explore this finding. As shown in Figure 4. 2, TCR4 recognised the VLP 18mer, in addition to four different overlapping 11mers within this 18mer peptide (Table 4. 3). We speculated that these 11mers would be presented differentially on HLA-A*02:01 and HLA-B*35:01, thus new BCLs expressing only one of HLA-A*02:01 or B*35:01 were used in further peptide stimulation assays to present the 11mers to the TCR4 cells. In addition, a modified version of the .221 BCL which was previously transduced in our lab to express HLA-A*02:01, was used. The .221 cell line is devoid of all HLA class I molecules, although recently they have been shown to express low levels of HLA-C*01:02 (Partridge et al., 2018). Despite this, as this HLA-C allele is not compatible with our TCR donor, we deemed this .221_A2 cell line to be a suitable antigen presenting cell line to confirm whether the TCR4 cells do in fact recognise peptide presented on HLA-A*02:01. The data in Figure 4. 3 confirms that TCR4 can recognise 2 different, overlapping 11mers EPLPQGQLTAY and LPQGQLTAYHV, presented on both HLA-A*02:01 or HLA-B*35:01. In addition, the 11mers LPEPLPQGQLT and PEPLPQGQLTA are also presented by HLA-B*35:01 but not by HLA-A*02:01, explaining why there was CD69 upregulation amongst the TCR4 cells when co-cultured with autologous BCLs loaded with these 11mers (Table 4. 3).

Furthermore, Figure 4. 4 demonstrates that this is not due to presentation by HLA-C*07:01, which is shared by donor 2 and the IAVI 3572 BCL used in the confirmation assay. Finally, stimulation with the irrelevant 9mer (FLRGRAYGL, from a late stage EBV antigen) showed that the TCR does not recognise non-specific peptide (Figure 4. 4). All these data indicate that the TCR4 specifically recognises the two 11mers EPL and LPQ when presented on HLA-A*02:01 and HLA-B*35:01.

The region of the ZEBRA peptide that encompasses the EPL and LPQ epitopes recognised by TCR4 is known to harbour 3 well-characterized overlapping sequences of various lengths, all of which are restricted to HLA-B*35:01 (Miles et al., 2005, Green et al., 2004). Although these correlate with the data in Table 4.4, which indicates that TCR4 responds to 13mers and the two 11mers, it did not recognise the previously characterized 9-mer LPQGQLTAY (Appendix 8), indicating that the TCR itself is most likely different from that previously characterized (Green et al., 2004).

Miles et al. described several EPL-11mer-specific HLA-B*35:01-restricted TCRs from different unrelated donors which shared closely related TCR sequences and particular CDR3 motifs. The authors showed that this TCR repertoire often consists of a selected group of TCR- α and - β variable and joining genes, with specific central residues present within the CDR3 regions (Miles et al., 2005). Although TCR4 does not fully conform to this described pattern of TCR gene usage, it does possess part of the described amino acid motif in its TCR β CDR3 region; the PG amino acids from the described LPG motif is present in the central residues of the TCR4 CDR3 β , (CASSQSPGTGVGYTF), possibly explaining why TCR4 is able to interact with HLA-B*35:01 presenting the EPL peptide.

The most polymorphic region within each HLA molecule is within the peptide binding groove, which has specificity for a motif within its epitope (Falk et al., 1991). The EPLPQGQLTAY 11mer conforms to the requirements of binding to HLA-B*35:01 in that it has a proline residue (P) at position 2 (P2) and a tyrosine residue (Y) at the C-terminus (Falk et al., 1993, Hill et al., 1992, Schonbach et al., 1996). Although the LPQGQLTAYHV 11mer does not possess a Y residue at its C-terminus, it does have the required P anchor residue at P2, possibly explaining its recognition by TCR4 on HLA-B*35:01. This is in contrast with the PLPQGQLTAYH-11mer which contains the LPQGQLTAY 9mer sequence; the 11mer has a P residue at position 3 and does not have the typical Y anchor residue at the C-terminus, and is thus not predicted to bind by the NetMHCpan predictor (www.cbs.dtu.dk › NetMHCpan).

Although the combination of HLA-B*35:01 and the EPLPQGQLTAY peptide is well established, it has not previously been described in association with HLA-A*02:01. The sequence motifs important for binding to HLA-A*02:01 include L at P2, and V or L at the C-terminus (Parker et al., 1992, Rasmussen et al., 2014, Drijfhout et al., 1995). According to the NetMHCpan predictor however, HLA-A*02:01 is not predicted to bind to the EPLPQGQLTAY or LPQGQLTAYHV 11mers, presumably due to the absence of the required anchor residues at P2 and P9. It is however predicted to bind weakly to the 13mer

VLPEPLPQGQLTA, which we observed in our hands (Table 4.4.). Although the P2 anchor requirements are not strictly met by the EPLPQGQLTAY and LPQGQLTAYHV 11mer epitopes, the presence of the V residue at the C-terminus of the latter may help to explain the stabilization of this peptide on the A*02:01 molecule. Furthermore, the epitopes are 11mers, and it has been shown that epitopes greater than 9 amino acids in length may adopt a highly bulged conformation in order to fit into the MHC groove (Miles et al., 2005, Tynan et al., 2005, Hassan et al., 2015). Owing to this bulging, it may be speculated that some shifting of the peptide may occur within the binding groove, possibly altering the contacts of the peptide residues with those of the MHC groove. This may permit binding of the EPLPQGQLTAY and LPQGQLTAYHV within the A*02:01 and B*35:01 grooves despite the residues not strictly being in the typical required position. To confirm this, the full structural biology of the complex will need to be examined to assess the contact points between the TCR and the pMHC.

Although the observation that TCR4 binds to the highly immunogenic EPLP epitope via HLA-A*02:01, in addition to the already described B*35:01, is a new finding, the cross-reactivity of a single TCR with two HLA molecules is not unique. Many studies have described the T cell cross-recognition of allo-HLA molecules, whether within the same HLA supertype or across superotypes (Frahm et al., 2007, Burrows et al., 1994, Koelle et al., 2002, Amir et al., 2010, Leslie et al., 2006, van den Heuvel et al., 2017). This promiscuity and cross-reactivity is believed to be important for successful surveillance against a variety of different antigens (Koelle et al., 2002). Furthermore, an EBV-specific CTL which recognises the immunodominant latent epitope FLRGRAYGL when presented on HLA-B8, and also recognises HLA-B*4402 as an alloantigen has been well-characterized (Burrows et al., 1994, Burrows et al., 1997, D'Orsogna et al., 2012). Although these studies suggest HLA class I promiscuity as being common amongst virus-specific CD8⁺ T cells, they all describe the phenomenon in allogeneic donors. No studies have yet been described whereby the cross-reactivity of T cells occurs to overlapping peptides on self-HLA molecules present in the same donor.

In Figure 4.3, the levels of CD69 upregulation are mainly higher when the cognate peptides are presented to TCR4 cells via the autologous donor BCL (~20% CD69+), which present via both HLA molecules, in comparison to the BCLs expressing only HLA-A*02:01 or B*35:01 (~5-9% CD69+). This stronger activation of the T cells in response to the peptide on the autologous donor BCL may be attributed to the co-expression of both HLA molecules simultaneously, resulting in double the amount of peptide being presented, thus offering the

host a possible survival advantage. In terms of clinical applicability, such a dual-HLA-specific TCR would be advantageous because it could be used for immunotherapy in both HLA-A*02:01⁺ or B*35:01⁺ individuals.

4.5.3 TCRs from donor 2 recognise various epitopes within the same peptide region of ZEBRA, presented on various HLA molecules

The five EBV-specific TCRs cloned from Donor 2 (TCR9, TCR16, TCR34, TCR131 and TCR132) were characterized in terms of their HLA-restriction and mapped to their peptide epitopes.

The TCRs are all restricted to various HLAs (Figure 4. 5); TCRs 9, 131 and 132 are restricted to HLA B*18:01, whilst TCRs 16 and 34 are both HLA A*23:01-restricted.

All of the TCRs recognise the 18mer peptide CDSELEIKRYKNRVASRK (Figure 4. 6B), demonstrating the immunogenicity of this epitope within this donor.

TCRs 9, 16, 34, 131 and 132 map to different epitopes of the CDS 18mer (Table 4. 5). The HLA-B*18:01-restricted TCRs 9 and 131 are specific for the DSELEIKRY 9mer, whereas TCR 132 maps to the overlapping CDSELEIKR 9mer. Although there is no observed homology between the sequences of these TCRs, there are similarities in their CDR3 residues; all three TCRs share a motif of GXG within the central residues of their CDR3 α , and TCRs 9 and 131 both also have a DRG motif within their CDR3 β central residues (Table 4. 6). These shared central residues may explain the shared epitope specificity for all three TCRs.

The 8mer epitope SELEIKRY has been previously reported to induce a strong CD8⁺ T cell response in HLA-B*18:01⁺ individuals (Rist et al., 2013). In addition, the predictions on NetMHCpan state that the SELEIKRY 8mer binds to HLA-B*18:01 strongly, whereas the binding of DSELEIKRY and CDSELEIKR 9mers are predicted to be weaker. Thus, perhaps if the peptides had been truncated further to 8mers, the optimal epitope for TCRs 9, 131 and 132 would have been elucidated. However, the HLA-B*18:01 restricted TCRs which recognise SELEIKRY have previously been shown to predominantly use TRBV10, but this is not the case for our SELEIKRY-specific B*18:01-restricted TCRs (Rist et al., 2015a).

The HLA-A*23:01-restricted TCR16 maps to two overlapping 9mers (EIKRYKNRV and IKRYKNRVA), with similar levels of CD69 upregulation. Although these 9mers, both share the 8 amino acid sequence IKRYKNRV, the binding prediction levels according to

NetMHCpan predictor are not high.

Although the 9mer KRYKNRVAS which induced a response in TCR34 cells is not predicted to bind strongly to HLA-A*23:01, the overlapping 9mer RYKNRVASR has a stronger predicted binding. Although there is no sequence homology or similarity between the sequences of these TCRs, they do share a common KLXF motif at their 3' end, suggesting that this may be relevant for their recognition of overlapping peptides on the same HLA molecule. Unlike HLA-B*18:01, very few HLA-A-restricted ZEBRA epitopes have been described in literature (Rist et al., 2015b), and HLA-A*23:01 has not yet been described to bind to any known ZEBRA epitopes. The finding that two of the dominant TCRs from this healthy donor are restricted to this HLA allele is worthy of further investigation as it expands the potential HLA alleles which can be relevant clinically.

4.5.4 Clustering of ZEBRA-specific TCR epitopes

The ZEBRA antigen is known to be a critical component of the EBV life cycle as it is essential for the switch from latent to lytic gene expression (Miller, 1990). Several immunodominant CD8⁺ T cell epitopes have been characterized, and they have been shown to be restricted to several different HLA alleles, mainly HLA-B and HLA-C alleles (Rist et al., 2015b). Rist et al. demonstrated that the CD8⁺ T cell epitopes within the ZEBRA peptide are clustered within certain regions of the peptide. They suggested that certain regions of the protein do not contain any known epitopes due to the presence of “immune blind spots” which share sequence similarity with host proteins (Rist et al., 2015b). Our data shows a similar pattern of epitope distribution amongst the six dominant ZEBRA-specific TCRs sequenced from 2 healthy donors. The HLA-A*02:01/ B*35:01-restricted EPLPQGQLTAY and LPQGQLTAYHV epitopes lie within the highly immunogenic transactivation domain (aa 1-166) of ZEBRA, whereas the HLA-B*18:01-restricted DSELEIKRY and CDSELEIKR, and the HLA-A*23:01-restricted EIKRYKNRV and RYKNRVASR epitopes are present in the DNA recognition domain (aa 178-194) (Flemington et al., 1992). Figure 4.7 shows the clustered distribution of these epitopes within the ZEBRA peptide sequence. Characterizing more of the dominant TCRs from healthy controls would likely display further clustered distribution, supporting the findings of Rist and colleagues (Rist et al., 2015b).

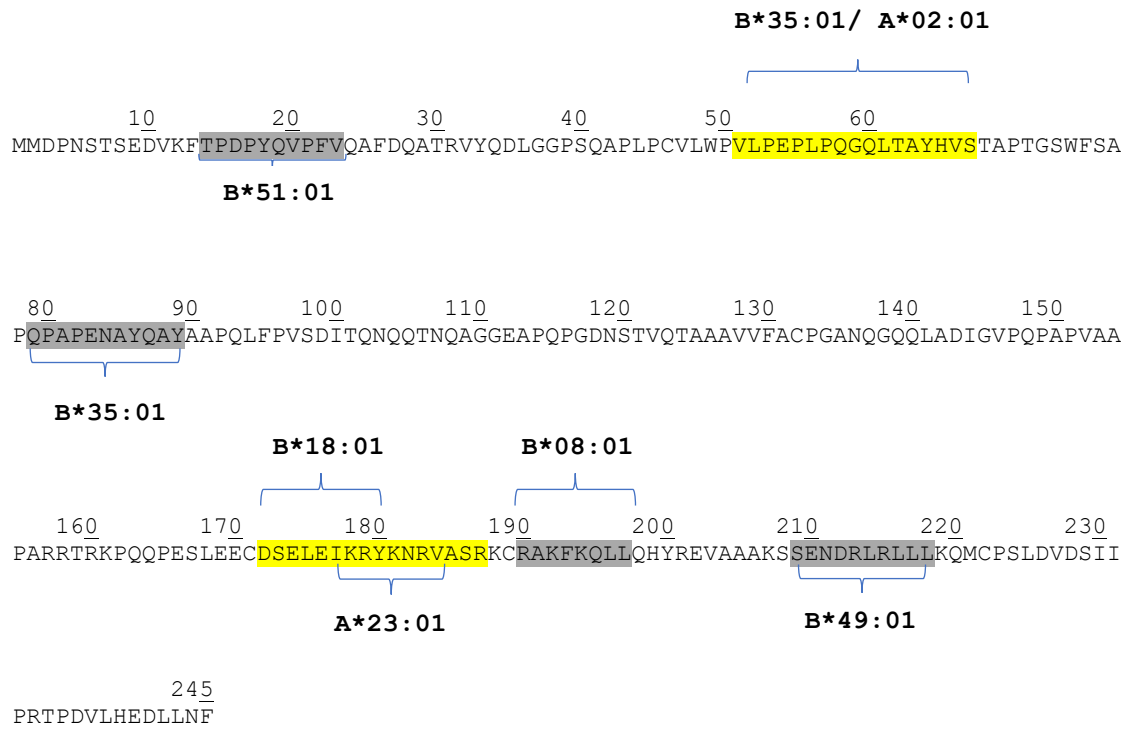


Figure 4. 7 Clustered distribution of T cell epitopes within EBV ZEBRA antigen

The amino acid structure of ZEBRA is shown with clustered epitopes identified in this study highlighted in yellow, and selected previously described epitopes highlighted in grey (Rist et al., 2015b). The known HLA restrictions are indicated.

4.5.5 Future Studies

In future studies, it would be useful to prepare tetramers specific for each of the HLA-peptide combinations described in this data. This would be particularly helpful for the confirmation of the dual-HLA-restriction of TCR4, as tetramer staining could support the data presented in this chapter. In terms of clinical application, these ZEBRA-specific tetramers could be used to isolate specific CD8⁺ T cells from donors for the purpose of expansion for adoptive therapy.

Another way to confirm the dual HLA-restriction of TCR4 would be to use completely HLA-deficient target cells. These could be naturally HLA class-I deficient as in the case of K562 cells (Sutherland et al., 1985), or all HLA-A, B and C genes could be knocked out from target cells and the HLA molecule of interest re-expressed in order to eliminate any potential of cross-reactivity from other HLA molecules (Kula et al., 2019). Although a similar method was used here utilizing the .221 cells which were transduced to express HLA-A*02:01 only, using the latter techniques may prove useful in terms of further confirmation of all the observed HLA-restrictions.

Finally, it will be interesting to assess the structural biology of the binding of TCR4 to HLA-A*02:01 and B*35:01 peptide complexes to see how the points of contact may differ, and how the same TCR is able to recognise the overlapping peptides on the two HLA molecules. Further studies such as these would help to strengthen the findings presented in this chapter and to confirm the clinical relevance of each TCR for use in adoptive T cell therapy against EBV-associated malignancies.

5

**Recognition of EBV-associated Gastric Carcinoma Cells
by ZEBRA-specific TCRs**

5.1 Introduction

Persistent EBV infection is associated with malignancies in both lymphoid cells and epithelial cells (zur Hausen et al., 1970, Burke et al., 1990). In addition to Burkitt's lymphoma and nasopharyngeal carcinoma, EBV is thought to be a causative factor in approximately 10% of all gastric carcinomas globally (Shibata and Weiss, 1992, Tokunaga et al., 1993, Takada, 2000). Nearly all cancerous cells in EBV-associated gastric carcinoma (EBVaGC) contain EBV DNA, and express the latent genes EBNA1, EBERs, BARTs, and may express the latent membrane protein 2A (LMP2A) (Imai et al., 1994, Fukayama et al., 1994, El-Sharkawy et al., 2018). Tumour infiltrating lymphocytes (TILs) have been shown to increase prognosis in EBVaGC, suggesting that T cells can recognise latent EBV antigens and mediate control of infected cells (Lee et al., 2008, Kang et al., 2016).

Despite the existence of specific T cell responses against both lytic and latent stages of infection, EBV has evolved to cause persistent infection and cancer through an arsenal of survival and immune evasion techniques, including downregulation of viral proteins, direct interference with host immunity, expression of specific immune evasion and oncogenic proteins, and instigating T cell exhaustion and death (Sasaki et al., 2019, Pender et al., 2017, Macedo et al., 2011, Quan et al., 2015, Fathallah et al., 2010, Blake et al., 1997).

Gastric cancers are the second leading cause of cancer-related mortality globally (Ferlay et al., 2010). If detected early, the 5-year survival rate can exceed 90% in some countries, such as in Japan (Nishikawa et al., 2018). Currently, surgery is the only successful treatment for gastric carcinoma, whilst adjuvant chemotherapy or radiation can also improve the outcome, depending on the stage of disease at diagnosis (Camargo et al., 2014, Orditura et al., 2014). If detected at an advanced stage however, even after surgical resection more than half of patients relapse and less than 10% of these patients survive for more than 5 years (Orditura et al., 2014). Alternative treatment options for advanced stage EBVaGC currently encompass improving the immune response to the virally-infected cells, such as immune-checkpoint blockade (Kang et al., 2017). Another immune-mediated approach is adoptive T cell therapy with EBV-specific CTLs, which has shown highly effective results in studies of other EBV-associated malignancies (Haque et al., 2001, Straathof et al., 2005b, Wildeman et al., 2012, Cho et al., 2018). However, most of these cancers exhibit different EBV latency types which involve the expression of more immunogenic antigens, compared with the low antigenicity and limited antigens of EBVaGC, which is of type I latency (Young and Dawson, 2014,

lizasa et al., 2012, El-Sharkawy et al., 2018). A way to overcome this limited antigenicity is to reactivate the more immunogenic lytic infection via treatment with latency reversal agents (Archin et al., 2012, Deeks, 2012). This encompasses the “shock and kill” method of attacking latent viruses, whereby the silent virus is “shocked” out of latency using specific agents and “killed” in its lytic state by antiviral agents or by the immune system. Numerous studies have thus far demonstrated the efficacy of this approach (Lee et al., 2015, Hui et al., 2016, Hui and Chiang, 2010, Wildeman et al., 2012). One group of agents which have been shown to successfully induce lytic reactivation of latent EBV are histone deacetylase inhibitors (HDACi) (Wildeman et al., 2012, Hui et al., 2016). These agents act on the chromatin to induce gene expression, thereby can upregulate transcription of highly immunogenic lytic stage antigens in EBV-infected cells. Such antigens include the immediate early protein ZEBRA, which is known to be primary targets of the powerful CTL response that eliminates most of the replicating virus during primary infection (Steven et al., 1997, Callan et al., 1998).

To date, studies which have used latency reversal agents to induce lytic activation have followed with antiviral agents such as ganciclovir to directly kill the reactivated virus (Hui et al., 2016, Wildeman et al., 2012).

Although several groups have demonstrated the efficacy of adoptive T cell therapy using CTLs against latent EBV antigens in other cancers, whilst others have utilized lytic reactivation as a tool to render the virus susceptible to killing, no studies have explored the outcome of combining the two approaches. This chapter addresses the combined approach of lytic stage reactivation followed by subsequent T cell therapy with CTLs specific to lytic stage antigens. I investigated the effect of HDACi treatment of EBVaGC cell lines, and the ability of ZEBRA-specific TCR-transduced T cells to recognise and kill EBVaGC cells after latency reversal.

5.1.1 Chapter-specific aims

There were 2 key aims for this chapter;

1. To demonstrate the ability of a panel of HDACi to induce lytic reactivation in selected EBVaGC cell lines
2. To assess the ability of EBV-specific TCR-transduced T cells to recognise and kill EBVaGC following HDACi treatment

5.2 HDACi treatment of EBV-associated gastric carcinoma cells

EBV ZEBRA-specific T cells were tested for their ability to recognise ZEBRA antigen expressed on gastric carcinoma cells. To investigate this, the gastric carcinoma cell lines AGS and OE19 were utilized, alongside their artificially-infected recombinant EBV_GFP⁺ counterparts, AGS_rEBV-GFP and OE19_rEBV-GFP (henceforth referred to as AGS_rEBV and OE19_rEBV, respectively). The cells were a kind gift from Professor Xin Lu at the Ludwig Institute for Cancer Research, Oxford University.

Table 5. 1 shows the HLA types of the TCR donors, and the AGS and OE19 cell lines, with matching alleles highlighted in red; both gastric cell lines share the common A*02:01 allele with TCR donor 1, whilst OE19 shares the B*18:01 allele with TCR donor 2. Both donors also share the Cw*07:01 allele with the OE19 cell line, but this is not relevant for studies using our TCRs. The HLA matching permits the use of these cell lines as target cells for downstream EBV-specific T cell mediated killing experiments as TCR4 recognises ZEBRA epitopes on A*02:01, and TCRs 9, 131 and 132 are restricted to B*18:01.

Table 5. 1 The HLA-A, -B and -C alleles of TCR Donors and the Gastric cell lines

		HLA-A		HLA-B		HLA-C	
Donor 1	TCR 4	A*02:01	A*11:01	B*35:01	B*49:01	Cw*04:01	Cw*07:01
Donor 2	TCRs 9, 131 132	A*23:01	A*31:01	B*18:01	B*40:01	Cw*03:04	Cw*07:01
Gastric cell	AGS	A*02:01	A*02:01	B*52:01	B*52:01	Cw*03:03	Cw*03:03
Gastric cell	OE19	A*01:01	A*02:01	B*18:01	B*45:01	Cw*05:01	Cw*07:01

¹ The matching HLA alleles between the donors and the gastric cell lines are highlighted

The gastric cell lines were treated with three different HDACi to reactivate the lytic infection cycle of EBV, thus inducing expression of ZEBRA antigen and rendering the cells susceptible to recognition by the ZEBRA-specific T cells.

Three HDACi which have previously been shown to reactivate lytic EBV or have shown promising results as anticancer agents, were used in this investigation; SAHA, chidamide, and a novel HDACi, CXD101 (Shi et al., 2015, Hui and Chiang, 2010, Hui et al., 2012, Eyre et al., 2016).

As preliminary assays, the cells were treated with increasing doses of each of the agents to confirm the dose required for optimal ZEBRA protein induction. The cells were treated with each HDACi for 48 hours at each concentration (1, 2.5, 5 or 10 μ M). The treated cells were stained with Live/Dead stain and anti-ZEBRA antibody before analysing on the flow cytometer. The gating strategy is shown in Figure 5. 1. The percentage of cells expressing ZEBRA vs the percentage of live cells was calculated and is shown in Figure 5. 2.

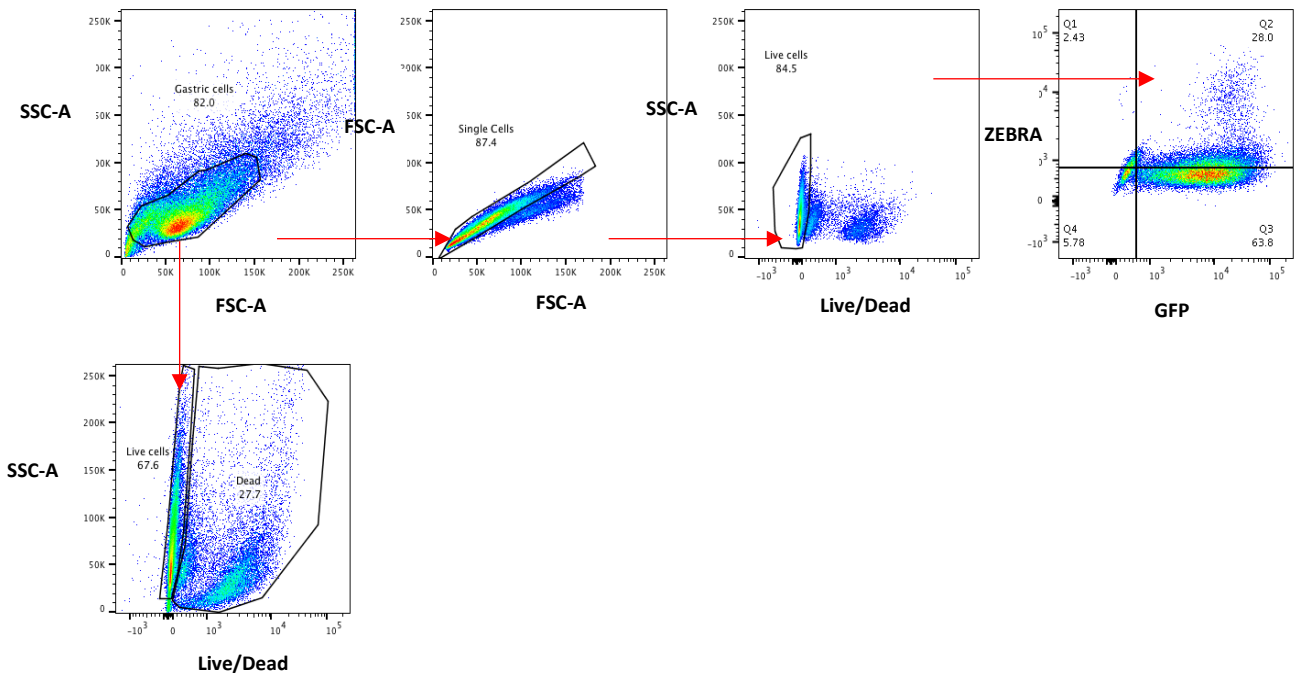


Figure 5. 1 The gating strategy for assessment of ZEBRA induction Vs toxicity post-HDACi treatment

The AGS_rEBV and OE19_rEBV were treated with HDACi for 48 hours and ZEBRA expression analysed. To assess the percentage of ZEBRA positive cells, the gastric cells were gated on single cells, live cells, and GFP+ ZEBRA+ cells (upper plots). To assess the overall percentage of live cells, the gastric cells were gated on live cells and dead cells using live/dead stain (lower plot).

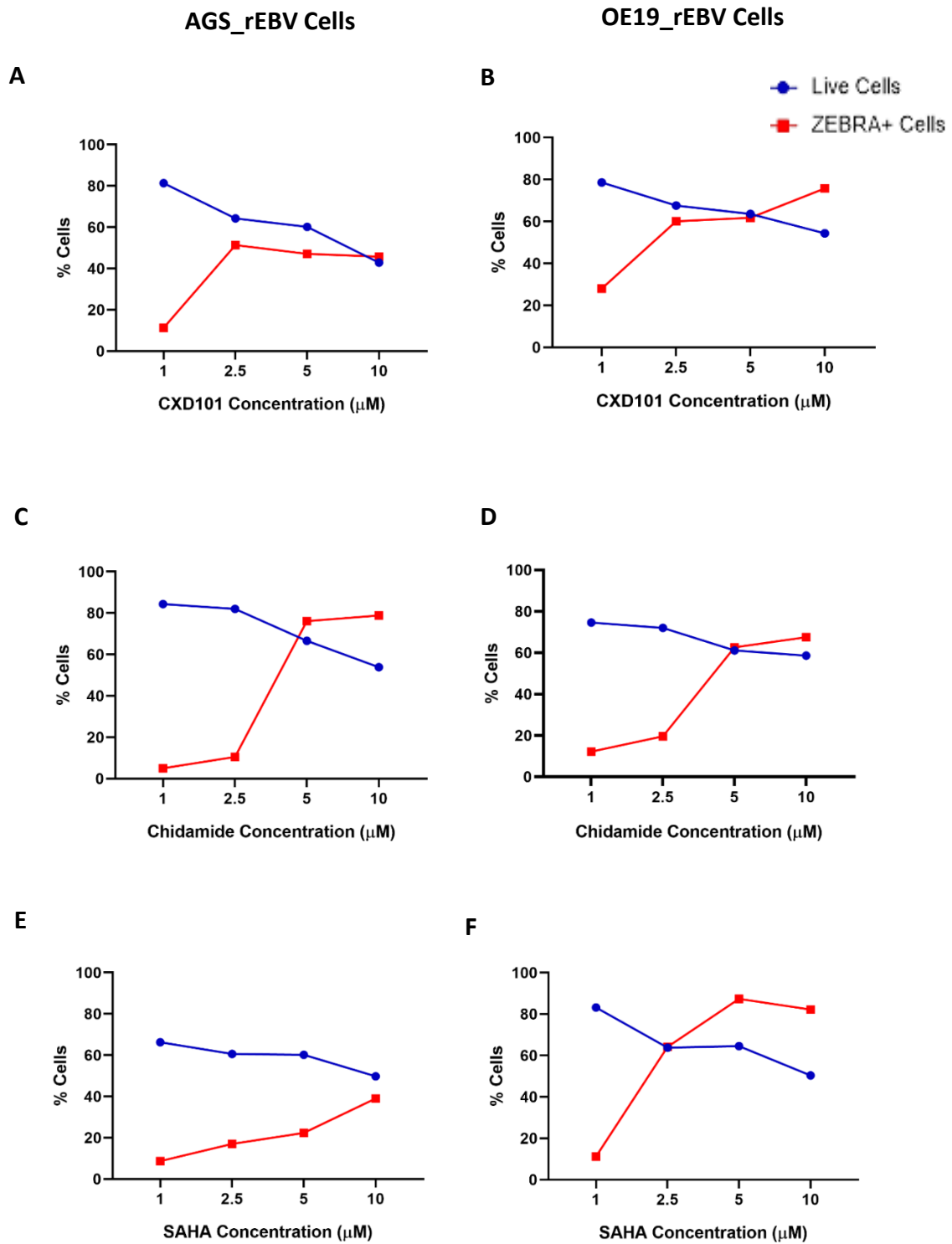


Figure 5. 2 The effect of increasing doses of HDACi treatment on EBVaGC cells

The EBV-associated gastric carcinoma cells AGS_rEBV and OE19_rEBV were treated with HDACis CXD101 (A-B), Chidamide (C-D) and SAHA (E-F) at concentrations of 1, 2.5, 5 and 10 μM for 48 hours before being analysed via flow cytometry. The percentage of live cells and the percentage of ZEBRA expression are shown. Data is from single experiment as was used to confirm dosages used previously.

The data indicate that the HDACi vary in their levels of toxicity versus their ability to induce ZEBRA expression. None of the compounds can induce high levels of ZEBRA expression in either cell line at 1 μM , but viability is preserved in most cells. CXD101 can induce ZEBRA expression in over 50% of cells with approximately 70% viability. With increasing doses of CXD101, there is little change in ZEBRA expression, but the viability of the cells decreases, indicating that higher doses of CXD101 are more toxic to these cells and that the optimal dose is 2.5 μM CXD101.

At 2.5 μM Chidamide, only 10-20% ZEBRA expression is seen in both cell types whilst 70-80% of cells remain alive. When the dose is increased to 5 μM however the ZEBRA induction increases dramatically to between 60-80%, while the percentage of live cells remains at approximately 60-70%. At 10 μM Chidamide however the ZEBRA induction increases very slightly but the cell death increases, indicating that 5 μM Chidamide is the optimal dose. SAHA has different effects on the two cell lines; at 2.5 μM concentration, although it does not cause high levels of cell death in AGS_rEBV cells, it induces relatively low levels of ZEBRA expression compared to the other HDACi (approximately 20% ZEBRA⁺). In OE19_rEBV cells however, 2.5 μM SAHA treatment induces more than 60% ZEBRA induction, although cell viability is also affected (approximately 65% live cells). SAHA seems to have more toxic effects overall on OE19_rEBV cells despite greater ability to induce ZEBRA. At 10 μM concentration of SAHA, the percentage of ZEBRA positive cells increases in AGS_rEBV cells and remains high in OE19_rEBV cells. However, this higher dose is also more toxic to both cell types, indicating that 5 μM is the optimal dose for SAHA treatment.

The optimal doses of each HDACi determined from this experiment were used to treat the cell lines for 48 hours, alongside a DMSO negative control. The relevant flow cytometry plots from each EBVaGC cell line is shown (Figure 5. 3). Figure 5. 4 shows the percentage ZEBRA expression in all the gastric carcinoma cell lines post-HDACi treatment.

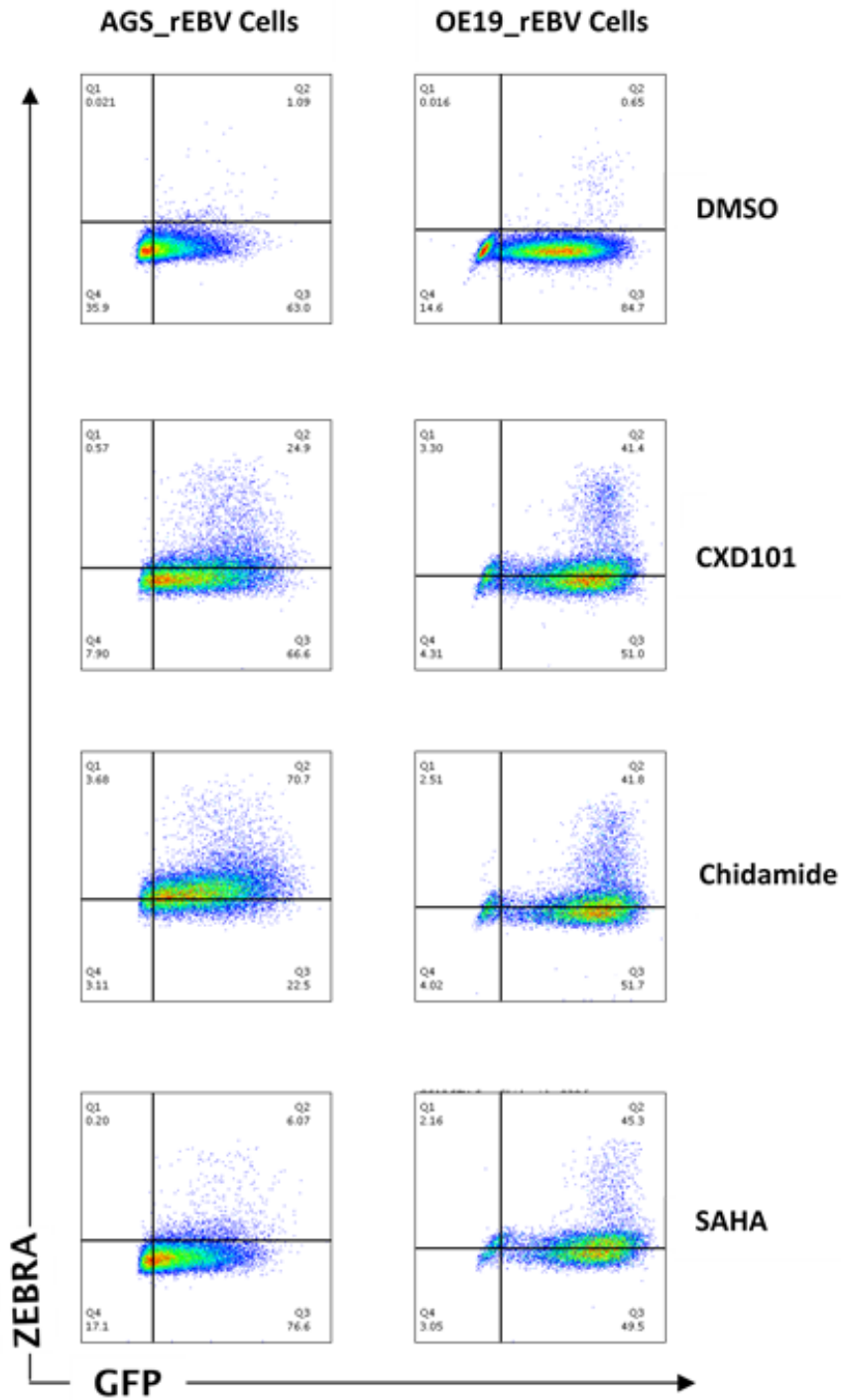


Figure 5. 3 Assessment of ZEBRA induction in EBV-associated gastric carcinoma cells post-HDACi treatment

The EBVaGC cell lines AGS_rEBV and OE19_rEBV were treated with HDACi CXD101 (2.5 μ M), Chidamide (5 μ M) and SAHA (5 μ M), and DMSO for 48 hours. The gating strategy used for analysis of ZEBRA expression is the same as that used in Figure 5.1. Representative dot plots of the EBVaGC cell lines post-treatment with each HDACi, or DMSO control, is shown.

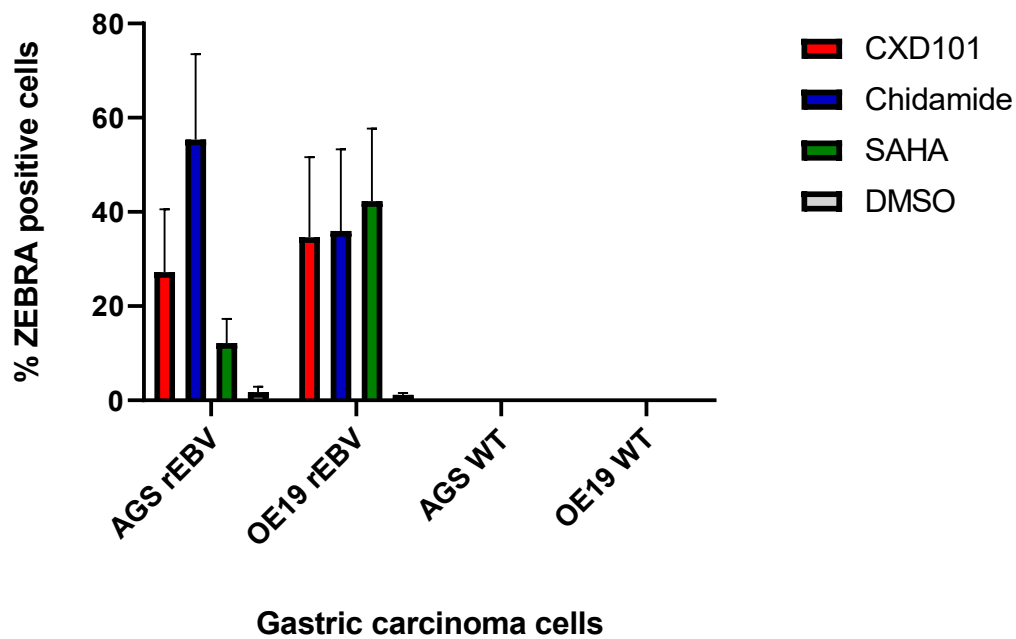


Figure 5. 4 Percentage of ZEBRA positive gastric carcinoma cells post-HDACi treatment

The AGS and OE19 cell lines (rEBV and WT) were treated with CXD101, Chidamide and SAHA, and DMSO for 48 hours. ZEBRA expression was measured in each cell type via flow cytometry. Data shown is the mean of 3 separate experiments, with SEM as error bars.

The data shows that all three HDACi are able to induce ZEBRA expression in AGS_rEBV and OE19_rEBV cell lines, but not in their EBV-negative counterparts (Figure 5. 3 and Figure 5. 4). The different compounds have various effects on the cell types; Chidamide can induce ZEBRA expression in nearly 60% of AGS_rEBV cells whereas this is less than 40% in OE19_rEBV cells. Similarly, whilst SAHA is able to induce ZEBRA induction in almost 50% of OE19_rEBV cells, this is seen in only 15% of AGS_rEBV cells. ZEBRA expression induced by CXD101 has the least variability between the cell types; approximately 30% of AGS_rEBV cells expressed ZEBRA after CXD101 treatment whilst this was approximately 40% OE19_rEBV cells.

These data indicate that CXD101, Chidamide and SAHA are all able to induce the lytic reactivation in EBV to varying degrees, thus HDACi-treated cells are expected to be suitable targets for the HLA-matched ZEBRA-specific T cells.

5.3 EBV-specific TCRs recognise ZEBRA peptide-pulsed gastric cells

In order to confirm the compatibility of the gastric cells with the ZEBRA-specific TCRs, the recognition of exogenously-loaded ZEBRA antigen on the HLA-matched gastric cells was investigated. The ZEBRA-specific SKW3 T cells were assessed for CD69 upregulation after 18 hours co-culture with HLA-matched gastric cell lines that had been pulsed with the ZEBRA peptide pool. The data in Figure 5. 5 indicates that each EBV-specific T cell is able to successfully recognise ZEBRA peptide presented on the surface of the HLA-matched gastric cell line, compared to controls with no peptide. TCR4 can recognise ZEBRA peptide presented on both AGS_rEBV and OE19_rEBV, as both these cell lines express the HLA-A*02:01. This contrasts with TCRs 9, 131 and 132, which only upregulate CD69 in response to ZEBRA peptide presented on OE19_rEBV cells, but not on AGS-rEBV cells. This is due to their restriction to HLA-B*18:01, which is only expressed by OE19_rEBV cells. These data indicate that the ZEBRA-specific TCRs can recognise ZEBRA presented on HLA-matched gastric cells and are thus compatible for the assessment of ZEBRA recognition on the cells post HDACi-treatment.

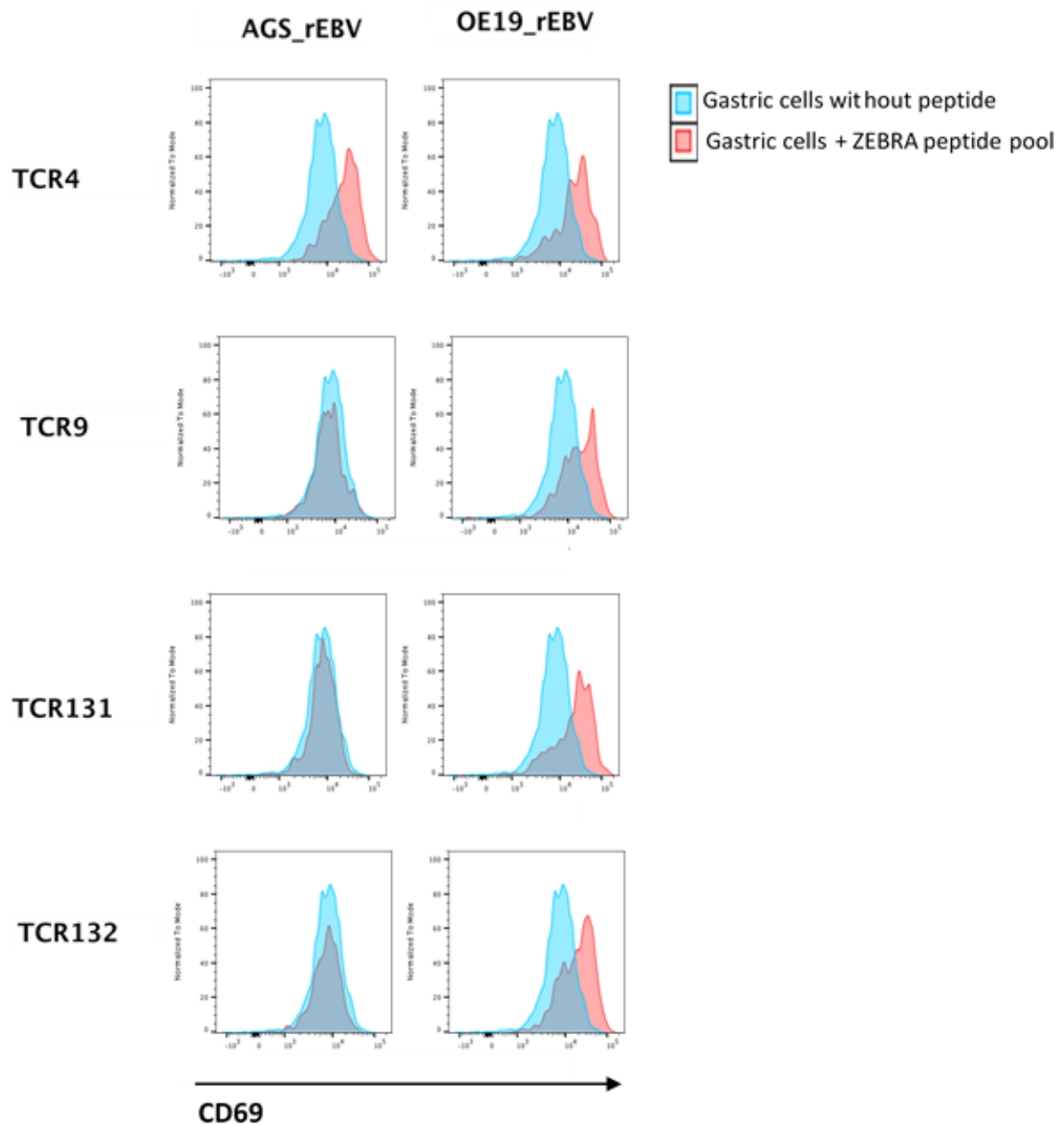


Figure 5.5 CD69 upregulation on ZEBRA-specific SKW3 T cells post peptide-pulsing of gastric cells

SKW3 T cells expressing the indicated ZEBRA-specific TCRs were co-cultured with ZEBRA peptide-pulsed gastric cells AGS_rEBV and OE19_rEBV, or gastric cells without peptide. CD69 upregulation was assessed and compared after 18 hours of co-culture. Histograms are representative of data from 3 separate experiments.

5.4 EBV-specific TCRs recognise ZEBRA on HDACi-treated EBVaGC cells

Next, the EBV-specific SKW3 T cells were tested for their ability to recognise endogenous ZEBRA peptide on gastric carcinoma cells post HDACi-treatment. The SKW3 T cell clones were co-cultured with HDACi-treated gastric carcinoma cells for 18 hours, and then the culture supernatant was collected for measurement of IL-2, IFN- γ and TNF α via the MSD system in order to assess activation of the T cell clones. Only single replicates of supernatants could be analysed due to limited space on the MSD plate (Figure 5. 6). The data shows that compared with DMSO-treated controls, all the T cell clones can recognise ZEBRA induced on their HLA-matched gastric carcinoma cell lines post-HDACi treatment. Overall, the levels of IL-2 are higher after co-culture with HDACi-treated gastric cells compared to DMSO-treated cells, with the highest levels being produced from all clones in response to CXD101-treated gastric cells. ZEBRA-specific activation is also confirmed by the increased levels of cytotoxic cytokines detected in culture supernatants. The levels of IFN- γ and TNF- α production is much higher in T cells co-cultured with HDACi-treated gastric cells compared with the DMSO controls, indicating that these are sensitive assays for the assessment of T cell activation after recognition of ZEBRA antigen. In both AGS_rEBV and OE19_rEBV cells overall, there were higher levels of IFN- γ produced in response to CXD101-treated cells compared to DMSO-treated controls and treatment with other HDACi, similar to the pattern of observed IL-2 secretion. This is especially true in the case of TCR4 clones, which produced up to ~25pg/ml compared to 10-15pg/ml by other T cell clones. The levels of IFN- γ produced in response to cells treated with Chidamide and SAHA are variable, with some TCR clones responding better to the former than the latter and vice versa. The levels of TNF- α production on the other hand are relatively consistent amongst all TCR clones and all HDACi-treated cells, although these are still higher (approximately 10pg/ml) compared with <2pg/ml in the DMSO controls.

These data confirm the recognition of ZEBRA by the TCRs, and demonstrates that this can lead to production of cytokines after recognition of ZEBRA expressed in EBVaGC cells following HDACi treatment.

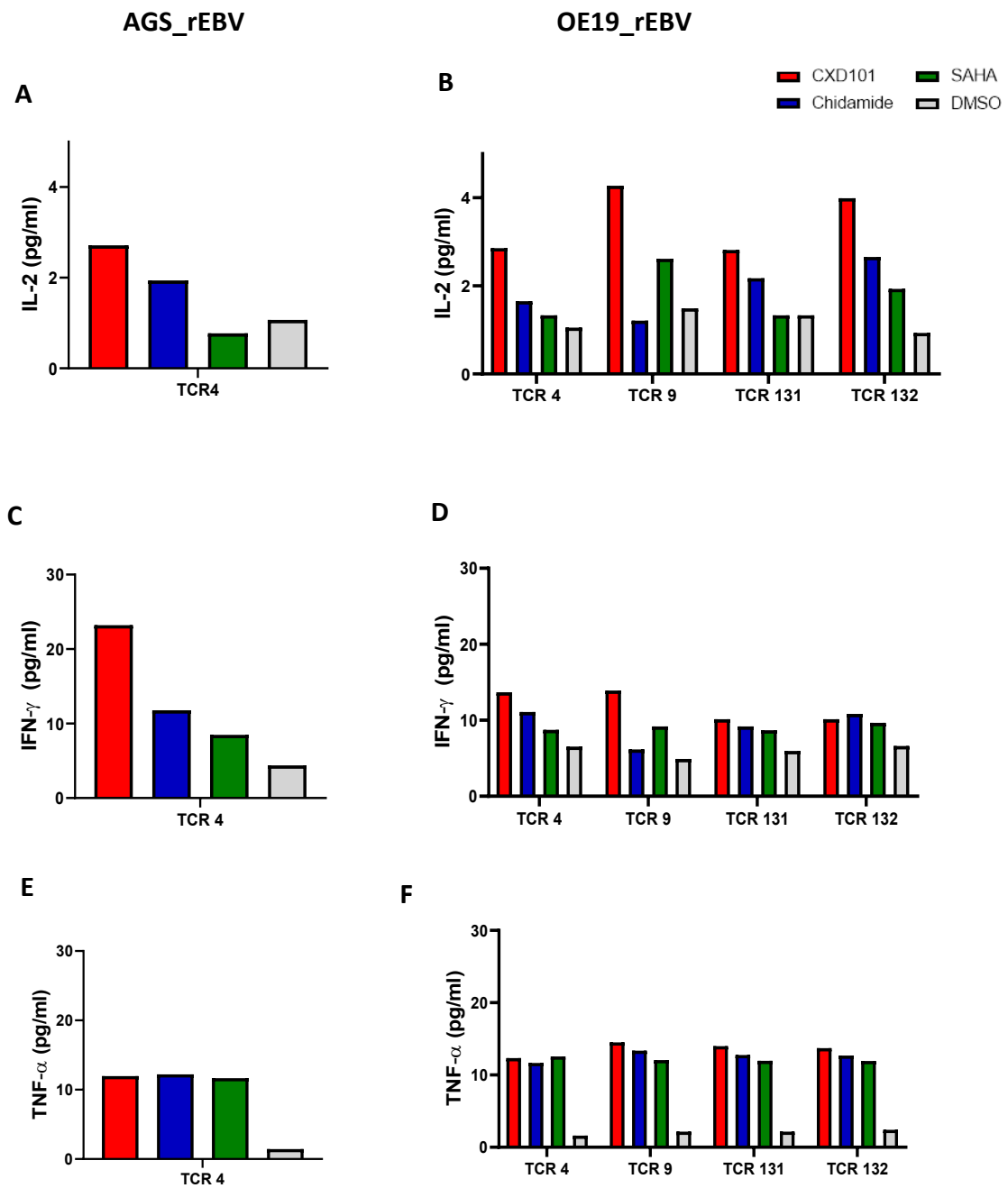


Figure 5. 6 SKW3 T cell clones produce cytokines upon recognition of HDACi-induced ZEBRA on gastric carcinoma cells

AGS_rEBV and OE19_rEBV were treated with HDACi or DMSO for 48 hours before co-culturing with HLA-matched SKW3 T cell clones for 18 hours. Supernatant was collected for assessment of IL-2, IFN- γ and TNF- α .

5.5 Expression of EBV-specific TCRs in primary T cells

In order to assess the full functional abilities of T cells expressing EBV-specific TCRs, the ZEBRA-specific TCRs were transduced into primary T cells. These cells were obtained from a healthy donor who had previously screened negative for IFN- γ responses to the EBV ZEBRA peptide pool. Activated T cells were transduced with TCR-encoding retroviral particles and the efficiency of transduction in CD8⁺ T cells were assessed 2-3 days later by analysis of GFP expression (Figure 5. 7). The transduction efficiency in primary T cells was extremely low compared to that in SKW3 cells; in the latter, GFP positive cells made up to 95% of the cells (Figure 3.18), however in primary T cells the GFP positive cells only made up to approximately 20% of cells.

Due to the limited number of GFP-expressing primary T cells, they were expanded for approximately a week before sorting for enrichment. CD3⁺ CD8⁺ GFP⁺ T cells were sorted and used immediately for functional studies.

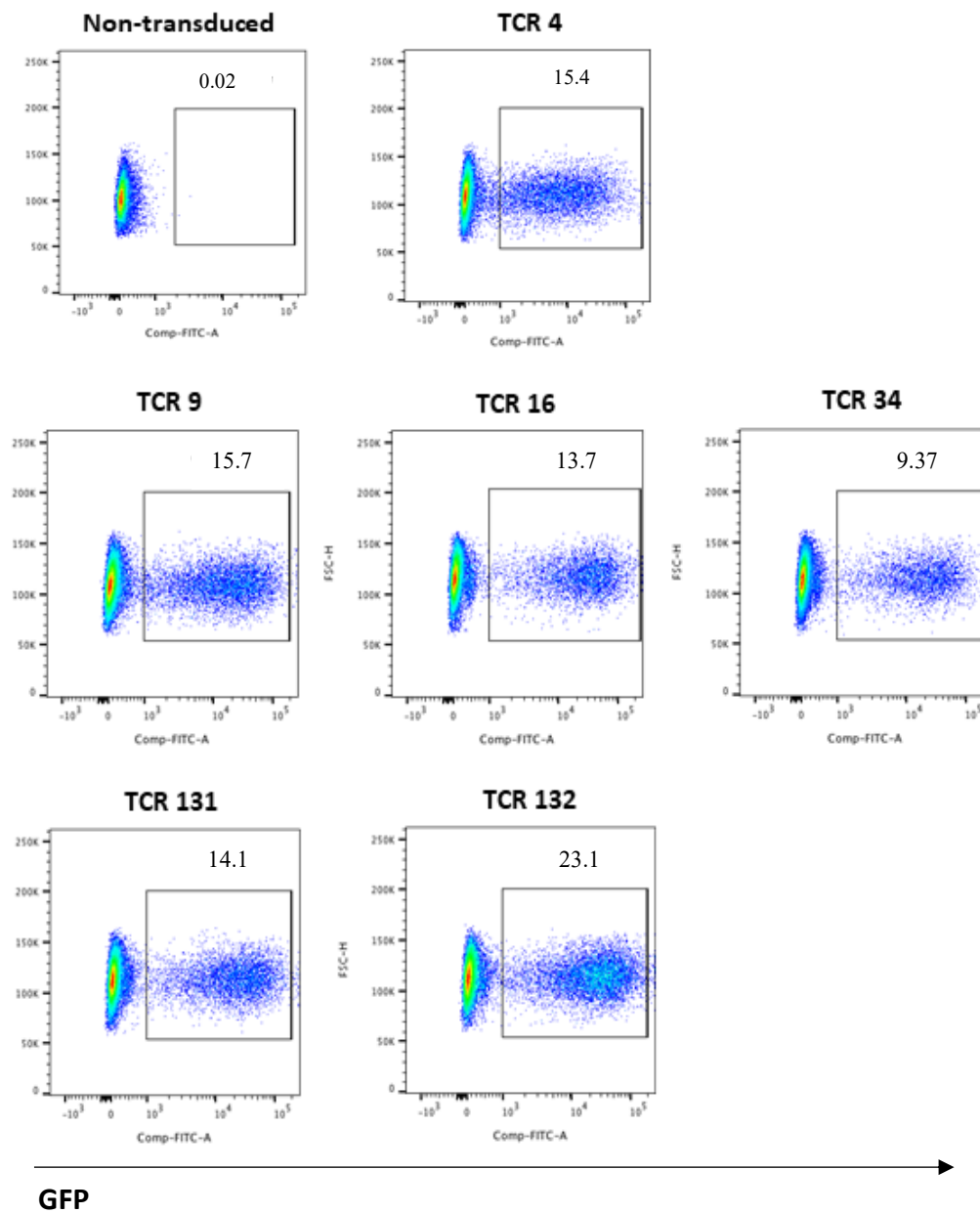


Figure 5. 7 Transduction efficiency of primary T cells with TCR-encoding retrovirus

Primary T cells were transduced with retroviral particles encoding EBV-specific TCRs and the transduction efficiency assessed using GFP expression analysis 2-3 days post transduction.

5.6 Recognition of exogenous ZEBRA antigen by primary T cells transduced with ZEBRA-specific TCRs

The enriched CD3⁺ CD8⁺ GFP⁺ primary T cells were assessed for their ability to recognise ZEBRA peptide presented on peptide-pulsed autologous B cell lines (BCLs). The transduced primary T cells were co-cultured for 18 hours with BCLs pulsed with either the ZEBRA peptide pool or an irrelevant peptide. Counting beads were used during flow cytometry; exactly 5000 events gated on the beads were acquired for each peptide stimulation well. The addition of the beads acts as an internal counting standard so that the absolute cell counts can reliably be calculated and normalized between each sample and its control. Thus, acquiring a fixed number of events from each sample ensured that the same number of cells were taken up for each condition. During analysis, the cells were gated on lymphocytes and singlets, live cells, and CD19 vs CD3 (Figure 5. 8). The number of live B cells present in each condition was counted and percentage cell death calculated in relation to a BCL only control which represents 100% survival. Percentage cell death was compared between cognate peptide-pulsed BCLs and irrelevant-peptide-pulsed BCLs. Upregulation of CD69 expression on T cell surfaces, and cytokine secretion in the culture supernatant was also assessed (Figure 5. 9).

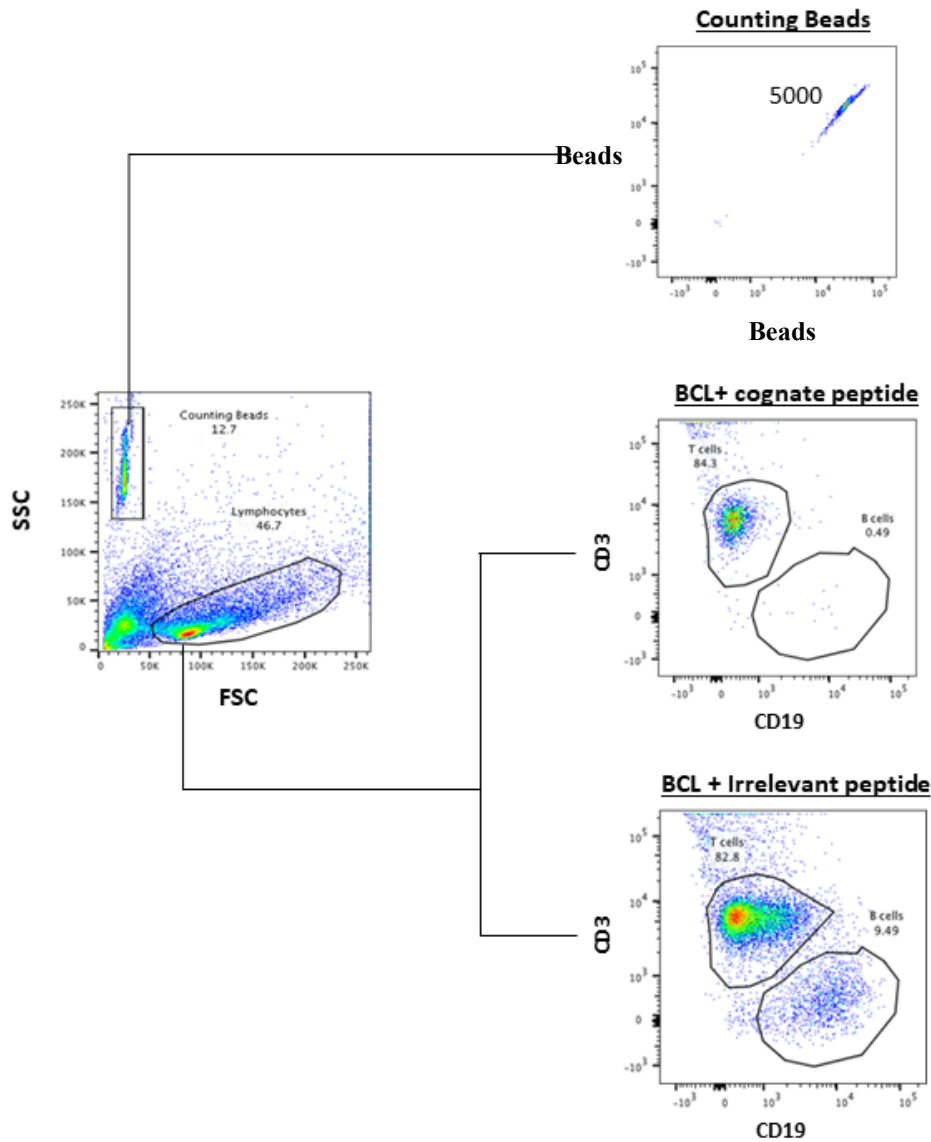


Figure 5. 8 Gating Strategy for B cell killing assay

The primary T cell clones were stimulated with autologous B cells pulsed with ZEBRA peptide pool or an irrelevant peptide (FLR from EBV EBNA antigen). 5000 counting beads were taken up according to the smaller gate in the FSC vs SSC panel to enable normalization of the number of cells taken up from each sample. The live lymphocytes were gated on CD3 vs CD19 to distinguish between the T cell and B cell populations, and the cells within the B cell gate were counted.

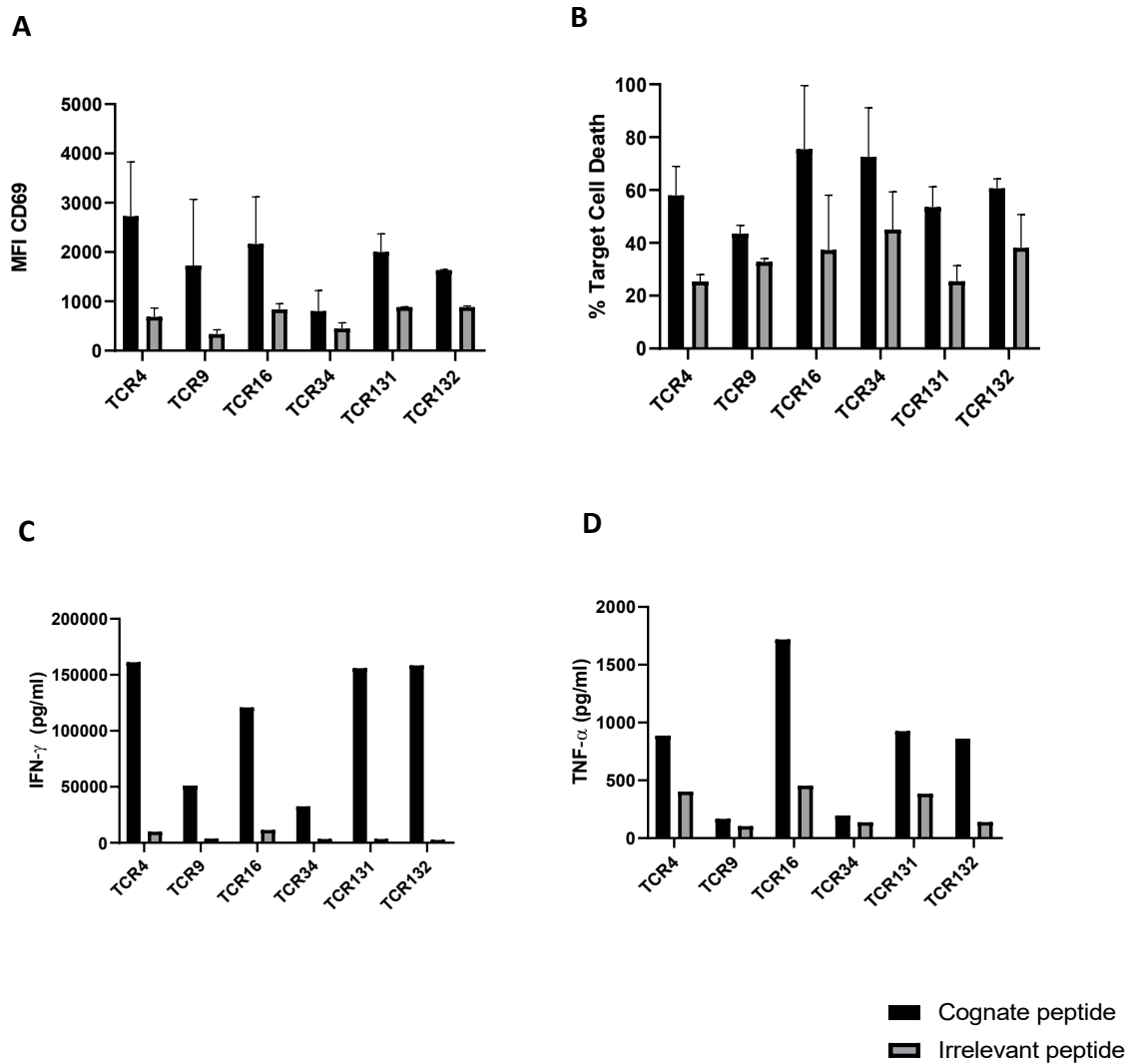


Figure 5.9 Killing of ZEBRA peptide-pulsed B cells by activated T cell clones

Autologous BCLs pulsed with ZEBRA peptide (black bars) or an irrelevant peptide (grey bars) and were co-cultured with primary T cell clones. T cell activation and killing were assessed. A) CD69 upregulation was measured on the primary T cells. Data shows the mean of two replicates from the same experiment. B) ZEBRA peptide-pulsed B cell death compared to death of irrelevant peptide-pulsed B cells. Target cell death was calculated as a percentage of BCL only controls. Data shows the mean of two replicates from the same experiment. C) IFN- γ and (D) TNF- α were measured in single replicates of co-culture supernatant via the MSD system.

The data in Figure 5. 9B indicates that the percentage cell death in B cells that presented ZEBRA peptides was higher than that in the B cells which presented an irrelevant peptide. In addition, the levels of CD69 upregulation on the T cell clones are similar to the percentage killing; the T cells which were presented with cognate peptides had higher CD69 upregulation levels than the T cell clones which were presented with irrelevant peptides (Figure 5. 9A). This not only confirms that the transduced TCR is functioning correctly in primary T cells in its ability to recognise its cognate peptide, but also that it can efficiently activate the primary T cell in an antigen-specific manner.

The cytokines in the co-culture supernatant from the B cell killing assay were analysed for IFN- γ and TNF- α (Figure 5. 9 C and D). As with the antigen-specific B cell death and CD69 upregulation, both cytokines are significantly increased when the T cell clones are presented with cognate peptide but not when presented with the irrelevant peptide. This demonstrates that the primary T cells transduced with EBV-specific TCR can recognise and respond to ZEBRA peptide in an antigen-specific manner.

5.7 TCR-transduced primary T cells recognise HDACi-treated EBVaGC cells

The ultimate test was to assess the ability of ZEBRA-specific primary T cells to recognise and kill EBV-associated gastric carcinoma cells post-latency reversal. To do this, we utilized the IncuCyte S3 Live-Cell analysis system to visually analyse the interactions between the ZEBRA-specific TCR-transduced primary T cells and their target EBV-associated gastric cells over a period of 24 hours. The cells were cultured at an Effector:Target ratio of 10:1 and a red apoptosis marker (IncuCyte Cytotox Red Reagent) for counting dead cells was added to each well at the start of incubation. After treatment with CXD101, Chidamide or SAHA, or with DMSO, the AGS_rEBV cells were co-cultured with the HLA-matched TCR4-transduced primary T cell clones, and an HLA-mismatched negative control clone, TCR9. The OE19_rEBV cells were also treated with the same HDACi and co-cultured with TCR4-transduced primary T cells, or primary T cells transduced with HLA-B*18:01-restricted TCR9, TCR131 or TCR132. Thus, whilst only HLA-A*02:01-restricted TCR4 is HLA-matched to AGS_rEBV, all of the TCR clones are HLA-matched to the OE19_rEBV cells, either via B*18:01 or via A*02:01 (Table 5. 1).

The ability of the clones to kill the target cells was assessed using the automated IncuCyte analysis software; initially the background levels of fluorescence were set, in addition to a GFP threshold level to distinguish between the GFP-low T cells and the GFP-high gastric cells. In addition to being larger in cell size, the GFP levels in the gastric cells were considerably brighter than the T cells, making it easy to distinguish between the two cell types. During the assay, the red marker was taken up by cells undergoing apoptosis, and the overlap area of this red fluorescence with the larger, very bright GFP cells was measured (μM^2) per replicate well at each set time point of 0, 8, 12, 18 and 24 hours. Cells which have an overlap of red dye and GFP thus indicate EBV-associated gastric cells that have undergone apoptosis. Figure 5. 10 shows representative images of cells with high-GFP and red overlap in CXD101- or DMSO-treated AGS_rEBV_GFP and OE19_rEBV_GFP cells; red staining increases in both cell lines over the 24-hour period after treatment with CXD101, in the presence of an HLA-matched TCR4 cells, but does not increase at the same levels in the presence of HLA-mismatched TCR9 cells. At 0 hours, there is some red staining visible, which is expected as the HDACi-treatment is known to cause cell death (Hui et al., 2012). In the DMSO-treated and HLA-mismatched wells however, there is very minimal red staining, indicating that there is no induction of apoptosis.

Figure 5. 11A demonstrates that CXD101-treated AGS_rEBV_GFP cells which take up the

red stain are surrounded by HLA-matched TCR4 cells (smaller GFP-low cells). In contrast, the gastric cells surrounded by HLA-mismatched TCR9 T cells do not undergo apoptosis despite also being treated with CXD101 (Figure 5. 11B). This indicates that the cell death is most likely due to recognition and killing by the ZEBRA-specific T cells. The area of apoptotic red and bright GFP overlap in the replicates is represented as cell death in Figure 5. 12 and Figure 5. 13.

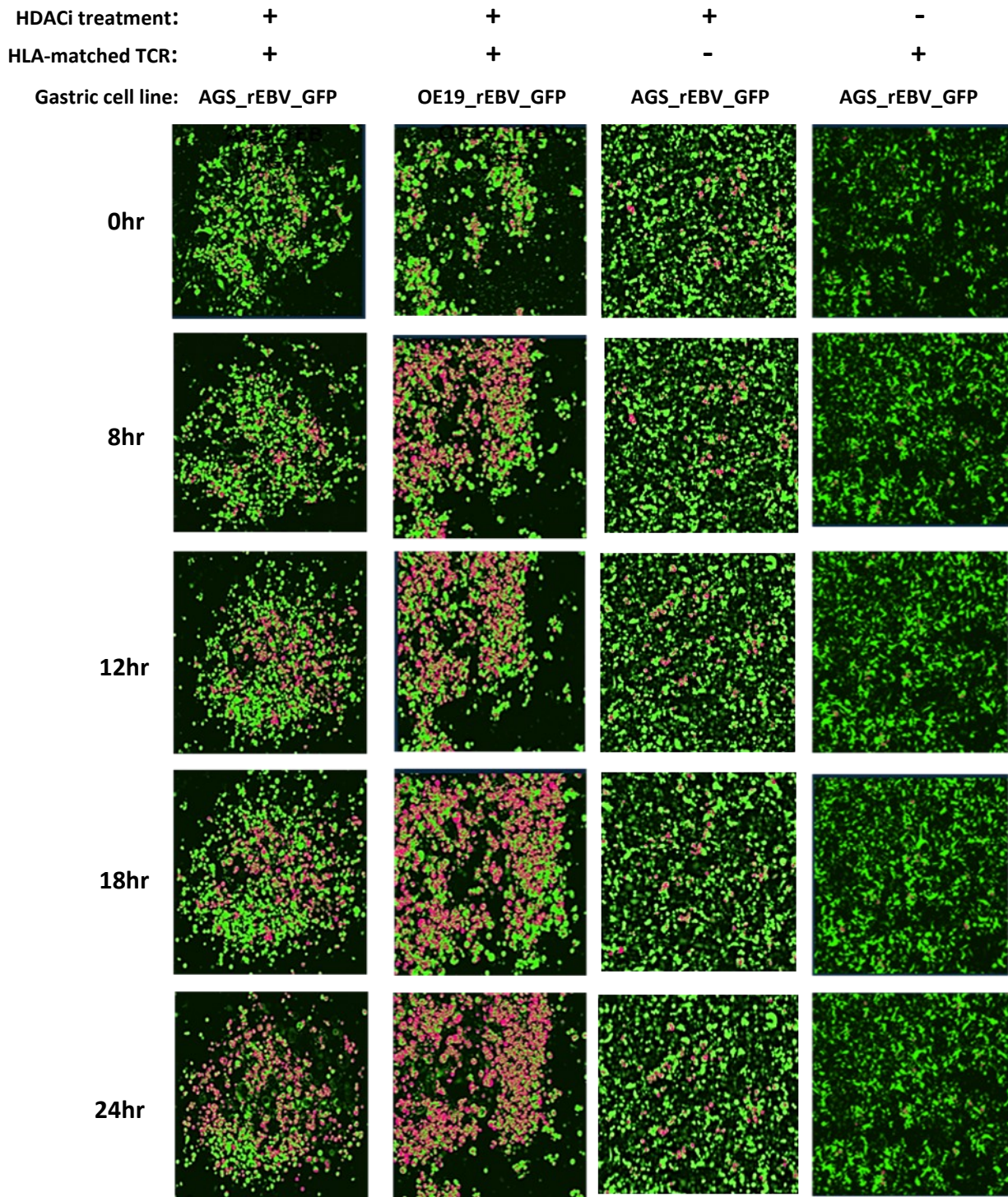


Figure 5. 10 Time course staining of HDACi-treated gastric cell death

Representative IncuCyte images of HDACi-treated (CXD101-treated) or untreated (DMSO-treated) gastric cells co-cultured with HLA-matched TCR4 or HLA-mismatched TCR9 transduced primary T cells. The images show the overlap red stain of cells that are double-positive for red apoptotic marker and high GFP at the times indicated. Representative figures show images from 4 selected wells. The images were captured at 10x magnification and manually zoomed in on the IncuCyte analysis software to view specific areas of interest.

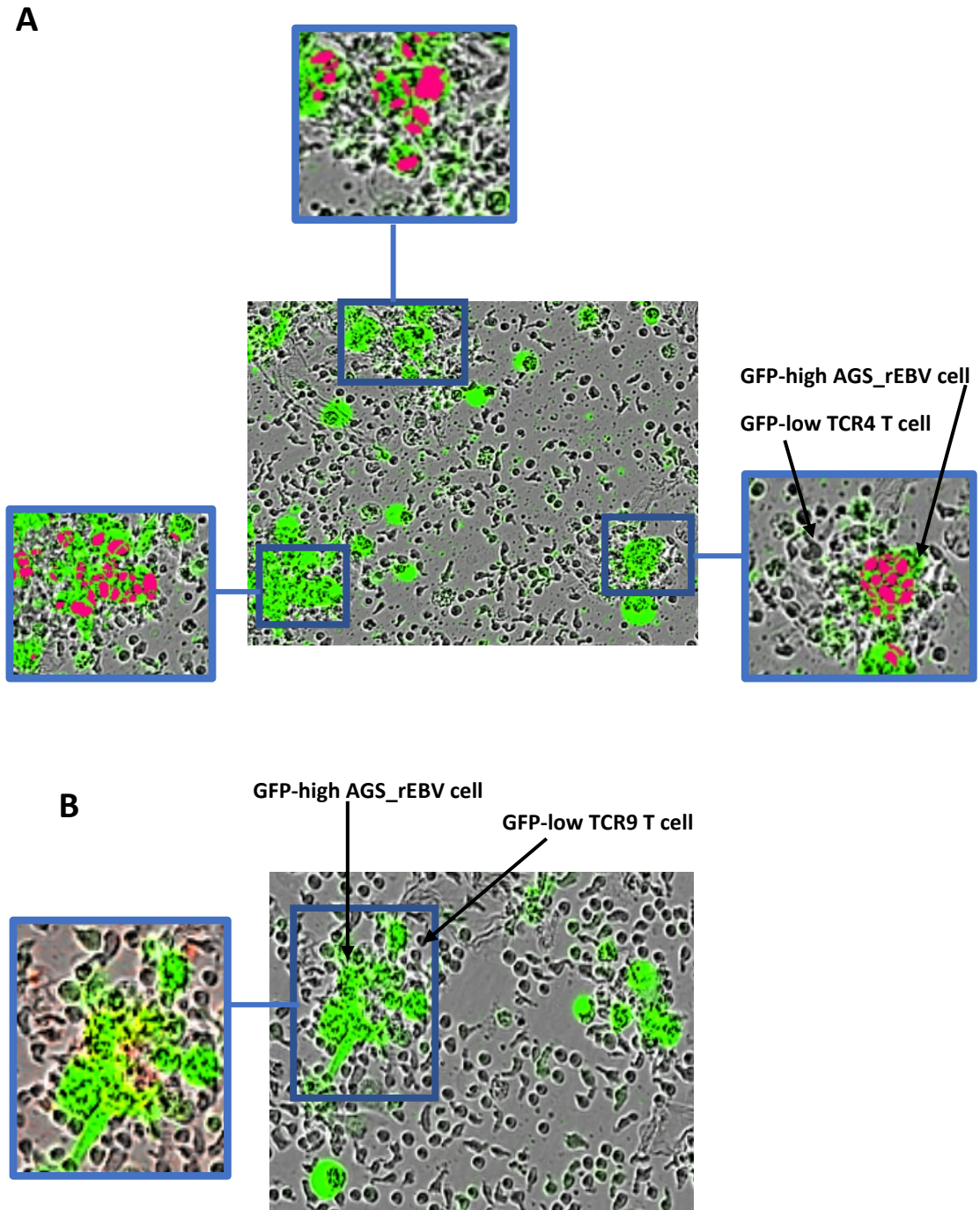


Figure 5. 11 Specific interaction of HLA-matched T cells with HDACi-treated gastric cells is associated with cell death

Representative phase contrast images from co-culture of CXD101-treated AGS_rEBV_GFP cells with HLA-matched TCR4 T cells (A), and HLA-mismatched TCR9 T cells (B). The large central phase contrast images show the larger, GFP-bright gastric cells surrounded by smaller GFP-low T cells. When the overlap red filter is applied (smaller surrounding panels highlighted in blue), gastric cells stain red, indicating cell death.

The images were captured at 10x magnification. The smaller panels were created by manually zooming into the 10x image on the IncuCyte analysis software.

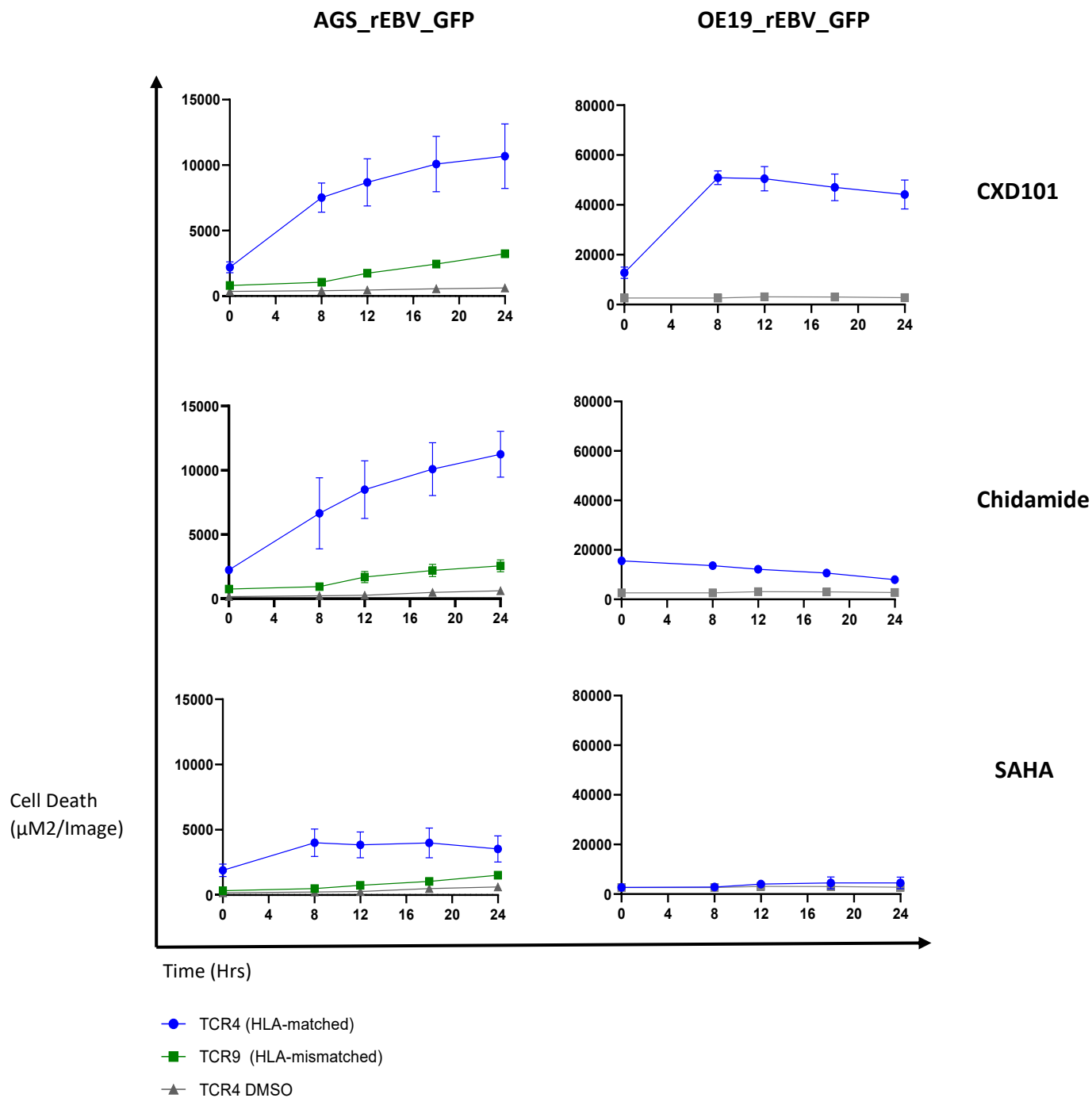


Figure 5. 12 TCR4-transduced primary T cells kill HDACi-treated EBVaGC cells

AGS_rEBV and OE19_rEBV were pre-treated with HDACi or DMSO for 48 hours before co-culturing with TCR4-transduced primary T cells for 24 hours. TCR4 is HLA-matched to the AGS- and OE19 cell lines whilst TCR9 is HLA-mismatched to AGS. Cell death is represented as μM^2 / per image, which represents the area of cells with fluorescence overlap of very high GFP (EBV-positive gastric cells) with red apoptosis marker in each replicate. Data shown is the mean of 4 replicates from the same experiment, with error bars representing SEM. The Wilcoxon's matched pairs signed rank test was performed and showed no statistical significance.

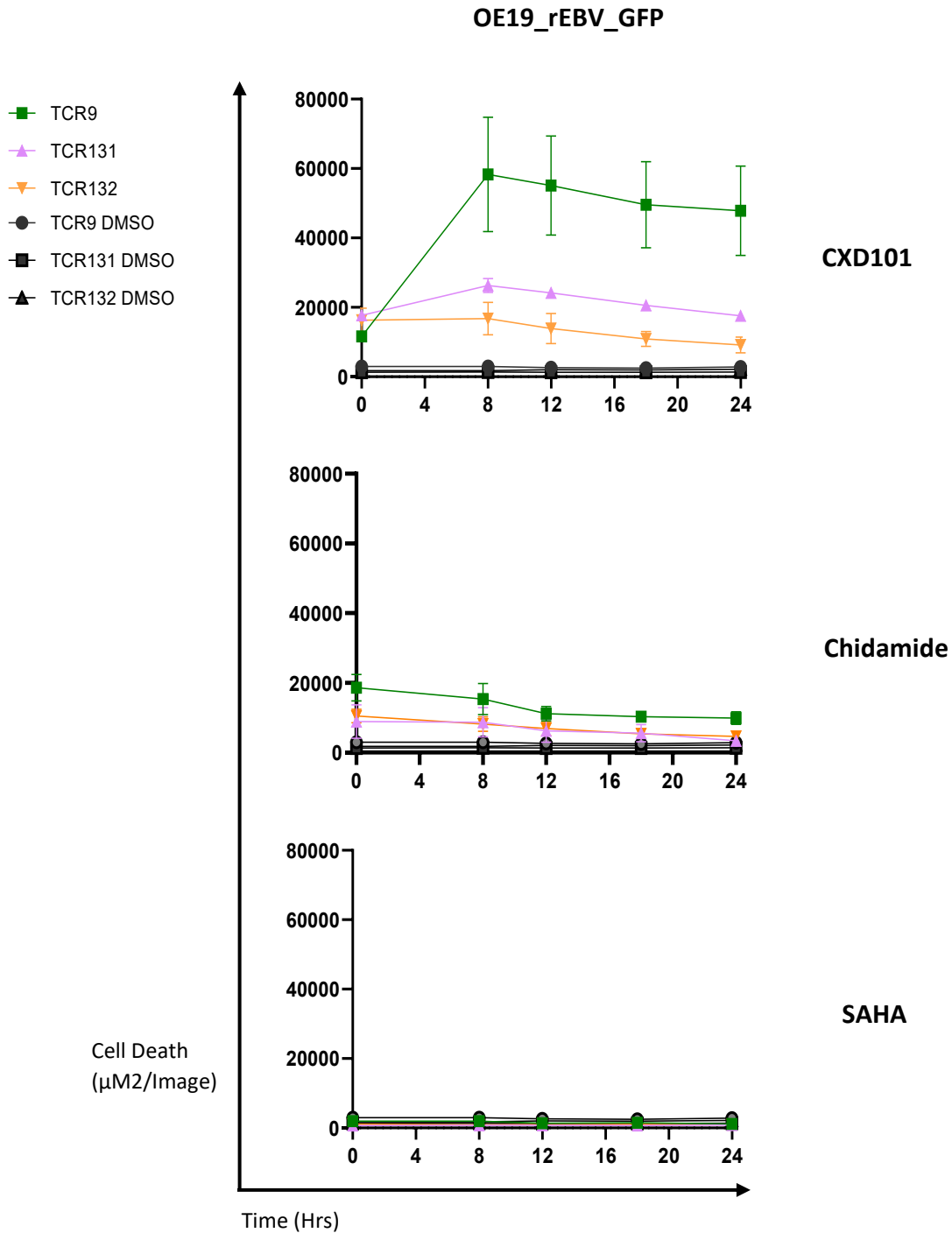


Figure 5. 13 Donor 2 ZEBRA-specific primary T cell clones kill HDACi-treated OE19_rEBV cells

OE19_rEBV were pre-treated with HDACi or DMSO for 48 hours before co-culturing with primary T cells for 24 hours. The TCRs HLA-B*18:01-restricted, thus are HLA-matched to the OE19 cell line. Cell death is represented as μM^2 / per image, which represents the area of cells with fluorescence overlap of very high GFP (EBV-positive gastric cells) with red apoptosis marker in each replicate. Data shown is the mean of 3 replicates from the same experiment, with error bars representing SEM. The Wilcoxon's matched pairs signed rank test was performed and showed no statistical significance.

The images in Figure 5. 12 and Figure 5. 13 show that the ZEBRA-specific T cells can kill HDACi-treated gastric cells but not DMSO-treated gastric cells. Primary T cells transduced with the HLA-A*02:01-restricted TCR4 cells can induce higher cell death in AGS_rEBV cells, compared to the HLA-mismatched TCR9 clone and in the DMSO-treated controls. Killing of OE19_rEBV cells by TCR4 is greatest after treatment with CXD101, compared to treatment with Chidamide or SAHA. Levels of TCR4-mediated cell death in SAHA-treated OE19_rEBV are similar to DMSO-treated cells. Overall, the data in Figure 5. 12 demonstrate that TCR4 is able to mediate the specific killing of HLA-A*02:01-expressing EBVaGC cells after treatment with HDACi.

All of the HLA-B*18:01-restricted TCR-transduced primary T cells are able to kill CXD101-treated OE19_rEBV cells compared to DMSO-treated controls (Figure 5. 13). The majority of killing occurs between 0-8 hours before reaching a plateau in CXD101-treated cells. TCR131 and TCR132 also induce higher levels of OE19_rEBV cell death compared to their DMSO-treated controls. T-cell mediated killing of Chidamide and SAHA-treated OE19_rEBV cells are substantially lower compared to CXD101-treated cells, but still higher than DMSO-treated cells. Overall, the data in Figure 5. 13 demonstrate that HLA-B*18:01-restricted TCRs 9, 131 and 132 are able to mediate the specific killing of HLA-matched OE19_rEBV cells after treatment with HDACi.

In the case of both cell lines and all the TCRs however, the differences in cell death in the HDACi-treated vs DMSO-treated controls were not statistically significant.

In addition to assessment of killing via the IncuCyte system, the cytokines in the supernatant of these assays were measured (Figure 5. 14).

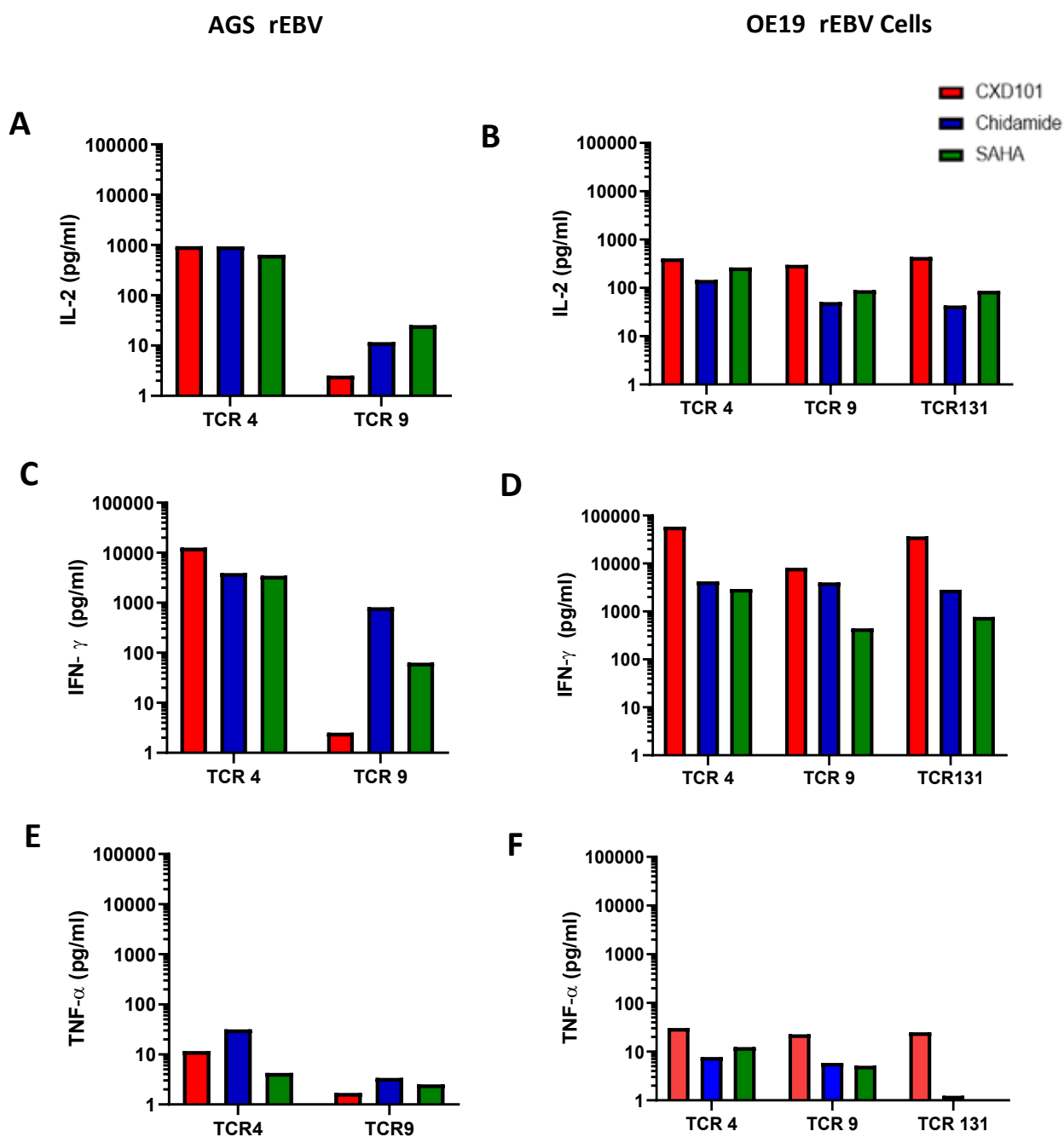


Figure 5. 14 ZEBRA-specific primary T cells secrete IL-2, IFN- γ and TNF- α in response to HDACi-treated gastric carcinoma cells

AGS_rEBV and OE19_rEBV were pre-treated with HDACi or DMSO for 48 hours and co-cultured with primary T cell clones for 24 hours. Co-culture supernatant was collected after 24 hours and cytokines were measured. Data shown is the value of the cytokine minus the background (DMSO control value) in single replicates.

The data in Figure 5. 14 indicates that all the TCR-transduced primary T cells produced IL-2, TNF- α , and IFN- γ in response to their HLA-matched HDACi-treated cells, and that overall this pattern compares with the levels of killing by each TCR seen in Figure 5. 12 and Figure 5. 13. There is however some non-specific cytokine production by TCR9 cells in response to HDACi-treated AGS_rEBV cells.

Although there are clear differences in the levels of killing observed in Figure 5. 12 and Figure 5. 13 depending on the HDACi used, cytokines measured from these wells indicate similar levels of IL-2, TNF- α , and IFN- γ , irrelevant of the treatment.

Overall, although there is very little difference between the levels of cytokines produced in response to the various HDACi-treated cells, the production of cytokines are consistent with the levels of cell death observed in the killing assay (Figure 5. 12 and Figure 5. 13), and support the conclusion that the ZEBRA-specific T cells are able recognise and induce cell death in EBVaGC cells which have undergone latency reversal of EBV via HDACi treatment.

5.8 Discussion

5.8.1 Summary

The ability of three different HDAC inhibitors to induce latency reversal in two EBVaGC cell lines has been confirmed through analysis of ZEBRA antigen expression 48 hours post-treatment. Furthermore, the ability of HLA-A*02:01 and HLA-B*18:01-restricted EBV-specific TCRs to recognise ZEBRA on HLA-matched EBVaGC cells has been demonstrated. Importantly, primary T cells transduced with ZEBRA-specific TCRs have been shown to recognise and kill HLA-matched EBVaGC cells post-HDACi treatment. This data suggests that a novel combination therapy consisting of HDACi treatment to reactivate the lytic stage of EBV infection, followed by adoptive T cell therapy with CTLs specific to these highly immunogenic lytic stage antigens, may be a promising novel approach to the treatment of EBV-associated malignancies.

5.8.2 EBVaGC cells express lytic stage antigen ZEBRA after HDACi-treatment

The artificially infected EBVaGC cell lines AGS_rEBV-GFP and OE19_rEBV-GFP (AGS_rEBV and OE19_rEBV, respectively) were used to test the ability of EBV-specific TCRs to recognise ZEBRA on HDACi-treated cells. Four of the cloned TCRs were suitable for studies using these gastric cell lines owing to their HLA-compatibility. These were HLA-A*02:01-restricted TCR4, which is HLA-matched with A*02:01⁺ AGS and OE19 cell lines, and TCRs 9, 131 and 132, all of which are B*18:01-restricted, thus are compatible for targeting the OE19 cell line (Table 5.1).

Preliminary assays were performed to determine the optimal dose of each HDACi on AGS_rEBV and OE19_rEBV. The cells were treated with CXD101, Chidamide, or SAHA at concentrations of 1, 2.5, 5 or 10 μ M for 48 hours. As shown in Figure 5. 2, each HDACi induces different levels of ZEBRA expression versus cytotoxicity. CXD101 is able to induce ZEBRA expression in the highest percentage of cells (60%) at 2.5 μ M, whereas Chidamide and SAHA require concentrations of at least 5 μ M to achieve this. This correlates with previous studies where SAHA has been shown to induce ZEBRA expression in EBV-associated carcinomas at minimum concentrations of 5 μ M (Hui and Chiang, 2010, Hui et al., 2012). Chidamide has previously been shown to induce high rates of cell death at 10 μ M in Hodgkin Lymphoma cell lines (Jiang et al., 2017). This is not the case when the same dose is used to treat the EBVaGC cell lines however, where cell viability is preserved to over 60%

even at 10 μ M concentration. This may be attributed to the different natures of the respective cell lines, and the various epigenetic mechanisms which contribute to their survival. The differences in the levels of ZEBRA upregulation post-treatment with the HDACi may also be due to the mechanism of actions of the respective agents. SAHA is known to be a potent HDACi (Richon, 2006), and this is reflected in the high levels of ZEBRA expression induced in OE19_rEBV cells (Figure 5. 2 and Figure 5. 4). However it did not induce as much ZEBRA expression in AGS_rEBV cells, suggesting that perhaps these cells are more resistant to treatment than the OE19_rEBV cells.

In keeping with previous reports of the ability of HDACi to reactivate lytic EBV infection and induce ZEBRA antigen expression in various EBV-associated cancer cells, our data shows that SAHA, Chidamide and CXD101 are all able to induce ZEBRA expression in up to 60% of AGS_rEBV and OE19_rEBV, but not in their EBV-negative counterparts (Figure 5. 3 and Figure 5. 4), indicating that these HDACi can act specifically on EBV-infected cells and reverse the latent stage of infection to the highly immunogenic lytic state (Shi et al., 2015, Hui and Chiang, 2010, Hui et al., 2012, Eyre et al., 2016).

5.8.3 EBV-specific SKW3 T cells recognise ZEBRA on HLA-matched gastric carcinoma cells

The ability of the EBV-specific T cells to recognise ZEBRA antigen on HLA-matched gastric cells was analysed. This was initially investigated by pulsing the HLA-matched EBVaGC cell lines with the ZEBRA peptide pool and co-culturing with EBV-specific SKW3 T cells. The recognition of presented peptide antigen was assessed by measuring the upregulation of CD69 on the surface of the T cells. Each of the respective TCRs was able to successfully recognise ZEBRA peptide presented on its HLA-matched gastric cells, but not on cells with mismatched HLAs (Figure 5. 5). This confirms that the TCRs can specifically recognise ZEBRA peptide presented on the surface of the HLA-matched gastric cells.

Following this, the ability of the SKW3 T cells to produce cytokines in response to ZEBRA antigen induced by HDACi treatment of the EBVaGC cells was tested. The ZEBRA-specific SKW3 T cells were cultured with HDACi-treated EBVaGC cells and the culture supernatant was assessed for IL-2, IFN- γ and TNF α (Figure 5. 6). Compared with DMSO-treated controls, all the HLA-matched SKW3 T cells produced cytokines in response to HDACi-treated EBVaGC cells. Overall, CXD101 treated cells induce the highest amounts of cytokines from all the TCRs, regardless of the cell type. This contrasts with the data in Figure

5. 4, which indicate that Chidamide treatment induces the highest levels of ZEBRA in AGS_rEBV cells and SAHA treatment in OE19_rEBV cells. Thus, considering the latter data, it is surprising that the SKW3 T cells produce the highest amounts of cytokines to CXD101-treated cells. Perhaps analysis of the ZEBRA expression levels in the HDACi-treated EBVaGC cells simultaneously may have shown that in this particular instance, Chidamide and SAHA treatment induced the highest levels of ZEBRA in AGS_rEBV and OE19_rEBV cells respectively. In addition, the T cells were not analysed for CD69 upregulation in this instance, and this may have helped to support the data. Nonetheless, the overall data confirms that the ZEBRA-specific SKW3 T cell clones are able to recognise ZEBRA antigen expressed in gastric carcinoma cells following HDACi treatment, indicating that these cells are suitable targets for ZEBRA-specific TCR-mediated killing post-HDACi treatment.

5.8.4 EBV-specific TCRs can be expressed in primary T cells and can recognise ZEBRA peptide-pulsed autologous B cells

The ZEBRA-specific TCRs were expressed in activated primary T cells isolated from a donor who had previously tested negative for IFN- γ responses to the EBV ZEBRA. The TCRs were successfully expressed in the primary T cells, as indicated by the expression of GFP in transduced cells compared to mock-transduced cells (Figure 5. 7). The transduction levels are not as high as in the SKW3 T cell line, but this was expected as primary T cells are known to be more challenging to transduce (Kennedy and Cribbs, 2016). As retroviral vectors need T cells to be activated for efficient infection, the transduction efficiency may have been impacted by the activation state of the primary T cells, which may have been heterogeneous amongst the cells. Perhaps performing the transduction using highly concentrated virus would have increased this efficiency (Kahn et al., 1992). In the future, tetramer staining could be used to analyse the exact levels of expression of transduced TCR, as GFP expression is only an indicator of transduction of efficiency and not gene expression.

The GFP⁺ primary T cells transduced with ZEBRA-specific TCRs were enriched and assessed for their ability to recognise and kill autologous B cells pulsed with the ZEBRA peptide pool.

Target B cell death was used as an indication of killing of antigen-expressing cells by ZEBRA-specific T cells. Counting beads were used to maintain absolute cell counts within

all the samples, allowing unbiased analysis of the number of surviving B cells compared to a BCL only control which represents 100% survival. The data in (Figure 5. 9) indicates that the TCR-transduced primary T cells recognise ZEBRA on their target B cells, and mediate specific killing, leading to between 40-60% target cell death. A greater percentage of B cells presenting ZEBRA peptide were killed compared to B cells presenting the irrelevant FLR peptide of the late stage EBV antigen EBNA-3. This indicates that the target cells are being killed in an antigen-specific manner by the transduced T cells. In correlation with this, CD69 upregulation and secretion of IFN- γ and TNF- α are higher when ZEBRA peptides are presented on the B cells as opposed to the irrelevant peptide. This confirms that the transduced TCRs can be expressed correctly in primary T cells and suggests that they can successfully activate the primary T cell in an antigen-specific manner to induce killing of target cells. Perhaps this data could be further supported by performing a conventional cytotoxicity assay using chromium release or another non-radioactive alternative assay (Karimi et al., 2014).

It was encouraging to see successful recognition and killing by the transduced primary T cells in the absence of endogenous TCR knockout, as it is known that transduced TCRs must compete with endogenous TCR chains, in addition to any mis-paired TCRs for expression on the cell surface in association with CD3 (Heemskerk et al., 2007). However, the primary T cells that were transduced with ZEBRA-specific TCRs are able to recognise their cognate antigen successfully, indicating that they are expressed in their correct $\alpha\beta$ pairs. This may be attributed to the additional cysteine residues that were included in the constant regions of the transduced TCR α and β chains, as it has been shown that introducing an additional disulphide bond can mediate correct expression of the introduced TCR (Cohen et al., 2007, Kuball et al., 2007). Perhaps knocking out the endogenous TCRs from the primary T cells would have increased target cell killing further by allowing more ZEBRA-specific TCRs to be expressed (Legut et al., 2018, Ochi et al., 2011).

5.8.5 TCR-transduced primary T cells recognise HDACi-treated EBVaGC cells and mediate killing

The IncuCyte Live-Cell analysis system was used to analyse the interactions between TCR-transduced T cells and HDACi-treated HLA-matched EBVaGC cells. Figure 5. 10 shows that HDACi-treated AGS_rEBV and OE19_rEBV cells both display increased levels of cell death over a 24-hour period, compared to the DMSO-treated OE19_rEBV cells and HDACi-treated cells co-cultured with HLA-mismatched T cells. There is strong evidence that the increased cell death observed is due to the killing action of the ZEBRA-specific T cells; this is demonstrated in Figure 5. 11A, where HLA-matched TCR4 cells can be seen surrounding CXD101-treated gastric cells, which obtain the red apoptotic stain. In contrast, this apoptotic stain is absent in the CXD101-treated cells surrounded by HLA-mismatched TCR9 cells (Figure 5. 11B). This strongly suggests that only ZEBRA-specific T cells selectively kill the HDACi-treated EBVaGC cells after treatment with HDACi due to the reactivation of lytic EBV infection.

The data presented in Figure 5. 12 and Figure 5. 13 indicate that ZEBRA-specific primary T cells can kill HDACi-treated EBVaGC cells but not their DMSO-treated counterparts, in an HLA-dependent manner. This is displayed by the higher levels of AGS_rEBV cell death induced by the HLA-A*02:01-restricted TCR4 cells compared to the HLA-mismatched TCR9 cells and DMSO-treated controls. Similarly, all of the HLA-matched T cells are able to induce higher levels of cell death in HDACi-treated OE19_rEBV cells compared to DMSO-treated controls. This strongly suggests that the T cell mediated-cell death is dependent on the expression of EBV ZEBRA antigen after treatment with HDACi. There were relatively low levels of killing of SAHA-treated gastric cells compared to cells treated with the other HDACi, but this may be attributed to the greater levels of toxicity of SAHA, as shown in Figure 5. 2. One of the limitations of this experiment was the limited number of effector T cells that were available, even after expansion. High levels of T cell death occurred after transduction, and the rates of GFP were also seen to decrease in surviving cells over time, thus it was necessary to transduce as many activated T cells as possible and extensively enrich the GFP⁺ cells before immediately using them for the killing assay. For future experiments this could be mitigated by transducing even larger numbers of primary T cells to maximise the number of GFP⁺ cells available for the assays.

To support this data, the supernatant was measured for IL-2, IFN- γ and TNF α (Figure 5. 14). In support of the killing assay observations, increased levels of all cytokines were secreted by

the transduced primary T cells in response to their HLA-matched EBVaGC post HDACi-treatment, but not in response to DMSO controls or mismatched control. Of note, TNF- α levels produced by all the T cells against CXD101-treated OE19_rEBV are almost double that in response to OE19_rEBV cells treated with Chidamide or SAHA. This correlates with the highest rates of CXD101-treated OE19_rEBV cell death seen in Figure 5. 12 and Figure 5. 13. The high levels of TNF- α contrast with previous studies, which have shown many HDACi, including SAHA, to mediate downregulation of the cytokine storm (Li et al., 2008, Dobrev et al., 2018). Although taken together it may suggest that CXD101 is the optimal HDACi for induction of ZEBRA-dependent killing, the significantly higher levels of TNF- α produced may indicate the risk of this treatment to induce a cytokine storm, whose detrimental effects may outweigh the benefits of the induced killing.

Taken together, the data presented here demonstrate that primary T cells can be utilized to successfully express functional ZEBRA-specific TCRs, even without prior knockout of endogenous TCRs. These transduced cells can recognise EBV ZEBRA antigen expressed on EBVaGC cells after HDACi-treatment, producing cytokines and mediating cell death in the EBVaGC in an HLA-restricted manner. The data provide a rationale for combination therapy between HDACi treatment and adoptive cell therapy using lytic EBV-specific T cells.

5.8.6 Future work

For future experiments, it may be helpful to knockout the endogenous TCRs from the primary T cells before transducing with the ZEBRA-specific TCRs. This would be expected to lead to even greater levels of ZEBRA-specific cell death due to lack of competition with endogenous TCRs for CD3 and reduced risk of mispairing occurring (Legut et al., 2018, Ochi et al., 2011).

Additionally, it will be interesting to test TCRs against other immediate early and early lytic antigens, as they have also been shown to be dominant during lytic infection, thus may be highly functional in their killing ability of HDACi-treated EBVaGC cells (Steven et al., 1997, Steven et al., 1996). Perhaps combining T cells with various antigen-specificities during treatment would also increase the cell death.

Many current studies investigating lytic reactivation of EBV have demonstrated the success of combination therapies using various reactivation agents and antiviral agents (Lee et al.,

2015, Hui et al., 2016, Hui and Chiang, 2010, Wildeman et al., 2012). It would be interesting to investigate the effect of a new combination therapy using HDACi and adoptive T cell therapy in addition to antiviral agents, as this would target the virus directly in addition to virally-infected cells (Hui et al., 2016, Wildeman et al., 2012).

A key limitation of the HDACi treatments investigated in the current study is that not all of the cells undergo lytic reactivation, as indicated by the ZEBRA negative populations in Figure 5. 3. This may represent a population of cells that are resistant to HDACi treatment, and suggest that lytic induction in this manner may not be an option for all EBVaGC cells. This is concerning as it would seriously hinder the success of any related treatments and requires further investigation. Perhaps a solution would be to target those cells which do respond to HDACi-treatment with lytic-specific T cells, and to use a different approach to target the resistant cells. One such approach could be to target the existing anti-latent EBV T cells and increase their functionality. One way in which to do this would be to combine HDACi treatment and adoptive T cell therapy with anti-PD-1 antibodies, as PD-L1 has been shown to be overexpressed in EBVaGC (Sasaki et al., 2019, Topalian et al., 2012). This would further enhance the T cell response against the viral antigens and may allow increased functional responses from T cells.

One of the limitations of the AGS_rEBV and OE19_rEBV cell lines used in the current study is that they are artificially infected with a recombinant EBV construct, so they do not represent the natural state of EBVaGC cells that would be found in patients. One of the reasons we were limited to using these particular cell lines was due to their HLA-compatibility with our TCRs. Using TCRs which are HLA-matched to a naturally-infected EBVaGC would give a more representative interpretation of the HDACi and T cell therapy combination explored in this chapter.

Finally, *in vivo* studies would allow the functional analysis of the ZEBRA-specific T cells in a more biologically reliable environment, allowing monitoring of EBVaGC killing within a living organism and confirming the efficacy of this proposed novel combination therapy.

6 Discussion

6.1 Results Summary

I have developed and validated an efficient platform for the cloning of paired full-length TCR $\alpha\beta$ chains from single antigen-specific T cells. This optimized platform overcomes many limitations of existing primary T cell cloning methods, such as lengthy in vitro culture and the outgrowth of certain clones over others, which can create bias and inefficiency. In addition, our optimized set of TCR-specific PCR and cloning primers allow easy cloning into a single pre-prepared retroviral vector, bypassing the need for lengthy subcloning and expensive gene synthesis. The capability of this method was demonstrated via the cloning of EBV ZEBRA-specific TCRs from two healthy donors. The most dominant TCRs made up approximately 21% of sequenced TCRs in each donor, and many of these were successfully expressed in TCR-negative T cell lines and in primary T cells. The transduced TCRs efficiently recognised their cognate peptide antigen, upregulating the early activation marker CD69 and secreting TNF- α and IFN- γ upon recognition of their MHC-restricted epitopes. After HDACi-mediated latency reversal of EBV-associated gastric carcinoma cells, primary T cells transduced with these ZEBRA-specific TCRs could recognise and kill these EBV-infected target cells. Characterization of a dominant TCR from one healthy donor revealed the ability to recognise two overlapping 11mers when presented on two different self-HLA alleles, HLA-A*02:01 and HLA-B*35:01. Such cross-reactivity to self-HLA molecules within the same donor has not yet been described in literature and may hold promise for T cell therapy for patients carrying both, or either, of these HLA alleles. Moreover, the functional data suggest that a novel combination therapy encompassing HDACi treatment to reactivate the lytic stage of EBV infection, followed by adoptive T cell therapy with CTLs redirected to specifically recognize these highly immunogenic lytic stage antigens, may be a promising novel approach to the treatment of EBV-associated malignancies.

Overall, the data shows that our single TCR cloning platform can identify and clone antigen-specific TCRs accurately, preserving their ability to recognise and mediate effector functions upon recognition of their target antigen. Our platform allows efficient mapping of T cell epitopes and MHC restriction determination, allowing fast and convenient characterization of the cloned TCRs. Importantly, our platform facilitates T cell epitope mapping, MHC restriction analysis and functional assessment of cloned TCRs in T cell lines and in primary T cells in vitro, and presents the possibility of further confirmation in vivo in xenograft murine models. An overall summary of the single TCR cloning platform is depicted in Figure 6. 1.

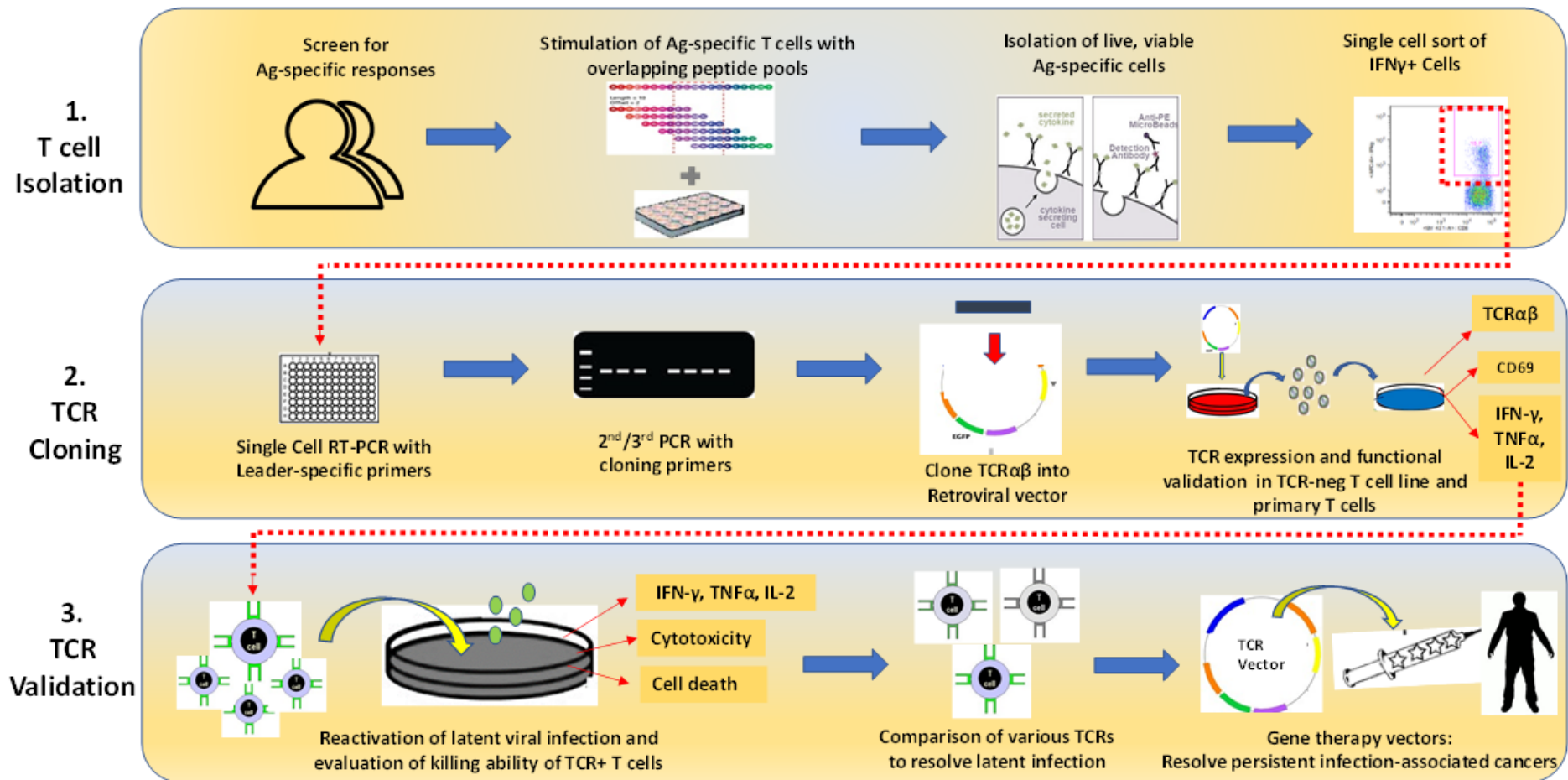


Figure 6. 1 Summary of Single TCR Cloning Platform

1. Antigen-specific TCRs corresponding to any infectious agent can be used to screen for antigen-specific T cell responses in healthy donors or patients. In our study, after initial screening of healthy volunteers, freshly-isolated PBMCs were stimulated with a pool of overlapping peptides. Live, IFN- γ + T cells were isolated using a capture assay, and IFN- γ + CD8+ T cells were single sorted into 96 well PCR plates.
2. Single TCRs can be cloned using the optimized 3-step PCR method and cloned into a universal pre-prepared retroviral vector using Gibson Assembly. The TCRs are stably transduced into target cells (TCR-negative T cell lines or primary T cells) and tested for TCR expression, and recognition of specific peptide via expression of CD69, IL-2 and IFN- γ , and TNF- α .
3. Killing capacity of primary T cells transduced with TCRs specific to lytic stage viral antigens is tested on virus-associated cancer cells after treatment with latency reversal agents. TCRs displaying the greatest ability to kill virus-associated cells after latency reversal will be most promising for immunotherapy against latent virus-associated cancers.

6.2 General Discussion

The single TCR cloning platform outlined in this thesis has its advantages and novelties compared to other methods, but also some limitations which should be addressed. In addition, there are further developments that can be made to strengthen the findings from the cloning of EBV-specific TCRs.

Compared to many conventional methods of T cell cloning, our single TCR cloning method does not require the expansion of primary T cells in culture. In vitro expansion used in these typical methods are not only lengthy and labour intensive, but also present bias in selection of TCR clones, as certain clones may be resistant to outgrowth compared to others, and lead to terminal differentiation.

One of the novelties and advantages of our TCR cloning platform lies in its convenience; it does not rely on expensive outsourced single-cell technologies but uses standard laboratory techniques to produce full-length, paired TCR sequences that retain their ability to mediate effector functions after stable expression in the T cell line or in primary T cells. A feature that grants this convenience is the use of the novel pre-prepared universal retroviral vector and the novel compatible 3rd round PCR primers. These were designed to allow seamless cloning of any full-length TCR $\alpha\beta$ pair into the single vector for stable expression. This avoids the synthesis of full-length gene blocks for each TCR sequence, or extensive subcloning to insert the genes into the desired expression vector, as is required with other published methods (Linnemann et al., 2013, Hu et al., 2018). Gibson assembly has not been used often in the context of TCR cloning, and in one instance where it was described, it required extensive prior artificial TCR gene synthesis, which is lengthy and costly (Guo et al., 2016). Thus, the incorporation of the Gibson assembly method to clone any complete TCR α and β genes directly from purified PCR products into a single universal retroviral vector is a novel approach which to our knowledge has not been described previously.

Although our method is simple and seamless in design, it is not automated and contains some lengthy steps. However, despite this, it is highly adaptable in a basic laboratory for use in the context of any disease, can rapidly and easily identify and clone full-length TCR $\alpha\beta$ pairs without prior in vitro expansion, and is less costly than using external companies to synthesise TCR genes of interest.

It is interesting to note good expression levels of our EBV-specific TCRs in SKW3 cells (which express both CD4 and CD8 endogenously) without the use of separate CD3- and CD8-encoding vectors. This is in contrast to the study by Nguyen and colleagues, where they

reported lack of tetramer binding to transduced CMV-specific TCRs, and weak CD69 upregulation upon stimulation (Nguyen et al., 2014). We bypassed the use of an additional CD8-expressing vector by sorting on CD8⁺ SKW3 cells, though perhaps incorporating an additional CD3 component to the TCR expression vector would increase expression rates of transduced TCRs in primary T cells where CD3 is believed to be the limiting factor for optimal TCR expression (Ahmadi et al., 2011a). In addition to its TCR-deficient nature, another advantage of using the SKW3 cell line is that it permits the mapping of epitopes and defining of MHC-restriction much easier compared to using primary T cell clones.

The SKW3 cells transduced with ZEBRA-specific TCRs upregulated CD69 expression in response to both 5 μ M and 10 μ M of peptide pool, and also secreted IL-2, TNF- α and IFN- γ upon stimulation. This demonstrates the ability of our platform to preserve the TCR sequence during the cloning method, allowing expression of correctly functioning TCRs which retain their ability to recognize their cognate antigen and activate the T cell. It would have been useful to titrate the specific mapped peptides, in order to assess the relative affinity and functional avidity of each of the TCRs. This may have shed light on the relative potency of each TCR to induce effector functions, for example the TCR which recognised antigen at the lowest concentration may be optimal for therapy. However, it is also important to consider the autoreactive effects of such high-affinity TCRs (Zhong et al., 2013).

One of the significant limitations to efficacy and safety aspects concerning TCR gene therapy is the potential of mispairing between the transduced and endogenous TCR chains in the target T cell (van Loenen et al., 2010, Bendle et al., 2010). In light of data from studies demonstrating that reducing the expression of endogenous TCR enhances the efficacy and expression levels of the transduced TCRs, we attempted to knock down endogenous TCR expression in target cells via the use of siRNA against endogenous TCR constant region genes (Bunse et al., 2014, Legut et al., 2018, Ochi et al., 2011). However, this was not successful in stably knocking down TCRs, probably due to low transduction efficiency or due to the siRNA targets being suboptimal. Future endeavours could consider improvement of the protocol to include a mechanism for simultaneous endogenous TCR knock down within the same T cells that the transgenic TCR is to be expressed, decreasing production time. This may involve the inclusion of endogenous TCR-specific siRNA, CRISPR or TALENs in the same vector as the TCR transgene (Legut et al., 2018, Ochi et al., 2011). Including such a mechanism would allow the vector to be used as a direct TCR replacement method as opposed to the generation of autologous TCR knockout cells beforehand or attempting to find

HLA-matching donor cells in a TCR knockout line. However major changes in our TCR vector would be required to accommodate the use of such gene-editing methods. In our current platform, the sites of sequence mismatch between the codon-optimized and endogenous constant regions are so limited that it would not have been possible to design a CRISPR-Cas9 or TALENs-based TCR knock out system as these require much longer target sequences to function (Jinek et al., 2012, Ran et al., 2013, Bogdanove and Voytas, 2011). In addition, the CRISPR-Cas9 system has its own disadvantages which must be considered in future treatment designs, including potential immunogenicity of the Cas9 protein (Charlesworth et al., 2018, Crudele and Chamberlain, 2018).

Another safety aspect of our current vector design which would need to be addressed in future is the use of the retroviral vector. Although the use of retroviral vectors in TCR gene therapy protocols is popular, there is a well-known associated risk of insertional mutagenesis due to the preferred sites of integration near promoter sites (Sinn et al., 2005). This poses a risk for oncogenesis because the vector may directly act to influence gene expression, or may lead to production of full length gene transcript owing to its own LTR promoter (Sinn et al., 2005). In the now infamous case involving a trial for gene-therapy to treat X-linked SCID, three out of 11 children developed leukaemia following *ex vivo* gene transfer of the common γ -chain into hematopoietic stem cells (Hacein-Bey-Abina et al., 2003). Similar to the pMX vector used in our platform, the vector used was based on the murine leukaemia virus (MuLV). In subsequent trials of immunodeficiencies using similar MuLV vectors however, no adverse effects had been reported (Gaspar et al., 2004, Aiuti et al., 2002). It has thus been suggested that the risks of insertional mutagenesis depend not only on the vector system, but also the target cells and the expressed transgene combined (Sinn et al., 2005). In contrast to the observed promoter site integration preferences of retroviral vectors, lentivirus vectors are believed to possess no preference sites for integration, with lower chances of promoter activation after integration. Thus, they may be less predisposed to insertional mutagenesis, suggesting they may be the safer option for gene therapy (Trono, 2003, Mamcarz et al., 2019).

A further limitation of using retroviral vectors is that they are incapable of transducing non-dividing cells, and it has been suggested from a murine model of adoptive cell therapy that transduced quiescent cells may be more effective in mediating effector responses against tumours compared to stimulated, dividing cells (Gattinoni et al., 2005). An alternative to using viral vectors to transduce dividing cells is the use of non-viral transposons, which can be conveniently electroporated into target cells. They have been shown to mediate highly

efficient transfer of TCR genes to PBMCs and confer levels of antitumor activity that are comparable to retroviral vector systems (Peng et al., 2009, Chicaybam et al., 2013). These important considerations can be taken into account in future experiments and applications; the universal nature of the cloning primers designed for our platform ensure that the vector backbone can easily be substituted whilst still maintaining the convenience and universal nature of the TCR cloning technology.

The cloning system could be improved in its screening of relevant TCRs. Although required for producing stable TCR-engineered T cells, the generation of retroviral particles is time consuming during the initial screening process when assessing TCR function and specificity. One way to improve this aspect of the system would be to use a reporter cell line system expressing luciferase or GFP. Such a cell line could be transfected with the TCR vector directly and stimulated with peptide, using the marker as a readout for function and specificity. Other groups have used such systems as a way to overcome the cumbersome nature of retroviral particle production and transduction, demonstrating that reporter cell lines can be used to easily screen for relevant TCRs (Hamana et al., 2016, Guo et al., 2016). Although these cells cannot be used directly for functional and killing assays, they could fast-track the screening stage to select TCRs of interest by as much as 2 weeks due to bypassing of retroviral particle generation and SKW3 transduction and culture.

The ZEBRA-specific TCRs which were dominant in the two healthy donors were characterized in terms of their HLA-specificity and mapped to their specific epitopes. One of the dominant TCRs, TCR4, comprised up 13% of all the TCRs sequenced from donor 1. Several peptide stimulation assays demonstrated that TCR4 can recognise two overlapping 11-mer epitopes, EPLPQGQLTAY and LPQGQLTAYHV, presented on both HLA-A*02:01 and HLA-B*35:01 molecules. The EPL-11mer is a well-known immunodominant epitope in HLA-B*35:01⁺ individuals, however, it has not previously been associated with HLA-A*02:01 (Miles et al., 2005, Green et al., 2004). Many studies have described the T cell cross-recognition of allo-HLA molecules, whether within the same HLA supertype or across superotypes (Frahm et al., 2007, Burrows et al., 1994, Koelle et al., 2002, Amir et al., 2010, Leslie et al., 2006, van den Heuvel et al., 2017). Moreover, an EBV-specific CTL which has dual specificity for the latent epitope FLRGRAYGL presented on HLA-B8, and the alloantigen HLA-B*44:02, has been well-characterized (Burrows et al., 1994, Burrows et al., 1997, D'Orsogna et al., 2012). It is important to note however that although HLA class I promiscuity has been shown to be common amongst virus-specific CD8⁺ T cells in allogeneic

donors, this phenomenon has not yet been described, to our knowledge, within the context of self-HLA molecules in the same individual. Furthermore, the stronger observed response to the autologous BCL (Figure 4.3) may be attributed to the co-expression of both HLA molecules simultaneously, thus the presentation of twice the amount of peptide compared to the single HLA-expressing cells. It could be speculated that such an effect could present the host with a possible survival advantage. In terms of clinical applicability, the dual-specificity of this TCR suggests it may be a potential candidate for use in immunotherapy in both HLA-A*02:01⁺ or HLA-B*35:01⁺ patients.

Although HLA-A*02:01 is not predicted to bind to the 11mer peptides, it is predicted to bind weakly to the 13mer VLPEPLPQGQLTA, which we observed in our hands (Table 4.4.).

Furthermore, it has been shown that epitopes greater than 9 amino acids in length must adopt a highly bulged conformation in order to fit into the MHC groove (Miles et al., 2005, Tynan et al., 2005, Hassan et al., 2015). Thus, despite the lack of strict conformation to the required anchor residues, this bulging may permit the binding of the EPLPQGQLTAY and LPQGQLTAYHV 11mers within both the A*02:01 and B*35:01 grooves. To confirm this, the full structural biology of the complex will need to be examined in future to assess the points of contact between the peptide and the MHC grooves. Perhaps single residue mutations would also shed light on which residues are essential for this dual-HLA specificity. It is interesting to note that several of the other TCRs in this donor possess the characteristics of B*35:01-restricted EPL-specific TCRs described by Miles et al (Miles et al., 2005). TCRs 10, 7 and 2 all use the described TRBJ-1-5 gene in their beta chain, whilst TCRs 1, 10, 16, 18, 19 and 20 all contain the SGGS motif in their central CDR3 α residues (Table 3.3). The presence of these shared CDR3 motifs and TCR gene usage strongly suggest that these TCRs will also be B*35:01-EPL restricted. As most of these TCRs were not as dominant as the TCRs selected for cloning, they were not analysed in this study. It would thus be very useful to express these and test whether any of them also recognise peptide on HLA-A*02:01 and B*35:01 in the same manner as TCR4.

Finally, we have identified two different HLA-A*23:01-restricted ZEBRA-specific TCRs from donor 2 (TCR16 and TCR34, Table 4.6). Very few HLA-A-restricted ZEBRA epitopes have been described in literature, and HLA-A*23:01 has not yet been described to bind to any known ZEBRA epitopes (Rist et al., 2015b). Thus, the finding that two of the dominant TCRs from this healthy donor are restricted to this HLA allele is worthy of further investigation as it expands the potential HLA alleles which can be relevant clinically. Other HLA-A-restricted ZEBRA-specific TCRs which would be useful are those restricted to HLA-

A*11:01 as 40% of nasopharyngeal carcinoma (NPC) patients are positive for this allele (Zheng et al., 2015). Additionally, HLA-A*24 and B*40- restricted TCRs would also be useful, as along with HLA-A*11:01, these HLA alleles are present at high frequency in the Chinese population where NPC is highly prevalent (Lee et al., 2000, Wu et al., 2018). It would be interesting to assess whether other TCRs from donor 1 also cross-react with more than one HLA molecule in the same manner as TCR4. In addition, it will also be of value to assess the function and specificities of other more dominant TCRs in each donor, such as TCR1 and TCR10, which composed 21% and 13% of sequences in donor 1, and TCR8 which made up 15% of donor 2 sequences. In order to strengthen the findings of this chapter, it would be useful to use HLA-blocking antibodies or to generate multimers against all of the TCRs for confirmation. This would be particularly helpful for the validation of the dual-HLA-restriction of TCR4 and, in terms of clinical application, for the isolation of specific CD8⁺ T cells from donors for expansion for adoptive therapy. Finally, knowledge of how common the ZEBRA-specific TCRs are in the population could be further indication of their importance in terms of protection against EBV. Searches on the Immune Epitope Database (iedb.org), VDJ data base (vdjdb.cdr3.net) and Protein Databank (pdb.org) yielded no results matching to the TCR sequences discussed in our work, suggesting that they are not known public TCRs.

Although all three HDACi used in this study, CXD101, Chidamide and SAHA, induced ZEBRA induction in both the AGS_rEBV and OE19_rEBV cells, it is important to note that not all of the cells undergo lytic reactivation, as indicated by the ZEBRA negative populations in Figure 5.3. This may represent a population of cells that are resistant to HDACi treatment and suggest that lytic induction in this manner may not be an option for all EBVaGC cells. This is concerning as it would greatly hinder the success of any related treatments and thus requires further investigation. A solution may be to combine different HDACi to maximise EBV reactivation, but this may also have implications with increased levels of toxicities. Perhaps an alternative combined solution would be to target HDACi-sensitive cells with lytic-specific T cells, and to use a different approach to target the resistant cells. One such approach could be to target the existing anti-latent EBV T cells by increasing their functionality. A way to do this may be to combine HDACi treatment and adoptive T cell therapy with anti-PD-1 antibodies, as PD-L1 has been shown to be overexpressed in EBVaGC (Sasaki et al., 2019, Topalian et al., 2012). This combination may enhance the T cell responses against the viral antigens and allow increased functional responses from T

cells. Finally, an important consideration is the effect of the HDACi on the CTLs themselves; it has been shown that certain latency reversal agents inhibit the functions of CTLs and even promote the formation of Tregs (Walker-Sperling et al., 2016, Jones et al., 2014, Tao et al., 2007). Although these studies investigated these effects in the context of anti-HIV responses, it will be important to assess the impact of potential HDACi-related CTL inhibition during treatment of EBV-associated malignancies with genetically-modified T cells. Although our data do not appear to show inhibition of CTL activity post-treatment with our chosen HDACis, it should be highlighted that the HDACi were washed away before trypsinization of treated cells during our experiments, so this may have inadvertently avoided T cell inhibition during the killing assay.

One of the major caveats of this work was that the transduction efficiency of the primary T cells was low ($\leq 25\%$). In addition, we found that the GFP expression levels diminished over time, further reducing the available cells for use. This may have been due to faster outgrowth of the GFP negative cells in comparison to GFP⁺ cells, as there was no antibiotic selection used to favour transduced cells. Thus, we were only able to expand sorted cells for a week before promptly performing assays. This posed a limitation on the number of assays, and in the case of the HDACi-treated gastric cell killing assay, we could only perform the experiment once in the available time, though with several replicate wells. Furthermore, it would have been useful to also analyse other markers of cytotoxic killing, such as CD107a, granzyme B and perforin staining. Analysis of these markers would have allowed comparison of the relative cytotoxicity of each TCR and shed more light on their abilities. Unfortunately, the low number of cells and their short-lived nature hindered the collection of more data for the consolidation of our findings. Critically, the short-term nature of transduction effects will need to be re-examined and improved if this is to be a viable, long term immunotherapy. Perhaps the phenotype of the transduced T cell is an important factor in the success of treatment, and transduction of naïve T cells may be a better option for longer-term, efficient immunotherapy (Joglekar et al., 2018, Klebanoff et al., 2005, Gattinoni et al., 2005). Finally, in future, it may also be interesting to test the effector functions of TCRs against other immediate early and early lytic antigens that have also been shown to be immunodominant targets during lytic infection (Steven et al., 1997, Steven et al., 1996). Perhaps combining T cells with various antigen-specificities during treatment would also increase cancer cell death and provide optimal clinical outcome.

6.3 Future Directions

As the killing abilities of the transduced primary T cells were evaluated on artificially-infected EBVaGC cells, it is difficult to comprehensively conclude that the TCRs will recognise and mediate effector functions towards naturally infected GC cells in the same manner. The levels of EBV infection and ZEBRA reactivation may be variable amongst naturally infected cells, and may in fact be lower than their recombinant EBV-infected counterparts used in this work. Thus, it will be important to assess this and examine the functionality of our TCRs against them. In future studies, using TCRs that are HLA-matched to a naturally infected EBVaGC would give a more representative interpretation of the HDACi and T cell therapy combination explored in this thesis. One of the limitations of executing this is the availability of cancer cells that are HLA-matched to our TCRs. A way to overcome this may be to express the relevant HLA molecules in the target cancer cells artificially before assessment.

In addition, it will be extremely useful to repeat the HDACi-treated EBVaGC cell killing experiment using primary T cells whose TCRs have been knocked out prior to ZEBRA-specific TCR transduction. One would expect that this would lead to increased EBV-specific TCR expression, resulting in increased levels of target cell killing (Legut et al., 2018, Ochi et al., 2011). Performing this experiment in TCR-KO cells would also remove any possibility of cross-reactivity and background killing of the T cells mediated by the endogenous TCRs.

Furthermore, it would be interesting to see if our TCRs also recognise ZEBRA antigen induced on other EBV-associated cancer cells, such as nasopharyngeal carcinoma, especially as this is such a major public health issue in certain parts of south east Asia (Wu et al., 2018).

Finally, *in vivo* studies using a xenograft mouse model would allow the functional analysis of the ZEBRA-specific T cells in a more biologically reliable environment. Introducing a luciferase reporter into the cancer cells would allow monitoring of EBVaGC killing within a model organism. This would confirm the efficacy of our proposed combination therapy and the experiments are currently ongoing.

6.4 Final Conclusions

Taken together, the work in this thesis outlines the development and validation of a highly accessible novel single TCR cloning platform that overcomes many problems associated with conventional T cell cloning methods. Furthermore, the use of a TCR-negative T cell line allows efficient and convenient epitope mapping and determination of MHC-restriction of the cloned TCRs. Crucially, our platform permits rapid functional analysis of cloned TCRs in cell lines and in primary T cells, and can easily be adapted for future *in vivo* xenograft murine models.

This novel platform was used to clone and functionally characterize several EBV ZEBRA-specific TCRs, which could mediate specific killing of EBVaGC cells post treatment with latency reversal agents. Based on our functional data, we propose a novel combination therapy consisting of HDACi-mediated latency reversal of EBV infection, followed by adoptive T cell therapy with lytic stage-specific TCR-engineered T cells, as a potential treatment of EBV-associated malignancies.

References

- ABBAS, A. K. & JANEWAY, C. A. 2000. Immunology: Improving on nature in the twenty-first century. *Cell*, 100, 129-138.
- ABBOTT, R. J., QUINN, L. L., LEESE, A. M., SCHOLLES, H. M., PACHNIO, A. & RICKINSON, A. B. 2013. CD8⁺ T cell responses to lytic EBV infection: late antigen specificities as subdominant components of the total response. *J Immunol*, 191, 5398-409.
- ABDEL-HAKEEM, M. S., BOISVERT, M., BRUNEAU, J., SOUDEYNS, H. & SHOUKRY, N. H. 2017. Selective expansion of high functional avidity memory CD8 T cell clonotypes during hepatitis C virus reinfection and clearance. *PLoS pathogens*, 13, e1006191-e1006191.
- AHMADI, M., KING, J., XUE, S. A., VOISINE, C., HOLLER, A., WRIGHT, G., WAXMAN, J. & STAUSS, H. 2011a. CD3 limits the Efficacy of TCR Gene Therapy in vivo. *Blood*, 118, 3528-37.
- AIUTI, A., SLAVIN, S., AKER, M., FICARA, F., DEOLA, S., MORTELLARO, A., MORECKI, S., ANDOLFI, G., TABUCCHI, A., CARLUCCI, F., MARINELLO, E., CATTANEO, F., VAI, S., SERVIDA, P., MINIERO, R., RONCAROLO, M. G. & BORDIGNON, C. 2002. Correction of ADA-SCID by stem cell gene therapy combined with nonmyeloablative conditioning. *Science*, 296, 2410-3.
- ALLISON, J. P., MCINTYRE, B. W. & BLOCH, D. 1982. Tumor-specific antigen of murine T-lymphoma defined with monoclonal antibody. *J Immunol*, 129, 2293-300.
- ALVES SOUSA, A. D. P., JOHNSON, K. R., OHAYON, J., ZHU, J., MURARO, P. A. & JACOBSON, S. 2019. Comprehensive Analysis of TCR- β Repertoire in Patients with Neurological Immune-mediated Disorders. *Scientific Reports*, 9, 344.
- AMIR, A. L., D'ORSOGNA, L. J., ROELEN, D. L., VAN LOENEN, M. M., HAGEDOORN, R. S., DE BOER, R., VAN DER HOORN, M. A., KESTER, M. G., DOXIADIS, II, FALKENBURG, J. H., CLAAS, F. H. & HEEMSKERK, M. H. 2010. Allo-HLA reactivity of virus-specific memory T cells is common. *Blood*, 115, 3146-57.
- AMYES, E., HATTON, C., MONTAMAT-SICOTTE, D., GUDGEON, N., RICKINSON, A. B., MCMICHAEL, A. J. & CALLAN, M. F. C. 2003. Characterization of the CD4⁺ T cell response to Epstein-Barr virus during primary and persistent infection. *The Journal of experimental medicine*, 198, 903-911.
- ANDERSEN, M. H., SCHRAMA, D., THOR STRATEN, P. & BECKER, J. C. 2006. Cytotoxic T Cells. *Journal of Investigative Dermatology*, 126, 32-41.
- ANNELS, N. E., CALLAN, M. F., TAN, L. & RICKINSON, A. B. 2000. Changing patterns of dominant TCR usage with maturation of an EBV-specific cytotoxic T cell response. *The Journal of Immunology*, 165, 4831-4841.
- ARCHIN, N. M., LIBERTY, A. L., KASHUBA, A. D., CHOUDHARY, S. K., KURUC, J. D., CROOKS, A. M., PARKER, D. C., ANDERSON, E. M., KEARNEY, M. F., STRAIN, M. C., RICHMAN, D. D., HUDGENS, M. G., BOSCH, R. J., COFFIN, J. M., ERON, J. J., HAZUDA, D. J. & MARGOLIS, D. M. 2012. Administration of vorinostat disrupts HIV-1 latency in patients on antiretroviral therapy. *Nature*, 487, 482-5.
- ARSTILA, T. P., CASROUGE, A., BARON, V., EVEN, J., KANELLOPOULOS, J. & KOURILSKY, P. 1999. A direct estimate of the human alpha T cell receptor diversity. *Science*, 286, 958-61.

- BAER, R., BANKIER, A. T., BIGGIN, M. D., DEININGER, P. L., FARRELL, P. J., GIBSON, T. J., HATFULL, G., HUDSON, G. S., SATCHWELL, S. C., SEGUIN, C. & ET AL. 1984. DNA sequence and expression of the B95-8 Epstein-Barr virus genome. *Nature*, 310, 207-11.
- BANU, N., CHIA, A., HO, Z. Z., GARCIA, A. T., PARAVASIVAM, K., GROTENBREG, G. M., BERTOLETTI, A. & GEHRING, A. J. 2014. Building and optimizing a virus-specific T cell receptor library for targeted immunotherapy in viral infections. *Sci Rep*, 4, 4166.
- BARKER, J. N., DOUBROVINA, E., SAUTER, C., JAROSCAK, J. J., PERALES, M. A., DOUBROVIN, M., PROCKOP, S. E., KOEHNE, G. & O'REILLY, R. J. 2010. Successful treatment of EBV-associated posttransplantation lymphoma after cord blood transplantation using third-party EBV-specific cytotoxic T lymphocytes. *Blood*, 116, 5045-9.
- BARQUINERO, J., EIXARCH, H. & PÉREZ-MELGOSA, M. 2004. Retroviral vectors: new applications for an old tool. *Gene Therapy*, 11, S3-S9.
- BASU, R., WHITLOCK, B. M., HUSSON, J., LE FLOC'H, A., JIN, W., OYLER-YANIV, A., DOTIWALA, F., GIANNONE, G., HIVROZ, C., BIAIS, N., LIEBERMAN, J., KAM, L. C. & HUSE, M. 2016. Cytotoxic T Cells Use Mechanical Force to Potentiate Target Cell Killing. *Cell*, 165, 100-110.
- BAUMANN, M., MISCHAK, H., DAMMEIER, S., KOLCH, W., GIRES, O., PICH, D., ZEIDLER, R., DELECLUSE, H.-J. & HAMMERSCHMIDT, W. 1998. Activation of the Epstein-Barr Virus Transcription Factor BZLF1 by 12-O-Tetradecanoylphorbol-13-Acetate-Induced Phosphorylation. *Journal of Virology*, 72, 8105-8114.
- BECATTINI, S., LATORRE, D., MELE, F., FOGlierINI, M., DE GREGORIO, C., CASSOTTA, A., FERNANDEZ, B., KELDERMAN, S., SCHUMACHER, T. N., CORTI, D., LANZAVECCHIA, A. & SALLUSTO, F. 2015. T cell immunity. Functional heterogeneity of human memory CD4(+) T cell clones primed by pathogens or vaccines. *Science*, 347, 400-6.
- BENDLE, G. M., LINNEMANN, C., HOOIJKAAS, A. I., BIES, L., DE WITTE, M. A., JORRITSMA, A., KAISER, A. D., POUW, N., DEBETS, R., KIEBACK, E., UCKERT, W., SONG, J. Y., HAANEN, J. B. & SCHUMACHER, T. N. 2010. Lethal graft-versus-host disease in mouse models of T cell receptor gene therapy. *Nat Med*, 16, 565-70, 1p following 570.
- BERDIEN, B., MOCK, U., ATANACKOVIC, D. & FEHSE, B. 2014. TALEN-mediated editing of endogenous T-cell receptors facilitates efficient reprogramming of T lymphocytes by lentiviral gene transfer. *Gene Ther*, 21, 539-48.
- BLAKE, N., HAIGH, T., SHAKA'A, G., CROOM-CARTER, D. & RICKINSON, A. 2000. The importance of exogenous antigen in priming the human CD8+ T cell response: lessons from the EBV nuclear antigen EBNA1. *J Immunol*, 165, 7078-87.
- BLAKE, N., LEE, S., REDCHENKO, I., THOMAS, W., STEVEN, N., LEESE, A., STEIGERWALD-MULLEN, P., KURILLA, M. G., FRAPPIER, L. & RICKINSON, A. 1997. Human CD8+ T cell responses to EBV EBNA1: HLA class I presentation of the (Gly-Ala)-containing protein requires exogenous processing. *Immunity*, 7, 791-802.
- BOETTCHER, M. & MCMANUS, M. T. 2015. Choosing the Right Tool for the Job: RNAi, TALEN, or CRISPR. *Molecular cell*, 58, 575-585.
- BOGDANOVA, A. J. & VOYTAS, D. F. 2011. TAL effectors: customizable proteins for DNA targeting. *Science*, 333, 1843-6.

- BOGEDAIN, C., WOLF, H., MODROW, S., STUBER, G. & JILG, W. 1995. Specific cytotoxic T lymphocytes recognize the immediate-early transactivator Zta of Epstein-Barr virus. *J Virol*, 69, 4872-9.
- BOLLARD, C. M., AGUILAR, L., STRAATHOF, K. C., GAHN, B., HULS, M. H., ROUSSEAU, A., SIXBEY, J., GRESIK, M. V., CARRUM, G., HUDSON, M., DILLOO, D., GEE, A., BRENNER, M. K., ROONEY, C. M. & HESLOP, H. E. 2004. Cytotoxic T lymphocyte therapy for Epstein-Barr virus+ Hodgkin's disease. *J Exp Med*, 200, 1623-33.
- BOMMHARDT, U., BASSON, M. A., KRUMMREI, U. & ZAMOYSKA, R. 1999. Activation of the extracellular signal-related kinase/mitogen-activated protein kinase pathway discriminates CD4 versus CD8 lineage commitment in the thymus. *J Immunol*, 163, 715-22.
- BOSE, P., DAI, Y. & GRANT, S. 2014. Histone deacetylase inhibitor (HDACI) mechanisms of action: emerging insights. *Pharmacology & therapeutics*, 143, 323-336.
- BOWLES, N. E., EISENSMITH, R. C., MOHUIDDIN, R., PYRON, M. & WOO, S. L. 1996. A simple and efficient method for the concentration and purification of recombinant retrovirus for increased hepatocyte transduction in vivo. *Hum Gene Ther*, 7, 1735-42.
- BRACIALE, T. J., MORRISON, L. A., SWEETSER, M. T., SAMBROOK, J., GETHING, M. J. & BRACIALE, V. L. 1987. Antigen presentation pathways to class I and class II MHC-restricted T lymphocytes. *Immunological reviews*, 98, 95-114.
- BRUMMELKAMP, T. R., BERNARDS, R. & AGAMI, R. 2002. A System for Stable Expression of Short Interfering RNAs in Mammalian Cells. *Science*, 296, 550-553.
- BUBNA, A. K. 2015. Vorinostat-An Overview. *Indian journal of dermatology*, 60, 419-419.
- BUNSE, M., BENDLE, G. M., LINNEMANN, C., BIES, L., SCHULZ, S., SCHUMACHER, T. N. & UCKERT, W. 2014. RNAi-mediated TCR knockdown prevents autoimmunity in mice caused by mixed TCR dimers following TCR gene transfer. *Mol Ther*, 22, 1983-91.
- BURKE, A. P., YEN, T. S., SHEKITKA, K. M. & SOBIN, L. H. 1990. Lymphoepithelial carcinoma of the stomach with Epstein-Barr virus demonstrated by polymerase chain reaction. *Mod Pathol*, 3, 377-80.
- BURROWS, S. R., KHANNA, R., BURROWS, J. M. & MOSS, D. J. 1994. An alloresponse in humans is dominated by cytotoxic T lymphocytes (CTL) cross-reactive with a single Epstein-Barr virus CTL epitope: implications for graft-versus-host disease. *J Exp Med*, 179, 1155-61.
- BURROWS, S. R., SILINS, S. L., KHANNA, R., BURROWS, J. M., RISCHMUELLER, M., MCCLUSKEY, J. & MOSS, D. J. 1997. Cross-reactive memory T cells for Epstein-Barr virus augment the alloresponse to common human leukocyte antigens: degenerate recognition of major histocompatibility complex-bound peptide by T cells and its role in alloreactivity. *Eur J Immunol*, 27, 1726-36.
- CACCIA, N., KRONENBERG, M., SAXE, D., HAARS, R., BRUNS, G. A., GOVERMAN, J., MALISSEN, M., WILLARD, H., YOSHIKAI, Y., SIMON, M. & ET AL. 1984. The T cell receptor beta chain genes are located on chromosome 6 in mice and chromosome 7 in humans. *Cell*, 37, 1091-9.
- CALLAN, M. F., STEVEN, N., KRAUSA, P., WILSON, J. D., MOSS, P. A., GILLESPIE, G. M., BELL, J. I., RICKINSON, A. B. & MCMICHAEL, A. J. 1996. Large clonal expansions of CD8+ T cells in acute infectious mononucleosis. *Nat Med*, 2, 906-11.
- CALLAN, M. F., TAN, L., ANNELS, N., OGG, G. S., WILSON, J. D., O'CALLAGHAN, C. A., STEVEN, N., MCMICHAEL, A. J. & RICKINSON, A. B. 1998. Direct

- visualization of antigen-specific CD8⁺ T cells during the primary immune response to Epstein-Barr virus In vivo. *J Exp Med*, 187, 1395-402.
- CAMARGO, M. C., KIM, W.-H., CHIARAVALLI, A. M., KIM, K.-M., CORVALAN, A. H., MATSUO, K., YU, J., SUNG, J. J. Y., HERRERA-GOEPFERT, R., MENESES-GONZALEZ, F., KIJIMA, Y., NATSUGOE, S., LIAO, L. M., LISSOWSKA, J., KIM, S., HU, N., GONZALEZ, C. A., YATABE, Y., KORIYAMA, C., HEWITT, S. M., AKIBA, S., GULLEY, M. L., TAYLOR, P. R. & RABKIN, C. S. 2014. Improved survival of gastric cancer with tumour Epstein-Barr virus positivity: an international pooled analysis. *Gut*, 63, 236-243.
- CARRASCO-AVINO, G., RIQUELME, I., PADILLA, O., VILLASECA, M., AGUAYO, F. R. & CORVALAN, A. H. 2017. The conundrum of the Epstein-Barr virus-associated gastric carcinoma in the Americas. *Oncotarget*, 8, 75687-75698.
- CATALINA, M. D., SULLIVAN, J. L., BAK, K. R. & LUZURIAGA, K. 2001. Differential evolution and stability of epitope-specific CD8(+) T cell responses in EBV infection. *J Immunol*, 167, 4450-7.
- CHARLESWORTH, C. T., DESHPANDE, P. S., DEVER, D. P., DEJENE, B., GOMEZ-OSPINA, N., MANTRI, S., PAVEL-DINU, M., CAMARENA, J., WEINBERG, K. I. & PORTEUS, M. H. 2018. Identification of Pre-Existing Adaptive Immunity to Cas9 Proteins in Humans. *bioRxiv*, 243345.
- CHEN, H., NDHLOVU, Z. M., LIU, D., PORTER, L. C., FANG, J. W., DARKO, S., BROCKMAN, M. A., MIURA, T., BRUMME, Z. L., SCHNEIDEWIND, A., PIECHOCKA-TROCHA, A., CESA, K. T., SELA, J., CUNG, T. D., TOTH, I., PEREYRA, F., YU, X. G., DOUEK, D. C., KAUFMANN, D. E., ALLEN, T. M. & WALKER, B. D. 2012. TCR clonotypes modulate the protective effect of HLA class I molecules in HIV-1 infection. *Nat Immunol*, 13, 691-700.
- CHICAYBAM, L., SODRE, A. L., CURZIO, B. A. & BONAMINO, M. H. 2013. An efficient low cost method for gene transfer to T lymphocytes. *PLoS One*, 8, e60298.
- CHLEWICKI, L. K., HOLLER, P. D., MONTI, B. C., CLUTTER, M. R. & KRANZ, D. M. 2005. High-affinity, peptide-specific T cell receptors can be generated by mutations in CDR1, CDR2 or CDR3. *J Mol Biol*, 346, 223-39.
- CHO, H.-I., KIM, U.-H., SHIN, A. R., WON, J.-N., LEE, H.-J., SOHN, H.-J. & KIM, T.-G. 2018. A novel Epstein-Barr virus-latent membrane protein-1-specific T-cell receptor for TCR gene therapy. *British journal of cancer*, 118, 534-545.
- CLAY, T. M., CUSTER, M. C., SACHS, J., HWU, P., ROSENBERG, S. A. & NISHIMURA, M. I. 1999. Efficient transfer of a tumor antigen-reactive TCR to human peripheral blood lymphocytes confers anti-tumor reactivity. *J Immunol*, 163, 507-13.
- CLUTE, S. C., WATKIN, L. B., CORNBERG, M., NAUMOV, Y. N., SULLIVAN, J. L., LUZURIAGA, K., WELSH, R. M. & SELIN, L. K. 2005. Cross-reactive influenza virus-specific CD8⁺ T cells contribute to lymphoproliferation in Epstein-Barr virus-associated infectious mononucleosis. *The Journal of clinical investigation*, 115, 3602-3612.
- CLUTTON, G. T. & JONES, R. B. 2018. Diverse Impacts of HIV Latency-Reversing Agents on CD8⁺ T-Cell Function: Implications for HIV Cure. *Frontiers in immunology*, 9, 1452-1452.
- COHEN, C. J., LI, Y. F., EL-GAMIL, M., ROBBINS, P. F., ROSENBERG, S. A. & MORGAN, R. A. 2007. Enhanced antitumor activity of T cells engineered to express T-cell receptors with a second disulfide bond. *Cancer research*, 67, 3898-3903.
- COHEN, C. J., ZHAO, Y., ZHENG, Z., ROSENBERG, S. A. & MORGAN, R. A. 2006. Enhanced antitumor activity of murine-human hybrid T-cell receptor (TCR) in human

- lymphocytes is associated with improved pairing and TCR/CD3 stability. *Cancer research*, 66, 8878-8886.
- COHEN, J. I. 2000. Epstein-Barr virus infection. *N Engl J Med*, 343, 481-92.
- COLLINS, M. K., GOODFELLOW, P. N., SPURR, N. K., SOLOMON, E., TANIGAWA, G., TONEGAWA, S. & OWEN, M. J. 1985. The human T-cell receptor alpha-chain gene maps to chromosome 14. *Nature*, 314, 273-4.
- COORAY, S., HOWE, S. J. & THRASHER, A. J. 2012. Retrovirus and lentivirus vector design and methods of cell conditioning. *Methods Enzymol*, 507, 29-57.
- COSTA, A. I., KONING, D., LADELL, K., MCLAREN, J. E., GRADY, B. P., SCHELLENS, I. M., VAN HAM, P., NIJHUIS, M., BORGHANS, J. A., KESMIR, C., PRICE, D. A. & VAN BAARLE, D. 2015. Complex T-cell receptor repertoire dynamics underlie the CD8⁺ T-cell response to HIV-1. *J Virol*, 89, 110-9.
- COUNTRYMAN, J., JENSON, H., SEIBL, R., WOLF, H. & MILLER, G. 1987. Polymorphic proteins encoded within BZLF1 of defective and standard Epstein-Barr viruses disrupt latency. *J Virol*, 61, 3672-9.
- COUNTRYMAN, J. & MILLER, G. 1985. Activation of expression of latent Epstein-Barr herpesvirus after gene transfer with a small cloned subfragment of heterogeneous viral DNA. *Proceedings of the National Academy of Sciences*, 82, 4085-4089.
- CRESCENZI, A., TAFFON, C., DONATI, M., GUARINO, M. P., VALERI, S. & COPPOLA, R. 2017. PD-L1/PD-1 check-point in gastric carcinoma with lymphoid stroma case report with immunochemical study. *Medicine (Baltimore)*, 96, e5730.
- CRUDELE, J. M. & CHAMBERLAIN, J. S. 2018. Cas9 immunity creates challenges for CRISPR gene editing therapies. *Nature Communications*, 9, 3497.
- D'ORSOGNA, L. J., VAN DEN HEUVEL, H., VAN DER MEER-PRINS, E. M. W., ROELEN, D. L., DOXIADIS, I. I. N. & CLAAS, F. H. J. 2012. Stimulation of Human EBV- and CMV-Specific Cytolytic Effector Function Using Allogeneic HLA Molecules. *The Journal of Immunology*, 1201034.
- DASH, P., MCCLAREN, J. L., OGUIN, T. H., 3RD, ROTHWELL, W., TODD, B., MORRIS, M. Y., BECKSFORT, J., REYNOLDS, C., BROWN, S. A., DOHERTY, P. C. & THOMAS, P. G. 2011. Paired analysis of TCRalpha and TCRbeta chains at the single-cell level in mice. *J Clin Invest*, 121, 288-95.
- DEEKS, S. G. 2012. HIV: Shock and kill. *Nature*, 487, 439-40.
- DELVES, P. J. & ROITT, I. M. 2000. The Immune System. *New England Journal of Medicine*, 343, 37-49.
- DOBREVA, Z. G., GRIGOROV, B. G. & STANILOVA, S. A. 2018. Effect of a Histone Deacetylases Inhibitor of IL-18 and TNF-Alpha Secretion in Vitro. *Open access Macedonian journal of medical sciences*, 6, 269-273.
- DONNELLY, M. L., LUKE, G., MEHROTRA, A., LI, X., HUGHES, L. E., GANI, D. & RYAN, M. D. 2001. Analysis of the aphthovirus 2A/2B polyprotein 'cleavage' mechanism indicates not a proteolytic reaction, but a novel translational effect: a putative ribosomal 'skip'. *J Gen Virol*, 82, 1013-25.
- DRIJFHOUT, J. W., BRANDT, R. M. P., D'AMARO, J., KAST, W. M. & MELIEF, C. J. M. 1995. Detailed motifs for peptide binding to HLA-A*0201 derived from large random sets of peptides using a cellular binding assay. *Human Immunology*, 43, 1-12.
- DUAN, L. & GRUNEBAUM, E. 2018. Hematological Malignancies Associated With Primary Immunodeficiency Disorders. *Clin Immunol*, 194, 46-59.
- DUDLEY, M. E., WUNDERLICH, J. R., ROBBINS, P. F., YANG, J. C., HWU, P., SCHWARTZENTRUBER, D. J., TOPALIAN, S. L., SHERRY, R., RESTIFO, N. P. & HUBICKI, A. M. 2002. Cancer regression and autoimmunity in patients after clonal repopulation with antitumor lymphocytes. *Science*, 298, 850-854.

- DUNMIRE, S. K., GRIMM, J. M., SCHMELING, D. O., BALFOUR, H. H., JR. & HOGQUIST, K. A. 2015. The Incubation Period of Primary Epstein-Barr Virus Infection: Viral Dynamics and Immunologic Events. *PLoS Pathog*, 11, e1005286.
- DURGEAU, A., VIRK, Y., CORGNAC, S. & MAMI-CHOUAIB, F. 2018. Recent Advances in Targeting CD8 T-Cell Immunity for More Effective Cancer Immunotherapy. *Frontiers in immunology*, 9, 14-14.
- ECKSCHLAGER, T., PLCH, J., STIBOROVA, M. & HRABETA, J. 2017. Histone Deacetylase Inhibitors as Anticancer Drugs. *International journal of molecular sciences*, 18, 1414.
- EGERTON, M., SHORTMAN, K. & SCOLLAY, R. 1990. The kinetics of immature murine thymocyte development in vivo. *International Immunology*, 2, 501-507.
- EL-SHARKAWY, A., AL ZAIDAN, L. & MALKI, A. 2018. Epstein–Barr Virus-Associated Malignancies: Roles of Viral Oncoproteins in Carcinogenesis. *Frontiers in Oncology*, 8.
- ELBASHIR, S. M., HARBORTH, J., LENDECKEL, W., YALCIN, A., WEBER, K. & TUSCHL, T. 2001. Duplexes of 21-nucleotide RNAs mediate RNA interference in cultured mammalian cells. *Nature*, 411, 494-498.
- ELLIOTT, S. L., PYE, S. J., SCHMIDT, C., CROSS, S. M., SILINS, S. L. & MISKO, I. S. 1997. Dominant cytotoxic T lymphocyte response to the immediate-early trans-activator protein, BZLF1, in persistent type A or B Epstein-Barr virus infection. *J Infect Dis*, 176, 1068-72.
- EPSTEIN, A. 2012. Burkitt lymphoma and the discovery of Epstein-Barr virus. *Br J Haematol*, 156, 777-9.
- EYRE, T. A., COLLINS, G. P., GUPTA, A., SHEIKH, S., WOODCOCK, V., WHITTAKER, J., WANG, L. M., SOILLEUX, E., TYSOE, F., COUSINS, R., LA THANGUE, N., KERR, D. & MIDDLETON, M. R. 2016. Results of a Phase I Study to Assess the Safety, Tolerability, Pharmacokinetics and Pharmacodynamics of CXD101: Preliminary Safety and Activity in Relapsed or Refractory Hodgkin and Non-Hodgkin Lymphoma Patients. *Blood*, 128, 1817-1817.
- FAINT, J. M., PILLING, D., AKBAR, A. N., KITAS, G. D., BACON, P. A. & SALMON, M. 1999. Quantitative flow cytometry for the analysis of T cell receptor Vbeta chain expression. *J Immunol Methods*, 225, 53-60.
- FALK, K., ROTZSCHKE, O., GRAHOVAC, B., SCHENDEL, D., STEVANOVIC, S., JUNG, G. & RAMMENSEE, H. G. 1993. Peptide motifs of HLA-B35 and -B37 molecules. *Immunogenetics*, 38, 161-2.
- FALK, K., ROTZSCHKE, O., STEVANOVIC, S., JUNG, G. & RAMMENSEE, H. G. 1991. Allele-specific motifs revealed by sequencing of self-peptides eluted from MHC molecules. *Nature*, 351, 290-6.
- FARRELL, P. J. 2019. Epstein-Barr Virus and Cancer. *Annu Rev Pathol*, 14, 29-53.
- FARRELL, P. J., ROWE, D. T., ROONEY, C. M. & KOUZARIDES, T. 1989. Epstein-Barr virus BZLF1 trans-activator specifically binds to a consensus AP-1 site and is related to c-fos. *Embo j*, 8, 127-32.
- FATHALLAH, I., PARROCHE, P., GRUFFAT, H., ZANNETTI, C., JOHANSSON, H., YUE, J., MANET, E., TOMMASINO, M., SYLLA, B. S. & HASAN, U. A. 2010. EBV Latent Membrane Protein 1 Is a Negative Regulator of TLR9. *The Journal of Immunology*, 185, 6439-6447.
- FEEDERLE, R., KOST, M., BAUMANN, M., JANZ, A., DROUET, E., HAMMERSCHMIDT, W. & DELECLUSE, H. J. 2000. The Epstein-Barr virus lytic program is controlled by the co-operative functions of two transactivators. *The EMBO journal*, 19, 3080-3089.

- FELLMANN, C. & LOWE, S. W. 2013. Stable RNA interference rules for silencing. *Nature Cell Biology*, 16, 10.
- FENG, W.-H., WESTPHAL, E., MAUSER, A., RAAB-TRAUB, N., GULLEY, M. L., BUSSON, P. & KENNEY, S. C. 2002. Use of Adenovirus Vectors Expressing Epstein-Barr Virus (EBV) Immediate-Early Protein BZLF1 or BRLF1 To Treat EBV-Positive Tumors. *Journal of Virology*, 76, 10951-10959.
- FERLAY, J., SHIN, H. R., BRAY, F., FORMAN, D., MATHERS, C. & PARKIN, D. M. 2010. Estimates of worldwide burden of cancer in 2008: GLOBOCAN 2008. *Int J Cancer*, 127, 2893-917.
- FERNANDEZ, A. F., ROSALES, C., LOPEZ-NIEVA, P., GRAÑA, O., BALLESTAR, E., ROPERO, S., ESPADA, J., MELO, S. A., LUJAMBIO, A. & FRAGA, M. F. 2009. The dynamic DNA methylomes of double-stranded DNA viruses associated with human cancer. *Genome research*, 19, 438-451.
- FLEISHER, G., HENLE, W., HENLE, G., LENNETTE, E. T. & BIGGAR, R. J. 1979. Primary infection with Epstein-Barr virus in infants in the United States: clinical and serologic observations. *J Infect Dis*, 139, 553-8.
- FLEMINGTON, E. K., BORRAS, A. M., LYTLE, J. P. & SPECK, S. H. 1992. Characterization of the Epstein-Barr virus BZLF1 protein transactivation domain. *Journal of virology*, 66, 922-929.
- FRAHM, N., YUSIM, K., SUSCOVICH, T. J., ADAMS, S., SIDNEY, J., HRABER, P., HEWITT, H. S., LINDE, C. H., KAVANAGH, D. G., WOODBERRY, T., HENRY, L. M., FAIRCLOTH, K., LISTGARTEN, J., KADIE, C., JOJIC, N., SANGO, K., BROWN, N. V., PAE, E., ZAMAN, M. T., BIHL, F., KHATRI, A., JOHN, M., MALLAL, S., MARINCOLA, F. M., WALKER, B. D., SETTE, A., HECKERMAN, D., KORBER, B. T. & BRANDER, C. 2007. Extensive HLA class I allele promiscuity among viral CTL epitopes. *Eur J Immunol*, 37, 2419-33.
- FREEMAN, J. D., WARREN, R. L., WEBB, J. R., NELSON, B. H. & HOLT, R. A. 2009. Profiling the T-cell receptor beta-chain repertoire by massively parallel sequencing. *Genome research*, 19, 1817-1824.
- FUCHS, C. S., DOI, T., JANG, R. W.-J., MURO, K., SATOH, T., MACHADO, M., SUN, W., JALAL, S. I., SHAH, M. A. & METGES, J.-P. 2017. KEYNOTE-059 cohort 1: Efficacy and safety of pembrolizumab (pembro) monotherapy in patients with previously treated advanced gastric cancer. American Society of Clinical Oncology.
- FUKAYAMA, M., HAYASHI, Y., IWASAKI, Y., CHONG, J., Ooba, T., TAKIZAWA, T., KOIKE, M., MIZUTANI, S., MIYAKI, M. & HIRAI, K. 1994. Epstein-Barr virus-associated gastric carcinoma and Epstein-Barr virus infection of the stomach. *Laboratory investigation; a journal of technical methods and pathology*, 71, 73-81.
- GALON, J., COSTES, A., SANCHEZ-CABO, F., KIRILOVSKY, A., MLECNIK, B., LAGORCE-PAGÈS, C., TOSOLINI, M., CAMUS, M., BERGER, A. & WIND, P. 2006. Type, density, and location of immune cells within human colorectal tumors predict clinical outcome. *Science*, 313, 1960-1964.
- GAN, Y. J., CHODOSH, J., MORGAN, A. & SIXBEY, J. W. 1997. Epithelial cell polarization is a determinant in the infectious outcome of immunoglobulin A-mediated entry by Epstein-Barr virus. *J Virol*, 71, 519-26.
- GARBER, K. 2018. Driving T-cell immunotherapy to solid tumors. *Nature Biotechnology*, 36, 215-219.
- GARCIA, K. C. & ADAMS, E. J. 2005. How the T Cell Receptor Sees Antigen—A Structural View. *Cell*, 122, 333-336.
- GARRIDO, F., RUIZ-CABELLO, F., CABRERA, T., PEREZ-VILLAR, J. J., LÓPEZ-BOTET, M., DUGGAN-KEEN, M. & STERN, P. L. 1997. Implications for

- immunosurveillance of altered HLA class I phenotypes in human tumours. *Immunology today*, 18, 89-95.
- GARZELLI, C., TAUB, F. E., SCHARFF, J. E., PRABHAKAR, B. S., GINSBERG-FELLNER, F. & NOTKINS, A. L. 1984. Epstein-Barr virus-transformed lymphocytes produce monoclonal autoantibodies that react with antigens in multiple organs. *Journal of virology*, 52, 722-725.
- GASPAR, H. B., PARSLEY, K. L., HOWE, S., KING, D., GILMOUR, K. C., SINCLAIR, J., BROUNS, G., SCHMIDT, M., VON KALLE, C., BARINGTON, T., JAKOBSEN, M. A., CHRISTENSEN, H. O., AL GHONAIUM, A., WHITE, H. N., SMITH, J. L., LEVINSKY, R. J., ALI, R. R., KINNON, C. & THRASHER, A. J. 2004. Gene therapy of X-linked severe combined immunodeficiency by use of a pseudotyped gammaretroviral vector. *Lancet*, 364, 2181-7.
- GATTINONI, L., KLEBANOFF, C. A., PALMER, D. C., WRZESINSKI, C., KERSTANN, K., YU, Z., FINKELSTEIN, S. E., THEORET, M. R., ROSENBERG, S. A. & RESTIFO, N. P. 2005. Acquisition of full effector function in vitro paradoxically impairs the in vivo antitumor efficacy of adoptively transferred CD8⁺ T cells. *The Journal of clinical investigation*, 115, 1616-1626.
- GIBSON, D. G., YOUNG, L., CHUANG, R. Y., VENTER, J. C., HUTCHISON, C. A., 3RD & SMITH, H. O. 2009. Enzymatic assembly of DNA molecules up to several hundred kilobases. *Nat Methods*, 6, 343-5.
- GONG, Q., WANG, C., ZHANG, W., IQBAL, J., HU, Y., GREINER, T. C., CORNISH, A., KIM, J. H., RABADAN, R., ABATE, F., WANG, X., INGHIRAMI, G. G., MCKEITHAN, T. W. & CHAN, W. C. 2017. Assessment of T-cell receptor repertoire and clonal expansion in peripheral T-cell lymphoma using RNA-seq data. *Sci Rep*, 7, 11301.
- GOTTSCHALK, S. & ROONEY, C. M. 2015. Adoptive T-Cell Immunotherapy. *Current topics in microbiology and immunology*, 391, 427-454.
- GRAKOU, A., BROMLEY, S. K., SUMEN, C., DAVIS, M. M., SHAW, A. S., ALLEN, P. M. & DUSTIN, M. L. 1999. The immunological synapse: a molecular machine controlling T cell activation. *Science*, 285, 221-7.
- GRAWUNDER, U., WEST, R. B. & LIEBER, M. R. 1998. Antigen receptor gene rearrangement. *Current Opinion in Immunology*, 10, 172-180.
- GREEN, K. J., MILES, J. J., TELLAM, J., VAN ZUYLEN, W. J., CONNOLLY, G. & BURROWS, S. R. 2004. Potent T cell response to a class I-binding 13-mer viral epitope and the influence of HLA micropolymorphism in controlling epitope length. *Eur J Immunol*, 34, 2510-9.
- GROGAN, E., JENSON, H., COUNTRYMAN, J., HESTON, L., GRADOVILLE, L. & MILLER, G. 1987. Transfection of a rearranged viral DNA fragment, WZhet, stably converts latent Epstein-Barr viral infection to productive infection in lymphoid cells. *Proceedings of the National Academy of Sciences*, 84, 1332-1336.
- GROGG, K. L., LOHSE, C. M., PANKRATZ, V. S., HALLING, K. C. & SMYRK, T. C. 2003. Lymphocyte-rich gastric cancer: associations with Epstein-Barr virus, microsatellite instability, histology, and survival. *Mod Pathol*, 16, 641-51.
- GROSS, G., WAKS, T. & ESHHAR, Z. 1989. Expression of immunoglobulin-T-cell receptor chimeric molecules as functional receptors with antibody-type specificity. *Proceedings of the National Academy of Sciences*, 86, 10024-10028.
- GRULICH, A. E., VAN LEEUWEN, M. T., FALSTER, M. O. & VAJDIC, C. M. 2007. Incidence of cancers in people with HIV/AIDS compared with immunosuppressed transplant recipients: a meta-analysis. *Lancet*, 370, 59-67.

- GUEDAN, S., CALDERON, H., POSEY, A. D., JR. & MAUS, M. V. 2019. Engineering and Design of Chimeric Antigen Receptors. *Mol Ther Methods Clin Dev*, 12, 145-156.
- GUO, X. Z., DASH, P., CALVERLEY, M., TOMCHUCK, S., DALLAS, M. H. & THOMAS, P. G. 2016. Rapid cloning, expression, and functional characterization of paired alphabeta and gammadelta T-cell receptor chains from single-cell analysis. *Mol Ther Methods Clin Dev*, 3, 15054.
- GUST, J., HAY, K. A., HANAFI, L.-A., LI, D., MYERSON, D., GONZALEZ-CUYAR, L. F., YEUNG, C., LILES, W. C., WURFEL, M., LOPEZ, J. A., CHEN, J., CHUNG, D., HARJU-BAKER, S., ÖZPOLAT, T., FINK, K. R., RIDDELL, S. R., MALONEY, D. G. & TURTLE, C. J. 2017. Endothelial Activation and Blood–Brain Barrier Disruption in Neurotoxicity after Adoptive Immunotherapy with CD19 CAR-T Cells. *Cancer Discovery*.
- GUTCHER, I. & BECHER, B. 2007. APC-derived cytokines and T cell polarization in autoimmune inflammation. *The Journal of Clinical Investigation*, 117, 1119-1127.
- HACEIN-BEY-ABINA, S., VON KALLE, C., SCHMIDT, M., MCCORMACK, M. P., WULFFRAAT, N., LEBOULCH, P., LIM, A., OSBORNE, C. S., PAWLIUK, R., MORILLON, E., SORENSEN, R., FORSTER, A., FRASER, P., COHEN, J. I., DE SAINT BASILE, G., ALEXANDER, I., WINTERGERST, U., FREBOURG, T., AURIAS, A., STOPPA-LYONNET, D., ROMANA, S., RADFORD-WEISS, I., GROSS, F., VALENSI, F., DELABESSE, E., MACINTYRE, E., SIGAUX, F., SOULIER, J., LEIVA, L. E., WISSLER, M., PRINZ, C., RABBITTS, T. H., LE DEIST, F., FISCHER, A. & CAVAZZANA-CALVO, M. 2003. LMO2-associated clonal T cell proliferation in two patients after gene therapy for SCID-X1. *Science*, 302, 415-9.
- HAMANA, H., SHITAOKA, K., KISHI, H., OZAWA, T. & MURAGUCHI, A. 2016. A novel, rapid and efficient method of cloning functional antigen-specific T-cell receptors from single human and mouse T-cells. *Biochem Biophys Res Commun*, 474, 709-714.
- HAMANN, D., BAARS, P. A., REP, M. H., HOOIBRINK, B., KERKHOF-GARDE, S. R., KLEIN, M. R. & VAN LIER, R. A. 1997. Phenotypic and functional separation of memory and effector human CD8+ T cells. *J Exp Med*, 186, 1407-18.
- HAN, A., GLANVILLE, J., HANSMANN, L. & DAVIS, M. M. 2014. Linking T-cell receptor sequence to functional phenotype at the single-cell level. *Nat Biotechnol*, 32, 684-92.
- HAN, Y., LIU, C., LI, G., LI, J., LV, X., SHI, H., LIU, J., LIU, S., YAN, P., WANG, S., SUN, Y. & SUN, M. 2018. Antitumor effects and persistence of a novel HER2 CAR T cells directed to gastric cancer in preclinical models. *Am J Cancer Res*, 8, 106-119.
- HANTO, D. W., FRIZZERA, G., PURTILO, D. T., SAKAMOTO, K., SULLIVAN, J. L., SAEMUNDSEN, A. K., KLEIN, G., SIMMONS, R. L. & NAJARIAN, J. S. 1981. Clinical spectrum of lymphoproliferative disorders in renal transplant recipients and evidence for the role of Epstein-Barr virus. *Cancer Res*, 41, 4253-61.
- HAQUE, T., TAYLOR, C., WILKIE, G. M., MURAD, P., AMLLOT, P. L., BEATH, S., MCKIERNAN, P. J. & CRAWFORD, D. H. 2001. Complete regression of posttransplant lymphoproliferative disease using partially HLA-matched Epstein Barr virus-specific cytotoxic T cells. *Transplantation*, 72, 1399-402.
- HAQUE, T., WILKIE, G. M., JONES, M. M., HIGGINS, C. D., URQUHART, G., WINGATE, P., BURNS, D., MCAULAY, K., TURNER, M., BELLAMY, C., AMLLOT, P. L., KELLY, D., MACGILCHRIST, A., GANDHI, M. K., SWERDLOW, A. J. & CRAWFORD, D. H. 2007. Allogeneic cytotoxic T-cell therapy for EBV-

- positive posttransplantation lymphoproliferative disease: results of a phase 2 multicenter clinical trial. *Blood*, 110, 1123-31.
- HAQUE, T., WILKIE, G. M., TAYLOR, C., AMLOT, P. L., MURAD, P., ILEY, A., DOMBAGODA, D., BRITTON, K. M., SWERDLOW, A. J. & CRAWFORD, D. H. 2002. Treatment of Epstein-Barr-virus-positive post-transplantation lymphoproliferative disease with partly HLA-matched allogeneic cytotoxic T cells. *Lancet*, 360, 436-42.
- HARDWICK, J. M., LIEBERMAN, P. M. & HAYWARD, S. D. 1988. A new Epstein-Barr virus transactivator, R, induces expression of a cytoplasmic early antigen. *J Virol*, 62, 2274-84.
- HASSAN, C., CHABROL, E., JAHN, L., KESTER, M. G. D., DE RU, A. H., DRIJFHOUT, J. W., ROSSJOHN, J., FALKENBURG, J. H. F., HEEMSKERK, M. H. M., GRAS, S. & VAN VEELLEN, P. A. 2015. Naturally Processed Non-canonical HLA-A*02:01 Presented Peptides. *Journal of Biological Chemistry*, 290, 2593-2603.
- HEEMSKERK, M. H. M., HAGEDOORN, R. S., VAN DER HOORN, M. A. W. G., VAN DER VEKEN, L. T., HOOGEBOOM, M., KESTER, M. G. D., WILLEMZE, R. & FALKENBURG, J. H. F. 2007. Efficiency of T-cell receptor expression in dual-specific T cells is controlled by the intrinsic qualities of the TCR chains within the TCR-CD3 complex. *Blood*, 109, 235-243.
- HENDRIKS, J., GRAVESTSTEIN, L. A., TESSELAAR, K., VAN LIER, R. A., SCHUMACHER, T. N. & BORST, J. 2000. CD27 is required for generation and long-term maintenance of T cell immunity. *Nat Immunol*, 1, 433-40.
- HENNECKE, J. & WILEY, D. C. 2001. T cell receptor-MHC interactions up close. *Cell*, 104, 1-4.
- HESLOP, H. E., NG, C. Y., LI, C., SMITH, C. A., LOFTIN, S. K., KRANCE, R. A., BRENNER, M. K. & ROONEY, C. M. 1996. Long-term restoration of immunity against Epstein-Barr virus infection by adoptive transfer of gene-modified virus-specific T lymphocytes. *Nat Med*, 2, 551-5.
- HILL, A. V. S., ELVIN, J., WILLIS, A. C., AIDOO, M., ALLSOPP, C. E. M., GOTCH, F. M., MING GAO, X., TAKIGUCHI, M., GREENWOOD, B. M., TOWNSEND, A. R. M., MCMICHAEL, A. J. & WHITTLE, H. C. 1992. Molecular analysis of the association of HLA-B53 and resistance to severe malaria. *Nature*, 360, 434-439.
- HINO, R., UOZAKI, H., MURAKAMI, N., USHIKU, T., SHINOZAKI, A., ISHIKAWA, S., MORIKAWA, T., NAKAYA, T., SAKATANI, T., TAKADA, K. & FUKAYAMA, M. 2009. Activation of DNA Methyltransferase 1 by EBV Latent Membrane Protein 2A Leads to Promoter Hypermethylation of *PTEN* Gene in Gastric Carcinoma. *Cancer Research*, 69, 2766-2774.
- HIRANO, T., KISHIMOTO, T., KURITANI, T., MURAGUCHI, A., YAMAMURA, Y., RALPH, P. & GOOD, R. A. 1979. In vitro immune response of human peripheral lymphocytes. IV. Specific induction of human suppressor T cells by an antiserum to the T leukemia cell line HSB. *J Immunol*, 123, 1133-40.
- HISLOP, A. D., ANNELS, N. E., GUDGEON, N. H., LEESE, A. M. & RICKINSON, A. B. 2002. Epitope-specific evolution of human CD8(+) T cell responses from primary to persistent phases of Epstein-Barr virus infection. *The Journal of experimental medicine*, 195, 893-905.
- HISLOP, A. D., GUDGEON, N. H., CALLAN, M. F., FAZOU, C., HASEGAWA, H., SALMON, M. & RICKINSON, A. B. 2001. EBV-specific CD8+ T cell memory: relationships between epitope specificity, cell phenotype, and immediate effector function. *J Immunol*, 167, 2019-29.

- HISLOP, A. D., TAYLOR, G. S., SAUCE, D. & RICKINSON, A. B. 2007. Cellular responses to viral infection in humans: lessons from Epstein-Barr virus. *Annu Rev Immunol*, 25, 587-617.
- HOCHBERG, D., MIDDELDORP, J. M., CATALINA, M., SULLIVAN, J. L., LUZURIAGA, K. & THORLEY-LAWSON, D. A. 2004. Demonstration of the Burkitt's lymphoma Epstein-Barr virus phenotype in dividing latently infected memory cells *in vivo*. *Proceedings of the National Academy of Sciences*, 101, 239-244.
- HOWIE, B., SHERWOOD, A. M., BERKEBILE, A. D., BERKA, J., EMERSON, R. O., WILLIAMSON, D. W., KIRSCH, I., VIGNALI, M., RIEDER, M. J., CARLSON, C. S. & ROBINS, H. S. 2015. High-throughput pairing of T cell receptor alpha and beta sequences. *Sci Transl Med*, 7, 301ra131.
- HU, Z., ANANDAPPA, A. J., SUN, J., KIM, J., LEET, D. E., BOZYM, D. J., CHEN, C., WILLIAMS, L., SHUKLA, S. A., ZHANG, W., TABBAA, D., STEELMAN, S., OLIVE, O., LIVAK, K. J., KISHI, H., MURAGUCHI, A., GULERIA, I., STEVENS, J., LANE, W. J., BURKHARDT, U. E., FRITSCH, E. F., NEUBERG, D., OTT, P. A., KESKIN, D. B., HACOEN, N. & WU, C. J. 2018. A cloning and expression system to probe T-cell receptor specificity and assess functional avidity to neoantigens. *Blood*, 132, 1911-1921.
- HUGHES, M. S., YU, Y. Y. L., DUDLEY, M. E., ZHENG, Z., ROBBINS, P. F., LI, Y., WUNDERLICH, J., HAWLEY, R. G., MOAYERI, M., ROSENBERG, S. A. & MORGAN, R. A. 2005. Transfer of a TCR gene derived from a patient with a marked antitumor response conveys highly active T-cell effector functions. *Human gene therapy*, 16, 457-472.
- HUI, K. F., CHEUNG, A. K., CHOI, C. K., YEUNG, P. L., MIDDELDORP, J. M., LUNG, M. L., TSAO, S. W. & CHIANG, A. K. 2016. Inhibition of class I histone deacetylases by romidepsin potently induces Epstein-Barr virus lytic cycle and mediates enhanced cell death with ganciclovir. *Int J Cancer*, 138, 125-36.
- HUI, K. F. & CHIANG, A. K. 2010. Suberoylanilide hydroxamic acid induces viral lytic cycle in Epstein-Barr virus-positive epithelial malignancies and mediates enhanced cell death. *Int J Cancer*, 126, 2479-89.
- HUI, K. F., HO, D. N., TSANG, C. M., MIDDELDORP, J. M., TSAO, G. S. & CHIANG, A. K. 2012. Activation of lytic cycle of Epstein-Barr virus by suberoylanilide hydroxamic acid leads to apoptosis and tumor growth suppression of nasopharyngeal carcinoma. *Int J Cancer*, 131, 1930-40.
- HUNDER, N. N., WALLEN, H., CAO, J., HENDRICKS, D. W., REILLY, J. Z., RODMYRE, R., JUNGLUTH, A., GNJATIC, S., THOMPSON, J. A. & YEE, C. 2008. Treatment of Metastatic Melanoma with Autologous CD4+ T Cells against NY-ESO-1. *New England Journal of Medicine*, 358, 2698-2703.
- HUPPA, J. B. & DAVIS, M. M. 2003. T-cell-antigen recognition and the immunological synapse. *Nat Rev Immunol*, 3, 973-983.
- IIZASA, H., NANBO, A., NISHIKAWA, J., JINUSHI, M. & YOSHIYAMA, H. 2012. Epstein-Barr Virus (EBV)-associated gastric carcinoma. *Viruses*, 4, 3420-3439.
- IMAI, S., KOIZUMI, S., SUGIURA, M., TOKUNAGA, M., UEMURA, Y., YAMAMOTO, N., TANAKA, S., SATO, E. & OSATO, T. 1994. Gastric carcinoma: monoclonal epithelial malignant cells expressing Epstein-Barr virus latent infection protein. *Proc Natl Acad Sci U S A*, 91, 9131-5.
- JANEWAY, C., TRAVERS, P., WALPORT, M. & SHLOMCHIK, M. 2005. *Immunobiology: The Immune System in Health and Disease*, Garland Science.

- JANEWAY, C. A. 2001. How the immune system protects the host from infection. *Microbes and Infection*, 3, 1167-1171.
- JANSSEN, E. & ZHANG, W. G. 2003. Adaptor proteins in lymphocyte activation. *Current Opinion in Immunology*, 15, 269-276.
- JANSSEN, E. M., LEMMENS, E. E., WOLFE, T., CHRISTEN, U., VON HERRATH, M. G. & SCHOENBERGER, S. P. 2003. CD4+ T cells are required for secondary expansion and memory in CD8+ T lymphocytes. *Nature*, 421, 852-6.
- JAYASOORIYA, S., DE SILVA, T. I., NJIE-JOBE, J., SANYANG, C., LEESE, A. M., BELL, A. I., MCAULAY, K. A., YANCHUN, P., LONG, H. M., DONG, T., WHITTLE, H. C., RICKINSON, A. B., ROWLAND-JONES, S. L., HISLOP, A. D. & FLANAGAN, K. L. 2015. Early Virological and Immunological Events in Asymptomatic Epstein-Barr Virus Infection in African Children. *PLOS Pathogens*, 11, e1004746.
- JI, J., WERNLI, M., KLIMKAIT, T. & ERB, P. 2003. Enhanced gene silencing by the application of multiple specific small interfering RNAs. *FEBS Letters*, 552, 247-252.
- JIANG, T., WANG, F., HU, L., CHENG, X., ZHENG, Y., LIU, T. & JIA, Y. 2017. Chidamide and decitabine can synergistically induce apoptosis of Hodgkin lymphoma cells by up-regulating the expression of PU.1 and KLF4. *Oncotarget*, 8, 77586-77594.
- JINEK, M., CHYLINSKI, K., FONFARA, I., HAUER, M., DOUDNA, J. A. & CHARPENTIER, E. 2012. A Programmable Dual-RNA-Guided DNA Endonuclease in Adaptive Bacterial Immunity. *Science*, 337, 816.
- JOGLEKAR, A. V., LIU, Z., WEBER, J. K., OUYANG, Y., JEPPSON, J. D., NOH, W. J., LAMOTHE-MOLINA, P. A., CHEN, H., KANG, S. G., BETHUNE, M. T., ZHOU, R., WALKER, B. D. & BALTIMORE, D. 2018. T cell receptors for the HIV KK10 epitope from patients with differential immunologic control are functionally indistinguishable. *Proc Natl Acad Sci U S A*, 115, 1877-1882.
- s expressing cognate antigen. *Blood*, 114, 535-546.
- JOHNSON, L. A., MORGAN, R. A., DUDLEY, M. E., CASSARD, L., YANG, J. C., HUGHES, M. S., KAMMULA, U. S., ROYAL, R. E., SHERRY, R. M., WUNDERLICH, J. R., LEE, C. C., RESTIFO, N. P., SCHWARZ, S. L., COGDILL, A. P., BISHOP, R. J., KIM, H., BREWER, C. C., RUDY, S. F., VANWAES, C., DAVIS, J. L., MATHUR, A., RIPLEY, R. T., NATHAN, D. A., LAURENCOT, C. M. & ROSENBERG, S. A. 2009. Gene therapy with human and mouse T-cell receptors mediates cancer regression and targets normal tissues expressing cognate antigen. *Blood*, 114, 535-46.
- JONES, R. B., O'CONNOR, R., MUELLER, S., FOLEY, M., SZETO, G. L., KAREL, D., LICHTERFELD, M., KOVACS, C., OSTROWSKI, M. A., TROCHA, A., IRVINE, D. J. & WALKER, B. D. 2014. Histone Deacetylase Inhibitors Impair the Elimination of HIV-Infected Cells by Cytotoxic T-Lymphocytes. *PLOS Pathogens*, 10, e1004287.
- JUNE, C. H., O'CONNOR, R. S., KAWALEKAR, O. U., GHASSEMI, S. & MILONE, M. C. 2018. CAR T cell immunotherapy for human cancer. *Science*, 359, 1361-1365.
- JUNE, C. H., RIDDELL, S. R. & SCHUMACHER, T. N. 2015. Adoptive cellular therapy: a race to the finish line. *Sci Transl Med*, 7, 280ps7.
- KAGEYAMA, S., IKEDA, H., MIYAHARA, Y., IMAI, N., ISHIHARA, M., SAITO, K., SUGINO, S., UEDA, S., ISHIKAWA, T., KOKURA, S., NAOTA, H., OHISHI, K., SHIRAIISHI, T., INOUE, N., TANABE, M., KIDOKORO, T., YOSHIOKA, H., TOMURA, D., NUKAYA, I., MINENO, J., TAKESAKO, K., KATAYAMA, N. & SHIKU, H. 2015. Adoptive Transfer of MAGE-A4 T-cell Receptor Gene-Transduced Lymphocytes in Patients with Recurrent Esophageal Cancer. *Clin Cancer Res*, 21, 2268-77.

- KAHN, M. L., LEE, S. W. & DICHEK, D. A. 1992. Optimization of retroviral vector-mediated gene transfer into endothelial cells in vitro. *Circ Res*, 71, 1508-17.
- KALOS, M., LEVINE, B. L., PORTER, D. L., KATZ, S., GRUPP, S. A., BAGG, A. & JUNE, C. H. 2011. T Cells with Chimeric Antigen Receptors Have Potent Antitumor Effects and Can Establish Memory in Patients with Advanced Leukemia. *Science Translational Medicine*, 3, 95ra73-95ra73.
- KANG, B. W., SEO, A. N., YOON, S., BAE, H. I., JEON, S. W., KWON, O. K., CHUNG, H. Y., YU, W., KANG, H. & KIM, J. G. 2016. Prognostic value of tumor-infiltrating lymphocytes in Epstein-Barr virus-associated gastric cancer. *Ann Oncol*, 27, 494-501.
- KANG, M.-S. & KIEFF, E. 2015. Epstein-Barr virus latent genes. *Experimental & Molecular Medicine*, 47, e131-e131.
- KANG, Y. K., BOKU, N., SATOH, T., RYU, M. H., CHAO, Y., KATO, K., CHUNG, H. C., CHEN, J. S., MURO, K., KANG, W. K., YEH, K. H., YOSHIKAWA, T., OH, S. C., BAI, L. Y., TAMURA, T., LEE, K. W., HAMAMOTO, Y., KIM, J. G., CHIN, K., OH, D. Y., MINASHI, K., CHO, J. Y., TSUDA, M. & CHEN, L. T. 2017. Nivolumab in patients with advanced gastric or gastro-oesophageal junction cancer refractory to, or intolerant of, at least two previous chemotherapy regimens (ONO-4538-12, ATTRACTION-2): a randomised, double-blind, placebo-controlled, phase 3 trial. *Lancet*, 390, 2461-2471.
- KAPPLER, J., KUBO, R., HASKINS, K., HANNUM, C., MARRACK, P., PIGEON, M., MCINTYRE, B., ALLISON, J. & TROWBRIDGE, I. 1983. The major histocompatibility complex-restricted antigen receptor on T cells in mouse and man: identification of constant and variable peptides. *Cell*, 35, 295-302.
- KARIMI, M. A., LEE, E., BACHMANN, M. H., SALICIONI, A. M., BEHRENS, E. M., KAMBAYASHI, T. & BALDWIN, C. L. 2014. Measuring cytotoxicity by bioluminescence imaging outperforms the standard chromium-51 release assay. *PLoS one*, 9, e89357-e89357.
- KAWAKAMI, Y., ELIYAHU, S., DELGADO, C. H., ROBBINS, P. F., SAKAGUCHI, K., APPELLA, E., YANNELLI, J. R., ADEMA, G. J., MIKI, T. & ROSENBERG, S. A. 1994. Identification of a human melanoma antigen recognized by tumor-infiltrating lymphocytes associated with in vivo tumor rejection. *Proceedings of the National Academy of Sciences*, 91, 6458-6462.
- KAWANISHI, M. 1993. Epstein-Barr virus induces fragmentation of chromosomal DNA during lytic infection. *J Virol*, 67, 7654-8.
- KAYE, J., HSU, M. L., SAURON, M. E., JAMESON, S. C., GASCOIGNE, N. R. & HEDRICK, S. M. 1989. Selective development of CD4+ T cells in transgenic mice expressing a class II MHC-restricted antigen receptor. *Nature*, 341, 746-9.
- KEBSCHULL, J. M. & ZADOR, A. M. 2015. Sources of PCR-induced distortions in high-throughput sequencing data sets. *Nucleic Acids Res*, 43, e143.
- KENNEDY, A. & CRIBBS, A. P. 2016. Production and Concentration of Lentivirus for Transduction of Primary Human T Cells. In: FEDERICO, M. (ed.) *Lentiviral Vectors and Exosomes as Gene and Protein Delivery Tools*. New York, NY: Springer New York.
- KHAN, G. & HASHIM, M. J. 2014. Global burden of deaths from Epstein-Barr virus attributable malignancies 1990-2010. *Infect Agent Cancer*, 9, 38.
- KHANNA, R., MOSS, D. J. & BURROWS, S. R. 1999. Vaccine strategies against Epstein-Barr virus-associated diseases: lessons from studies on cytotoxic T-cell-mediated immune regulation. *Immunol Rev*, 170, 49-64.
- KIEFF, E. A. R., A.B. 2007. Epstein-Barr virus and its replication. In: Field's Virology, Lippincott Williams & Wilkins, Philadelphia. 2603-2654.

- KIM, S. M., BHONSLE, L., BESGEN, P., NICKEL, J., BACKES, A., HELD, K., VOLLMER, S., DORNMAIR, K. & PRINZ, J. C. 2012. Analysis of the paired TCR alpha- and beta-chains of single human T cells. *PLoS One*, 7, e37338.
- KIM, S. T., CRISTESCU, R., BASS, A. J., KIM, K. M., ODEGAARD, J. I., KIM, K., LIU, X. Q., SHER, X., JUNG, H., LEE, M., LEE, S., PARK, S. H., PARK, J. O., PARK, Y. S., LIM, H. Y., LEE, H., CHOI, M., TALASAZ, A., KANG, P. S., CHENG, J., LOBODA, A., LEE, J. & KANG, W. K. 2018. Comprehensive molecular characterization of clinical responses to PD-1 inhibition in metastatic gastric cancer. *Nat Med*, 24, 1449-1458.
- KITAMURA, T., KOSHINO, Y., SHIBATA, F., OKI, T., NAKAJIMA, H., NOSAKA, T. & KUMAGAI, H. 2003. Retrovirus-mediated gene transfer and expression cloning: powerful tools in functional genomics. *Experimental Hematology*, 31, 1007-1014.
- KLEBANOFF, C. A., GATTINONI, L., TORABI-PARIZI, P., KERSTANN, K., CARDONES, A. R., FINKELSTEIN, S. E., PALMER, D. C., ANTONY, P. A., HWANG, S. T., ROSENBERG, S. A., WALDMANN, T. A. & RESTIFO, N. P. 2005. Central memory self/tumor-reactive CD8+ T cells confer superior antitumor immunity compared with effector memory T cells. *Proc Natl Acad Sci U S A*, 102, 9571-6.
- KNIPPING, F., OSBORN, M. J., PETRI, K., TOLAR, J., GLIMM, H., VON KALLE, C., SCHMIDT, M. & GABRIEL, R. 2017. Genome-wide Specificity of Highly Efficient TALENs and CRISPR/Cas9 for T Cell Receptor Modification. *Molecular Therapy - Methods & Clinical Development*, 4, 213-224.
- KOBAYASHI, E., MIZUKOSHI, E., KISHI, H., OZAWA, T., HAMANA, H., NAGAI, T., NAKAGAWA, H., JIN, A., KANEKO, S. & MURAGUCHI, A. 2013. A new cloning and expression system yields and validates TCRs from blood lymphocytes of patients with cancer within 10 days. *Nat Med*, 19, 1542-6.
- KOELLE, D. M., CHEN, H. B., MCCLURKAN, C. M. & PETERSDORF, E. W. 2002. Herpes simplex virus type 2-specific CD8 cytotoxic T lymphocyte cross-reactivity against prevalent HLA class I alleles. *Blood*, 99, 3844-7.
- KOLMAN, J. L., TAYLOR, N., MARSHAK, D. R. & MILLER, G. 1993. Serine-173 of the Epstein-Barr virus ZEBRA protein is required for DNA binding and is a target for casein kinase II phosphorylation. *Proceedings of the National Academy of Sciences*, 90, 10115-10119.
- KUBALL, J., DOSSETT, M. L., WOLFL, M., HO, W. Y., VOSS, R.-H., FOWLER, C. & GREENBERG, P. D. 2007. Facilitating matched pairing and expression of TCR chains introduced into human T cells. *Blood*, 109, 2331-2338.
- KULA, T., DEZFULIAN, M. H., WANG, C. I., ABDELFATTAH, N. S., HARTMAN, Z. C., WUCHERPFENNIG, K. W., LYERLY, H. K. & ELLEDGE, S. J. 2019. T-Scan: A Genome-wide Method for the Systematic Discovery of T Cell Epitopes. *Cell*, 178, 1016-1028.e13.
- KUZUSHIMA, K., NAKAMURA, S., NAKAMURA, T., YAMAMURA, Y., YOKOYAMA, N., FUJITA, M., KIYONO, T. & TSURUMI, T. 1999. Increased frequency of antigen-specific CD8(+) cytotoxic T lymphocytes infiltrating an Epstein-Barr virus-associated gastric carcinoma. *The Journal of clinical investigation*, 104, 163-171.
- LEE, H. E., CHAE, S. W., LEE, Y. J., KIM, M. A., LEE, H. S., LEE, B. L. & KIM, W. H. 2008. Prognostic implications of type and density of tumour-infiltrating lymphocytes in gastric cancer. *Br J Cancer*, 99, 1704-11.
- LEE, H. G., KIM, H., KIM, E. J., PARK, P. G., DONG, S. M., CHOI, T. H., KIM, H., CHONG, C. R., LIU, J. O., CHEN, J., AMBINDER, R. F., HAYWARD, S. D.,

- PARK, J. H. & LEE, J. M. 2015. Targeted therapy for Epstein-Barr virus-associated gastric carcinoma using low-dose gemcitabine-induced lytic activation. *Oncotarget*, 6, 31018-29.
- LEE, S. P., CHAN, A. T., CHEUNG, S. T., THOMAS, W. A., CROOMCARTER, D., DAWSON, C. W., TSAI, C. H., LEUNG, S. F., JOHNSON, P. J. & HUANG, D. P. 2000. CTL control of EBV in nasopharyngeal carcinoma (NPC): EBV-specific CTL responses in the blood and tumors of NPC patients and the antigen-processing function of the tumor cells. *J Immunol*, 165, 573-82.
- LEFRANC, M.-P. & LEFRANC, G. 2001a. 2 - T cell receptor structural and biological properties. In: LEFRANC, M.-P. & LEFRANC, G. (eds.) *The T Cell Receptor FactsBook*. London: Academic Press.
- LEFRANC, M.-P. & LEFRANC, G. 2001b. 3 - Synthesis of the T cell receptor chains. In: LEFRANC, M.-P. & LEFRANC, G. (eds.) *The T Cell Receptor FactsBook*. London: Academic Press.
- LEGUT, M., DOLTON, G., MIAN, A. A., OTTMANN, O. G. & SEWELL, A. K. 2018. CRISPR-mediated TCR replacement generates superior anticancer transgenic T cells. *Blood*, 131, 311-322.
- LENSCHOW, D. J., WALUNAS, T. L. & BLUESTONE, J. A. 1996. CD28/B7 system of T cell costimulation. *Annual Review of Immunology*, 14, 233-258.
- LESLIE, A., PRICE, D. A., MKHIZE, P., BISHOP, K., RATHOD, A., DAY, C., CRAWFORD, H., HONEYBORNE, I., ASHER, T. E., LUZZI, G., EDWARDS, A., ROSSEAU, C. M., MULLINS, J. I., TUDOR-WILLIAMS, G., NOVELLI, V., BRANDER, C., DOUEK, D. C., KIEPIELA, P., WALKER, B. D. & GOULDER, P. J. R. 2006. Differential Selection Pressure Exerted on HIV by CTL Targeting Identical Epitopes but Restricted by Distinct HLA Alleles from the Same HLA Supertype. *The Journal of Immunology*, 177, 4699.
- LEVITSKAYA, J., CORAM, M., LEVITSKY, V., IMREH, S., STEIGERWALD-MULLEN, P. M., KLEIN, G., KURILLA, M. G. & MASUCCI, M. G. 1995. Inhibition of antigen processing by the internal repeat region of the Epstein-Barr virus nuclear antigen-1. *Nature*, 375, 685.
- LI, N., ZHAO, D., KIRSCHBAUM, M., ZHANG, C., LIN, C.-L., TODOROV, I., KANDEEL, F., FORMAN, S. & ZENG, D. 2008. HDAC inhibitor reduces cytokine storm and facilitates induction of chimerism that reverses lupus in anti-CD3 conditioning regimen. *Proceedings of the National Academy of Sciences of the United States of America*, 105, 4796-4801.
- LI, Y. & SETO, E. 2016. HDACs and HDAC Inhibitors in Cancer Development and Therapy. *Cold Spring Harbor perspectives in medicine*, 6, a026831.
- LI, Z., LIU, G., TONG, Y., ZHANG, M., XU, Y., QIN, L., WANG, Z., CHEN, X. & HE, J. 2015. Comprehensive analysis of the T-cell receptor beta chain gene in rhesus monkey by high throughput sequencing. *Sci Rep*, 5, 10092.
- LIEBERMAN, J., MANJUNATH, N. & SHANKAR, P. 2002. Avoiding the kiss of death: how HIV and other chronic viruses survive. *Curr Opin Immunol*, 14, 478-86.
- LIN, D. & MAECKER, H. T. 2018. Mass Cytometry Assays for Antigen-Specific T Cells Using CyTOF. *Methods Mol Biol*, 1678, 37-47.
- LIN, Z., SWAN, K., ZHANG, X., CAO, S., BRETT, Z., DRURY, S., STRONG, M. J., FEWELL, C., PUETTER, A., WANG, X., FERRIS, M., SULLIVAN, D. E., LI, L. & FLEMINGTON, E. K. 2016. Secreted Oral Epithelial Cell Membrane Vesicles Induce Epstein-Barr Virus Reactivation in Latently Infected B Cells. *J Virol*, 90, 3469-79.

- LINDAHL, T., ADAMS, A., BJURSELL, G., BORNKAMM, G. W., KASCHKA-DIERICH, C. & JEHN, U. 1976. Covalently closed circular duplex DNA of Epstein-Barr virus in a human lymphoid cell line. *J Mol Biol*, 102, 511-30.
- LINETTE, G. P., STADTMAUER, E. A., MAUS, M. V., RAPOPORT, A. P., LEVINE, B. L., EMERY, L., LITZKY, L., BAGG, A., CARRENO, B. M., CIMINO, P. J., BINDER-SCHOLL, G. K., SMETHURST, D. P., GERRY, A. B., PUMPHREY, N. J., BENNETT, A. D., BREWER, J. E., DUKES, J., HARPER, J., TAYTON-MARTIN, H. K., JAKOBSEN, B. K., HASSAN, N. J., KALOS, M. & JUNE, C. H. 2013. Cardiovascular toxicity and titin cross-reactivity of affinity-enhanced T cells in myeloma and melanoma. *Blood*, 122, 863-871.
- LINNEMANN, C., HEEMSKERK, B., KVISTBORG, P., KLUIN, R. J., BOLOTIN, D. A., CHEN, X., BRESSER, K., NIEUWLAND, M., SCHOTTE, R., MICHELS, S., GOMEZ-EERLAND, R., JAHN, L., HOMBRINK, P., LEGRAND, N., SHU, C. J., MAMEDOV, I. Z., VELDS, A., BLANK, C. U., HAANEN, J. B., TURCHANINOVA, M. A., KERKHOVEN, R. M., SPITS, H., HADRUP, S. R., HEEMSKERK, M. H., BLANKENSTEIN, T., CHUDAKOV, D. M., BENDLE, G. M. & SCHUMACHER, T. N. 2013. High-throughput identification of antigen-specific TCRs by TCR gene capture. *Nat Med*, 19, 1534-41.
- LIU, P. & SPECK, S. H. 2003. Synergistic autoactivation of the Epstein-Barr virus immediate-early BRLF1 promoter by Rta and Zta. *Virology*, 310, 199-206.
- LONG, H. M., CHAGOURY, O. L., LEESE, A. M., RYAN, G. B., JAMES, E., MORTON, L. T., ABBOTT, R. J. M., SABBAAH, S., KWOK, W. & RICKINSON, A. B. 2013. MHC II tetramers visualize human CD4+ T cell responses to Epstein-Barr virus infection and demonstrate atypical kinetics of the nuclear antigen EBNA1 response. *The Journal of Experimental Medicine*, 210, 933-949.
- LONG, H. M., HAIGH, T. A., GUDGEON, N. H., LEEN, A. M., TSANG, C. W., BROOKS, J., LANDAIS, E., HOUSSAINT, E., LEE, S. P., RICKINSON, A. B. & TAYLOR, G. S. 2005. CD4+ T-cell responses to Epstein-Barr virus (EBV) latent-cycle antigens and the recognition of EBV-transformed lymphoblastoid cell lines. *J Virol*, 79, 4896-907.
- LONG, H. M., LEESE, A. M., CHAGOURY, O. L., CONNERTY, S. R., QUARCOOPOME, J., QUINN, L. L., SHANNON-LOWE, C. & RICKINSON, A. B. 2011. Cytotoxic CD4+ T cell responses to EBV contrast with CD8 responses in breadth of lytic cycle antigen choice and in lytic cycle recognition. *Journal of immunology (Baltimore, Md. : 1950)*, 187, 92-101.
- LU, Y. C., YAO, X., CRYSTAL, J. S., LI, Y. F., EL-GAMIL, M., GROSS, C., DAVIS, L., DUDLEY, M. E., YANG, J. C., SAMUELS, Y., ROSENBERG, S. A. & ROBBINS, P. F. 2014. Efficient identification of mutated cancer antigens recognized by T cells associated with durable tumor regressions. *Clin Cancer Res*, 20, 3401-10.
- MA, C. K., BLYTH, E., CLANCY, L., SIMMS, R., BURGESS, J., BROWN, R., DEO, S., MICKLETHWAITE, K. P. & GOTTLIEB, D. J. 2015. Addition of varicella zoster virus-specific T cells to cytomegalovirus, Epstein-Barr virus and adenovirus tri-specific T cells as adoptive immunotherapy in patients undergoing allogeneic hematopoietic stem cell transplantation. *Cytotherapy*, 17, 1406-20.
- MACEDO, C., WEBBER, S. A., DONNENBERG, A. D., POPESCU, I., HUA, Y., GREEN, M., ROWE, D., SMITH, L., BROOKS, M. M. & METES, D. 2011. EBV-Specific CD8⁺ T Cells from Asymptomatic Pediatric Thoracic Transplant Patients Carrying Chronic High EBV Loads Display Contrasting Features: Activated Phenotype and Exhausted Function. *The Journal of Immunology*, 186, 5854-5862.
- MAINI, M. K., GUDGEON, N., WEDDERBURN, L. R., RICKINSON, A. B. & BEVERLEY, P. C. L. 2000. Clonal Expansions in Acute EBV Infection Are

- Detectable in the CD8 and not the CD4 Subset and Persist with a Variable CD45 Phenotype. *The Journal of Immunology*, 165, 5729-5737.
- MAMCARZ, E., ZHOU, S., LOCKEY, T., ABDELSAMED, H., CROSS, S. J., KANG, G., MA, Z., CONDORI, J., DOWDY, J., TRIPLETT, B., LI, C., MARON, G., ALDAVE BECERRA, J. C., CHURCH, J. A., DOKMECI, E., LOVE, J. T., DA MATTA AIN, A. C., VAN DER WATT, H., TANG, X., JANSSEN, W., RYU, B. Y., DE RAVIN, S. S., WEISS, M. J., YOUNGBLOOD, B., LONG-BOYLE, J. R., GOTTSCHALK, S., MEAGHER, M. M., MALECH, H. L., PUCK, J. M., COWAN, M. J. & SORRENTINO, B. P. 2019. Lentiviral Gene Therapy Combined with Low-Dose Busulfan in Infants with SCID-X1. *New England Journal of Medicine*, 380, 1525-1534.
- MATSUMURA, M., FREMONT, D., PETERSON, P. & WILSON, I. 1992. Emerging principles for the recognition of peptide antigens by MHC class I molecules. *Science*, 257, 927-934.
- MATSUSAKA, K., KANEDA, A., NAGAE, G., USHIKU, T., KIKUCHI, Y., HINO, R., UOZAKI, H., SETO, Y., TAKADA, K., ABURATANI, H. & FUKAYAMA, M. 2011. Classification of Epstein–Barr Virus–Positive Gastric Cancers by Definition of DNA Methylation Epigenotypes. *Cancer Research*, 71, 7187-7197.
- MAUDE, S. L., FREY, N., SHAW, P. A., APLENC, R., BARRETT, D. M., BUNIN, N. J., CHEW, A., GONZALEZ, V. E., ZHENG, Z., LACEY, S. F., MAHNKE, Y. D., MELENHORST, J. J., RHEINGOLD, S. R., SHEN, A., TEACHEY, D. T., LEVINE, B. L., JUNE, C. H., PORTER, D. L. & GRUPP, S. A. 2014. Chimeric antigen receptor T cells for sustained remissions in leukemia. *N Engl J Med*, 371, 1507-17.
- MECKIFF, B. J., LADELL, K., MCLAREN, J. E., RYAN, G. B., LEESE, A. M., JAMES, E. A., PRICE, D. A. & LONG, H. M. 2019. Primary EBV Infection Induces an Acute Wave of Activated Antigen-Specific Cytotoxic CD4⁺ T Cells. *The Journal of Immunology*, 203, 1276-1287.
- MILES, J. J., DOUEK, D. C. & PRICE, D. A. 2011. Bias in the $\alpha\beta$ T-cell repertoire: implications for disease pathogenesis and vaccination. *Immunology & Cell Biology*, 89, 375-387.
- MILES, J. J., ELHASSEN, D., BORG, N. A., SILINS, S. L., TYNAN, F. E., BURROWS, J. M., PURCELL, A. W., KJER-NIELSEN, L., ROSSJOHN, J., BURROWS, S. R. & MCCLUSKEY, J. 2005. CTL recognition of a bulged viral peptide involves biased TCR selection. *J Immunol*, 175, 3826-34.
- MILLER, G. 1990. The Switch between Latency and Replication of Epstein-Barr Virus. *The Journal of Infectious Diseases*, 161, 833-844.
- MOORE, K. W., VIEIRA, P., FIORENTINO, D. F., TROUNSTINE, M. L., KHAN, T. A. & MOSMANN, T. R. 1990. Homology of cytokine synthesis inhibitory factor (IL-10) to the Epstein-Barr virus gene BCRF1. *Science*, 248, 1230-1234.
- MOOSMANN, A., BIGALKE, I., TISCHER, J., SCHIRRMANN, L., KASTEN, J., TIPPMER, S., LEEPING, M., PREVALSEK, D., JAEGER, G., LEDDEROSE, G., MAUTNER, J., HAMMERSCHMIDT, W., SCHENDEL, D. J. & KOLB, H. J. 2010. Effective and long-term control of EBV PTLD after transfer of peptide-selected T cells. *Blood*, 115, 2960-70.
- MORGAN, R. A., CHINNASAMY, N., ABATE-DAGA, D., GROS, A., ROBBINS, P. F., ZHENG, Z., DUDLEY, M. E., FELDMAN, S. A., YANG, J. C., SHERRY, R. M., PHAN, G. Q., HUGHES, M. S., KAMMULA, U. S., MILLER, A. D., HESSMAN, C. J., STEWART, A. A., RESTIFO, N. P., QUEZADO, M. M., ALIMCHANDANI, M., ROSENBERG, A. Z., NATH, A., WANG, T., BIELEKOVA, B., WUEST, S. C., AKULA, N., MCMAHON, F. J., WILDE, S., MOSETTER, B., SCHENDEL, D. J.,

- LAURENCOT, C. M. & ROSENBERG, S. A. 2013. Cancer regression and neurological toxicity following anti-MAGE-A3 TCR gene therapy. *Journal of immunotherapy (Hagerstown, Md. : 1997)*, 36, 133-151.
- MORGAN, R. A., DUDLEY, M. E., WUNDERLICH, J. R., HUGHES, M. S., YANG, J. C., SHERRY, R. M., ROYAL, R. E., TOPALIAN, S. L., KAMMULA, U. S. & RESTIFO, N. P. 2006. Cancer regression in patients after transfer of genetically engineered lymphocytes. *Science*, 314, 126-129.
- MORGAN, R. A., YANG, J. C., KITANO, M., DUDLEY, M. E., LAURENCOT, C. M. & ROSENBERG, S. A. 2010. Case report of a serious adverse event following the administration of T cells transduced with a chimeric antigen receptor recognizing ERBB2. *Molecular Therapy*, 18, 843-851.
- MORRISON, T. E., MAUSER, A., KLINGELHUTZ, A. & KENNEY, S. C. 2004. Epstein-Barr virus immediate-early protein BZLF1 inhibits tumor necrosis factor alpha-induced signaling and apoptosis by downregulating tumor necrosis factor receptor 1. *Journal of virology*, 78, 544-549.
- MORRISON, T. E., MAUSER, A., WONG, A., TING, J. P.-Y. & KENNEY, S. C. 2001. Inhibition of IFN- γ signaling by an Epstein-Barr virus immediate-early protein. *Immunity*, 15, 787-799.
- MUNSON, D. J., EGELSTON, C. A., CHIOTTI, K. E., PARRA, Z. E., BRUNO, T. C., MOORE, B. L., NAKANO, T. A., SIMONS, D. L., JIMENEZ, G., YIM, J. H., ROZANOV, D. V., FALTA, M. T., FONTENOT, A. P., REYNOLDS, P. R., LEACH, S. M., BORGES, V. F., KAPPLER, J. W., SPELLMAN, P. T., LEE, P. P. & SLANSKY, J. E. 2016. Identification of shared TCR sequences from T cells in human breast cancer using emulsion RT-PCR. *Proc Natl Acad Sci U S A*, 113, 8272-7.
- MÜNZ, C. 2019. Latency and lytic replication in Epstein-Barr virus-associated oncogenesis. *Nature Reviews Microbiology*, 17, 691-700.
- MÜNZ, C., BICKHAM, K. L., SUBKLEWE, M., TSANG, M. L., CHAHROUDI, A., KURILLA, M. G., ZHANG, D., O'DONNELL, M. & STEINMAN, R. M. 2000. Human Cd4⁺ T Lymphocytes Consistently Respond to the Latent Epstein-Barr Virus Nuclear Antigen Ebnal. *The Journal of Experimental Medicine*, 191, 1649-1660.
- MURO, K., CHUNG, H. C., SHANKARAN, V., GEVA, R., CATENACCI, D., GUPTA, S., EDER, J. P., GOLAN, T., LE, D. T., BURTNESSE, B., MCREE, A. J., LIN, C. C., PATHIRAJA, K., LUNCEFORD, J., EMANCIPATOR, K., JUCO, J., KOSHIJI, M. & BANG, Y. J. 2016. Pembrolizumab for patients with PD-L1-positive advanced gastric cancer (KEYNOTE-012): a multicentre, open-label, phase 1b trial. *Lancet Oncol*, 17, 717-726.
- MURRAY, R., KURILLA, M., BROOKS, J., THOMAS, W., ROWE, M., KIEFF, E. & RICKINSON, A. 1992. Identification of target antigens for the human cytotoxic T cell response to Epstein-Barr virus (EBV): implications for the immune control of EBV-positive malignancies. *Journal of Experimental Medicine*, 176, 157-168.
- NAKAYAMADA, S., TAKAHASHI, H., KANNO, Y. & O'SHEA, J. J. 2012. Helper T cell diversity and plasticity. *Current opinion in immunology*, 24, 297-302.
- NASEEM, M., BARZI, A., BREZDEN-MASLEY, C., PUCCINI, A., BERGER, M. D., TOKUNAGA, R., BATTAGLIN, F., SONI, S., MCSKANE, M., ZHANG, W. & LENZ, H.-J. 2018. Outlooks on Epstein-Barr virus associated gastric cancer. *Cancer treatment reviews*, 66, 15-22.
- NEMEROW, G. R., MOLD, C., SCHWEND, V. K., TOLLEFSON, V. & COOPER, N. R. 1987. Identification of gp350 as the viral glycoprotein mediating attachment of

- Epstein-Barr virus (EBV) to the EBV/C3d receptor of B cells: sequence homology of gp350 and C3 complement fragment C3d. *Journal of Virology*, 61, 1416.
- NEPARIDZE, N. & LACY, J. 2014. Malignancies associated with Epstein-Barr virus: pathobiology, clinical features, and evolving treatments. *Clin Adv Hematol Oncol*, 12, 358-71.
- NGUYEN, T. H., ROWNTREE, L. C., PELLICCI, D. G., BIRD, N. L., HANDEL, A., KJER-NIELSEN, L., KEDZIERSKA, K., KOTSIMBOS, T. C. & MIFSUD, N. A. 2014. Recognition of distinct cross-reactive virus-specific CD8⁺ T cells reveals a unique TCR signature in a clinical setting. *J Immunol*, 192, 5039-49.
- NING, R. J., XU, X. Q., CHAN, K. H. & CHIANG, A. K. 2011. Long-term carriers generate Epstein-Barr virus (EBV)-specific CD4⁺ and CD8⁺ polyfunctional T-cell responses which show immunodominance hierarchies of EBV proteins. *Immunology*, 134, 161-171.
- NING, Z.-Q., LI, Z.-B., NEWMAN, M. J., SHAN, S., WANG, X.-H., PAN, D.-S., ZHANG, J., DONG, M., DU, X. & LU, X.-P. 2012. Chidamide (CS055/HBI-8000): a new histone deacetylase inhibitor of the benzamide class with antitumor activity and the ability to enhance immune cell-mediated tumor cell cytotoxicity. *Cancer Chemotherapy and Pharmacology*, 69, 901-909.
- NISHIKAWA, J., IIZASA, H., YOSHIYAMA, H., SHIMOKURI, K., KOBAYASHI, Y., SASAKI, S., NAKAMURA, M., YANAI, H., SAKAI, K., SUEHIRO, Y., YAMASAKI, T. & SAKAIDA, I. 2018. Clinical Importance of Epstein-Barr Virus-Associated Gastric Cancer. *Cancers*, 10, 167.
- OCHI, T., FUJIWARA, H., OKAMOTO, S., AN, J., NAGAI, K., SHIRAKATA, T., MINENO, J., KUZUSHIMA, K., SHIKU, H. & YASUKAWA, M. 2011. Novel adoptive T-cell immunotherapy using a WT1-specific TCR vector encoding silencers for endogenous TCRs shows marked antileukemia reactivity and safety. *Blood*, 118, 1495-503.
- ORDITURA, M., GALIZIA, G., SFORZA, V., GAMBARDELLA, V., FABOZZI, A., LATERZA, M. M., ANDREOZZI, F., VENTRIGLIA, J., SAVASTANO, B., MABILIA, A., LIETO, E., CIARDIELLO, F. & DE VITA, F. 2014. Treatment of gastric cancer. *World journal of gastroenterology*, 20, 1635-1649.
- ORENTAS, R. J., ROSKOPF, S. J., NOLAN, G. P. & NISHIMURA, M. I. 2001. Retroviral transduction of a T cell receptor specific for an Epstein-Barr virus-encoded peptide. *Clin Immunol*, 98, 220-8.
- PADOVAN, E., CASORATI, G., DELLABONA, P., MEYER, S., BROCKHAUS, M. & LANZAVECCHIA, A. 1993. Expression of two T cell receptor alpha chains: dual receptor T cells. *Science*, 262, 422-4.
- PALENDIRA, U. & RICKINSON, A. B. 2015. Primary immunodeficiencies and the control of Epstein-Barr virus infection. *Ann N Y Acad Sci*, 1356, 22-44.
- PARENTE-PEREIRA, A. C., WILKIE, S., VAN DER STEGEN, S. J. C., DAVIES, D. M. & MAHER, J. 2014. Use of retroviral-mediated gene transfer to deliver and test function of chimeric antigen receptors in human T-cells. 2014.
- PARK, J. H., RIVIERE, I., GONEN, M., WANG, X., SENECHAL, B., CURRAN, K. J., SAUTER, C., WANG, Y., SANTOMASSO, B., MEAD, E., ROSHAL, M., MASLAK, P., DAVILA, M., BRENTJENS, R. J. & SADELAIN, M. 2018. Long-Term Follow-up of CD19 CAR Therapy in Acute Lymphoblastic Leukemia. *N Engl J Med*, 378, 449-459.
- PARKER, K. C., BEDNAREK, M. A., HULL, L. K., UTZ, U., CUNNINGHAM, B., ZWEERINK, H. J., BIDDISON, W. E. & COLIGAN, J. E. 1992. Sequence motifs

- important for peptide binding to the human MHC class I molecule, HLA-A2. *J Immunol*, 149, 3580-7.
- PARKHURST, M. R., YANG, J. C., LANGAN, R. C., DUDLEY, M. E., NATHAN, D. A., FELDMAN, S. A., DAVIS, J. L., MORGAN, R. A., MERINO, M. J., SHERRY, R. M., HUGHES, M. S., KAMMULA, U. S., PHAN, G. Q., LIM, R. M., WANK, S. A., RESTIFO, N. P., ROBBINS, P. F., LAURENCOT, C. M. & ROSENBERG, S. A. 2011. T cells targeting carcinoembryonic antigen can mediate regression of metastatic colorectal cancer but induce severe transient colitis. *Mol Ther*, 19, 620-6.
- PARKIN, J. & COHEN, B. 2001. An overview of the immune system. *Lancet*, 357, 1777-1789.
- PAROLINI, S., BOTTINO, C., FALCO, M., AUGUGLIARO, R., GILIANI, S., FRANCESCHINI, R., OCHS, H. D., WOLF, H., BONNEFOY, J. Y., BIASSONI, R., MORETTA, L., NOTARANGELO, L. D. & MORETTA, A. 2000. X-linked lymphoproliferative disease. 2B4 molecules displaying inhibitory rather than activating function are responsible for the inability of natural killer cells to kill Epstein-Barr virus-infected cells. *J Exp Med*, 192, 337-46.
- PARTRIDGE, T., NICASTRI, A., KLISZCZAK, A. E., YINDOM, L.-M., KESSLER, B. M., TERNETTE, N. & BORROW, P. 2018. Discrimination Between Human Leukocyte Antigen Class I-Bound and Co-Purified HIV-Derived Peptides in Immunopeptidomics Workflows. *Frontiers in Immunology*, 9.
- PELLETIER, J. & SONENBERG, N. 1988. Internal initiation of translation of eukaryotic mRNA directed by a sequence derived from poliovirus RNA. *Nature*, 334, 320-325.
- PENDER, M. P., CSURHES, P. A., BURROWS, J. M. & BURROWS, S. R. 2017. Defective T-cell control of Epstein-Barr virus infection in multiple sclerosis. *Clinical & translational immunology*, 6, e126-e126.
- PENG, P. D., COHEN, C. J., YANG, S., HSU, C., JONES, S., ZHAO, Y., ZHENG, Z., ROSENBERG, S. A. & MORGAN, R. A. 2009. Efficient nonviral Sleeping Beauty transposon-based TCR gene transfer to peripheral blood lymphocytes confers antigen-specific antitumor reactivity. *Gene Ther*, 16, 1042-9.
- PING, Y., LIU, C. & ZHANG, Y. 2018. T-cell receptor-engineered T cells for cancer treatment: current status and future directions. *Protein & Cell*, 9, 254-266.
- POPE, J., HORNE, M. & SCOTT, W. 1968. Transformation of foetal human leukocytes in vitro by filtrates of a human leukaemic cell line containing herpes-like virus. *International journal of cancer*, 3, 857-866.
- PORTER, D. L., HWANG, W. T., FREY, N. V., LACEY, S. F., SHAW, P. A., LOREN, A. W., BAGG, A., MARCUCCI, K. T., SHEN, A., GONZALEZ, V., AMBROSE, D., GRUPP, S. A., CHEW, A., ZHENG, Z., MILONE, M. C., LEVINE, B. L., MELENHORST, J. J. & JUNE, C. H. 2015. Chimeric antigen receptor T cells persist and induce sustained remissions in relapsed refractory chronic lymphocytic leukemia. *Sci Transl Med*, 7, 303ra139.
- POTAPOV, V. & ONG, J. L. 2017. Examining Sources of Error in PCR by Single-Molecule Sequencing. *PLOS ONE*, 12, e0169774.
- PRECOPIO, M. L., SULLIVAN, J. L., WILLARD, C., SOMASUNDARAN, M. & LUZURIAGA, K. 2003. Differential kinetics and specificity of EBV-specific CD4+ and CD8+ T cells during primary infection. *J Immunol*, 170, 2590-8.
- PROVASI, E., GENOVESE, P., LOMBARDO, A., MAGNANI, Z., LIU, P. Q., REIK, A., CHU, V., PASCHON, D. E., ZHANG, L., KUBALL, J., CAMISA, B., BONDANZA, A., CASORATI, G., PONZONI, M., CICERI, F., BORDIGNON, C., GREENBERG, P. D., HOLMES, M. C., GREGORY, P. D., NALDINI, L. & BONINI, C. 2012.

- Editing T cell specificity towards leukemia by zinc finger nucleases and lentiviral gene transfer. *Nat Med*, 18, 807-815.
- PUDNEY, V. A., LEESE, A. M., RICKINSON, A. B. & HISLOP, A. D. 2005. CD8+ immunodominance among Epstein-Barr virus lytic cycle antigens directly reflects the efficiency of antigen presentation in lytically infected cells. *J Exp Med*, 201, 349-60.
- QUAN, L., CHEN, X., LIU, A., ZHANG, Y., GUO, X., YAN, S. & LIU, Y. 2015. PD-1 Blockade Can Restore Functions of T-Cells in Epstein-Barr Virus-Positive Diffuse Large B-Cell Lymphoma In Vitro. *PLoS One*, 10, e0136476.
- QUINN, L. L., ZUO, J., ABBOTT, R. J., SHANNON-LOWE, C., TIERNEY, R. J., HISLOP, A. D. & ROWE, M. 2014. Cooperation between Epstein-Barr virus immune evasion proteins spreads protection from CD8+ T cell recognition across all three phases of the lytic cycle. *PLoS Pathog*, 10, e1004322.
- RAMSDEN, D. A., BAETZ, K. & WU, G. E. 1994. Conservation of sequence in recombination signal sequence spacers. *Nucleic acids research*, 22, 1785-1796.
- RAN, F. A., HSU, P. D., LIN, C. Y., GOOTENBERG, J. S., KONERMANN, S., TREVINO, A. E., SCOTT, D. A., INOUE, A., MATOBA, S., ZHANG, Y. & ZHANG, F. 2013. Double nicking by RNA-guided CRISPR Cas9 for enhanced genome editing specificity. *Cell*, 154, 1380-9.
- RAO, D. D., VORHIES, J. S., SENZER, N. & NEMUNAITIS, J. 2009. siRNA vs. shRNA: Similarities and differences. *Advanced Drug Delivery Reviews*, 61, 746-759.
- RAPOPORT, A. P., STADTMAUER, E. A., BINDER-SCHOLL, G. K., GOLOUBEVA, O., VOGL, D. T., LACEY, S. F., BADROS, A. Z., GARFALL, A., WEISS, B. & FINKLESTEIN, J. 2015. NY-ESO-1-specific TCR-engineered T cells mediate sustained antigen-specific antitumor effects in myeloma. *Nature medicine*, 21, 914.
- RASMUSSEN, M., HARND AHL, M., STRYHN, A., BOUCHERMA, R., NIELSEN, L. L., LEMONNIER, F. A., NIELSEN, M. & BUUS, S. 2014. Uncovering the peptide-binding specificities of HLA-C: a general strategy to determine the specificity of any MHC class I molecule. *J Immunol*, 193, 4790-802.
- REDMOND, D., PORAN, A. & ELEMENTO, O. 2016. Single-cell TCRseq: paired recovery of entire T-cell alpha and beta chain transcripts in T-cell receptors from single-cell RNAseq. *Genome medicine*, 8, 80-80.
- RENAUD-GABARDOS, E., HANTELYS, F., MORFOISSE, F., CHAUFOR, X., GARMY-SUSINI, B. & PRATS, A.-C. 2015. Internal ribosome entry site-based vectors for combined gene therapy. *World journal of experimental medicine*, 5, 11-20.
- RIBAS, A. & WOLCHOK, J. D. 2018. Cancer immunotherapy using checkpoint blockade. *Science*, 359, 1350-1355.
- RICHMAN, S. A., NUNEZ-CRUZ, S., MOGHIMI, B., LI, L. Z., GERSHENSON, Z. T., MOURELATOS, Z., BARRETT, D. M., GRUPP, S. A. & MILONE, M. C. 2018. High-affinity GD2-specific CAR T cells induce fatal encephalitis in a preclinical neuroblastoma model. *Cancer immunology research*, 6, 36-46.
- RICHON, V. M. 2006. Cancer biology: mechanism of antitumour action of vorinostat (suberoylanilide hydroxamic acid), a novel histone deacetylase inhibitor. *British Journal of Cancer*, 95, S2-S6.
- RICKINSON, A. & KIEFF, E. 2007. Fields virology 4th ed. Lippincott Williams & Wilkins, Philadelphia.
- RIDDELL, S. R., WATANABE, K. S., GOODRICH, J. M., LI, C. R., AGHA, M. E. & GREENBERG, P. D. 1992. Restoration of viral immunity in immunodeficient humans by the adoptive transfer of T cell clones. *Science*, 257, 238-41.
- RIST, M. J., HIBBERT, K. M., CROFT, N. P., SMITH, C., NELLER, M. A., BURROWS, J. M., MILES, J. J., PURCELL, A. W., ROSSJOHN, J., GRAS, S. & BURROWS, S. R.

- 2015a. T Cell Cross-Reactivity between a Highly Immunogenic EBV Epitope and a Self-Peptide Naturally Presented by HLA-B*18:01<sup>+</sup> Cells. *The Journal of Immunology*, 194, 4668.
- RIST, M. J., NELLER, M. A., BURROWS, J. M. & BURROWS, S. R. 2015b. T cell epitope clustering in the highly immunogenic BZLF1 antigen of Epstein-Barr virus. *J Virol*, 89, 703-12.
- RIST, M. J., THEODOSSIS, A., CROFT, N. P., NELLER, M. A., WELLAND, A., CHEN, Z., SULLIVAN, L. C., BURROWS, J. M., MILES, J. J., BRENNAN, R. M., GRAS, S., KHANNA, R., BROOKS, A. G., MCCLUSKEY, J., PURCELL, A. W., ROSSJOHN, J. & BURROWS, S. R. 2013. HLA Peptide Length Preferences Control CD8⁺ T Cell Responses. *The Journal of Immunology*, 191, 561-571.
- ROBBINS, P. D., TAHARA, H. & GHIVIZZANI, S. C. 1998. Viral vectors for gene therapy. *Trends in Biotechnology*, 16, 35-40.
- ROBBINS, P. F., KASSIM, S. H., TRAN, T. L., CRYSTAL, J. S., MORGAN, R. A., FELDMAN, S. A., YANG, J. C., DUDLEY, M. E., WUNDERLICH, J. R., SHERRY, R. M., KAMMULA, U. S., HUGHES, M. S., RESTIFO, N. P., RAFFELD, M., LEE, C. C., LI, Y. F., EL-GAMIL, M. & ROSENBERG, S. A. 2015. A pilot trial using lymphocytes genetically engineered with an NY-ESO-1-reactive T-cell receptor: long-term follow-up and correlates with response. *Clin Cancer Res*, 21, 1019-27.
- ROBBINS, P. F., MORGAN, R. A., FELDMAN, S. A., YANG, J. C., SHERRY, R. M., DUDLEY, M. E., WUNDERLICH, J. R., NAHVI, A. V., HELMAN, L. J., MACKALL, C. L., KAMMULA, U. S., HUGHES, M. S., RESTIFO, N. P., RAFFELD, M., LEE, C.-C. R., LEVY, C. L., LI, Y. F., EL-GAMIL, M., SCHWARZ, S. L., LAURENCOT, C. & ROSENBERG, S. A. 2011. Tumor regression in patients with metastatic synovial cell sarcoma and melanoma using genetically engineered lymphocytes reactive with NY-ESO-1. *Journal of clinical oncology : official journal of the American Society of Clinical Oncology*, 29, 917-924.
- ROONEY, C. M., ROWE, D. T., RAGOT, T. & FARRELL, P. J. 1989. The spliced BZLF1 gene of Epstein-Barr virus (EBV) transactivates an early EBV promoter and induces the virus productive cycle. *J Virol*, 63, 3109-16.
- ROONEY, C. M., SMITH, C. A., NG, C. Y., LOFTIN, S., LI, C., KRANCE, R. A., BRENNER, M. K. & HESLOP, H. E. 1995. Use of gene-modified virus-specific T lymphocytes to control Epstein-Barr-virus-related lymphoproliferation. *Lancet*, 345, 9-13.
- ROSENBERG, S. A., PACKARD, B. S., AEBERSOLD, P. M., SOLOMON, D., TOPALIAN, S. L., TOY, S. T., SIMON, P., LOTZE, M. T., YANG, J. C. & SEIPP, C. A. 1988. Use of tumor-infiltrating lymphocytes and interleukin-2 in the immunotherapy of patients with metastatic melanoma. *New England Journal of Medicine*, 319, 1676-1680.
- ROSENBERG, S. A., YANNELLI, J. R., YANG, J. C., TOPALIAN, S. L., SCHWARTZENTRUBER, D. J., WEBER, J. S., PARKINSON, D. R., SEIPP, C. A., EINHORN, J. H. & WHITE, D. E. 1994. Treatment of patients with metastatic melanoma with autologous tumor-infiltrating lymphocytes and interleukin 2. *J Natl Cancer Inst*, 86, 1159-66.
- ROTH, D. B. 2014. V(D)J Recombination: Mechanism, Errors, and Fidelity. *Microbiol Spectr*, 2.
- ROWE, D. T., ROWE, M., EVAN, G. I., WALLACE, L., FARRELL, P. J. & RICKINSON, A. B. 1986. Restricted expression of EBV latent genes and T-lymphocyte-detected membrane antigen in Burkitt's lymphoma cells. *The EMBO journal*, 5, 2599-2607.

- ROWEN, L., KOOP, B. F. & HOOD, L. 1996. The Complete 685-Kilobase DNA Sequence of the Human β T Cell Receptor Locus. *Science*, 272, 1755-1762.
- RUDOLPH, M. G., STANFIELD, R. L. & WILSON, I. A. 2006. How TCRs bind MHCs, peptides, and coreceptors. *Annu Rev Immunol*, 24, 419-66.
- RUSSELL, J. H. & LEY, T. J. 2002. Lymphocyte-mediated cytotoxicity. *Annual Review of Immunology*, 20, 323-370.
- RYAN, M. D., KING, A. M. & THOMAS, G. P. 1991. Cleavage of foot-and-mouth disease virus polyprotein is mediated by residues located within a 19 amino acid sequence. *J Gen Virol*, 72 (Pt 11), 2727-32.
- SADELAIN, M., RIVIÈRE, I. & RIDDELL, S. 2017. Therapeutic T cell engineering. *Nature*, 545, 423-431.
- SAIKI, Y., OHTANI, H., NAITO, Y., MIYAZAWA, M. & NAGURA, H. 1996. Immunophenotypic characterization of Epstein-Barr virus-associated gastric carcinoma: massive infiltration by proliferating CD8⁺ T-lymphocytes. *Lab Invest*, 75, 67-76.
- SALLUSTO, F., GEGINAT, J. & LANZAVECCHIA, A. 2004. Central memory and effector memory T cell subsets: function, generation, and maintenance. *Annu Rev Immunol*, 22, 745-63.
- SASAKI, S., NISHIKAWA, J., SAKAI, K., IIZASA, H., YOSHIYAMA, H., YANAGIHARA, M., SHUTO, T., SHIMOKURI, K., KANDA, T., SUEHIRO, Y., YAMASAKI, T. & SAKAIDA, I. 2019. EBV-associated gastric cancer evades T-cell immunity by PD-1/PD-L1 interactions. *Gastric Cancer*, 22, 486-496.
- SCHOLTEN, K. B., KRAMER, D., KUETER, E. W., GRAF, M., SCHOEDL, T., MEIJER, C. J., SCHREURS, M. W. & HOOIJBERG, E. 2006. Codon modification of T cell receptors allows enhanced functional expression in transgenic human T cells. *Clinical Immunology*, 119, 135-145.
- SCHONBACH, C., MIWA, K., IBE, M., SHIGA, H., NOKIHARA, K. & TAKIGUCHI, M. 1996. Refined peptide HLA-B*3501 binding motif reveals differences in 9-mer to 11-mer peptide binding. *Immunogenetics*, 45, 121-9.
- SEBZDA, E., MARIATHASAN, S., OHTEKI, T., JONES, R., BACHMANN, M. F. & OHASHI, P. S. 1999. Selection of the T cell repertoire. *Annu Rev Immunol*, 17, 829-74.
- SHI, Y., DONG, M., HONG, X., ZHANG, W., FENG, J., ZHU, J., YU, L., KE, X., HUANG, H., SHEN, Z., FAN, Y., LI, W., ZHAO, X., QI, J., HUANG, H., ZHOU, D., NING, Z. & LU, X. 2015. Results from a multicenter, open-label, pivotal phase II study of chidamide in relapsed or refractory peripheral T-cell lymphoma. *Annals of Oncology*, 26, 1766-1771.
- SHIBATA, D. & WEISS, L. M. 1992. Epstein-Barr virus-associated gastric adenocarcinoma. *Am J Pathol*, 140, 769-74.
- SHIN, H. J., KIM, D. N. & LEE, S. K. 2011. Association between Epstein-Barr virus infection and chemoresistance to docetaxel in gastric carcinoma. *Mol Cells*, 32, 173-9.
- SHINKAI, Y., RATHBUN, G., LAM, K. P., OLTZ, E. M., STEWART, V., MENDELSON, M., CHARRON, J., DATTA, M., YOUNG, F., STALL, A. M. & ALT, F. W. 1992. RAG-2-DEFICIENT MICE LACK MATURE LYMPHOCYTES OWING TO INABILITY TO INITIATE V(D)J REARRANGEMENT. *Cell*, 68, 855-867.
- SHINOZAKI-USHIKU, A., KUNITA, A. & FUKAYAMA, M. 2015. Update on Epstein-Barr virus and gastric cancer (review). *Int J Oncol*, 46, 1421-34.
- SHITAOKA, K., HAMANA, H., KISHI, H., HAYAKAWA, Y., KOBAYASHI, E., SUKEGAWA, K., PIAO, X., LYU, F., NAGATA, T., SUGIYAMA, D.,

- NISHIKAWA, H., TANEMURA, A., KATAYAMA, I., MURAHASHI, M., TAKAMATSU, Y., TANI, K., OZAWA, T. & MURAGUCHI, A. 2018. Identification of Tumoricidal TCRs from Tumor-Infiltrating Lymphocytes by Single-Cell Analysis. *Cancer Immunol Res*, 6, 378-388.
- SILINS, S. L., SHERRITT, M. A., SILLERI, J. M., CROSS, S. M., ELLIOTT, S. L., BHARADWAJ, M., LE, T. T., MORRISON, L. E., KHANNA, R. & MOSS, D. J. 2001. Asymptomatic primary Epstein-Barr virus infection occurs in the absence of blood T-cell repertoire perturbations despite high levels of systemic viral load. *Blood*, 98, 3739-3744.
- SIMON, P., OMOKOKO, T. A., BREITKREUZ, A., HEBICH, L., KREITER, S., ATTIG, S., KONUR, A., BRITTEN, C. M., PARET, C., DHAENE, K., TURECI, O. & SAHIN, U. 2014. Functional TCR retrieval from single antigen-specific human T cells reveals multiple novel epitopes. *Cancer Immunol Res*, 2, 1230-44.
- SINCLAIR, A. J., BRIMMELL, M., SHANAHAN, F. & FARRELL, P. J. 1991. Pathways of activation of the Epstein-Barr virus productive cycle. *Journal of Virology*, 65, 2237-2244.
- SINGH, S. & JHA, H. C. 2017. Status of Epstein-Barr Virus Coinfection with Helicobacter pylori in Gastric Cancer. *J Oncol*, 2017, 3456264.
- SINN, P. L., SAUTER, S. L. & MCCRAY, P. B. 2005. Gene Therapy Progress and Prospects: Development of improved lentiviral and retroviral vectors – design, biosafety, and production. *Gene Therapy*, 12, 1089-1098.
- SIXBEY, J. W., LEMON, S. M. & PAGANO, J. S. 1986. A second site for Epstein-Barr virus shedding: the uterine cervix. *Lancet*, 2, 1122-4.
- SIXBEY, J. W., NEDRUD, J. G., RAAB-TRAUB, N., HANES, R. A. & PAGANO, J. S. 1984. Epstein-Barr virus replication in oropharyngeal epithelial cells. *N Engl J Med*, 310, 1225-30.
- SMATTI, M. K., AL-SADEQ, D. W., ALI, N. H., PINTUS, G., ABOU-SALEH, H. & NASRALLAH, G. K. 2018. Epstein–Barr Virus Epidemiology, Serology, and Genetic Variability of LMP-1 Oncogene Among Healthy Population: An Update. *Frontiers in Oncology*, 8.
- SMITH-GARVIN, J. E., KORETZKY, G. A. & JORDAN, M. S. 2009. T cell activation. *Annu Rev Immunol*, 27, 591-619.
- SONG, H. & YANG, P.-C. 2010. Construction of shRNA lentiviral vector. *North American journal of medical sciences*, 2, 598-601.
- SPRUNT, T. P. & EVANS, F. A. 1920. Mononuclear leucocytosis in reaction to acute infections (“infectious mononucleosis”). *Bull Johns Hopkins Hosp*, 31, 410-417.
- STADTMAUER, E. A., FAITG, T. H., LOWTHER, D. E., BADROS, A. Z., CHAGIN, K., DENGEL, K., IYENGAR, M., MELCHIORI, L., NAVENOT, J.-M., NORRY, E., TRIVEDI, T., WANG, R., BINDER, G. K., AMADO, R. & RAPOPORT, A. P. 2019. Long-term safety and activity of NY-ESO-1 SPEAR T cells after autologous stem cell transplant for myeloma. *Blood advances*, 3, 2022-2034.
- STEVANOVIC, S., DRAPER, L. M., LANGHAN, M. M., CAMPBELL, T. E., KWONG, M. L., WUNDERLICH, J. R., DUDLEY, M. E., YANG, J. C., SHERRY, R. M., KAMMULA, U. S., RESTIFO, N. P., ROSENBERG, S. A. & HINRICHS, C. S. 2015. Complete regression of metastatic cervical cancer after treatment with human papillomavirus-targeted tumor-infiltrating T cells. *J Clin Oncol*, 33, 1543-50.
- STEVEN, N. M., ANNELS, N. E., KUMAR, A., LEESE, A. M., KURILLA, M. G. & RICKINSON, A. B. 1997. Immediate early and early lytic cycle proteins are frequent targets of the Epstein-Barr virus-induced cytotoxic T cell response. *J Exp Med*, 185, 1605-17.

- STEVEN, N. M., LEESE, A. M., ANNELS, N. E., LEE, S. P. & RICKINSON, A. B. 1996. Epitope focusing in the primary cytotoxic T cell response to Epstein-Barr virus and its relationship to T cell memory. *J Exp Med*, 184, 1801-13.
- STRAATHOF, K. C., BOLLARD, C. M., POPAT, U., HULS, M. H., LOPEZ, T., MORRISS, M. C., GRESIK, M. V., GEE, A. P., RUSSELL, H. V., BRENNER, M. K., ROONEY, C. M. & HESLOP, H. E. 2005. Treatment of nasopharyngeal carcinoma with Epstein-Barr virus--specific T lymphocytes. *Blood*, 105, 1898-904.
- STRANG, G. & RICKINSON, A. B. 1987. Multiple HLA class I-dependent cytotoxicities constitute the "non-HLA-restricted" response in infectious mononucleosis. *Eur J Immunol*, 17, 1007-13.
- STUBBINGTON, M. J., LONNBERG, T., PROSERPIO, V., CLARE, S., SPEAK, A. O., DOUGAN, G. & TEICHMANN, S. A. 2016. T cell fate and clonality inference from single-cell transcriptomes. *Nat Methods*, 13, 329-32.
- SUN, Q., BURTON, R., REDDY, V. & LUCAS, K. G. 2002. Safety of allogeneic Epstein-Barr virus (EBV)-specific cytotoxic T lymphocytes for patients with refractory EBV-related lymphoma. *Br J Haematol*, 118, 799-808.
- SUN, Q., ZHANG, X., WANG, L., GAO, X., XIONG, Y., LIU, L., WEI, F., YANG, L. & REN, X. 2019. T-cell receptor gene therapy targeting melanoma-associated antigen-A4 by silencing of endogenous TCR inhibits tumor growth in mice and human. *Cell Death & Disease*, 10, 475.
- SUN, R., SHEPHERD, S. E., GEIER, S. S., THOMSON, C. T., SHEIL, J. M. & NATHANSON, S. G. 1995. Evidence that the antigen receptors of cytotoxic T lymphocytes interact with a common recognition pattern on the H-2Kb molecule. *Immunity*, 3, 573-582.
- SUN, X., SAITO, M., SATO, Y., CHIKATA, T., NARUTO, T., OZAWA, T., KOBAYASHI, E., KISHI, H., MURAGUCHI, A. & TAKIGUCHI, M. 2012. Unbiased analysis of TCRalpha/beta chains at the single-cell level in human CD8+ T-cell subsets. *PLoS One*, 7, e40386.
- SUNG, J. A., LAM, S., GARRIDO, C., ARCHIN, N., ROONEY, C. M., BOLLARD, C. M. & MARGOLIS, D. M. 2015. Expanded cytotoxic T-cell lymphocytes target the latent HIV reservoir. *J Infect Dis*, 212, 258-63.
- SUNG, J. A., PATEL, S., CLOHOSEY, M. L., ROESCH, L., TRIPIC, T., KURUC, J. D., ARCHIN, N., HANLEY, P. J., CRUZ, C. R., GOONETILLEKE, N., ERON, J. J., ROONEY, C. M., GAY, C. L., BOLLARD, C. M. & MARGOLIS, D. M. 2018. HIV-Specific, Ex Vivo Expanded T Cell Therapy: Feasibility, Safety, and Efficacy in ART-Suppressed HIV-Infected Individuals. *Molecular Therapy*, 26, 2496-2506.
- SUTHERLAND, J., MANNONI, P., ROSA, F., HUYAT, D., TURNER, A. R. & FELLOUS, M. 1985. Induction of the expression of HLA class I antigens on K562 by interferons and sodium butyrate. *Hum Immunol*, 12, 65-73.
- SZYMCZAK, A. L., WORKMAN, C. J., WANG, Y., VIGNALI, K. M., DILIOGLOU, S., VANIN, E. F. & VIGNALI, D. A. 2004. Correction of multi-gene deficiency in vivo using a single 'self-cleaving' 2A peptide-based retroviral vector. *Nat Biotechnol*, 22, 589-94.
- TAKADA, K. 2000. Epstein-Barr virus and gastric carcinoma. *Mol Pathol*, 53, 255-61.
- TAKADA, K., SHIMIZU, N., SAKUMA, S. & ONO, Y. 1986. trans activation of the latent Epstein-Barr virus (EBV) genome after transfection of the EBV DNA fragment. *Journal of Virology*, 57, 1016-1022.
- TAN, J. T., WHITMIRE, J. K., AHMED, R., PEARSON, T. C. & LARSEN, C. P. 1999a. 4-1BB ligand, a member of the TNF family, is important for the generation of antiviral CD8 T cell responses. *J Immunol*, 163, 4859-68.

- TAN, L. C., GUDGEON, N., ANNELS, N. E., HANSASUTA, P., O'CALLAGHAN, C. A., ROWLAND-JONES, S., MCMICHAEL, A. J., RICKINSON, A. B. & CALLAN, M. F. 1999b. A re-evaluation of the frequency of CD8⁺ T cells specific for EBV in healthy virus carriers. *J Immunol*, 162, 1827-35.
- TANNER, J., WEIS, J., FEARON, D., WHANG, Y. & KIEFF, E. 1987. Epstein-Barr virus gp350/220 binding to the B lymphocyte C3d receptor mediates adsorption, capping, and endocytosis. *Cell*, 50, 203-13.
- TAO, R., DE ZOETEN, E. F., ÖZKAYNAK, E., CHEN, C., WANG, L., PORRETT, P. M., LI, B., TURKA, L. A., OLSON, E. N., GREENE, M. I., WELLS, A. D. & HANCOCK, W. W. 2007. Deacetylase inhibition promotes the generation and function of regulatory T cells. *Nature Medicine*, 13, 1299-1307.
- TAYLOR, G. S., LONG, H. M., BROOKS, J. M., RICKINSON, A. B. & HISLOP, A. D. 2015. The immunology of Epstein-Barr virus-induced disease. *Annu Rev Immunol*, 33, 787-821.
- TEH, H. S., KISIELOW, P., SCOTT, B., KISHI, H., UEMATSU, Y., BLÜTHMANN, H. & VON BOEHMER, H. 1988. Thymic major histocompatibility complex antigens and the $\alpha\beta$ T-cell receptor determine the CD4/CD8 phenotype of T cells. *Nature*, 335, 229-233.
- THORLEY-LAWSON, D. A., HAWKINS, J. B., TRACY, S. I. & SHAPIRO, M. 2013. The pathogenesis of Epstein-Barr virus persistent infection. *Curr Opin Virol*, 3, 227-32.
- TILL, B. G., JENSEN, M. C., WANG, J., CHEN, E. Y., WOOD, B. L., GREISMAN, H. A., QIAN, X., JAMES, S. E., RAUBITSCHKE, A., FORMAN, S. J., GOPAL, A. K., PAGEL, J. M., LINDGREN, C. G., GREENBERG, P. D., RIDDELL, S. R. & PRESS, O. W. 2008. Adoptive immunotherapy for indolent non-Hodgkin lymphoma and mantle cell lymphoma using genetically modified autologous CD20-specific T cells. *Blood*, 112, 2261-71.
- TOKUNAGA, M., LAND, C. E., UEMURA, Y., TOKUDOME, T., TANAKA, S. & SATO, E. 1993. Epstein-Barr virus in gastric carcinoma. *Am J Pathol*, 143, 1250-4.
- TOPALIAN, S. L., HODI, F. S., BRAHMER, J. R., GETTINGER, S. N., SMITH, D. C., MCDERMOTT, D. F., POWDERLY, J. D., CARVAJAL, R. D., SOSMAN, J. A., ATKINS, M. B., LEMING, P. D., SPIGEL, D. R., ANTONIA, S. J., HORN, L., DRAKE, C. G., PARDOLL, D. M., CHEN, L., SHARFMAN, W. H., ANDERS, R. A., TAUBE, J. M., MCMILLER, T. L., XU, H., KORMAN, A. J., JURE-KUNKEL, M., AGRAWAL, S., MCDONALD, D., KOLLIA, G. D., GUPTA, A., WIGGINTON, J. M. & SZNOL, M. 2012. Safety, activity, and immune correlates of anti-PD-1 antibody in cancer. *N Engl J Med*, 366, 2443-54.
- TRAUTMANN, L., RIMBERT, M., ECHASSERIEAU, K., SAULQUIN, X., NEVEU, B., DECHANET, J., CERUNDOLO, V. & BONNEVILLE, M. 2005. Selection of T Cell Clones Expressing High-Affinity Public TCRs within Human Cytomegalovirus-Specific CD8 T Cell Responses. *The Journal of Immunology*, 175, 6123-6132.
- TRONO, D. 2003. Virology. Picking the right spot. *Science*, 300, 1670-1.
- TURNER, S. J., DOHERTY, P. C., MCCLUSKEY, J. & ROSSJOHN, J. 2006. Structural determinants of T-cell receptor bias in immunity. *Nature Reviews Immunology*, 6, 883-894.
- TYNAN, F. E., BORG, N. A., MILES, J. J., BEDDOE, T., EL-HASSEN, D., SILINS, S. L., VAN ZUYLEN, W. J., PURCELL, A. W., KJER-NIELSEN, L., MCCLUSKEY, J., BURROWS, S. R. & ROSSJOHN, J. 2005. High resolution structures of highly bulged viral epitopes bound to major histocompatibility complex class I. Implications for T-cell receptor engagement and T-cell immunodominance. *J Biol Chem*, 280, 23900-9.

- TZELLOS, S. & FARRELL, P. J. 2012. Epstein-barr virus sequence variation-biology and disease. *Pathogens (Basel, Switzerland)*, 1, 156-174.
- UEMATSU, Y., RYSER, S., DEMBIC, Z., BORGULYA, P., KRIMPENFORT, P., BERNIS, A., VON BOEHMER, H. & STEINMETZ, M. 1988. In transgenic mice the introduced functional T cell receptor beta gene prevents expression of endogenous beta genes. *Cell*, 52, 831-41.
- VAN BLEEK, G. M. & NATHENSON, S. G. 1991. The structure of the antigen-binding groove of major histocompatibility complex class I molecules determines specific selection of self-peptides. *Proceedings of the National Academy of Sciences of the United States of America*, 88, 11032-11036.
- VAN DEN HEUVEL, H., HEUTINCK, K. M., VAN DER MEER-PRINS, E. M. W., YONG, S. L., VAN MIERT, P., ANHOLTS, J. D. H., FRANKE-VAN DIJK, M. E. I., ZHANG, X. Q., ROELEN, D. L., TEN BERGE, R. J. M. & CLAAS, F. H. J. 2017. Allo-HLA Cross-Reactivities of Cytomegalovirus-, Influenza-, and Varicella Zoster Virus-Specific Memory T Cells Are Shared by Different Healthy Individuals. *Am J Transplant*, 17, 2033-2044.
- VAN DER MERWE, P. A. & DUSHEK, O. 2011. Mechanisms for T cell receptor triggering. *Nat Rev Immunol*, 11, 47-55.
- VAN LOENEN, M. M., DE BOER, R., AMIR, A. L., HAGEDOORN, R. S., VOLBEDA, G. L., WILLEMZE, R., VAN ROOD, J. J., FALKENBURG, J. H. & HEEMSKERK, M. H. 2010. Mixed T cell receptor dimers harbor potentially harmful neoreactivity. *Proc Natl Acad Sci U S A*, 107, 10972-7.
- VETSIKA, E. K. & CALLAN, M. 2004. Infectious mononucleosis and Epstein-Barr virus. *Expert Rev Mol Med*, 6, 1-16.
- VON BOEHMER, H., TEH, H. S. & KISIELOW, P. 1989. The thymus selects the useful, neglects the useless and destroys the harmful. *Immunology Today*, 10, 57-61.
- WÄLCHLI, S., LØSET, G. Å., KUMARI, S., JOHANSEN, J. N., YANG, W., SANDLIE, I. & OLWEUS, J. 2011. A practical approach to T-cell receptor cloning and expression. *PloS one*, 6, e27930-e27930.
- WALKER-SPERLING, V. E., POHLMAYER, C. W., TARWATER, P. M. & BLANKSON, J. N. 2016. The Effect of Latency Reversal Agents on Primary CD8+ T Cells: Implications for Shock and Kill Strategies for Human Immunodeficiency Virus Eradication. *EBioMedicine*, 8, 217-229.
- WANG, Y., WANG, F., WANG, R., ZHAO, P. & XIA, Q. 2015. 2A self-cleaving peptide-based multi-gene expression system in the silkworm *Bombyx mori*. *Scientific reports*, 5, 16273-16273.
- WEISS, A. & LITTMAN, D. R. 1994. Signal transduction by lymphocyte antigen receptors. *Cell*, 76, 263-74.
- WEISS, A. & STOBO, J. D. 1984. Requirement for the coexpression of T3 and the T cell antigen receptor on a malignant human T cell line. *J Exp Med*, 160, 1284-99.
- WHERRY, E. J., HA, S. J., KAECH, S. M., HAINING, W. N., SARKAR, S., KALIA, V., SUBRAMANIAM, S., BLATTMAN, J. N., BARBER, D. L. & AHMED, R. 2007. Molecular signature of CD8+ T cell exhaustion during chronic viral infection. *Immunity*, 27, 670-84.
- WIECZOREK, M., ABUALROUS, E. T., STICHT, J., ÁLVARO-BENITO, M., STOLZENBERG, S., NOÉ, F. & FREUND, C. 2017. Major Histocompatibility Complex (MHC) Class I and MHC Class II Proteins: Conformational Plasticity in Antigen Presentation. *Frontiers in immunology*, 8, 292-292.
- WILDEMAN, M. A., NOVALIC, Z., VERKUIJLEN, S. A., JUWANA, H., HUITEMA, A. D., TAN, I. B., MIDDELDORP, J. M., DE BOER, J. P. & GREIJER, A. E. 2012.

- Cytolytic virus activation therapy for Epstein-Barr virus-driven tumors. *Clin Cancer Res*, 18, 5061-70.
- WILLIAMS, H., MCAULAY, K., MACSWEEN, K. F., GALLACHER, N. J., HIGGINS, C. D., HARRISON, N., SWERDLOW, A. J. & CRAWFORD, D. H. 2005. The immune response to primary EBV infection: a role for natural killer cells. *Br J Haematol*, 129, 266-74.
- WILLIAMS, M. A. & BEVAN, M. J. 2007. Effector and memory CTL differentiation. *Annu Rev Immunol*, 25, 171-92.
- WILSON, R. C. & DOUDNA, J. A. 2013. Molecular mechanisms of RNA interference. *Annu Rev Biophys*, 42, 217-39.
- WOODBERRY, T., SUSCOVICH, T. J., HENRY, L. M., DAVIS, J. K., FRAHM, N., WALKER, B. D., SCADDEN, D. T., WANG, F. & BRANDER, C. 2005. Differential targeting and shifts in the immunodominance of Epstein-Barr virus--specific CD8 and CD4 T cell responses during acute and persistent infection. *J Infect Dis*, 192, 1513-24.
- WU, L., LI, C. & PAN, L. 2018. Nasopharyngeal carcinoma: A review of current updates. *Experimental and therapeutic medicine*, 15, 3687-3692.
- YOUNG, L. S. & DAWSON, C. W. 2014. Epstein-Barr virus and nasopharyngeal carcinoma. *Chinese journal of cancer*, 33, 581-590.
- ZERRAHN, J., HELD, W. & RAULET, D. H. 1997. The MHC Reactivity of the T Cell Repertoire Prior to Positive and Negative Selection. *Cell*, 88, 627-636.
- ZHANG, G.-Q., ZHAO, H., WU, J.-Y., LI, J.-Y., YAN, X., WANG, G., WU, L.-L., ZHANG, X.-G., SHAO, Y., WANG, Y. & JIAO, S.-C. 2015. Prolonged overall survival in gastric cancer patients after adoptive immunotherapy. *World journal of gastroenterology*, 21, 2777-2785.
- ZHANG, W. 2014. TCGA divides gastric cancer into four molecular subtypes: implications for individualized therapeutics. *Chin J Cancer*, 33, 469-70.
- ZHAO, Y., GE, X., HE, J., CHENG, Y., WANG, Z., WANG, J. & SUN, L. 2019. The prognostic value of tumor-infiltrating lymphocytes in colorectal cancer differs by anatomical subsite: a systematic review and meta-analysis. *World journal of surgical oncology*, 17, 85-85.
- ZHENG, Y., PARSONAGE, G., ZHUANG, X., MACHADO, L. R., JAMES, C. H., SALMAN, A., SEARLE, P. F., HUI, E. P., CHAN, A. T. & LEE, S. P. 2015. Human Leukocyte Antigen (HLA) A*1101-Restricted Epstein-Barr Virus-Specific T-cell Receptor Gene Transfer to Target Nasopharyngeal Carcinoma. *Cancer Immunol Res*, 3, 1138-47.
- ZHONG, S., MALECEK, K., JOHNSON, L. A., YU, Z., VEGA-SAENZ DE MIERA, E., DARVISHIAN, F., MCGARY, K., HUANG, K., BOYER, J., CORSE, E., SHAO, Y., ROSENBERG, S. A., RESTIFO, N. P., OSMAN, I. & KROGSGAARD, M. 2013. T-cell receptor affinity and avidity defines antitumor response and autoimmunity in T-cell immunotherapy. *Proceedings of the National Academy of Sciences of the United States of America*, 110, 6973-6978.
- ZIEGLER, J. L., DREW, W. L., MINER, R. C., MINTZ, L., ROSENBAUM, E., GERSHOW, J., LENNETTE, E. T., GREENSPAN, J., SHILLITOE, E., BECKSTEAD, J., CASAVANT, C. & YAMAMOTO, K. 1982. Outbreak of Burkitt's-like lymphoma in homosexual men. *Lancet*, 2, 631-3.
- ZUR HAUSEN, H., SCHULTE-HOLTHAUSEN, H., KLEIN, G., HENLE, W., HENLE, G., CLIFFORD, P. & SANTESSON, L. 1970. EBV DNA in biopsies of Burkitt tumours and anaplastic carcinomas of the nasopharynx. *Nature*, 228, 1056-8.

Appendices

**APPENDIX 1:
Primers and PCR conditions for 5'RACE PCR**

Table 1. Reverse Transcription Primers for 5'RACE PCR method

Primer	Primer Sequence
alpha-RT	5'-AGCAGTGTTTGGCAGCTCTT-3'
beta1-RT	5'-CTGGCAAAGAAGAATGTGT-3'
beta2-RT	5'-ACACAGATTGGGAGCAGGTA-3'

Table 2. Reverse Transcription mastermix and conditions for 5'RACE PCR method

	1 Rx	5 Rx
RT primer mix	0.5	2.5
10mM dNTP	0.5	2.5
H2O	3	15
RNA	1	5
	5	

Aliquot 5ul to individual tube and heat to 65C for 5 minutes

Add 5ul of enzyme mastermix below:

	1 Rx	5 Rx
10x RT buffer	1	5
25mM mgCl	2	10
DTT	1	5
Rnase Out	0.5	2.5
4 U Superscript III	0.5	2.5

Reaction: 50C for 1 hour, 70C 5 mins

Table 3. Poly-G tailing reaction for 5'RACE PCR method

	1x Rx	10x
14U TdT	0.4	4
0.5mM dGTP	0.05	0.5
0.4U Murine Rnase Inhibitor	0.01	0.1
0.2% Triton X-100	0.02	0.2
4mM MgCl	0.08	0.8
1X TdT buffer	1.5	15

Aliquot 2.06ul of MM into each RT tube (~15ul total)

Tailing reaction: 40 mins at 37C, then 20 mins at 75C

Table 4. 1st PCR Primers for 5'RACE PCR method

Primer	Primer Sequence
AP-1F	5'-ACAGCAGGTCAGTCAAGCAGTAGCAGCAGTTCGATAACTTCGAATT CTGCAGTCGACGGTACCGCGGGCCCCGGGATCCCCCCCCCCCCC-3'
alphaR-1 st	5'-AGAGGGGAGAAGAGGGGCAAT-3'
beta1R-1 st	5'-CCATGACGGGTTAGAAGCTC-3'
beta2R-1 st	5'-GGATGAAGAATGACCTGGGAT-3'

Table 5. 1st PCR mastermix for 5'RACE PCR method

	1Rx	5.3Rx
10x PCR Buffer	2.5	13.25
10mM dNTP	0.5	2.65
MgCl ₂	0.75	3.975
F primer	0.5	
R primer	0.5	
Plat Taq	0.2	1.06
H ₂ O	19.05	100.965
Total Mastermix	24	
Template		1

Table 6. 1st PCR conditions for 5'RACE PCR method

Temperature	
94°C for 2 min	
94 °C for 15 sec	45 cycles
60 °C for 30 sec	
72 °C for 1.30 min	
72 °C for 10 mins	
4 °C store	

Table 7. Nested (2nd) PCR Primers for 5'RACE PCR method

Primer	Primer Sequence
AP-2F	5'-AGCAGTAGCAGCAGTTCGATAA-3'
TCR α NestR	5'-GGTGAATAGGCAGACAGACTT-3'
TCR β NestR	5'-GTGGCCAGGCACACCAGTGT-3'

Table 8. Nested (2nd) PCR mastermix for 5'RACE PCR method

	25ul Rx	5.3 Rx
10x PCR Buffer	2.5	13.25
10mM dNTP	0.5	2.65
MgCl ₂	0.75	3.975
AP2 F	0.5	2.65
Alpha or Beta Nested R	0.5	2.65
Plat Taq	0.25	1.325
H ₂ O	18	95.4
Total	25	

Aliquot 23ul and add 2ul template

Table 9. Nested PCR conditions for 5'RACE PCR method

Temperature	
94°C for 2 min	
94 °C for 15 sec	35 cycles
60 °C for 30 sec	
72 °C for 45 sec	
72 °C for 10 mins	
4 °C store	

APPENDIX 2: EBV ZEBRA peptide Pool

18mer Peptide	Sequence
1	MMDPNSTSEDKFTDPY
2	STSEDKFTDPYQVPFV
3	VKFTDPYQVPFVQAFDQ
4	DPYQVPFVQAFDQATRVY
5	PFVQAFDQATRVYQDLGG
6	FDQATRVYQDLGGPSQAP
7	RVYQDLGGPSQAPLPCVL
8	LGGPSQAPLPCVLWPVLP
9	QAPLPCVLWPVLPPELPQ
10	CVLWPVLPPELPQGGQLTA
11	VLPELPQGGQLTAYHVSA
12	LPQGGQLTAYHVSAAPTGS
13	LTAYHVSAAPTGSWFPAP
14	VSAAPTGSWFPAPQPAPPE
15	TGSWFPAPQPAPENAYQA
16	PAPQPAPENAYQAYAAPQ
17	APENAYQAYAAPQLFPVS
18	YQAYAAPQLFPVSDITQN
19	APQLFPVSDITQNQLTNQ
20	PVSDITQNQLTNQAGGEA
21	TQNQLTNQAGGEAPQPGD
22	TNQAGGEAPQPGDNSTVQ
23	GEAPQPGDNSTVQPAAAV
24	PGDNSTVQPAAAVVLACP
25	TVQPAAAVVLACPGANQE
26	AAVVLACPGANQEQQLAD
27	ACPGANQEQQLADIGAPQ
28	NQEQQLADIGAPQPAPAA
29	LADIGAPQPAPAAAPARR
30	APQPAPAAAPARRTRKPL
31	PAAAPARRTRKPLQPESL
32	ARRTRKPLQPESLEECDS
33	KPLQPESLEECDSELEIK
34	ESLEECDSELEIKRYKNR
35	CDSELEIKRYKNRVASRK
36	EIKRYKNRVASRKCRAKF
37	KNRVASRKCRAKFKHLLQ
38	SRKCRAKFKHLLQHCREV

39	AKFKHLLQHCREVASAKS
40	LLQHCREVASAKSENDR
41	REVASAKSENDRLRLLL
42	AKSENDRLRLLLQMCP
43	NDRLRLLLQMCPSLDVD
44	LLKQMCPSLDVDSIIPR
45	MCPSLDVDSIIPRTPDVL
46	DVDSIIPRTPDVLHEDLL
47	DSIIPRTPDVLHEDLLNF

APPENDIX 3:
Paired TCR Sequences and frequencies obtained from Donor 1

TCR*	TRAV	TRAJ	CDR3 a	TRBV	TRBJ	CDR3 b	Freq	%
1	TRAV1- 2*01	TRAJ6*01	CAVLSSGGSYIPTF	TRBV12- 3*01	TRBJ1- 2*01	CASSFSTCSANYGYT F	16	21
10	TRAV3*0 1	TRAJ13*0 2	CAVRDYNSSGGYQKV TF	TRBV10- 3*02	TRBJ1- 5*01	CASSTGDSNQPQHF	10	13
4	TRAV20* 02	TRAJ24*0 2	CAFFSWGKQLQF	TRBV3- 1*01	TRBJ1- 2*01	CASSQSPGTGVGYT F	10	13
7	TRAV8- 6*02	TRAJ40*0 1	CAVSDQGTYKYIF	TRBV10- 3*02	TRBJ1- 5*01	CASSTGDSNQPQHF	5	6
2	TRAV4*0 1	TRAJ8*01	CLQNAFQKLVF	TRBV10- 3*02	TRBJ1- 5*01	CASSTGDSNLPQHF	5	6
16	TRAV3*0 1	TRAJ13*0 2	CAVRDYNNGNGYQK VTF	TRBV28* 01	TRBJ2- 1*01	CASRVPGNLDEQFF	4	5
19	TRAV3*0 1	TRAJ13*0 2	CAVRDYNSSGGYQKV TF	TRBV12- 3*01	TRBJ1- 2*01	CASSFSTCSANYGYT F	4	5
3	TRAV8- 6*02	TRAJ40*0 1	CAVSDQGTYKYIF	TRBV12- 3*01	TRBJ1- 2*01	CASSFSTCSANYGYT F	3	4
17	TRAV8- 4*01	TRAJ3*01	CAVSDLEPNSSASKII F	TRAV35* 02	TRBJ1- 2*01	CAGHFSTCSANYGY TF	3	4
18	TRAV3*0 1	TRAJ13*0 2	CAVRDYNSSGGYQKV TF	TRBV28* 01	TRBJ2- 1*01	CASRVPGNLDQFF	3	4
20	TRAV1- 2*01	TRAJ6*01	CAVLSSGGSYIPTF	TRBV28* 01	TRBJ2- 1*01	CASRVPGNLDQFF	2	3
61	TRAV20* 02	TRAJ24*0 2	CAFFSWGKQLQF	TRBV7- 9*01	TRBJ1- 1*01	CASSPQPTEAFF	2	3
14	TRAV20* 02	TRAJ24*0 2	CAFFSWGKQLQF	TRBV28* 01	TRBJ2- 1*01	CASRVPGNLDQFF	2	3
54	TRAV20* 02	TRAJ24*0 2	CAFVQWLKLF	TRAV35* 02	TRAJ40* 01	CAGHFSTYKYIF	1	1
70	TRAV8- 6*02	TRAJ23*0 1	CAVSRSNQGGKLIF	TRBV28* 01	TRBJ2- 1*01	CASRVPLDEYFF	1	1
33	TRAV8- 6*02	TRAJ40*0 1	CAVSDQGTYKYIF	TRBV3- 1*01 F	TRBJ1- 2*01	CASSQSPGTGVGYT F	1	1
5	TRAV4*0 1	TRAJ8*01	CLQNAFQKLVF	TRBV12- 3*01	TRBJ1- 2*01	CASSFSTCSANYGYT F	1	1
38	TRAV8- 6*02	TRAJ23*0 1	CAVSRSNQGGKLIF	TRBV3- 1*01	TRBJ1- 2*01	CASSQSPGTGVGYT F	1	1
71	TRAV21* 02	TRAJ4*01	CAVRPLIYGGYNKLIF	TRBV28* 01	TRBJ2- 3*01	CASSLPGAGGYTDT QYF	1	1
29	TRAV24* 01	TRAJ24*0 2	CALPWGTDSWGK QF	TRBV6- 4*01	TRBJ1- 1*01	CASSDTGTLNTEAFF	1	1
59	TRAV29* 01	TRAJ49*0 1	CPCRNTGNQFYF	TRBV28* 01	TRBJ1- 5*01	CASSFGLDSNQPQH F	1	1

*TCR No. has no bearing on frequency of clone. It was assigned during initial organization and grouping of TCR sequences during analysis. Only productive paired TCR $\alpha\beta$ sequences are shown. n= 77

APPENDIX 4: Paired TCR sequences and frequencies obtained from Donor 2

TCR *	TRAV	TRAJ	CDR3 α	TRBV	TRBJ	CDR3 β	Fre q	%
8	TRAV12- 3*01	TRAJ26*0 1	CAMRNYGQNFVF	TRBV25- 1*01	TRBJ1- 3*01	CASDGTGGENTIYF	21	15
131	TRAV26- 2*01	TRAJ47*0 1	CILRDGVGYGNKLVF	TRBV9*0 2	TRBJ2- 3*01	CASEDRGGTDTQYF	19	14
16	TRAV13- 2*01	TRAJ12*0 1	CAEKGWDSSYKLI	TRBV30* 02	TRBJ1- 2*01	CAWVDGVLDGYTF	19	14
9	TRAV13- 1*02	TRAJ42*0 1	CAASKEGGGSQGNLI F	TRBV20- 1*02	TRBJ2- 1*01	CSARDRGEHPPND QFF	14	10
132	TRAV14*0 1	TRAJ52*0 1	CAMREGSGVGTSGYK LTF	TRBV29- 1*01	TRBJ2- 5*01	CSAAGTSGSGETQY F	11	8
34	TRAV29* 01	TRAJ16* 01	CAASEGGQKLLF	TRBV7- 9*03	TRBJ24* 01	CASSAPNSDSAKNI QYF	11	8
25	TRAV13- 1*02	TRAJ42*0 1	CAASKEGGGSQGNLI F	TRBV12- 3*01	TRBJ1- 2*01	CASSFSTCSANYGYT F	4	3
51	TRAV14*0 1	TRAJ54*0 1	CAMREVQGAQKLVF	TRBV4- 2*01	TRBJ1- 3*01	CASSLSETGTGNTIY F	4	3
23	TRAV1- 2*01	TRAJ6*01	CAVLSSGGSYIPTF	TRBV12- 3*01	TRBJ1- 2*01	CASSFSTCSANYGYT F	4	3
29	TRAV13- 1*02	TRAJ42*0 1	CAASKEGGGSQGNLI F	TRBV4- 2*01	TRBJ1- 3*01	CASSLSETGTGNTIY F	4	3
45	TRAV8- 6*02	TRAJ40*0 1	CAVSDQGTYKYIF	TRBV10- 3*02	TRBJ1- 5*01	CASSTGDSNQPQH F	4	3
46	TRAV8- 6*02	TRAJ40*0 1	CAVSDQGTYKYIF	TRBV12- 3*01	TRBJ1- 2*01	CXSSFSTCSANYGYT F	4	3
14	TRAV26- 2*01	TRAJ47*0 1	CILRDGVNYGNKLVF	TRBV9*0 2	TRBJ2- 3*01	CASEDRNSGDTQY F	3	2
15	TRAV29*0 1	TRAJ16*0 1	CAASEGGQKLLF	TRBV9*0 1	TRBJ2- 1*01	CASSVPSGGAGE QFF	3	2
49	TRAV26- 2*01	TRAJ56*0 1	CILRGVYTGANSKLT	TRBV4- 1*01	TRBJ1- 2*01	CASSQGLSDDGYT F	2	1
55	TRAV13- 1*02	TRAJ42*0 1	CAASKEGGGSQGNLI F	TRBV7- 8*01	TRBJ2- 7*01	CASSLGQAYEQYF	1	1
54	TRAV27*0 1	TRAJ35*0 1	CAXXIGFGNVLHC	TRBV2*0 1	TRBJ1- 5*01	CASREEGSSHPQHF	1	1
112	TRAV12- 3*01	TRAJ42*0 1	CAMGNYGGSQGNLIF	TRBV10- 3*02	TRBJ1- 1*01	CAINDVGGTEAFF	1	1
15	TRAV26- 2*01	TRAJ56*0 1	CILRGVYTGANSKLT	TRBV4- 1*01	TRBJ1- 2*01	CASSQGLSDDGYT F	1	1
120	TRAV29* 01	TRAJ16* 01	CAASEGGQKLLF	TRBV12- 3*01	TRBJ1- 2*01	CASSFSTCSANYGYT F	1	1
98	TRAV12- 3*01	TRAJ26*0 1	CAMRNYGQNFVF	TRBV12- 3*01	TRBJ1- 2*01	CASSFSTCSANYGYT F	1	1
12	TRAV8- 6*02	TRAJ40*0 1	CAVSDQGTYKYIF	TRBV29- 1*01	TRBJ2- 5*01	CSAAGTSGSGETQY F	1	1
61	TRAV27*0 1	TRAJ35*0 1	CAXXIGFGNVLHC	TRBV12- 3*01	TRBJ1- 2*01	CASSFSTCSANYGYT F	1	1
73	TRAV4*01	TRAJ8*01	CLQNWVQKLVF	TRBV4- 2*01	TRBJ1- 3*01	CASSLSETGTGNTIY F	1	1
38	TRAV13- 2*01	TRAJ12*0 1	CAEKGWDSSYNLIF	TRBV30* 02	TRBJ1- 2*01	CAWVDGVLDGYTF	1	1

*TCR No. has no bearing on frequency of clone. It was assigned during initial organization and grouping of TCR sequences during analysis. Only productive paired TCR $\alpha\beta$ sequences are shown. n= 138

APPENDIX 5: HLA Alleles of BCL panels used to characterize TCRs

Table 1. The HLA alleles of the BCL panel used to characterize TCR4

BCL ID	HLA-A1	HLA-A2	HLA-B1	HLA-B2	HLA-C1	HLA-C2
Autologous	A*02:01	A*11:01	B*35:01	B*49:01	C*04:01	C*07:01
BJ004	A*02:01	A*33	B*58	B*58	C*08	C*03
BJ035	A*11:01	A*24	B*46	B*57	C*01	C*06
BJ043	A*31	A*31	B*35:01	B*35:01	C*03	C*03
HD12	A*02:05	A*30:04	B*45:01	B*49:01	C*07:02	C*12:03
IAVI 3572 BCL	A*03:01	A*24:02	B*18:01	B*35:01	C*04:01	C*07:01
IAVI 3374 BCL	A*02:01	A*25:01	B*18:01	B*35:30	C*04:01	C*12:03
.221 A2 Cell line	A*02:01	-	-	-	Low C*01:02	Low C*01:02
HC6	A*23:01	A*31:01	B*18:01	B*40:01	C*03:04	C*07:01
HK7	A*01	A*02:07	B*44	B*37	C*06:01	C*07:01

¹The alleles in red indicate matching alleles to TCR donor 1 (autologous)

Table 2. The HLA alleles of the BCL panel used to characterize donor 2 TCRs

BCL ID	HLA-A1	HLA-A2	HLA-B1	HLA-B2	HLA-C1	HLA-C2
Autologous	A*23:01	A*31:01	B*18:01	B*40:01	C*03:04	C*07:01
HC6	A*11:01	A*23:01	B*44:03	B*51:01	C*04:01	C*15:02
BJ043	A*31:01	A*31:01	B*35:01	B*35:01	C*04	C*04
IV3374	A*02:01	A*25:01	B*18:01	B*35:03	C*04:01	C*12:03
BJ096	A*24	A*24	B*40:01	B*54	C*01	C*03

¹The alleles in red indicate matching alleles to TCR donor 2 (autologous)

APPENDIX 6: Overlapping 9mer peptide sequences

The 18mer ZEBRA peptides and their overlapping 9mers used for epitope mapping

A 18mer: VLPEPLPQGQLTAYHVSA

Peptide number	9mer
1	VLPEPLPQG
2	LPEPLPQGQ
3	PEPLPQGQL
4	EPLPQGQLT
5	PLPQGQLTA
6	LPQGQLTAY
7	PQGQLTAYH
8	QGQLTAYHV
9	GQLTAYHVS

B 18mer: CDSELEIKRYKNRVASRK

Peptide number	9mer
1	CDSELEIKR
2	DSELEIKRY
3	SELEIKRYK
4	ELEIKRYKN
5	LEIKRYKNR
6	EIKRYKNRV
7	IKRYKNRVA
8	KRYKNRVAS
9	RYKNRVASR
10	YKNRVASRK

The VLPEPLPQGQLTAYHVSA and CDSELEIKRYKNRVASRK 18mers were used for the design of overlapping 9mers with an offset of 1 amino acid for TCR epitope mapping. These individual 9mers were used for peptide pulsing of the autologous BCLs and used for peptide stimulation as described previously.

APPENDIX 7: Peptide pulsing of TCR4 with 15-, 13- and 11mers

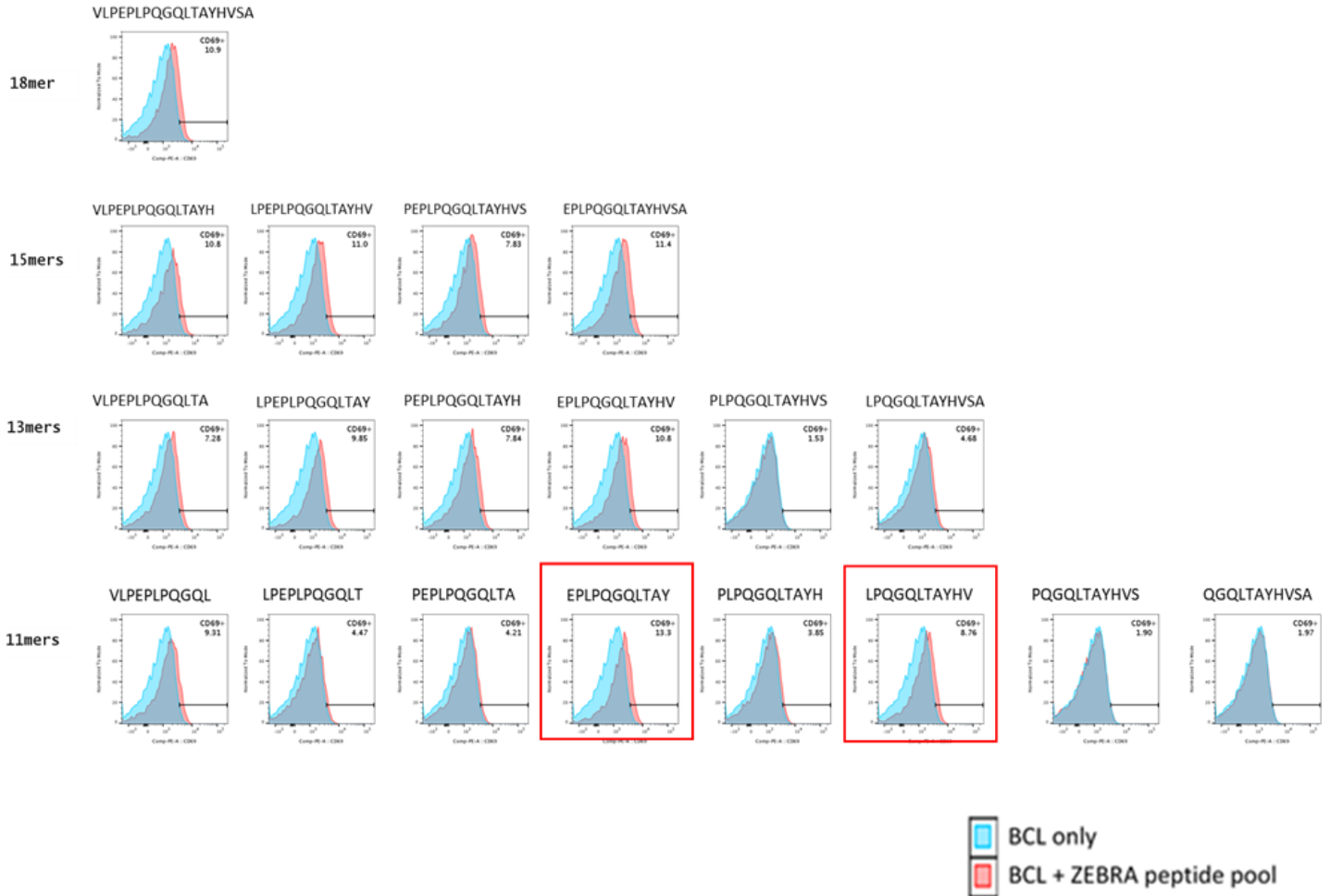


Figure 1. Peptide pulsing of TCR4 with 15-, 13- and 11mers

TCR4 SKW3 cells were stimulated with peptides of the indicated lengths. The red boxes indicate the 11mers which induced a positive CD69 response when presented on the autologous BCLs.

APPENDIX 8: Peptide pulsing of TCR4 with 9mers

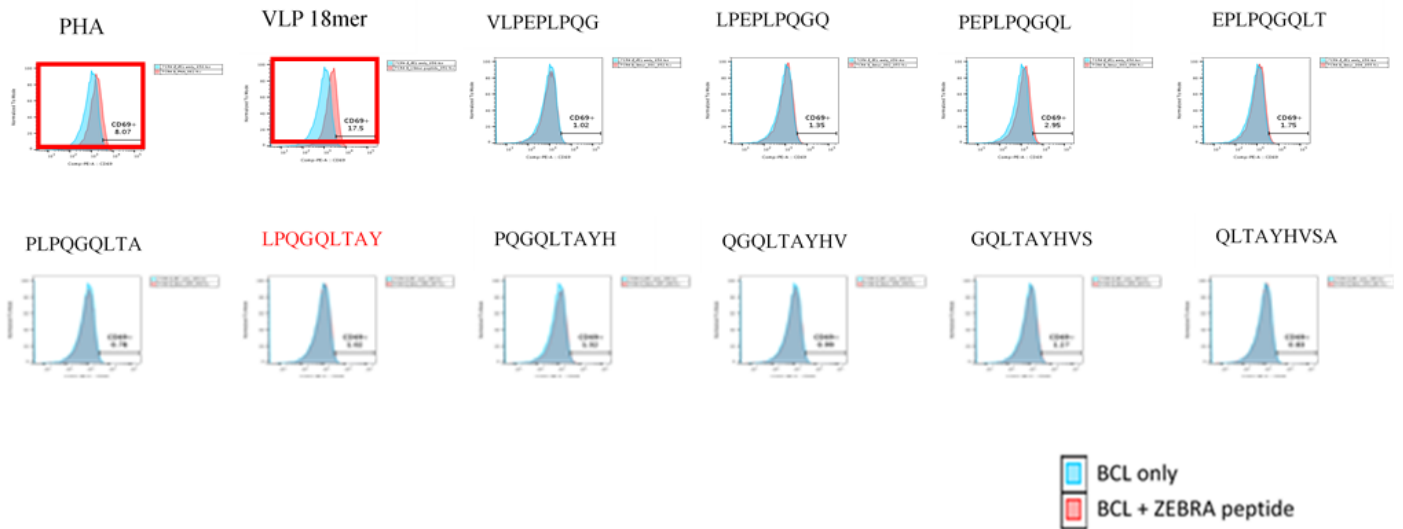


Figure 1. TCR4 does not recognise 9mers within the VLP 18mer

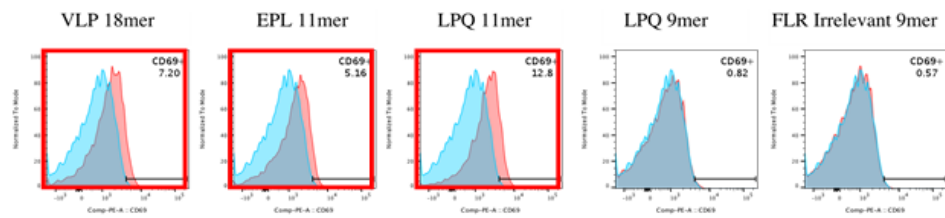
TCR4 SKW3 cells were stimulated with 9mers. No CD69 upregulation was observed. The peptide sequence highlighted in red indicates the overlapping sequence of the EPL and LPQ 11mers which induced a positive response in TCR4.

APPENDIX 9:
Further confirmation of TCR4 cross-reactivity
with HLA-A*02:01 and HLA-B*35:01

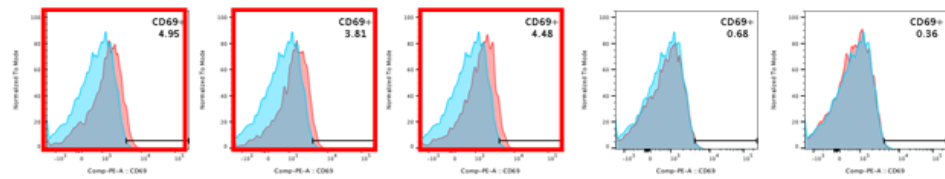
Table 1. A large panel of BCLs chosen to confirm the HLA-A*02:01 and HLA-B*35:01 cross-reactivity of TCR4

		HLA I Alleles						TCR 4
		A	A	B	B	C	C	CD69
1	Donor 1 Autologous BCL	A*02:01	A*11:01	B*35:01	B*49:01	Cw*04:01	Cw*07:01	+
2	GZ006 BCL	A*02:01	A*11:01	B*56	B*46	Cw*01	Cw*01	+
3	GZ055 BCL	A*02:01	A*24	B*40	B*46	Cw*01	Cw*07:02	+
4	GZ074 BCL	A*02:01	A*02:07	B*40	B*54	Cw*01	Cw*07:02	+
5	GZ092 BCL	A*02:01	A*03	B*44	B*51	Cw*04:01	Cw*14	+
6	IAVI 3374 BCL	A*02:01	A*25:01	B*18:01	B*35:30	Cw*04:01	Cw*12:03	+
7	H3N2 #2A BCL	A*02:01	A*26:01	B*18	B*40:01	Cw*03	Cw*07:01	+
8	IAVI 3572 BCL	A*03:01	A*24:02	B*35:01	B*18:01	Cw*04:01	Cw*07:01	+
9	HK-002 BCL	A*01	A*02:07	B*44	B*37	Cw*06	Cw*07:01	-
10	LG BCL	A*23:01	A*31:01	B*18:01	B*40:01	Cw*03:04	Cw*07:01	-
11	OE19 line	A*02:01	A*01:01	B*18:01	B*45:01	Cw*05:01	Cw*07:01	+
12	AGS line	A*02:01	A*02:01	B*52:01	B*52:01	Cw*03:03	Cw*03:03	+
13	BJ043 BCL	A*31	A*31	B*35:01	B*35:01	Cw*03	Cw*03	+
14	BJ096 BCL	A*24	A*24	B*40	B*54	Cw*01	Cw*03	-
15	BJ035 BCL	A*24	A*11:01	B*46	B*57	Cw*01	Cw*06	-

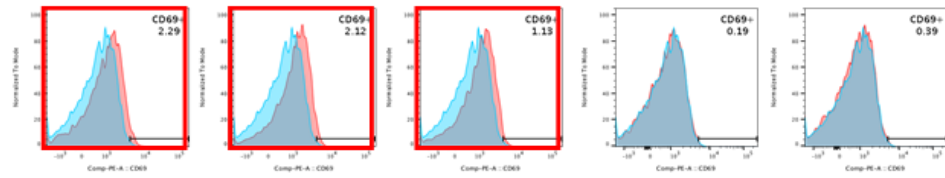
Autologous BCL:
HLA A*02:01, A*11:01,
B*35:01, B*49:01,
Cw*04:01, Cw*07:01



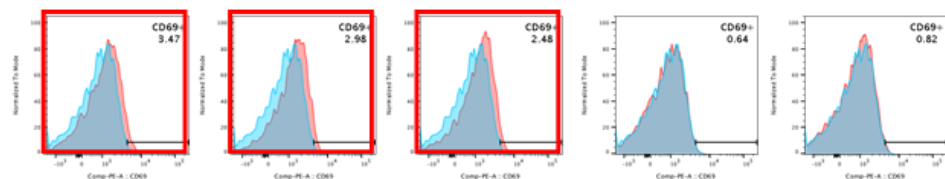
IAVI 3572 BCL:
HLA A*03:01, A*24:01,
B*35:01, B*18:01,
Cw*04:01, Cw*07:01



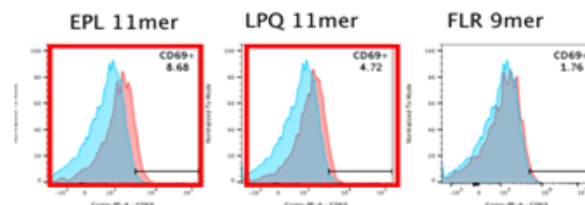
IAVI 3374 BCL:
HLA A*02:01, A*25:01,
B*35:03, B*18:01,
Cw*04:01, Cw*12:03



.221_A2 Line:
HLAA*02:01

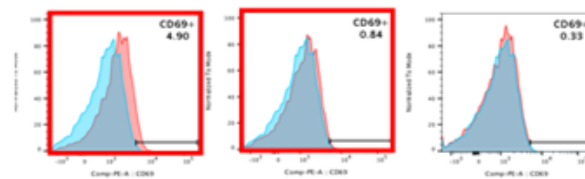


Autologous BCL:
HLA A*02:01, A*11:01,
B*35:01, B*49:01,
Cw*04:01, Cw*07:01

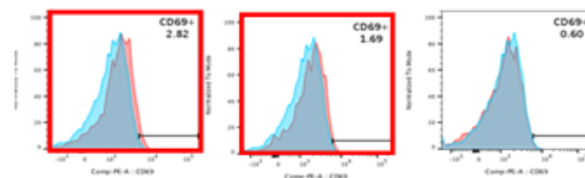


BCL only
BCL + ZEBRA peptide

.221_A2 Line:
HLA A*02:01



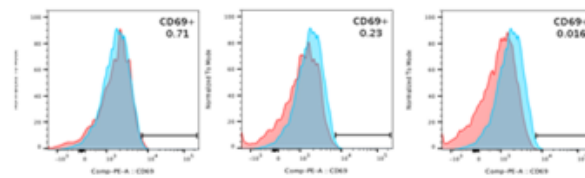
GZ74 BCL:
HLA A*02:01, A*02:07,
B*40:01, B*54:01,
Cw*01:01, Cw*07:02



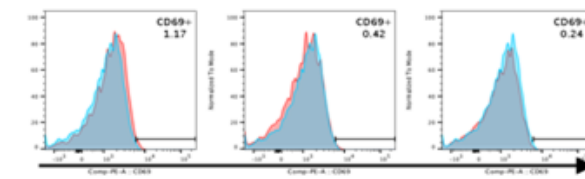
GZ55 BCL:
HLA A*02:01, A*24,
B*40:01, B*46,
Cw*01:01, Cw*07:02



HC3 BCL:
HLA A*23:01, A*31:01,
B*18:01, B*40:01,
Cw*03:04, Cw*07:01



HK2 BCL:
HLA A*01:01, A*02:07,
B*44:01, B*37:01,
Cw*06:01, Cw*07:01



CD69

Figure 1: Further confirmation of TCR4 HLA-A*02:01 and HLA-B*35:01 cross-reactivity

The peptide stimulation assays using the of HLA-A*02:01+ or HLA-B*35:01+ were repeated for confirmation. Only the BCLs which possess HLA-A*02:01 and HLA-B*35:01 are able to induce CD69 in TCR4.

APPENDIX 10: 9mer peptide pulsing of Donor 2 TCRs

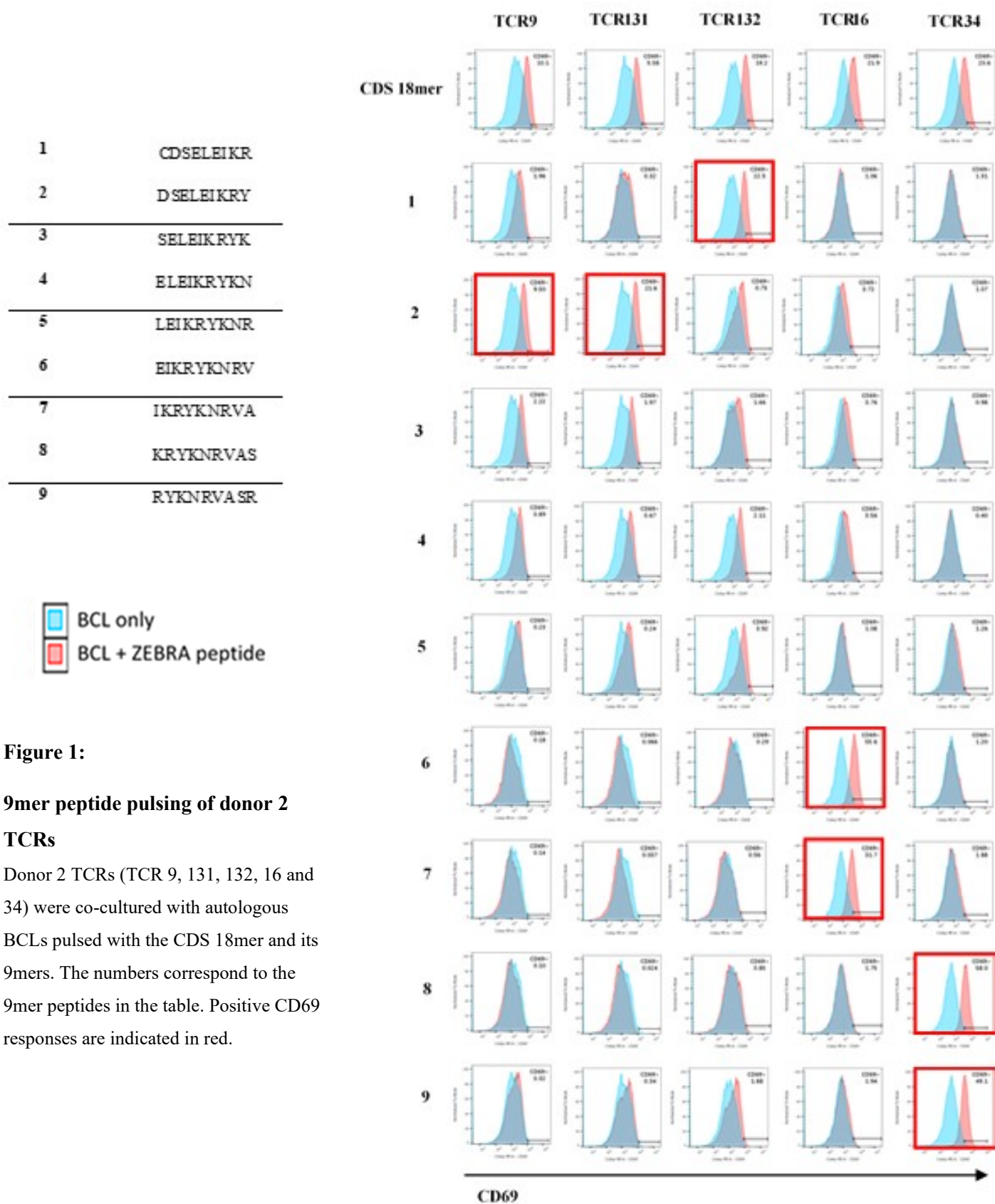


Figure 1:

9mer peptide pulsing of donor 2 TCRs

Donor 2 TCRs (TCR 9, 131, 132, 16 and 34) were co-cultured with autologous BCLs pulsed with the CDS 18mer and its 9mers. The numbers correspond to the 9mer peptides in the table. Positive CD69 responses are indicated in red.

APPENDIX 11: Licensing details and permission to use published images

License Details

This Agreement between Ms. Nadia Khan ("You") and Springer Nature ("Springer Nature") consists of your license details and the terms and conditions provided by Springer Nature and Copyright Clearance Center.

[Print](#) [Copy](#)

License Number	4751390220396
License date	Jan 17, 2020
Licensed Content Publisher	Springer Nature
Licensed Content Publication	Nature Reviews Immunology
Licensed Content Title	Structural determinants of T-cell receptor bias in immunity
Licensed Content Author	Stephen J. Turner et al
Licensed Content Date	Nov 17, 2006
Type of Use	Thesis/Dissertation
Requestor type	academic/university or research institute
Format	print and electronic
Portion	figures/tables/illustrations
Number of figures/tables/illustrations	1
High-res required	no
Will you be translating?	no
Circulation/distribution	1 - 29
Author of this Springer Nature content	no
Title	Characterization of T cell responses to EBV-associated gastric carcinoma using a single TCR cloning platform
Institution name	Imperial College London
Expected presentation date	Dec 2019
Portions	figure 1
Requestor Location	Ms. Nadia Khan 12 Brookesley Street London, E3 4QL United Kingdom Attn: Ms. Nadia Khan
Total	0.00 GBP

License Details

This Agreement between Ms. Nadia Khan ("You") and Elsevier ("Elsevier") consists of your license details and the terms and conditions provided by Elsevier and Copyright Clearance Center.

[Print](#) [Copy](#)

License Number	4746570604205
License date	Jan 12, 2020
Licensed Content Publisher	Elsevier
Licensed Content Publication	Journal of Investigative Dermatology
Licensed Content Title	Cytotoxic T Cells
Licensed Content Author	Mads Hald Andersen, David Schrama, Per thor Straten, Jürgen C. Becker
Licensed Content Date	Jan 1, 2006
Licensed Content Volume	126
Licensed Content Issue	1
Licensed Content Pages	10
Type of Use	reuse in a thesis/dissertation
Portion	figures/tables/illustrations
Number of figures/tables/illustrations	1
Format	both print and electronic
Are you the author of this Elsevier article?	No
Will you be translating?	No
Title	Characterization of T cell responses to EBV-associated gastric carcinoma using a single TCR cloning platform
Institution name	Imperial College London
Expected presentation date	Dec 2019
Portions	Figure 5
Requestor Location	Ms. Nadia Khan 12 Brookesley Street London, E3 4QL United Kingdom Attn: Ms. Nadia Khan
Publisher Tax ID	GB 494 6272 12
Total	0.00 GBP

License Details

This Agreement between Ms. Nadia Khan ("You") and Springer Nature ("Springer Nature") consists of your license details and the terms and conditions provided by Springer Nature and Copyright Clearance Center.

[Print](#) [Copy](#)

License Number	4747611022938
License date	Jan 14, 2020
Licensed Content Publisher	Springer Nature
Licensed Content Publication	Nature Reviews Microbiology
Licensed Content Title	Latency and lytic replication in Epstein-Barr virus-associated oncogenesis
Licensed Content Author	Christian Münz
Licensed Content Date	Sep 2, 2019
Type of Use	Thesis/Dissertation
Requestor type	academic/university or research institute
Format	print and electronic
Portion	figures/tables/illustrations
Number of figures/tables/illustrations	1
High-res required	no
Will you be translating?	no
Circulation/distribution	1 - 29
Author of this Springer Nature content	no
Title	Characterization of T cell responses to EBV-associated gastric carcinoma using a single TCR cloning platform
Institution name	Imperial College London
Expected presentation date	Dec 2019
Portions	figure 1
Requestor Location	Ms. Nadia Khan 12 Brookesley Street London, E3 4QL United Kingdom Attn: Ms. Nadia Khan
Total	0.00 GBP

License Details

This Agreement between Ms. Nadia Khan ("You") and Springer Nature ("Springer Nature") consists of your license details and the terms and conditions provided by Springer Nature and Copyright Clearance Center.

[Print](#) [Copy](#)

License Number	4746010897474
License date	Jan 11, 2020
Licensed Content Publisher	Springer Nature
Licensed Content Publication	Springer eBook
Licensed Content Title	Adoptive T-Cell Immunotherapy
Licensed Content Author	Stephen Gottschalk, Cliona M. Rooney
Licensed Content Date	Jan 1, 2015
Type of Use	Thesis/Dissertation
Requestor type	academic/university or research institute
Format	print and electronic
Portion	figures/tables/illustrations
Number of figures/tables/illustrations	1
Will you be translating?	no
Circulation/distribution	1 - 29
Author of this Springer Nature content	no
Title	Characterization of T cell responses to EBV-associated gastric carcinoma using a single TCR cloning platform
Institution name	Imperial College London
Expected presentation date	Dec 2019
Portions	figure 1
Requestor Location	Ms. Nadia Khan 12 Brookesley Street London, E3 4QL United Kingdom Attn: Ms. Nadia Khan
Total	0.00 GBP

LICENSED CONTENT

Gutcher and Becher 2007

Publication Title	The Journal of Clinical Investigation	Country	United States of America
Author/Editor	AMERICAN SOCIETY FOR CLINICAL INVESTIGATION., Robinson, George Canby	Rightholder	American Society for Clinical Investigation
Date	01/01/1924	Publication Type	Journal
Language	English		

REQUEST DETAILS

Portion Type	Image/photo/illustration	Distribution	U.K. and Commonwealth (excluding Canada)
Number of images / photos / illustrations	1	Translation	Original language of publication
Format (select all that apply)	Print, Electronic	Copies for the disabled?	No
Who will republish the content?	Academic institution	Minor editing privileges?	No
Duration of Use	Current edition and up to 5 years	Incidental promotional use?	No
Lifetime Unit Quantity	Up to 499	Currency	GBP
Rights Requested	Main product		

NEW WORK DETAILS

Title	Mrs	Institution name	Imperial College London
Instructor name	Nadia Khan	Expected presentation date	2020-01-31

ADDITIONAL DETAILS

Order reference number	N/A	The requesting person / organization to appear on the license	Nadia Khan
------------------------	-----	---	------------

REUSE CONTENT DETAILS

Title, description or numeric reference of the portion(s)	Figure 1	Title of the article/chapter the portion is from	N/A
Editor of portion(s)	N/A	Author of portion(s)	AMERICAN SOCIETY FOR CLINICAL INVESTIGATION.; Robinson, George Canby
Volume of serial or monograph	N/A	Issue, if republishing an article from a serial	N/A
Page or page range of portion	1	Publication date of portion	1924-01-01

ISSN	1545-3278	Publisher	ANNUAL REVIEWS
Type of Use	Republish in a thesis/dissertation	Portion	Image/photo/illustration

[Hide Details](#)

LICENSED CONTENT

Taylor et al 2015

Publication Title	Annual review of immunology	Rightholder	Annual Reviews, Inc.
Date	01/01/1983	Publication Type	e-Journal
Language	English	URL	http://arjournals.annualreviews.org/l...
Country	United States of America		

REQUEST DETAILS

Portion Type	Image/photo/illustration	Distribution	U.K. and Commonwealth (excluding Canada)
Number of images / photos / illustrations	1	Translation	Original language of publication
Format (select all that apply)	Print, Electronic	Copies for the disabled?	No
Who will republish the content?	Academic institution	Minor editing privileges?	No
Duration of Use	Life of current edition	Incidental promotional use?	No
Lifetime Unit Quantity	Up to 499	Currency	GBP
Rights Requested	Main product		

NEW WORK DETAILS

Title	Mrs	Institution name	Imperial College London
Instructor name	Nadia Khan	Expected presentation date	2020-01-31

ADDITIONAL DETAILS

Order reference number	N/A	The requesting person / organization to appear on the license	Nadia Khan
------------------------	-----	---	------------

REUSE CONTENT DETAILS

Title, description or numeric reference of the portion(s)	figure 3	Title of the article/chapter the portion is from	N/A
Editor of portion(s)	N/A	Author of portion(s)	N/A
Volume of serial or monograph	N/A	Issue, if republishing an article from a serial	N/A
Page or page range of portion	1	Publication date of portion	1983-01-01

[Remove](#)

